LUND UNIVERSITY

Cellular Processes and Mechanisms in Saccharomyces cerevisiae Influencing Anaerobic Xylose Fermentation

Bergdahl, Basti

2013

Link to publication

Citation for published version (APA):
Bergdahl, B. (2013). *Cellular Processes and Mechanisms in Saccharomyces cerevisiae Influencing Anaerobic Xylose Fermentation*. [Doctoral Thesis (compilation)]. Applied Microbiology (LTH).

Total number of authors:
1

General rights
Unless other specific re-use rights are stated the following general rights apply:
Copyright and moral rights for the publications made accessible in the public portal are retained by the authors and/or other copyright owners and it is a condition of accessing publications that users recognise and abide by the legal requirements associated with these rights.
• Users may download and print one copy of any publication from the public portal for the purpose of private study or research.
• You may not further distribute the material or use it for any profit-making activity or commercial gain
• You may freely distribute the URL identifying the publication in the public portal

Read more about Creative commons licenses: https://creativecommons.org/licenses/

Take down policy
If you believe that this document breaches copyright please contact us providing details, and we will remove access to the work immediately and investigate your claim.

LUND UNIVERSITY

PO Box 117
221 00 Lund
+46 46-222 00 00

Cellular Processes and Mechanisms in *Saccharomyces cerevisiae* Influencing Anaerobic Xylose Fermentation

BASTI BERGDAHL | APPLIED MICROBIOLOGY | LUND UNIVERSITY
DOCTORAL THESIS

Cellular Processes and Mechanisms in *Saccharomyces cerevisiae* Influencing Anaerobic Xylose Fermentation

In 2009 the EU approved two directives as a first initiative towards reducing greenhouse gas (GHG) emissions and becoming independent of fossil fuels: the Renewable Energy Directive (RED) and the Fuel Quality Directive (FQD). As a result, the demand for biofuels will increase enormously over the next decade, both nationally and in the entire EU. This huge demand will require a more advanced type of biofuels, produced from cellulosic and lignocellulosic raw materials that do not compete with the supply of food crops. These biofuels are referred to as second generation (2G) fuels. The production of 2G bioethanol at a commercial scale requires yeast strains capable of producing ethanol at high yield and high productivity from all sugars (hexoses and pentoses) extracted from the raw material. This thesis describes the cellular processes required for a high fermentation rate and the intracellular signals that regulate them. The aim of the work presented was to increase the knowledge about anaerobic xylose metabolism and to identify new biochemical mechanisms that limit anaerobic growth of recombinant *Saccharomyces cerevisiae* strains on this carbon source.

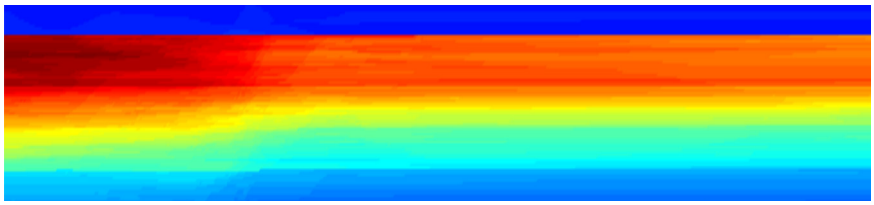

Cover art: The Thermodynamic Landscape in Recombinant *Saccharomyces cerevisiae*

Intracellular concentrations of 35 metabolites involved in the central carbon metabolism were measured in recombinant *S. cerevisiae* during a batch fermentation of glucose and xylose. Using the fermentation data, directions of intracellular fluxes were independently estimated by dynamic Flux Balance Analysis using a genome-scale model of the metabolic network in *S. cerevisiae*. By combining these two data sets the thermodynamic feasibility of 206 metabolic reactions and transport processes could be evaluated by calculating maximum and minimum values of the Gibbs energy of reaction ($\Delta rG'$). The horizontal axis in the picture above represents the progression of time through the batch fermentation. The vertical axis represents values of $\Delta rG'$ and the border between the red and blue areas indicate equilibrium ($\Delta rG' = 0$). The colours represent the fraction of reactions that can take on a given $\Delta rG'$ at a certain time point during the batch fermentation: red indicates a high fraction and blue indicates a low fraction.

LUND UNIVERSITY

ISBN 978-91-7422-318-7

Applied Microbiology, Lund University, 2013

Cellular Processes and Mechanisms in *Saccharomyces cerevisiae* Influencing Anaerobic Xylose Fermentation

Basti Bergdahl

Division of Applied Microbiology
Department of Chemistry
Faculty of Engineering
Lund University

Doctoral Thesis
2013

LUND
UNIVERSITY

Akademisk avhandling för avläggande av teknologie doktorsexamen vid Tekniska fakulteten, Lunds Universitet. Avhandlingen kommer att försvaras på engelska, fredagen den 17 maj, 2013, kl. 10.15 vid en offentlig disputation I hörsal K:B, Kemicentrum, Getingevägen 60, Lund. Fakultetens opponent är Prof. Jochen Förster, CTO vid Novo Nordisk Foundation Center for Biosustainability, Hørsholm, Danmark.

Academic thesis which, by due of permission of the Faculty of Engineering at Lund University, will be publicly defended on Friday 17th of May, at 10:15 am in Lecture Hall K:B, Center for Chemistry and Chemical Engineering, Getingevägen 60, Lund, for the degree of Philosophy in Engineering. Faculty opponent is Prof. Jochen Förster, CTO at the Novo Nordisk Foundation Center for Biosustainability, Hørsholm, Denmark.

Cellular Processes and Mechanisms in *Saccharomyces cerevisiae* Influencing Anaerobic Xylose Fermentation

Doctoral Thesis

Copyright © 2013 Basti Bergdahl

ISBN 978-91-7422-318-7

Division of Applied Microbiology
Department of Chemistry, Lund University
P.O. Box 124
SE-221 00 Lund
Sweden

Printed in Sweden by Media-Tryck, Lund University
Lund 2013

Populärvetenskaplig sammanfattning

Ett viktigt steg i strävan att ersätta fossila bränslen med biobränslen är ett effektivt utnyttjande av förnyelsebar lignocellulosa. Råmaterialet är restprodukter från skogs- och jordbruksindustrin och består bl. a. av komplexa kolhydrater som cellulosa. Efter nedbrytning till enkla sockermolekyler kan dessa omvandlas till bioetanol genom jäsning. Sockret som extraheras från vissa lignocellulosa material består upp till 30% av xylos. Xylos är en sockermolekyl med fem kolatomer och för en ekonomiskt lönsam process krävs fullständig förjäsning av xylos till etanol.

Kol är den grundläggande byggstenen i alla biologiska molekyler. Alla sockerarter, även xylos, är både viktiga energikällor och kolkällor. Vid produktion av bioetanol används vanligtvis bagerijäst, *Saccharomyces cerevisiae*. Tyvärr saknar *S. cerevisiae* flera gener som behövs för att tillgodogöra sig xylos. Under de senaste 20 åren har nya jäststammar utvecklats genom att introducera dessa gener i *S. cerevisiae*. En stor del av utvecklingsarbetet har lagts på att öka upptagningshastigheten av xylos och utbytet av etanol. Produktionshastigheten av etanol från xylos är dock fortfarande mycket lägre än den som erhålls vid jäsning av socker med sex kolatomer, som t.ex. glukos.

Målet med arbetet som presenteras i denna avhandling var att öka produktiviteten av etanol vid jäsning av glukos och xylos tillsammans. Tillväxten av jästceller har stort inflytande på etanolproduktiviteten. De jäststammar som finns idag växer tämligen dåligt på xylos. Många av de signaler som jästcellen använder för att reglera tillväxten beror på förändringar i koncentrationen av små molekyler inne i cellen, s.k. metaboliter. För att förstå xylos-metabolismen undersökte jag hur koncentrationer av metaboliter förändras vid jäsning av xylos och jämförde dessa med förändringar som sker vid jäsning av glukos. I mitt arbete identifierade och utvärderade jag cellulära processer och mekanismer som krävs för celltillväxt. Arbetet gav upphov till en ny hypotes: den långsamma tillväxten på xylos kan bero på begränsningar i veckningen av proteiner inuti i cellen. En essentiell process som ger proteinerna deras aktiva form.

Hexokinas 2 (Hxk2p) är ett bi-funktionellt protein som deltar i regleringen av processer specifika för produktionen av etanol. Enzymet inaktiveras av xylos med minskad kontroll som följd. Genom att kombinera metoder för att modifiera proteiner och mikroorganismer med jäsningsteknologi har jag identifierat en mutation i *HXK2*-genen som gör enzymet mindre känsligt för xylos. Det muterade enzymet medförde snabbare konsumtion av glukos i närvaro av xylos, men hade ingen uppenbar effekt på jäsningen av xylos. Det innebär att Hxk2p inte agerar på egen hand och att andra proteiner också påverkar regleringen. Vilka dessa proteiner är återstår att utforska.

I min avhandling har jag sammanfattat min kunskap om de intracellulära signaler som uppkommer vid jäsning av xylos. Jag visar också hur jag har använt dessa signaler för att identifiera biokemiska processer som potentiellt begränsar förmågan hos *S. cerevisiae* att växa på kol- och energikällan xylos.

Abstract

In 2009 the EU approved two directives as a first initiative towards reducing greenhouse gas emissions and becoming independent of fossil fuels: the Renewable Energy Directive and the Fuel Quality Directive. As a result, the demand for biofuels will increase enormously over the next decade, both nationally and in the entire EU. This huge demand will require a more advanced type of biofuels, produced from cellulosic and lignocellulosic raw materials that do not compete with the supply of food crops. These biofuels are referred to as second generation (2G) fuels. The production of 2G bioethanol at a commercial scale requires yeast strains capable of producing ethanol at high yield and high productivity from all sugars (hexoses and pentoses) extracted from the raw material.

The aim of the work presented in this thesis has been to increase the ethanol productivity of recombinant xylose-fermenting strains of the yeast *Saccharomyces cerevisiae* during batch fermentation of a glucose/xylose mixture. A parameter that has a big influence on productivity is cellular growth and the yeast strains currently used today grow rather poorly on xylose. Many of the signals cells use to regulate growth originate from changes in the concentrations of metabolites inside the cells. To increase our knowledge of xylose metabolism the dynamic changes in intracellular metabolite concentrations were measured during batch fermentation of a glucose/xylose mixture using LC-MS/MS. This study gave meaningful insights about important intracellular signals, biological phenomena and mechanism. The analysis of the metabolite data pointed toward limitations in the folding of proteins inside the ER, which might be the underlying cause of the slow growth on xylose.

Another important factor is the regulation of expression of genes required for sugar transport and those related to fermentative metabolism. Hexokinase 2 (Hxk2p) is an important bi-functional protein that acts both as a catalytic enzyme and a global transcription factor. This protein plays a role in the regulation of the above mentioned genes and becomes inactivated in the presence of xylose. As a consequence it loses its' regulatory function. In an effort to improve repression signals during xylose fermentation this protein was engineered to become immune towards inactivation by xylose. By combining methods for protein and genetic engineering with fermentation technology a mutation in the gene was identified which increased the catalytic activity by 64% in the presence of xylose. The new variant allowed faster glucose consumption in the presence of xylose, but had no obvious impact on xylose fermentation. These results indicate that Hxk2p does not act alone and other proteins are involved in the regulation. These proteins remain to be identified.

This thesis describes the cellular processes required for balanced anaerobic microbial growth and the intracellular signals that regulate them. The aim has been to identify biochemical mechanisms that limit anaerobic growth of recombinant *S. cerevisiae* strains on xylose.

List of Papers

This thesis is based on the following scientific articles which will be referred to by their Roman numbers in the text. The articles are found at the end of the thesis.

I. Parachin NS, Bergdahl B, van Niel EWJ, Gorwa-Grauslund MF: **Kinetic modeling reveals current limitations in the production of ethanol from xylose by recombinant *Saccharomyces cerevisiae***. *Metab Eng* 2011, 13:508-517.

II. Bergdahl B, Heer D, Sauer U, Hahn-Hägerdal B, van Niel EWJ: **Dynamic metabolomics differentiates between carbon and energy starvation in recombinant *Saccharomyces cerevisiae* fermenting xylose**. *Biotechnol Biofuels* 2012, 5:34.

III. Bergdahl B, Gorwa-Grauslund MF, van Niel EWJ: **Physiological effects of over-expressing compartment-specific components of the protein folding machinery in xylose-fermenting *Saccharomyces cerevisiae***. Manuscript 2013

IV. Bergdahl B, Sandström AG, van Niel EWJ, Gorwa-Grauslund MF: **Engineering yeast hexokinase 2 for improved tolerance toward xylose-induced inactivation**. Manuscript 2013

I have also contributed to the following publication which is not included in the thesis:

Carlquist M, Olsson C, Bergdahl B, van Niel EWJ, Gorwa-Grauslund MF, Frejd T: **Kinetic resolution of racemic 5,6-epoxy-bicyclo[2.2.1]heptane-2-one using genetically engineered *Saccharomyces cerevisiae***. *J Mol Catal B Enzym* 2009, 58:98-102

My Contribution to the Papers

I. I developed the kinetic models, performed the simulations and participated in analysing the results as well as describing the models in the manuscript.

II. I conceived of the study and designed the experiments together with Dr. Dominic Heer whom also helped me carry out the experimental work. I performed the statistical analysis and biological interpretation of the data. I wrote the manuscript with the assistance of my supervisors.

III. I conceived of the study and designed the experiments. I supervised the master student who performed most of the molecular biology work. I developed the enzymatic assay and performed the fermentation experiments. I analysed the data and wrote the manuscript.

IV. I conceived of the study and designed most of the experiments. The structural analysis of Hxk2p and design of mutations was performed by Dr. Anders Sandström and one master student. Dr. Sandström constructed the xylose-fermenting strains and performed the anaerobic batch fermentations together with me. I supervised the work of one master student and one undergraduate student who constructed the deletion strain. I performed the remaining molecular biology work, generated the *E. coli* and yeast libraries, performed the selection experiments and evaluated the identified protein variant in chemostat cultivations. I wrote the manuscript, except for the part related to protein engineering which was written by Dr. Sandström.

Abbreviations

1G	first generation biofuels
2G	second generation biofuels
AEC	adenylate energy charge
AK	adenylate kinase, EC 2.7.4.3
ALD, Ald6p	aldehyde dehydrogenase, EC 1.2.1.3
ARG-L, Arg	arginine
ASN-L, Asn	asparagine
ASP-L, Asp	aspartate
CE	capillary electrophoresis
df	degrees of freedom
E4P	erythrose 4-phosphate
ENO, Eno2p	enolase, EC 4.2.1.11
ER	endoplasmic reticulum
ERAD	ER-associated degradation
F26BP	fructose 2,6-bisphosphate
F6P	fructose 6-phophate
FAD	flavin adenine dinucleotide
FBP	fructose 1,6 bisphosphate
FMN	riboflavin 5'-monophosphate
FUMase	fumarate hydratase, EC 4.2.1.2
G6P	glucose 6-phosphate
GC	gas chromatography
GEC	guanylate energy charge
GFP	green fluorescence protein
GLN-L, Gln	glutamine
GLU-L, Glu	glutamate
HPLC	high pressure liquid chromatography
HXK2, Hxk2p	hexokinase 2, EC 2.7.1.1
M1P	mannitol 1-phosphate
M1PDH	mannitol-1-phosphate 5-dehydrogenase, EC 1.1.1.17
MDH	malate dehydrogenase, EC 1.1.1.37
MS	mass spectrometry
NES	nuclear export sequence
NLS	nuclear localisation sequence
NMR	nuclear magnetic resonance

OST	oligosaccharyltransferase, EC 2.4.1.119
PDI1, Pdi1p	protein disulphide isomerase, EC 5.3.4.1
PEP	phospho*enol*pyruvate
PFK	6-phosphofructo kinase, EC 2.7.1.11
PFK26	6-phosphofructo-2-kinase, EC 2.7.1.105
PHE-L	phenylalanine
PKA	protein kinase A
Pkc1p	protein kinase C
PPP	pentose phosphate pathway
PYK	pyruvate kinase, EC 2.7.1.40
PYR	pyruvate
R5P	ribose 5-phosphate
Ribi	Ribosome biogenesis
RP	Ribosomal protein
RU5P	ribulose 5-phosphate
S7P	sedoheptulose 7-phosphate
Ser	serine
SPC	signal peptidase complex
SRP	signal-recognition particle
SUC2	invertase encoding gene, EC 3.2.1.26
TAL	transaldolase, EC 2.2.1.2
Thr	threonine
TKL	transketolase, EC 2.2.1.1
TRP-L	tryptophan
TYR-L	tyrosine
UPR	unfolded protein response
UPLC	ultra performance liquid chromatography
XDH, *XYL2*	xylitol dehydrogenase, EC 1.1.1.9
XI, *xylA*	xylose isomerase, EC 5.3.1.5
XK, *XKS1*, *xylB*	xylulokinase, EC 2.7.1.17
XR, *XYL1*	xylose reductase, EC 1.1.1.307
XU5P	xylulose 5-phosphate

Table of Contents

Introduction

In 2009 the EU approved two directives, influencing the future use of energy, as a first initiative towards reducing greenhouse gas (GHG) emissions and becoming independent of fossil fuels. The first directive is called the Renewable Energy Directive (RED) which states that the fraction of energy derived from renewable resources should be at least 20% of the total energy consumption in the EU by the year 2020 [EU, 2009b]. All member states need to make adjustments in their energy production for this target to be achieved, but the extent of these changes depend on each state's starting point. The RED further mandates that by 2020, 10% of the energy consumed in the transport sector shall be derived from renewable fuels (biofuels). This target is equal for all member states. The biofuels used must fulfil specific criteria regarding sustainability and GHG emission savings in order to be eligible for tax exemptions and other financial support. Initially, the GHG emissions using a biofuel must be at least 35% less than using a reference fossil fuel, but this requirement will increase over time and by the year 2018 a 60% lower emission will be required. The second directive, the Fuel Quality Directive (FQD), obliges the producers and suppliers of fuels to reduce the GHG emissions with 6% by the year 2020 [EU, 2009a]. This can be achieved in different ways, e.g. by adapting all chains in the production process to use sustainable biofuels and energy from other renewable sources.

Figure 1A shows how the Swedish gross energy production was distributed between different energy carriers in 2011. The energy produced from renewable resources (i.e. biomass, district heating via heat pumps, wind and water power) constituted 43% of the total production which is far above the EU average around 10% [SCB, 2012]. This fraction should be increased to a minimum of 49% by 2020 according to the RED, which is the highest target of all the EU member states. The contribution from biomass has steadily increased since the 1970's and mainly consists of residues from forestry and agricultural sectors as well as peat and municipal waste [SCB, 2012]. In the transport sector the contribution from biomass was approximately 6% of the sector's total energy consumption in 2011, whereas more than 90% came from fossil fuels [SCB, 2013b]. To reach the 10% target set by the RED it is thus necessary to exchange the fossil fuels with sustainable biofuels. Bioethanol is a biofuel which has been available in Sweden since the beginning of 2000 as a blend (E85) containing 85% bioethanol and 15% gasoline. Although its use is increasing, the total volume delivered in 2011 was significantly lower than other petroleum based fuels (Fig. 1B) [SCB, 2013a]. Nevertheless, the demand for biofuels will increase

enormously over the next decade, both nationally and in the entire EU, which will most likely lead to the appearance of a whole new market in many countries [Alvfors *et al.*, 2010]. This huge demand will also require a more advanced type of biofuels, produced from cellulosic and lignocellulosic raw materials. These biofuels are referred to as second generation (2G) in contrast to first generation (1G) fuels which are produced from sugar- or starch-rich agricultural crops such as wheat, corn, sugar beets and sugar cane. In order to not compete with the supply of food crops the development of 2G biofuels is critical [Alvfors *et al.*, 2010].

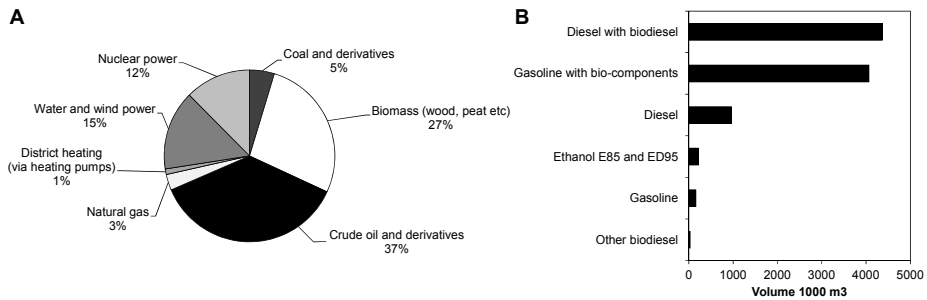

Figure 1. A) Distribution of the gross energy production between different energy carriers in Sweden in the year 2011. B) The total delivery of petroleum based fuels and biofuels in Sweden in the year 2011.
Definitions: biodiesel means FAME (fatty acid methyl esters) and HVO (hydrogenated vegetable oil); bio-components mean ethanol and ETBE (ethyl tertiary butyl ether). Source: [SCB, 2013b; SCB, 2013a]

To meet the targets set by the EU directives, production processes of several biofuel alternatives are under development and each has to be evaluated according to certain criteria. The main factors considered in such an evaluation are technical, economic, ecological and political as well as customer requirements (Fig. 2). Taken together, biofuels should as far as possible have a competitive production cost, not require additional distribution or infrastructure costs, have physical and chemical properties similar to existing fuels and different blends should be possible without problems [Festel, 2008]. There is no biofuel currently fulfilling all these criteria alone and it is thus necessary to produce different types of biofuels that complement each other, using the resources available locally. The commercialization of a biofuel is indeed a challenging task which requires collaboration of experts from many different areas. Still, studies have shown that the development of sustainable biofuels and the utilization of other renewable resources for energy production will not only contribute to reducing the GHG emissions, but also lead to higher security in energy supply, new job opportunities

and increased income to rural regions [Festel, 2008; APEC, 2010; Bessou *et al.*, 2011; Börjesson *et al.*, 2012].

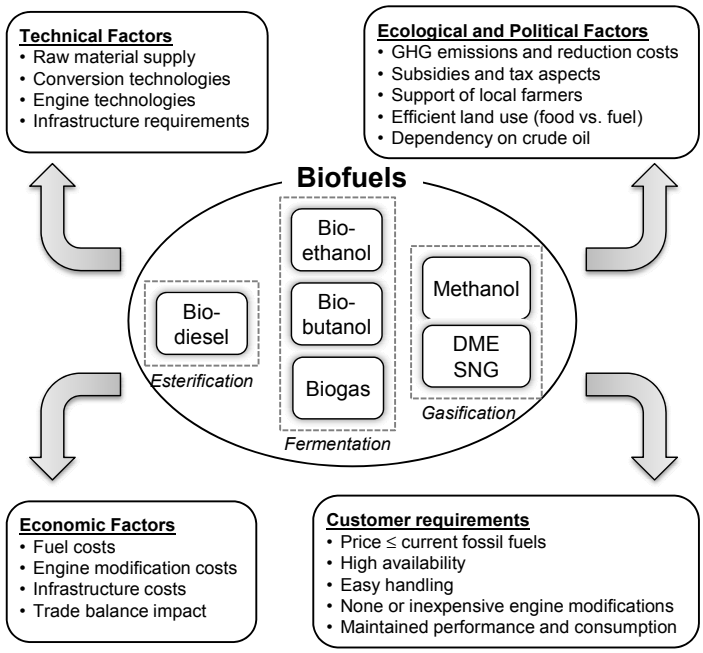

Figure 2. Factors influencing the evaluation of biofuels.
Abbreviations: GHG, greenhouse gas; SNG, synthetic natural gas; DME, dimethyl ether.

The potential for Sweden to increase its production of biofuels is high, mainly due to large forest resources, a well-established pulp and paper industry, favourable production conditions for energy crops (e.g. willow and red canary grass), a developed infrastructure and access to pilot and demonstration plants for technology development [Grahn and Hansson, 2009; Alvfors *et al.*, 2010]. Three main routes are being evaluated for the production of 2G biofuels from lignocellulosic materials: i) esterification of rapeseed and sunflower oil into biodiesel, ii) gasification of solid biomass or black liquor into DME (dimethyl ether), synthetic natural gas (methane) or methanol and iii) fermentation of sugar monomers into ethanol or butanol and anaerobic digestion of e.g. organic waste into biogas (Fig. 2). None of these processes is however economically feasible by itself. The key to an economically feasible production of 2G biofuels is to integrate several processes to generate heat, electricity, biogas and other high value biochemicals in a single production plant – a so called biorefinery [Alvfors *et al.*, 2010; Gallezot, 2012].

The process to ferment sugars into ethanol using the yeast *Saccharomyces cerevisiae* is well known and well established. However, since lignocellulosic

materials have a much more complex chemical structure than starch-rich crops, an initial pre-treatment of the material under harsh conditions is required to open the chemical structure [Girio *et al.*, 2010; Soccol *et al.*, 2011]. Due to the harsh conditions employed during the pre-treatment several inhibitory compounds are also formed which significantly reduce the fermentation efficiency of the yeast [Jönsson *et al.*, 2013]. After pre-treatment the cellulose and hemicellulose polymers are accessible for hydrolytic enzymes which break them down into fermentable sugar monomers [Galbe and Zacchi, 2007]. The composition of the resulting sugar fraction depends on the material used [Olofsson *et al.*, 2008; Girio *et al.*, 2010]. Softwood, such as pine and spruce, mainly contains glucans and only a small fraction of mannan and xylan. In other materials, such as wheat straw, corn stover, switch grass and willow, the fraction of xylan can be as much as 30% (Fig. 3). Conversion of the xylose sugar monomers can increase the final ethanol yield by 20% which will reduce the production cost significantly and is thus crucial for obtaining an economically feasible process [Sassner *et al.*, 2008]. In short, the production of 2G ethanol from lignocellulosic raw materials requires i) optimized conditions for pre-treatment for each material, ii) efficient and cheap hydrolytic enzymes and iii) robust yeast strains that are tolerant towards inhibitors and can produce ethanol at high yield and high productivity from all sugars (hexoses and pentoses) present in the hydrolysate.

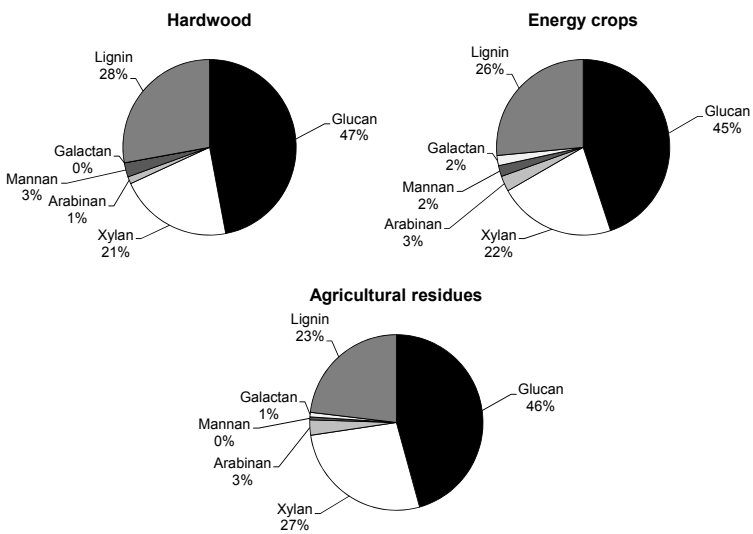

Figure 3. Average composition of some lignocellulosic raw materials.
Hardwood: Poplar and aspen. Energy crops: Switch grass and willow. Agricultural residues: Corn stover, rice straw, sugar cane bagasse and wheat straw. Fractions are given as per cent of dry matter. Source: [Olofsson *et al.*, 2008]

The aim of the work presented in this thesis has been to increase the ethanol productivity of recombinant xylose-fermenting strains of the yeast *S. cerevisiae* during batch fermentation of a glucose/xylose mixture. Chapter 1 gives an overview of the genetic modifications required to enable xylose utilization in *S. cerevisiae* and highlights a limitation in the initial xylose pathway [**Paper I**]. In Chapter 2 some analytical methods are briefly presented which are often used to obtain global information about cellular metabolism and physiology. As cellular growth is a key parameter with a significant impact on process productivity a comprehensive evaluation of signals given by intracellular metabolites during xylose metabolism was conducted [**Paper II**]. The results from this evaluation are presented in Chapter 3 in relation to the cellular processes that are required for balanced microbial growth. The analysis pointed towards a limitation in the protein folding machinery which was evaluated by over-expressing three different components of this pathway [**Paper III**]. Chapter 4 presents the role of hexokinase 2 (Hxk2p), an important bi-functional protein which acts both as a catalytic enzyme and a global transcription regulator. This protein is part of the signalling pathway that induces expression of genes required for sugar transport and represses the expression of genes involved in respiratory metabolism. In an effort to improve the transcriptional control of these genes during xylose fermentation Hxk2p was engineered to become immune towards inactivation by xylose [**Paper IV**].

Imagination is more important than knowledge.
Knowledge – is limited.
Imagination – encircles the world.

Albert Einstein

1. Metabolic Pathways for Xylose Utilization

The capability to utilize xylose as a carbon and energy source is more common among bacteria than among eukaryotes. The most studied xylose-utilizing eukaryote is *Scheffersomyces stipitis* (formerly *Pichia stipitis* [Kurtzman and Suzuki, 2010]) which has an oxido-reductive pathway for xylose assimilation. Bacteria, on the other hand, use a co-factor independent isomerization pathway. In this chapter both these pathways are described, with advantages and disadvantages associated with the introduction in *S. cerevisiae*.

1.1. The fungal oxido-reductive xylose pathway

Most species of yeast and fungi that can utilize xylose have an oxido-reductive pathway consisting of a xylose reductase (XR), a xylitol dehydrogenase (XDH) and a xylulokinase (XK) (Fig. 4) [Barnett, 1976]. The XR catalyses the conversion of xylose to xylitol while using electrons stored in reduced cofactors. Species such as *Candida utilis* and *C. tropicalis* have an XR which only use NADPH as cofactor, whereas the XR from *S. stipitis* has dual cofactor specificity and can use both NADPH and NADH [Bruinenberg *et al.*, 1984; Toivola *et al.*, 1984; Yokoyama *et al.*, 1995; Yablochkova *et al.*, 2003]. However, the specificity for NADPH is still higher than for NADH [Rizzi *et al.*, 1988]. The use of NADH in the reaction catalysed by the XR is important for obtaining a balanced pathway [Bruinenberg *et al.*, 1983]. The XDH enzyme catalyses the conversion of xylitol to xylulose and uses exclusively NAD as cofactor. This reaction is subject to thermodynamic limitations due to the very low equilibrium constant (K'_{eq}) [Rizzi *et al.*, 1989]. For this reaction to have a negative Gibbs free energy ($\Delta_r G'^{\circ}$) and proceed in the forward direction, the concentrations of the products NADH and xylulose have to be much lower than the concentration of the substrates. The importance of the XK enzyme is thus evident as it catalyses the phosphorylation of xylulose to xylulose 5-phosphate using ATP and thus ensures favourable conditions for the XDH reaction.

S. cerevisiae do possess the genes for an endogenous oxido-reductive pathway. There are several genes encoding enzymes for xylose reduction (*YJR096W*, *GCY1*, *GRE3* and *YPR1*), xylitol oxidation (*XYL2*, *SOR1*, *SOR2* and *XDH1*) but only one encoding a XK (*XKS1*) [Träff *et al.*, 2002; Toivari *et al.*, 2004; Chang *et al.*, 2007; Wenger *et al.*, 2010]. The expression levels of these genes are however very low, but the simultaneous over-expression of *GRE3* and *XYL2* has been shown to confer a xylose-positive phenotype [Träff *et al.*, 2002; Toivari *et al.*, 2004]. The *XDH1* gene was only recently identified and annotated as a xylitol dehydrogenase [Wenger *et al.*, 2010]. It was shown to enable xylose utilization in an otherwise wild-type and xylose-negative strain as well as being necessary for xylose utilization in those strains already carrying the gene. In addition, these experiments indicated that the other genes encoding XDH enzymes (i.e. *XYL2*, *SOR1* and *SOR2*) have a detrimental effect on the ability to utilize xylose [Wenger *et al.*, 2010]. In the same study it was also shown that only *GRE3* and *YPR1* can enable xylose utilization when expressed alone in a strain void of all XR activity. Since the enzyme encoded by *GRE3* is NADPH-dependent, there is a significant redox imbalance in this endogenous pathway which contributes to its inefficiency. It may be so that the enzyme encoded by *XDH1* has a higher affinity for NADPH which would balance the pathway and increase the efficiency, especially when the other genes are deleted.

1.2. The bacterial isomerization xylose pathway

The species of bacteria that can utilize xylose have a much simpler pathway than the oxido-reductive alternative (Fig. 4) [Jeffries, 1983]. This pathway has also been identified in the fungal species *Piromyces* sp. isolated from elephant faeces [Kuyper *et al.*, 2003]. It consists of two enzymes: a xylose isomerase (XI) and a XK. The XI catalyses the conversion of xylose directly to xylulose without the use of any cofactor. This is a huge advantage for metabolic engineering purposes. However, this reaction also has a positive $\Delta_rG'^{\circ}$ and is thus subject to the same thermodynamic limitations as the XDH reaction [Tewari *et al.*, 1985].

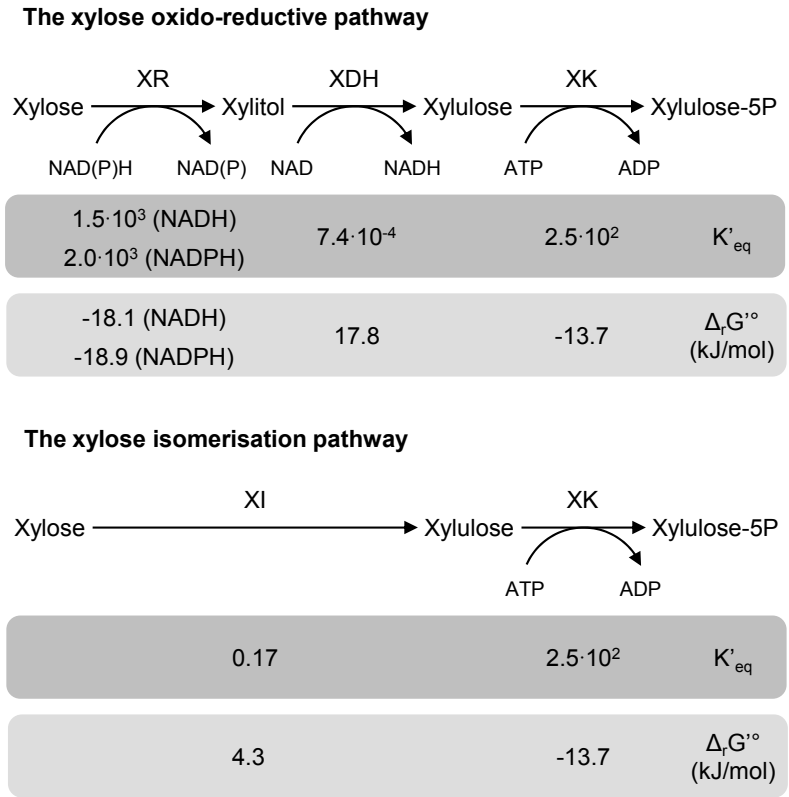

Figure 4. The two xylose utilization pathways present in yeast and bacterial species. The thermodynamic properties were calculated using the online tool eQuilibrator (http://milolab.webfactional.com).

1.3. Metabolic engineering of *Saccharomyces cerevisiae* for xylose assimilation

1.3.1. Choosing a xylose pathway

As highlighted above, the XR/XDH-pathway has a problem with cofactor balancing between the two first reactions. This means that the cells have to use other reactions and resources to maintain the proper balance. The importance of maintaining the redox balance is discussed in Chapter 3.3. The introduction of the *XYL1* and *XYL2* genes from *S. stipitis*, encoding the NAD(P)H-dependent XR and NAD-dependent XDH, respectively, in *S. cerevisiae* yielded a

recombinant strain capable of producing ethanol from xylose [Kötter *et al.*, 1990; Amore *et al.*, 1991]. However, the xylose consumption rate was low and the xylose was never completely consumed. Additionally, the ethanol yield was very low at ~11% of the theoretical yield. This was attributed to three possible reasons: i) low XK-activity, ii) a limited capacity of the pentose phosphate pathway (PPP) and iii) low uptake rate of xylose. The low ethanol yield and the absence of other fermentation products showed that the metabolism of xylose by *S. cerevisiae* was mainly oxidative. Further studies showed a significant accumulation of xylitol and a growth arrest on xylose in the absence of respiration [Kötter and Ciriacy, 1993]. This was due to two reasons: i) the strong preference for NADPH as cofactor by the XR and ii) the inability of the cells to oxidise the NADH produced by the XDH. Hence, the difference in co-factor specificity and the thermodynamic constraint of the XDH reaction led to an accumulation of xylitol in the absence of an external electron acceptor. The redox imbalance is the main disadvantage with the XR/XDH-pathway and several strategies have been explored to overcome this limitation (Table 1). The most successful strategy so far has been to engineer variants of XR with altered cofactor specificity. Strains expressing these engineered variants produce a higher yield of ethanol due to a significantly reduced production of xylitol and are also able to grow anaerobically on xylose as the sole carbon source [Runquist *et al.*, 2009b; Runquist *et al.*, 2010a]. However, the growth on xylose during batch fermentation of a glucose/xylose mixture remains low [Bengtsson *et al.*, 2009] (see also Fig. 11 in Chapter 3).

Due to the distinct problems with balancing the redox co-factors in the XR/XDH-pathway, efforts have been made to develop recombinant strains expressing a gene encoding XI [van Maris *et al.*, 2007]. The lack of co-factor involvement makes this a potentially good alternative to the XR/XDH-pathway. However, most genes encoding XI:s are of bacterial origin which are not translated into fully functional enzymes when expressed in yeast [Sarthy *et al.*, 1987; Amore *et al.*, 1989; Gardonyi and Hahn-Hägerdal, 2003]. The first gene encoding a XI that exhibited activity when expressed in *S. cerevisiae* was *xylA* from *Thermus thermophilus* [Walfridsson *et al.*, 1996]. The aerobic growth rate of the recombinant strain was, however, low due the reduced catalytic activity by the enzyme at 30 °C. Combining the expression of *xylA* from *T. thermophilus* with deletion of the endogenous aldose reductase encoded by *GRE3* reduced xylitol formation significantly [Träff *et al.*, 2001]. Strains with higher growth rates on xylose were obtained by adaptation of strains with increased activity of XK and the enzymes in the non-oxidative PPP [Karhumaa *et al.*, 2005]. The discovery of a eukaryotic XI from the fungus *Piromyces* sp., which could be functionally expressed in yeast with higher activity, presented new possibilities for this alternative [Kuyper *et al.*, 2003]. Even so, strains with the XI-pathway require extensive metabolic engineering combined with long adaptation in xylose medium before their performance can match that of less evolved XR/XDH-strains

[Kuyper *et al.*, 2005a; Kuyper *et al.*, 2005b; Wisselink *et al.*, 2009]. The main advantage of using the XI-pathway is still the potential of obtaining high ethanol yields since xylitol production will be very low.

Table 1. Metabolic engineering strategies explored to overcome the redox imbalance in a XR/XDH-pathway expressed in *S. cerevisiae*.

Genetic modification(s)	Species	Reference
Disruption of the *ZWF1* gene encoding G6PDH	*Saccharomyces cerevisiae*	[Jeppsson *et al.*, 2003a] [Jeppsson *et al.*, 2003b]
Engineering XDH toward higher preference for NADP	*Scheffersomyces stipitis*	[Metzger et al., 1995] [Watanabe *et al.*, 2007b] [Krahulec *et al.*, 2009]
Expression of wild-type XR with high preference for NADH	*Candida parapsilosis*	[Bengtsson *et al.*, 2009]
Engineering XR toward higher preference for NADH	*Scheffersomyces stipitis*	[Jeppsson *et al.*, 2006] [Watanabe *et al.*, 2007a] [Bengtsson *et al.*, 2009] [Runquist *et al.*, 2010a] [Krahulec *et al.*, 2009]
Optimization of XR/XDH expression levels	*Saccharomyces cerevisiae*	[Eliasson *et al.*, 2001] [Jeppsson *et al.*, 2003b] [Jin and Jeffries, 2003] [Karhumaa *et al.*, 2007]
Expression of *xfp* encoding a phosphoketolase	*Bifidobacterium lactis*	[Sonderegger *et al.*, 2004]
Alteration of cofactor requirement for ammonium assimilation by disruption of the *GDH1* gene (encoding NADPH-dependent glutamate dehydrogenase) and over-expression of *GDH2* (encoding NADH-dependent glutamate dehydrogenase)	*Saccharomyces cerevisiae*	[Grotkjaer *et al.*, 2005]
Expression of *gapN* encoding a non-phosphorylating, NADP-dependent glyceraldehyde 3-phosphate dehydrogenase	*Kluyveromyces lactis* *Streptococcus mutants*	[Verho *et al.*, 2003] [Bro *et al.*, 2006]
Over-expression of endogenous *POS5* encoding a NADH kinase	*Saccharomyces cerevisiae*	[Hou *et al.*, 2009]
Expression of *noxE* encoding a water-forming NADH oxidase	*Lactococcus lactis*	[Zhang *et al.*, 2012]
Implementation of a transhydrogenase-like shunt	*Saccharomyces cerevisiae*	[Suga *et al.*, 2013]

As shown in Figure 4 the XK is common for both pathways and is important for achieving a high flux through any of the pathways due to the thermodynamic constraint of the preceding enzyme. XI-strains with endogenous XK-activity consume only a fraction of the available xylose and excrete the xylulose formed intracellularly [Kuyper *et al.*, 2003; van Maris *et al.*, 2007; Madhavan *et al.*, 2009]. Similarly, low XK-activity in XR/XDH-strains leads to xylitol excretion and low ethanol production [Ho *et al.*, 1998]. Attempts to increase the XK activity in XR/XDH-strains by expressing the *XKS1* gene from an episomal multicopy plasmid resulted, as expected, in significantly reduced xylitol yield and increased ethanol yield [Johansson *et al.*, 2001; Lee *et al.*, 2003; Van Vleet *et al.*, 2008]. However, in all cases did this high activity also lead to a reduced xylose consumption rate as well as lower aerobic growth rate. Hence, the majority of current strains only have a single extra copy integrated in the genome to enable xylose utilization [Kuyper *et al.*, 2004; Karhumaa *et al.*, 2005]. The negative effect of very high XK activity has been ascribed to an excessive ATP usage in the initial phosphorylation reaction [Teusink *et al.*, 1998]. However, this would require a high rate of substrate supply, which conversely decreased. The gene *PHO13* was recently shown to encode a phosphatase capable of using xylulose 5-phosphate as substrate *in vitro* [Kim *et al.*, 2013]. Such a dephosphorylation reaction would not only lead to a futile cycle of ATP-utilization, but also to reduced concentrations of important intermediates required in both the PPP to create a pulling effect, and in the biosynthetic reactions of nucleotides (see below). A general reduction of nucleotide synthesis would most likely lead to a reduced growth rate as observed. Several studies have shown that deletion of the *PHO13* gene or the loss of enzyme-function improves both growth and fermentation performance on xylose [Van Vleet *et al.*, 2008; Fujitomi *et al.*, 2012; Kim *et al.*, 2013].

1.3.2. The pentose phosphate pathway

The PPP is divided into two parts, an oxidative and a non-oxidative pathway (Fig. 5). The oxidative pathway consists of three enzymes which converts glucose 6-phosphate (G6P) into the pentose ribulose 5-phosphate (RU5P). This is the final outcome of two oxidation reactions forming reduced NADPH cofactors and one decarboxylation reaction producing CO_2. The non-oxidative PPP begins with the isomerisation of RU5P into ribose 5-phosphate (R5P) and xylulose 5-phosphate (XU5P) via two different enzymes (Fig. 5). The subsequent reactions are a series of carbon-shuffling between different compounds, catalysed by the two enzymes transketolase (TKL) and transaldolase (TAL) (Fig. 5). While TAL covalently binds the ketone group (C_3) to be transferred to a lysine residue in the protein structure [Jia *et al.*, 1997], TKL is dependent on the cofactor thiamine

diphosphate (TPP) to transfer the carbonyl group (C_2) from XU5P to R5P or erythrose 4-phosphate (E4P) [Nilsson *et al.*, 1997]. The carbon channelled through the PPP during fermentative growth of *S. cerevisiae* is only around 15% of the glucose utilized [Frick and Wittmann, 2005] and the phospho*enol*pyruvate (PEP) generated by employing the PPP has been estimated to be less than 4% of the carbon taken up [Gancedo and Lagunas, 1973; Maaheimo *et al.*, 2001]. The role of the PPP has thus been suggested as exclusively anabolic and not catabolic [Maaheimo *et al.*, 2001].

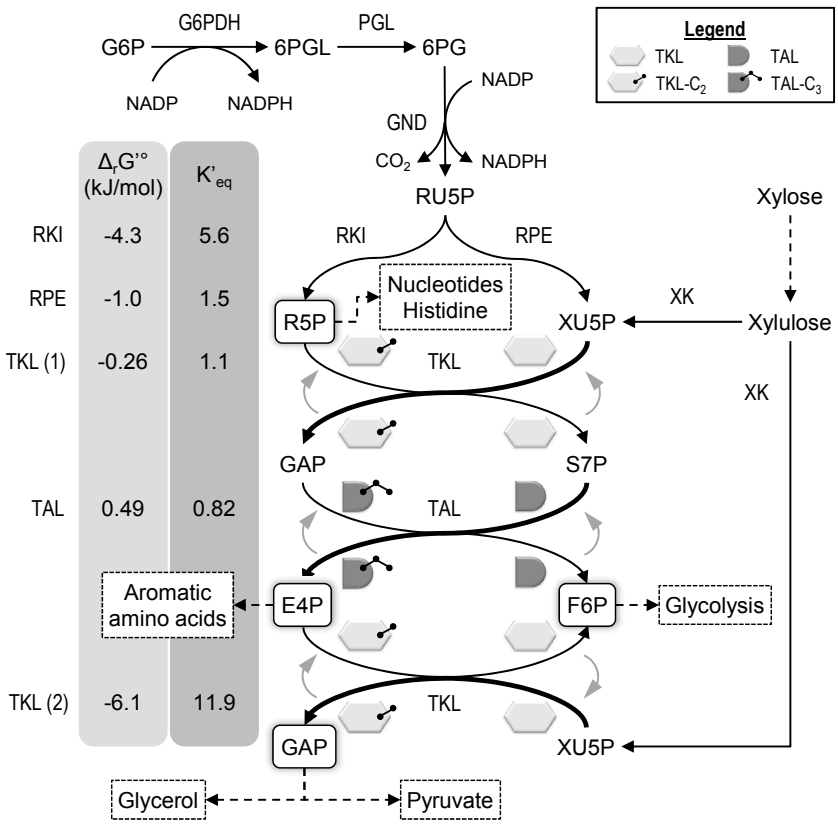

Figure 5. The pentose phosphate pathway.
In the oxidative part G6P is converted to RU5P through two oxidation reactions and a decarboxylation reaction. RU5P enters the non-oxidative part of the pathway and is isomerized to R5P and XU5P. E4P is formed through a series of carbon-shuffling reactions catalysed by the enzymes TKL and TAL. The thicker arrows indicate the first step of the reactions in which the carbonyl (C2) or ketone (C3) group is transferred to the enzyme. The thinner arrows indicate the second step of the reactions in which the carbon group is removed from the enzyme. The small, grey arrows indicate the transition from step one to step two. Thermodynamic data was obtained from http://xpdb.nist.gov/enzyme_thermodynamics/ [Goldberg *et al.*, 2004].

Many of the compounds formed in the PPP are indeed needed for biosynthesis of essential building blocks. R5P is the starting structure for the synthesis of histidine, co-factors (e.g. NAD, NADP, FAD) and nucelotides (ATP, GTP, CTP, UTP). The nucelotides are subsequently used to form nucleic acids necessary for DNA and RNA synthesis. E4P is the starting structure for the synthesis of aromatic amino acids and the NADPH generated in the oxidative PPP is an important source of electrons in anabolic reactions.

During fermentation of xylulose, native *S. cerevisiae* accumulates intracellular sedoheptulose 7-phosphate (S7P) which was interpreted as insufficient activity of subsequent PPP enzymes [Senac and Hahn-Hägerdal, 1990]. When the four genes of the non-oxidative PPP were over-expressed the rate of xylulose [Johansson and Hahn-Hägerdal, 2002] and xylose [Karhumaa *et al.*, 2005] fermentation did indeed increase. The limited capacity of the non-oxidative PPP for xylose utilization has since been established by recent metabolomics studies [Klimacek *et al.*, 2010; Wisselink *et al.*, 2010] and mathematical simulations [Song *et al.*, 2012]. As shown in Figure 5 most of the reactions in the non-oxidative PPP operate close to equilibrium at standard conditions (i.e. equal concentrations of all metabolites). Hence, the direction of these reactions is to a large extent determined by the individual metabolite concentrations and increasing the activity by over-expressing the genes will only be effective to a certain point.

Many recombinant xylose fermenting strains of *S. cerevisiae* currently carry additional copies of the genes encoding the enzymes in the non-oxidative PPP [Chu and Lee, 2007]. To evaluate whether this modification, together with deletion of the *GRE3* gene, shifts the bottleneck back to the initial xylose assimilation pathway two kinetic models were created: one describing the XR/XDH-pathway and the other the XI-pathway [**Paper I**]. Simulations using these models indicated that in both cases would an increase of the XK-activity increase xylose consumption and reduce xylitol formation. To confirm these results, the *xylB* gene from *E. coli* (encoding the XK) was over-expressed in a strain-background already carrying the before mentioned modifications, including an integrated extra copy of the endogenous *XKS1* gene. The XK enzyme of *E. coli* has nearly 400-fold higher turnover rate than the endogenous enzyme of *S. cerevisiae* [Richard *et al.*, 2000; Di Luccio *et al.*, 2007]. A higher XK-activity in the strain harbouring the XI-pathway led to a 38% increase in the total amount of xylose fermented in 100 h and a concomitant increase in the amount of ethanol produced [**Paper I**].

When the XK activity was increased in a strain harbouring the XR/XDH-pathway the xylitol yield was reduced by 88%, reaching a value even lower than that obtained with the XI-strain (0.01 g/g vs. 0.05 g/g, respectively) [**Paper I**]. The ethanol yield, however, only increased by 7% and the productivity was reduced due to a 14% reduction in the amount of xylose consumed [**Paper I**].

Still, these experiments clearly showed that the combination of these genetic modifications is highly beneficial for xylose fermentation using *S. cerevisiae*. However, these modifications did not enable anaerobic growth on xylose which indicates other bottlenecks exists either downstream the PPP or upstream the XR in the sugar transport system.

1.3.3. Glucose and xylose transporters

S. cerevisiae possesses a number of genes encoding transporters of sugars and sugar alcohols: *HXT1-17* (glucose and fructose), *AGT1* (maltose), *GAL2* (galactose) and *STL1* (glycerol) [Bisson *et al.*, 1993; Reifenberger *et al.*, 1995; Boles and Hollenberg, 1997; Pao *et al.*, 1998; Wieczorke *et al.*, 1999; Ferreira *et al.*, 2005]. The uptake of glucose is however mainly mediated by six primary transporters (*HXT1-4, 6* and *7*) whose expression are regulated via the Rgt2p and Snf3p glucose sensors [Moriya and Johnston, 2004]. The kinetic properties for glucose have been determined for each of these transporters individually under both repressive and non-repressing conditions (Table 2) [Reifenberger *et al.*, 1997].

Table 2. Kinetic parameters of individual transporters for glucose under repressive (100 mM) and non-repressive (5 mM) conditions. V_{max} values are given in units nmol/mg protein/min and K_m values are given in units mM. NR: not reported. Source: [Reifenberger *et al.*, 1997]

Gene	100 mM Glucose		5 mM Glucose	
	V_{max}	K_m	V_{max}	K_m
HXT1	NR	110 ± 25	690 ± 26	90 ± I5
HXT2	1.7 ± 0.8	10 ± 1	97 ± 8	1.5 ± 0.2
	–	–	450 ± 20	60 ± 10
HXT3	250 ± 50	65 ± 15	360 ± 20	55 ± 6
HXT4	100 ± 4	9.4 ± 0.7	160 ± 8	9.3 ± 0.7
HXT7	121 ± 4	2.1 ± 0.2	186 ± 7	1.1 ± 0.1
Wild type	15 ± 6	1.7 ± 0.8	167 ± 6	0.8 ± 0.1
	165 ± 6	46 ± 7	104 ± 8	21 ± 3

Based on the measured saturation constants, the order of increasing affinity among these transporters was: Hxt1p < Hxt3p < Hxt4p < Hxt2p < Hxt7p. The wild-type strain used in these experiments displayed a two-component system with high and low affinities for glucose, respectively. The high affinity system did however not contribute significantly to the transport capacity in conditions with high glucose concentration (Table 2). Although Hxt2p was characterized as a low affinity transporter, the kinetic properties appear to be dependent on the growth conditions as a low affinity component also appears under non-repressing

conditions (Table 2). As each individual transporter has different kinetic properties the expression of each gene is tuned according to the extracellular glucose concentration (Fig. 6) [Youk and van Oudenaarden, 2009].

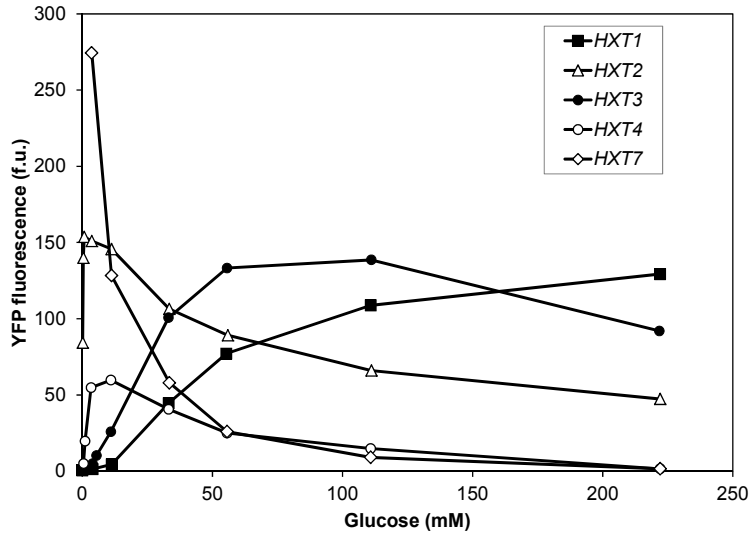

Figure 6. Expression levels of *HXT* genes measured using YFP reporter constructs in wild-type yeast strain CEN.PK2-1C.
The two membrane proteins Rgt2p and Snf3p sense the extracellular level of glucose and modulate the expression of each *HXT* gene according to their kinetic properties. High affinity transporters (*HXT7* and *HXT2*) are induced at low glucose concentrations while low affinity transporters (*HXT1* and *HXT3*) are induced at high concentrations. Source: [Youk and van Oudenaarden, 2009].

S. cerevisiae has no specific transporter for xylose but the Hxt transporters as well as the Gal2p transporter are able to facilitate the uptake of xylose [Sedlak and Ho, 2004; Saloheimo *et al.*, 2007]. The kinetic properties with regard to xylose have been determined for some individual transporters (Table 3). The affinity for xylose is on average 100-fold lower than for glucose. Hence, xylose will not be transported to any large extent when glucose is present at high concentration. The high-affinity transporters (Hxt2p, 4p and 7p) are more sensitive toward inhibition by glucose (50% reduction in uptake rate in the presence of 10 mM glucose) than the low-affinity transporter (Hxt1p; 50% reduction in uptake rate in the presence of 150 mM glucose).

The competition between glucose and xylose has been investigated using mathematical modelling [Bertilsson *et al.*, 2008]. In that model the uptake of sugar was assumed to follow a Michaelis-Menten rate equation with inhibition by the competing sugar. The model also included the glucose-dependent regulatory response of each individual transporter gene (cf. Fig. 6).

Table 3. Kinetic parameters for xylose transport of individual transporters expressed under the control of *TPI1*-promoter. The background strain harbours a XD/XDH-pathway and all strains were grown in 2% maltose medium. Source: [Saloheimo *et al.*, 2007]

Transporter gene	V_{max} (nmol/mg protein/min)	K_m (mM)
HXT1	750 ± 94	880 ± 8
HXT2	340 ± 10	260 ± 130
HXT4	190 ± 23	170 ± 120
HXT7	110 ± 7	130 ± 9

The simulations showed that the highest xylose transport rate was achieved at a glucose concentration around 2 g/L. The presence of a small amount of glucose ensured induction of both high-affinity (Hxt2p and 4p) and high-capacity (Hxt1p and 3p) transporters which combined is more efficient than having only the high-affinity transporters (Hxt2p, 6p and 7p) as would be the case with no glucose present. This highlights the importance of Hxt1p, Hxt2p and Hxt4p for obtaining the most efficient xylose transport. An increase in transport capacity (higher level of Hxt1p or Hxt3p) was shown to increase the xylose transport rate at low glucose concentration, while an increased affinity is necessary at high glucose concentration [Bertilsson *et al.*, 2008].

A more mechanistic model for the competition between glucose and xylose for a single transporter is illustrated in Figure 7. The derived rate equations for this mechanism are given by Equations 1-3.

$$v_{GLC}^{trsp} = \frac{v_{GLC}^{\max}\left\{\frac{C_{GLC}^{e}}{K_{GLC}}\left(1+\frac{\beta}{\gamma_{HXT}}\frac{C_{XYL}^{i}}{K_{XYL}}\right)-\frac{C_{GLC}^{i}}{K_{GLC}}\left(1+\frac{\beta}{\gamma_{HXT}}\frac{C_{XYL}^{e}}{K_{XYL}}\right)\right\}}{Denominator} \quad (1)$$

$$v_{XYL}^{trsp} = \frac{v_{XYL}^{\max}\left\{\frac{C_{XYL}^{e}}{K_{XYL}}\left(1+\frac{\alpha}{\gamma_{HXT}}\frac{C_{GLC}^{i}}{K_{GLC}}\right)-\frac{C_{XYL}^{e}}{K_{XYL}}\left(1+\frac{\alpha}{\gamma_{HXT}}\frac{C_{GLC}^{e}}{K_{GLC}}\right)\right\}}{Denominator} \quad (2)$$

$$Denominator = \left(1+\frac{C_{GLC}^{e}}{K_{GLC}}+\frac{C_{XYL}^{e}}{K_{XYL}}\right)\left(1+\frac{\alpha}{\gamma_{HXT}}\frac{C_{GLC}^{i}}{K_{GLC}}+\frac{\beta}{\gamma_{HXT}}\frac{C_{XYL}^{i}}{K_{XYL}}\right)+\ldots$$
$$\ldots+\left(1+\frac{C_{GLC}^{i}}{K_{GLC}}+\frac{C_{XYL}^{i}}{K_{XYL}}+\frac{C_{G6P}^{i}}{K_{I}}+\frac{C_{GLC}^{i}C_{G6P}^{i}}{K_{GLC}K_{II}}+\frac{C_{XYL}^{i}C_{G6P}^{i}}{K_{XYL}K_{II}}\right)\left(1+\frac{\alpha}{\gamma_{HXT}}\frac{C_{GLC}^{e}}{K_{GLC}}+\frac{\beta}{\gamma_{HXT}}\frac{C_{XYL}^{e}}{K_{XYL}}\right) \quad (3)$$

In this model the transporter is regarded as a carrier with two different conformations; the carrier is either open towards the extracellular medium or towards the cytoplasm. The general rate equation for transport of two competing substrates, previously derived by Geck [1971], is here extended to include the inhibition by G6P.

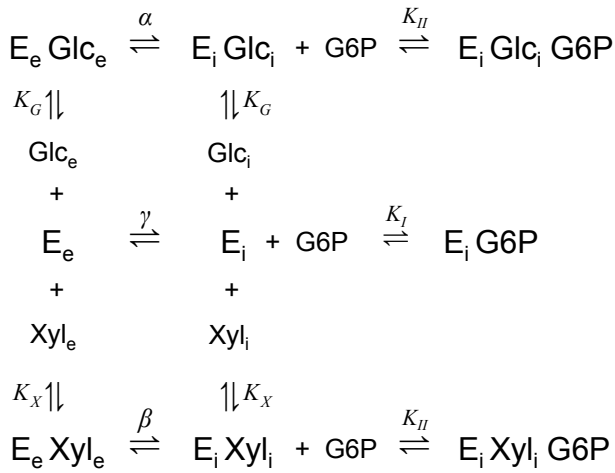

Figure 7. Mechanism of co-transport of glucose (Glc) and xylose (Xyl) with inhibition by G6P. The transporter is modelled as a shuttle with two different conformations. The transporter can be open towards the extracellular medium (E_e) or towards the cytoplasm (E_i). When G6P is bound to the transporter it cannot change its conformation.

C_{GLC} and C_{XYL}, in Equations 1-3, are the concentrations of the sugar being transported and the exponent indicates if it is the extracellular (*e*) or intracellular concentration (*i*). K_G and K_X are the dissociation constants of glucose and xylose, respectively, from the free transporter and can be assumed to represent the affinity of the transporter protein. K_I and K_{II} are the dissociation constants of G6P from unloaded and loaded carrier, respectively. The number of dissociation constants is reduced by assuming that the inhibition of the transporter-xylose complex by G6P is equal to the inhibition of the transporter-glucose complex. The free transporter is more strongly inhibited than the transporter-sugar complexes and the constants have been determined by Rizzi *et al.* [1996]: K_I = 1.2 mM and K_{II} = 7.2 mM. The inhibition of the sugar transporters by G6P is still a topic for discussion [Rizzi *et al.*, 1996]. However, it seems reasonable that there is some kind of control of the sugar uptake in order to prevent accumulation of usable glucose inside non-viable cells. The parameters α, β and γ are the rates of conformation change of loaded (α and β) and unloaded carrier (γ); these are assumed to be the rate limiting steps in the transport mechanism. If the loaded and unloaded carriers are assumed to have the same rate of conformation change, the ratios α/γ and β/γ can be set equal to unity. Whether this holds in reality needs to be verified experimentally. For a detailed description of the derivation together with the assumptions made, the reader is referred to the Appendix.

Improvements of the endogenous transport system of recombinant *S. cerevisiae* with the XI-pathway have been achieved by prolonged adaptation in

glucose/xylose mixtures [Kuyper *et al.*, 2005b]. The unknown changes led to a two-fold increase in V_{max} and a 25% decrease of the K_m for xylose in the adapted strain. This improvement conferred a faster overall fermentation rate and a 50% higher specific xylose consumption rate (0.9 g/g/h compared with 0.6 g/g/h for the non-adapted strain).

More rational approaches have been undertaken to improve xylose transport by introducing exogenous genes encoding sugar transporters from natural xylose-consuming organisms. Only a few of these are able to confer a xylose-positive phenotype in the absence of the endogenous transporters (Table 4). The expression of the transporters encoded by *GXF1* and *SUT1* as well as the loci *At5g59250* and *At5g17010* in XR/XDH-strains has a positive effect on fermentation performance [Hector *et al.*, 2008; Katahira *et al.*, 2008; Runquist *et al.*, 2009a]. In all experiments, the ethanol productivity increased due to an increased xylose consumption rate, but only after glucose had been depleted. The expression of *GXF1* in the XI-strain TMB3360 did not improve the performance significantly during anaerobic fermentation of 50 g/L xylose [**Paper I**]. The combination of *GXF1* and over-expression of *xylB* from *E. coli*, on the other hand, led to a 78% increase in specific ethanol productivity compared to the strain not carrying the *GXF1* gene [**Paper I**]. This shows very nicely how the location of a bottleneck in a pathway depends on the design of the whole network.

The transporters evaluated kinetically all show a higher affinity for glucose than for xylose, except the recently identified transporters encoded by *XYP29* from *S. stipitis* and *An25* from *N. crassa* which cannot transport glucose at all (Table 4) [Du *et al.*, 2010]. However, the effect of these transporters on the co-fermentation of glucose and xylose has not yet been evaluated. The genes *GXS1* and *XUT3* from *C. intermedia* and *S. stipitis*, respectively, have also undergone mutagenesis by error-prone PCR to generate transporters with improved characteristics for xylose transport [Young *et al.*, 2012]. The selected Gxs1p variants had a higher transport capacity and reduced affinity for xylose which increased the aerobic growth rate on xylose by 70%. These variants had, however, no effect on the fermentation of a glucose/xylose mixture. The best Xut3p variant had a 39% higher transport capacity and 50% lower K_m compared with the wild type transporter. Hence, in this case it was possible to improve efficiency and affinity at the same time. The XR/XDH-strain expressing this variant had a 27% higher growth rate on xylose aerobically and significantly increased consumption rates of both glucose and xylose using mixed substrates. The strain expressing the improved variant consumed 10 g/L glucose within 30 h whereas the control strain consumed less than 50% of the glucose in 100 h. A similar pattern was observed with xylose: the strain expressing the new variant consumed 7.5 g/L xylose in 100 h while the control strain only consumed 2 g/L.

Despite this large body of experimental work, a significant degree of glucose/xylose co-consumption has not yet been demonstrated. This will not be possible until a specific xylose transporter has been identified with an affinity for xylose that is at least equal that for glucose. Furthermore, the increased xylose consumption rates achieved by expressing additional transporters have not led to faster growth under anaerobic conditions. This indicates that other processes downstream the xylose pathway and PPP are still limiting the growth on xylose.

Table 4. Exogenous transporter genes cloned and expressed in *S. cerevisiae* strains with or without (*hxt*^{0}) native transporters. Kinetic parameters and the growth phenotype under aerobic conditions are also given where available. ND: not detected.

Organism	Transporter gene/locus	Strain	Xylose pathway	Aerobic performance		Kinetic parameters			Ref.
				Carbon source	Phenotype	Substrate	V_{max} [a] mmol/g CDW/h [b] nmol/mg CDW/min	K_m (mM)	
Arabidopsis thaliana	*STP2* *STP3*	TMB3201(*hxt*^{0})	XR, XDH	20 g/L xyl	No growth	–	–	–	[Hamacher *et al.*, 2002]
	At5g59250	TMB3201(*hxt*^{0})	XR, XDH	20 g/L xyl	No growth	–	–	–	[Hamacher *et al.*, 2002]
		TMB3418	XR(K270R), XDH	60 g/L xyl 15 g/L xyl 4 g/L xyl	μ = 0.16 μ = 0.04 μ = 0.002	Xylose	163 ± 7[b]	148 ± 39	[Runquist *et al.*, 2010b]
		EY12(*hxt*^{0})	XR, XDH	20 g/L glc 20 g/L xyl 5 g/L xyl	No growth No growth No growth	–	–	–	[Young *et al.*, 2011]
Candida intermedia	*GXF1*	TMB3201(*hxt*^{0})	XR, XDH	–	–	Glucose Xylose	~2.6[a] ~3.9[a]	2.0 ± 0.64 48.7±6.5	[Leandro *et al.*, 2006]
		TMB3416	XR(K270R), XDH	60 g/L xyl 15 g/L xyl 4 g/L xyl	μ = 0.16 μ = 0.04 μ = 0.008	Xylose	471 ± 10[b]	166 ± 6	[Runquist *et al.*, 2010b]
		EY12(*hxt*^{0})	XR, XDH	20 g/L glc 20 g/L xyl 5 g/L xyl	μ = 0.172 μ = 0.070 μ =0.085	–	–	–	[Young *et al.*, 2011]
	GXS1	TMB3201(*hxt*^{0})	XR, XDH	20 g/L xyl (solid)	Slow growth	Glucose Xylose	0.26 ± 0.02[a] 0.39 ± 0.09[a]	0.012 ± 0.004 0.4±0.1	[Leandro *et al.*, 2006]
		EY12(*hxt*^{0})	XR, XDH	20 g/L glc 20 g/L xyl 5 g/L xyl	μ = 0.051 μ = 0.049 μ =0.078	–	–	–	[Young *et al.*, 2011]

Table 4. Continued.

Chloella kessleri	*HUP1*	TMB3201(*hxt*^{0})	XR, XDH	20 g/L xyl	No growth	–	–	–	[Hamacher *et al.*, 2002]
Cryptococcus neoformans	*CNBC3990*	EY12(*hxt*^{0})	XR, XDH	20 g/L glc 20 g/L xyl 5 g/L xyl	No growth No growth No growth	–	–	–	[Young *et al.*, 2011]
Debaryomyces hansenii	*XylHP*	EY12(*hxt*^{0})	XR, XDH	20 g/L glc 20 g/L xyl 5 g/L xyl	μ = 0.073 μ = 0.065 μ =0.100	–	–	–	[Young *et al.*, 2011]
	DEHA0D02167	EY12(*hxt*^{0})	XR, XDH	20 g/L glc 20 g/L xyl 5 g/L xyl	μ = 0.045 No growth No growth	–	–	–	[Young *et al.*, 2011]
	DEHA2A14300p *DEHA2B14278p* *DEHA2F19140p*	EY12(*hxt*^{0})	XR, XDH	20 g/L glc 20 g/L xyl 5 g/L xyl	No growth No growth No growth	–	–	–	[Young *et al.*, 2011]
Escherichia coli	*xylE*	TMB3201(*hxt*^{0})	XR, XDH	20 g/L xyl	No growth	–	–	–	[Hamacher *et al.*, 2002]
Neurospora crassa	*An25*	EBY.VW4000(*hxt*^{0})	None	–	–	Glucose Xylose	ND 37 ± 3 [a]	ND 175 ± 21	[Du *et al.*, 2010]
Scheffersomyces stipitis	*SUT1*	RE700(*hxt*^{0})	None	–	–	Glucose Xylose	45.0 ± 1.0 [b] 132.0 ± 1.0 [b]	1.5 ± 0.1 145.0 ± 1.0	[Weierstall *et al.*, 1999]
		TMB3418	XR(K270R), XDH	60 g/L xyl 15 g/L xyl 4 g/L xyl	μ = 0.16 μ = 0.04 μ = 0.005	Xylose	178 ± 16[b]	96 ± 11	[Runquist *et al.*, 2010b]
	SUT2	RE700(*hxt*^{0})	None	–	–	Glucose Xylose	3.3±0.1/28.0±4.0 [b] 41.0 ± 1.0 [b]	1.1±0.1/55.0±11.0 49.0 ± 1.0	[Weierstall *et al.*, 1999]
	SUT3	RE700(*hxt*^{0})	None	–	–	Glucose Xylose	3.7±0.1/22.0±0.1 [b] 87.0 ± 2.0 [b]	0.8±0.1/31.0±0.1 103.0 ± 3.0	[Weierstall *et al.*, 1999]

Table 4. Continued.

Scheffersomyces stipitis	*XYP29*	EBY.VW4000(*hxt*^{0})	None	–	–	Glucose Xylose	ND 42 ± 2[a]	ND 56 ± 9	[Du *et al.*, 2010]
Trichoderma reesei (Hypocrea jecorina)	*xlt1*	H2219(*hxt*^{0})	XR, XDH	20 g/L xyl	No growth (adaptation required)	–	–	–	[Saloheimo *et al.*, 2007]
Yarrowia lipolytica	*YALI0C06424*	EY12(*hxt*^{0})	XR, XDH	20 g/L glc 20 g/L xyl 5 g/L xyl	μ = 0.043 No growth No growth	–	–	–	[Young *et al.*, 2011]
	YALI0B06391p *YALI0B01342p* *YALI0C08943p* *YALI0F06776p*	EY12(*hxt*^{0})	XR, XDH	20 g/L glc 20 g/L xyl 5 g/L xyl	No growth No growth No growth	–	–	–	[Young *et al.*, 2011]

All truths are easy to understand once they are discovered.
The point is to discover them.

Galileo Galilei

2. Global Analyses of Xylose Metabolism

To identify bottlenecks in xylose metabolism of recombinant *S. cerevisiae* strains downstream of the initial transport and assimilation pathways, knowledge of where the highest degree of functional information can be found is necessary. This chapter gives a short overview of the major intracellular 'omes and what information they can give.

2.1. The functional information residing in cellular entities

In the rational design of industrially applicable cell factories it is important to understand the underlying cellular processes which give rise to a certain phenotype. The phenotype of a microorganism, i.e. its growth characteristics and other observable traits such as product excretion, is determined by its interactions with the environment and its genetic potential (Fig. 8). The genome, as such, can provide information about the phylogeny of the organism and its structural components but the functional information provided is limited. The functional information is rather found in the biochemical processes that occur in response to the environmental conditions and is commonly viewed as the connection between the three major 'omes in the cell: transcriptome, proteome and metabolome (Fig. 8) [Smedsgaard and Nielsen, 2005].

The transcriptome can today easily be analysed using available DNA microarray technology for a relatively low cost [Ehrenreich, 2006] and has been applied frequently in the research of yeast metabolism [Hirasawa *et al.*, 2010]. Data on the expression pattern of genes give a higher degree of information than the genome since it can define which structural component are active under certain conditions. Properly designed experiment can also give an insight into the regulation of the metabolism (see for example Slattery *et al.* [2008] and Zaman *et al.* [2009]). However, mRNA molecules are merely the material used as templates for synthesizing new proteins and thus are not true functional entities, only

carriers of information [Delneri *et al.*, 2001]. The proteins and the metabolites on the other hand, are directly involved in the cellular biochemistry and thereby dictate more closely the function of the organism. Nevertheless, DNA microarrays have been used in several studies with the aim to better understand xylose metabolism in recombinant *S. cerevisiae* [Wahlbom *et al.*, 2003; Jin *et al.*, 2004; Salusjärvi *et al.*, 2006; Salusjärvi *et al.*, 2008; Runquist *et al.*, 2009b]. All these studies showed a significant up-regulation of genes involved in respiratory pathways, independent of the oxygenation level, as well as the high-affinity sugar transporters. The conclusion from these results is that xylose is not recognised as a fermentable carbon source by *S. cerevisiae* and cannot convey the same regulatory signals as glucose does.

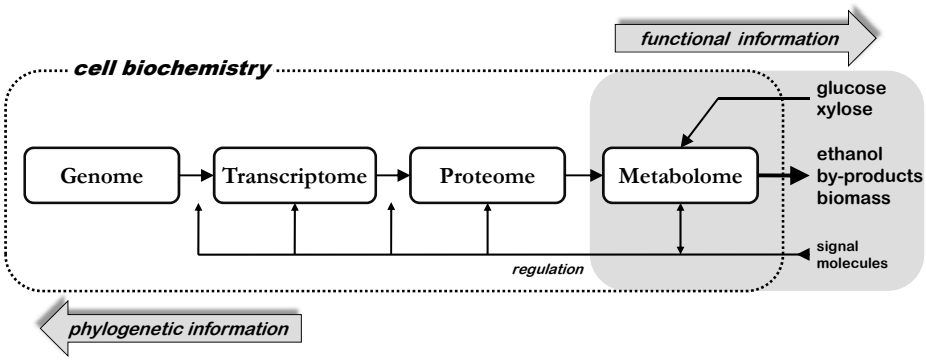

Figure 8. The degree and type of information residing in the different cellular 'omes.
Adapted from [Smedsgaard and Nielsen, 2005].

The intracellular proteins act as enzymes, catalysing many of the intracellular reactions, as well as the main regulatory components which control gene expression. Hence, proteins are indeed important cellular entities and the possibility to quantify the abundance of all cellular proteins would provide useful information regarding the metabolic status of the cell. Unfortunately, there is a low correlation between the transcriptome and proteome, mainly due to the separation of the two by the translation process, making it difficult to assess the protein abundance from transcriptional data [Gygi *et al.*, 1999; Griffin *et al.*, 2002; Greenbaum *et al.*, 2003]. The analysis of the proteome is further complicated by the fact that the mere presence of a protein does not mean it is active. For a protein to be functional it needs to be folded into a specific 3-dimensional structure, involving incorporation of disulphide bridges, and often requires additional post-translational modifications (PTM) such as

phosphorylation, acetylation and glycosylation.[1] Such modifications are regarded as an important regulatory event and need to be taken into account when assessing the role of a particular protein [Daran-Lapujade *et al.*, 2004; Oliveira *et al.*, 2012]. In addition, some proteins are part of a larger complex which is the active component inside the cell [Krogan *et al.*, 2006]. The proteome has nevertheless been the target of interest in several analyses of industrial wine and beer production strains [Joubert *et al.*, 2000; Kobi *et al.*, 2004; Hansen *et al.*, 2006; Zuzuarregui *et al.*, 2006; Cheng *et al.*, 2008]. Specific investigations of the proteome in recombinant *S. cerevisiae* strains metabolizing xylose are, however, few. The abundance of proteins has been compared between anaerobic chemostat cultivations of a XR/XDH-strain with different feed compositions: 10 g/L glucose or a mixture of 27 g/L xylose and 3 g/L glucose [Salusjärvi *et al.*, 2003]. The most significant changes in protein levels were related to glycerol metabolism (activation of NAD regeneration), ethanol and acetate utilization (increased NADPH and acetyl-CoA formation) and mitochondrial metabolism (reduced biosynthetic capacity). Proteomics was also used to investigate the underlying molecular changes in a mutated industrial *S. cerevisiae* strain with much improved xylose fermentation capability [Karhumaa *et al.*, 2009]. This analysis revealed higher protein levels in the improved strain of TKL in the PPP, Eno2p (enolase) in lower glycolysis and Ald6p (aldehyde dehydrogenase) used for NADPH formation through acetate production. In addition the enzyme Pdi1p (protein disulphide isomerase), which is involved in the folding of proteins in the ER, was found to be significantly higher in the improved strain. The protein level of Pdi1p was also reported as 84% lower in an XR/XDH-strain growing aerobically on xylose compared to glucose [Salusjärvi *et al.*, 2008]. This finding is discussed further in Chapter 3.5.

Recent advances in the discovery and identification of PTM:s through advanced algorithms [Potthast *et al.*, 2005] may substantially increase the information obtained from proteomic studies and thus motivate the undertaking of new investigations. With the advent of protein microarray technology it will be possible to analyse the proteome with regard to protein-protein, protein-DNA/RNA and protein-small molecule interactions, as well as different kinds of post-translational modifications, in a large-scale, high-throughput fashion [Chen and Snyder, 2010]. The main limitation of protein microarrays is still the high production cost of the chips and the small number of probes/enzymes that can be used per assay and array.

[1] A comprehensive list of post-translational modifications can be found at the UniProt Knowledgebase (http://www.uniprot.org/docs/ptmlist).

2.2. Discovering intracellular signals by metabolomics

The *metabolome* is the complete set of small, low-molecular-weight molecules, (i.e. *metabolites*) in a biological sample, which can be an organ, a tissue, an organism or biological fluid [Oliver *et al.*, 1998]. *Metabolomics* is the systematic characterization and quantification of small molecules in complex biological samples. Another term is *metabonomics* (from the Greek words *meta* and *nomos* meaning change and a rule set or set of laws, respectively) which further aims to measure the dynamic metabolic response of a biological system due to stimuli or manipulation [Nicholson and Lindon, 2008]. As the analytical and technical procedures used in these fields are the same, the two terms are also often used interchangeably. There are two main approaches within metabolomics, depending on the purpose of the investigation. *Metabolic fingerprinting* is a comprehensive, untargeted analysis of as many intracellular metabolites as possible with high biochemical relevance. This approach often only gives relative quantities and is thus used to obtain a rapid classification of the sample. The other approach, *metabolic profiling*, aims for a quantitative analysis of a set of pre-defined metabolites belonging to a class of compounds or members of particular pathways [Fiehn, 2002]. Metabolic profiling is less comprehensive than fingerprinting and the methodology does not allow the investigator to look for other metabolites than those pre-defined after the samples have been analysed. However, the absolute quantitation will provide information which can be used in more detailed analyses of the system, e.g. a thermodynamic evaluation of intracellular reactions [Soh *et al.*, 2012]. The work described in **Paper II** is one example of a metabonomics investigation where metabolic profiling was used to measure the dynamic changes in concentrations of targeted metabolites in two recombinant xylose-fermenting strains of *S. cerevisiae* during batch fermentation of a glucose/xylose mixture. The findings in this study are presented in Chapter 3.

The functional role of metabolites in the metabolism is eminent as they can i) influence the rate of conversion by an enzyme, either as substrate, product or allosteric effector, ii) act as signalling molecules (e.g. cAMP), iii) protect the cell from damage (e.g. glutathione) and iv) influence the directionality of enzymatic reactions through their thermodynamic properties. The technology to separate, detect and quantify intracellular metabolites has developed quickly in recent years. Several methods are now available to analyse substances with different chemical properties using GC/MS, LC/MS, EC/MS or NMR [Krishnan *et al.*, 2005; Villas-Boas *et al.*, 2005; Oldiges *et al.*, 2007; Werner *et al.*, 2008; Buscher *et al.*, 2009; Bowen and Northen, 2010]. Some advantages and disadvantages with these methods are summarized in Table 5.

To illustrate the steps involved in analysing the metabolome of a particular sample, the workflow adopted in **Paper II** is shown in Figure 9.

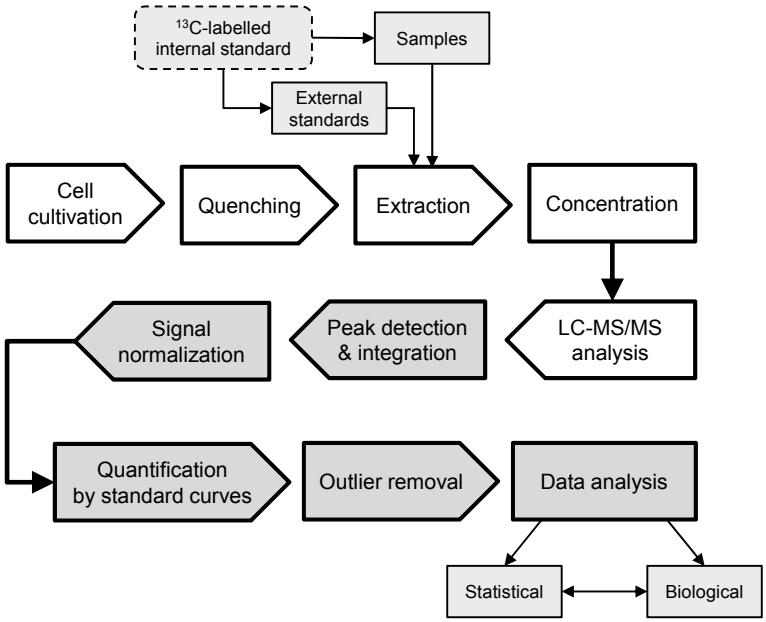

Figure 9. The workflow adopted in Paper II to quantify targeted metabolites.
The steps performed as wet-work are indicated in white while steps performed using a computer are indicated in dark grey. See text and **Paper II** for further details.

The quenching and extraction steps are the two most critical steps during sample preparation. The purpose of quenching the cells is to quickly stop all metabolic activity to preserve the metabolic state. Hence this step is performed by dispersing the cell culture into a buffered solution chilled to ca. -40 °C. The smaller the drops generated by the dispersion equipment the more efficient is the quenching. Depending on the solution used and the duration of the treatment, different degrees of leakage of metabolites into the solution are obtained [Canelas *et al.*, 2008a]. If this step is not intended as a combined quenching and extraction, a high degree of leakage will in the worst case lead to the generation of an unrepresentative sample. The conditions employed in the extraction step need to be harsh enough to break the cells and release the metabolites, but not so harsh that the metabolites are degraded. Due to the importance of these two steps, several methods for quenching and extraction have been developed for different organisms (reviewed by [Villas-Boas *et al.*, 2005; Dunn and Winder, 2011]. Some methods developed for *S. cerevisiae* are given in Table 5. Metabolites extracted from microorganisms generally need to be enriched before analysis. This is preferably performed using a vacuum centrifuge under moderate temperatures.

Hence, there is a direct advantage in using volatile solutions for the extraction as they readily evaporate under such conditions. By introducing an isotope-labelled internal standard to samples and external standards during the extraction step, metabolite losses (e.g. due to degradation) can be corrected for by normalizing the signal of each metabolite with its labelled counterpart. In addition, two important drawbacks with an LC-MS/MS analysis can be counteracted: i) matrix effects caused by the unique composition of a certain cell type or microorganism and ii) non-linear calibration curves due to high salt or organic solvent concentrations in the sample [Mashego *et al.*, 2004].

Table 5. Methods commonly used for quenching of cells, extraction, separation and detection of metabolites in *S. cerevisiae*. For more information see [Villas-Boas *et al.*, 2005].

Description	Advantages	Disadvantages
Quenching methods		
Cold methanol/water solution	• Cells can be separated from cultivation broth through centrifugation • Reduced organic solvent content • Fast drop in temperature	• Requires sample handling at low temperatures • May cause leakage due to cell wall disruption if the methanol:water ratio is not controlled
Cold glycerol/saline solution	• Cells can be separated from cultivation broth through centrifugation • No organic solvent • Reduced leakage	• Dominance of the glycerol peak may mask detection of other metabolites
Perchloric acid	• Rapid and efficient inactivation of enzymes • Preserves nucleotides and amines	• Low pH can degrade some metabolites • Very oxidative • No separation from cultivation broth • Low recovery
Liquid nitrogen	• Rapid freezing • Very low temperature • Easily evaporated from the sample	• Low reproducibility, no homogenous freezing • High leakage due to cold shock • No separation from cultivation broth
Extraction methods		
Cold buffered methanol:chloroform	• Efficient and reproducible • Denatures enzymes by chloroform • Preserves phosphorylated compounds • Can separate polar from non-polar metabolites	• Requires sample handling at low temperatures • Chloroform toxicity • Laborious

Table 5. Continued.

Description	Advantages	Disadvantages
Boiling ethanol	• Simple and fast • Accurate and reliable • Suitable for cultures with low cell density • High recovery of selected metabolites (e.g. G6P, ATP, NAD, NADH)	• Degradation of thermo-labile metabolites
Separation methods		
GC	• High chromatographic resolution of volatile compounds • Suitable for complex biological samples • Simultaneous analysis of different metabolite classes	• Unable to analyse thermo-labile metabolites • Non-volatile compounds must be derivatized before analysis • Derivatized unknown compounds difficult to identify
CE	• High resolution of polar metabolites • Small volumes • Suitable for complex biological samples	• High complexity • High maintenance
HPLC and UPLC	• Separates a broad group of metabolites • High sensitivity • Average to high resolution • Analysis of thermo-labile metabolites	• Matrix effects • Salt concentrations in samples should be low
Detection methods		
NMR	• No separation required • Non-destructive on samples • Very high analytical reproducibility • Minimal sample preparation	• Limited detection limit (micro molar) • High sample volume required (100-500 µL)
MS	• Low detection limit (≤ pico molar) • Low sample volume required (low µL range)	• Coupling to a separation step normally required • Destructive on samples • Fair analytical reproducibility • Substantial sample preparation may be required (e.g. salts need to be at low concentrations)

S. cerevisiae contains approximately 700-1100 unique metabolites [Herrgård *et al.*, 2008; Mo *et al.*, 2009] which is substantially lower than the ~6000 genes or proteins. It would therefore seem like a less daunting task to analyse metabolite data than e.g. transcription data. However, there are often several genes and proteins involved in the synthesis and degradation of a single metabolite which generates a rather complicated link between the genome and metabolome. In contrast, the genome, transcriptome and proteome are directly linked to each other through transcription and translation. The many roles of metabolites also add to the difficulty of interpreting metabolite data. It is thus necessary to use statistical methods to analyse such data and the most commonly used are clustering, PCA (principal component analysis), ICA (independent component analysis), correlation analysis and network analysis [Scholz *et al.*, 2004; Steuer, 2006; Steuer *et al.*, 2007]. In **Paper II** clustering of time course metabolite data was used to obtain a global overview of the dynamic changes in metabolite concentrations and PCA was used to identify key metabolites that had the highest contribution to the variation in all samples. This analysis also revealed three distinct phases during the batch fermentation: a glucose phase, a transition phase and a xylose phase. The most drastic changes in metabolite concentrations were observed in the transition phase.

Metabolomics is still an emerging field which combines knowledge in analytical biochemistry, cellular biology (e.g. physiology, metabolism, regulation etc.), statistical analysis and mathematical modelling to describe cellular status. As the concerted effects of changes in gene expression due to changes in the environment are ultimately reflected in the metabolome, a snap-shot of metabolite concentrations under a certain condition can therefore give a description of the phenotype and the cellular state with a higher degree of functional information. In the next chapter an overview is given of the cellular processes which are required for balanced microbial growth. The focus is on the signals provided by metabolites and how these factors influence xylose fermentation.

3. Cellular Processes Required for Balanced Microbial Growth

There are five cellular processes that need to be carefully coordinated for a microbial population to maintain a balanced growth: nutrient uptake, energy conservation (ATP generation), balancing of redox cofactors, biosynthesis and commitment to the cell division cycle (Fig. 10). A non-growing phenotype of a microorganism is due to two reasons: i) the cells do not have the ability to catalyse particular reactions partaking in these processes (i.e. the restriction lies in the genome) and/or ii) the cells fail to properly regulate one or more of these processes (i.e. the restriction most likely lies in the metabolome and proteome). TMB3422 is one of the best lab strains rationally designed for xylose fermentation currently available [Runquist *et al.*, 2010a]. It assimilates xylose through the XR/XDH-pathway and is able to grow anaerobically in defined mineral medium with xylose as the sole carbon source with a $\mu_{max} \approx 0.07$ h^{-1} (Fig. 11A). This demonstrates that *S. cerevisiae* has the ability to grow anaerobically on xylose, yet only at a fraction of the rate attained with glucose as the carbon source. However, if the same strain is used to ferment a mixture of glucose and xylose, the growth rate on xylose decreases drastically to ca. 0.015 h^{-1} (Fig. 11B). Hence, the regulatory signals required for the cells to reach their highest potential are not present under these conditions. This chapter presents an overview of the prerequisites for balanced growth.

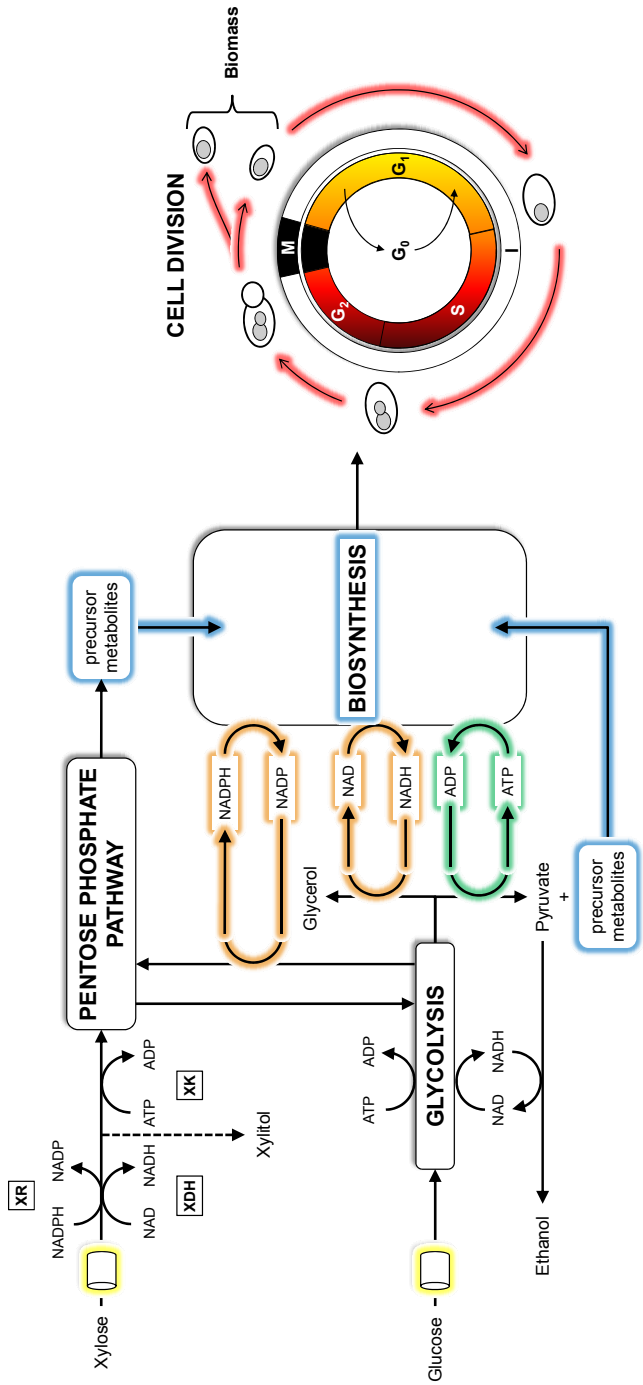

Figure 10. (See legend on next page)

(See figure on previous page.)

Figure 10. Organization of the cellular processes required for balanced growth.

There are five cellular processes needed for balanced microbial growth: nutrient uptake (yellow), transformation of energy to generate ATP (green), balancing of redox cofactors (orange), biosynthesis of macromolecules (blue) and commitment to the cell division cycle (red). The cell cycle is divided in an interphase (I) and mitosis (M). There are three distinct phases in the interphase: G_1, the cell increases in size and prepares for DNA synthesis; S, DNA is replicated; G_2, the cell increases in size and prepares for division. During mitosis the chromosomes are divided between the mother cell and the daughter cell followed by the separation of two distinct cells. G_0 is a state of quiescence and is entered by cells that have stopped dividing.

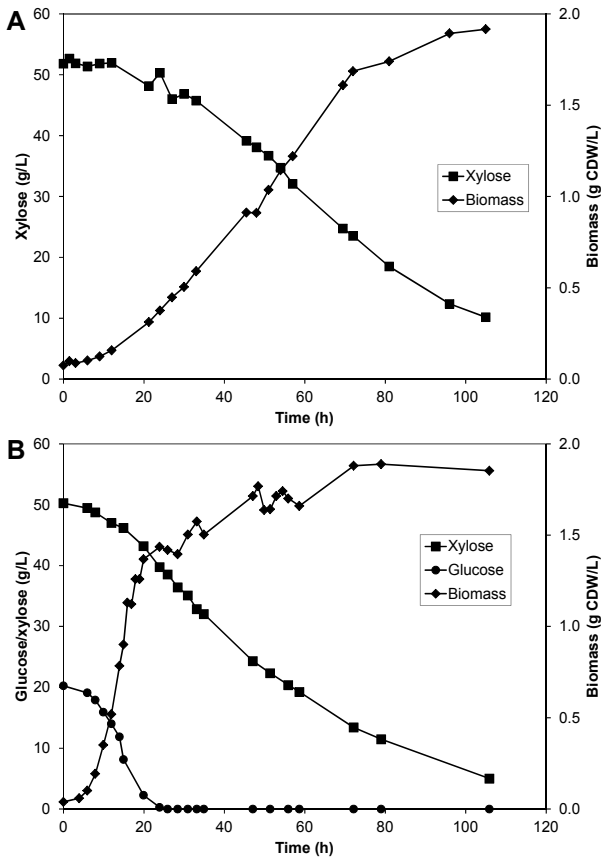

Figure 11. Growth profiles of TMB3422 in 2X YNB medium with xylose as sole carbon source (A) or a mixture of glucose and xylose (B).

The experimental data in Figure A was kindly provided by PhD student Raquel Cadete (Department of Microbiology, Federal University of Minas Gerais, Brazil).

3.1. Nutrient assimilation

The ability of the cells to take up and assimilate nutrients (carbon, nitrogen, vitamins, minerals etc.) is naturally a fundamental requisite for microbial growth. The molecular basis for the uptake of glucose and xylose as well as the pathways required to assimilate the latter have been described in Chapter 1 and will not be covered further here. Although increasing the transport capacity in a XI strain led to faster uptake rate of xylose and improved the ethanol productivity, it did not improve the anaerobic growth rate [**Paper I**]. In addition, these improvements have not been evaluated using a mixture of glucose and xylose. As shown in Figure 11, glucose has an inhibitory effect on the uptake of xylose and sets a cellular state manifested as a very slow anaerobic growth on xylose. The comparison between a XR/XDH-strain and a XI-strain presented in **Paper II** showed a 10-fold difference in xylose uptake rate (the XI-strain having the lowest uptake rate) but none of the two strains were able to grow anaerobically. These findings indicate that other factors than xylose transport are limiting anaerobic growth.

The simplest model describing microbial growth is the classical relationship proposed by Jacques Monod in which the growth rate is a hyperbolic function of the extracellular substrate concentration C_s (Equation 4).

$$\mu = \frac{\mu_{\max} C_s}{K_s + C_s} \tag{4}$$

The growth of wild-type *S. cerevisiae* strains on glucose can adequately be described using this model, but it fails to describe the growth behaviour of strains genetically modified to be unable to control expression of individual *HXT* genes through Snf3p and Rgt2p [Youk and van Oudenaarden, 2009] (cf. Fig. 6 in Chapter 1). The dependency of the growth rate on the glucose concentration varied significantly depending on which *HXT* gene was expressed, but in all cases investigated, Equation 4 was inadequate to describe the observed behaviour of the modified strains. The expression of *HXT3* and *HXT6* also indicated that the lack of proper control over the expression can even lead to growth arrest at high glucose concentrations. This behaviour was observed despite a monotonically increasing glucose uptake rate with increasing glucose concentration, showing that the perception of a nutrient (in this case the carbon source) is as important as the transport capacity in determining the cell's growth rate. By removing the two principal sensors Snf3p and Rgt2p, the growth rate of the single-*HXT* strains again increased with increasing glucose concentration, but at the cost of a much lower sensitivity. Based on these experimental results, it was proposed that the sensing of extracellular glucose has been developed by the cells to ensure that the growth rate always increases when the availability of glucose increase [Youk and

van Oudenaarden, 2009]. The role of Snf3p and Rgt2p in xylose signalling is further discussed in Chapter 4.

The uptake of sterols and unsaturated fatty acids is also a prerequisite for growth under anaerobic conditions since the synthesis of these compounds requires molecular oxygen [Rosenfeld and Beauvoit, 2003]. Media used for cultivation of *S. cerevisiae* under anaerobic conditions are thus supplemented with ergosterol and Tween 80 [Andreasen and Stier, 1953]. *SUT1* and *UPC2* are two genes encoding transcription factors that are induced under anaerobic conditions [Lai *et al.*, 2006; Runquist *et al.*, 2009b]. Together they induce the expression of *AUS1*, *DAN1* and *PDR11* which encode proteins that mediate the uptake of sterols [Ness *et al.*, 2001; Wilcox *et al.*, 2002]. However, none of these genes are differentially expressed during anaerobic xylose fermentation compared to glucose fermentation [Runquist *et al.*, 2009b] making the uptake of sterols an unlikely limitation in the growth on xylose.

3.2. Energy conservation

ATP is the most important energy carrier in the cell and is used to maintain all the necessary cellular processes and to drive the biosynthesis of macro molecules. When the cells have access to oxygen, ATP is generated by the ATP synthase complex located in the inner membrane of the mitochondria. This complex is driven by the proton motive force generated in the electron transport chain (Fig. 12A) [Dudkina *et al.*, 2010]. Under anaerobic conditions oxygen is no longer available as the final electron acceptor; hence the electron transport chain is of no use to the cell. However, the expression of the genes encoding the constituents of the electron transport chain is several folds higher during anaerobic xylose fermentation compared to glucose fermentation (Fig. 12B) [Runquist *et al.*, 2009b]. This is probably the most compelling evidence in favour of the hypothesis that xylose is not recognized as a fermentable carbon source by *S. cerevisiae*.

The generation of ATP under anaerobic conditions has to occur through substrate-level phosphorylation and thus depends on a high activity of pyruvate kinase (PYK) which catalyses the last reaction in glycolysis where PEP is converted to pyruvate (PYR) (Fig. 10, Fig. 13, Paper II: Fig. 1A). This enzyme requires both G6P and fructose 6-phophate (F6P) for induction [Boles *et al.*, 1993] and fructose 1,6-bisphosphate (FBP) for activation [Barwell *et al.*, 1971] (Fig. 13). FBP is formed from F6P and ATP in the reaction catalysed by 6-phosphofructo kinase (PFK) whose activity significantly increases in the presence of fructose 2,6-bisphosphate (F26BP) [Gad, 1981] (Fig. 13). The formation of F26BP is stimulated through activation of 6-phosphofructo-2-kinase (PFK26) by

protein kinase A (PKA) [Francois *et al.*, 1984] which is most active in the presence of glucose [Zaman *et al.*, 2008] (Fig. 13). This series of metabolic interactions could be the underlying mechanism of the stimulating effect low glucose concentration has on xylose uptake [Jeffries *et al.*, 1985; Öhgren *et al.*, 2006; Krahulec *et al.*, 2010].

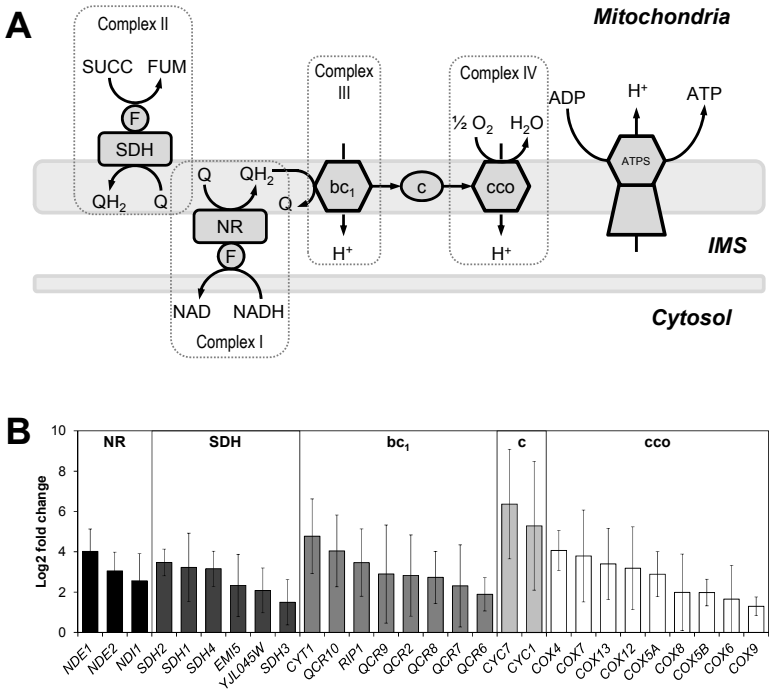

Figure 12. The electron transport chain.
A) The electrons sequestered from an energy source are transported through a series of cytochromes until they reach the final electron acceptor – oxygen. During the path through the electron transport chain a proton motive force is established by the difference in proton concentration between the two compartments which is utilized by the ATP synthase to generate ATP. **B**) The $\log_2$-fold change in expression of the structural genes constituting the electron transport chain during xylose fermentation compared to glucose fermentation. Error bars indicate the 95% confidence interval of the mean (*df* = 2) [Runquist *et al.*, 2009b].

During anaerobic fermentation of xylose the intracellular concentrations of G6P, F6P and FBP are significantly lower compared to glucose fermentation [**Paper II**]. In the XI strain investigated, which had the lowest uptake rate of xylose, the concentrations of these metabolites decreased between 33- to 88-fold. This shows the importance of having a high sugar uptake rate in order to

replenish the pools of metabolites that provide the regulatory signal for efficient production of ATP via substrate-level phosphorylation.

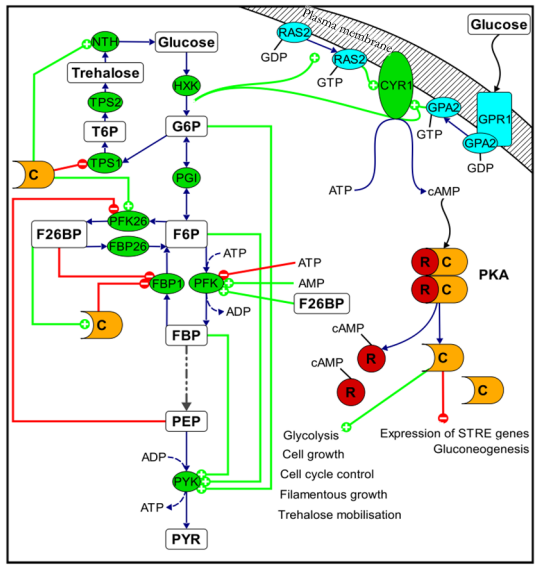

Figure 13. Activation of ATP generation through pyruvate kinase.
Glycolysis is activated through the induction of the Ras/cAMP/PKA pathway. cAMP formed by adenylate cyclase (*CYR1*) interacts with the regulatory subunits (R) of PKA which releases the catalytic subunits (C). The active PKA phosphorylates PFK26 which subsequently produces F26BP from F6P and ATP. F26BP is an essential activator of PFK which phosphorylates F6P to FBP. The production of FBP in turn activates PYK and ATP generation. Production of ATP and ethanol depends on a high catalytic activity of PYK which requires the simultaneous presence of G6P, F6P and FBP. PKA and F26BP also efficiently inactivate gluconeogenesis by inhibiting FBP1.

The most commonly used measure to assess the energetic status of cells is the adenylate energy charge (AEC) [Atkinson, 1968]. It is defined as the ratio between the total adenine nucleotide pool and the sum of the ATP pool and half the ADP pool:

$$(ATP + ½ADP)/(ATP + ADP + AMP) \qquad (5)$$

The adenine nucleotides are balanced by adenylate kinase (AK) which catalyses the reaction:

$$ATP + AMP \leftrightarrows 2\ ADP$$

Hence, the ADP pool can serve as an energy reserve to be used when ATP levels decrease. The AEC has been suggested as an important regulatory signal for controlling the energy balance by directly modulating enzyme activities

[Chapman and Atkinson, 1977; Knowles, 1977; Dombek and Ingram, 1988]. When the AEC is high, enzymes catalysing reactions using ATP are stimulated while the enzymes catalysing reactions in which ATP is produced are less active. When the value of the AEC is reduced, the opposite regulatory mechanism takes place in an effort to restore the AEC back to its optimal value. In *S. cerevisiae* actively growing on glucose the AEC has a value of 0.8 [Ball and Atkinson, 1975; Klimacek *et al.*, 2010; Wisselink *et al.*, 2010][**Paper II**]. When the cells are exposed to glucose depletion the AEC drops sharply to around 0.5 and continues to fall during prolonged glucose starvation [Ball and Atkinson, 1975; Klimacek *et al.*, 2010]. In light of the significantly reduced concentrations of G6P, F6P and FBP during xylose fermentation an alteration of the AEC would have been an expected consequence. However, measurements of the intracellular concentrations of the adenine nucleotides gave rise to a remarkable consistency in the AEC which remained at 0.8 during xylose fermentation, despite the reduced sugar uptake rate and concentrations of hexose sugar phosphates (Fig. 14) [**Paper II**]. This implies that the proposed regulatory signal provided by the AEC is the same during xylose fermentation as during glucose fermentation. Hence, these results strongly indicate that the AEC is not providing the required signal for continued growth on xylose after glucose depletion.

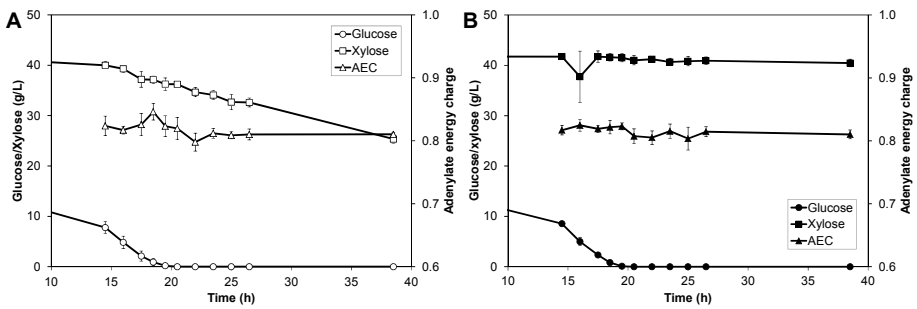

Figure 14. Dynamics of the AEC during batch fermentation of a glucose/xylose mixture.
A) TMB3057 (XR/XDH, white markers). **B**) TMB3359 (XI, black markers). Both strains were grown in anaerobic conditions using 2X YNB-medium with 20 g/L glucose and 40 g/L xylose as carbon sources.. Errors are given as 95% confidence intervals of the means calculated from duplicate experiments for each strain ($5 \leq n \leq 11$). Figure is adapted from Paper II.

3.3. Redox-balancing

As mentioned in the previous section the redox cofactors NAD and NADP serve as carriers of electrons sequestered during the catabolism of the energy source. An imbalance between the oxidised and reduced forms of these metabolites can have a detrimental effect on the cellular metabolism. Accumulation of NADH would hamper the catabolic reactions and diminished supply of NADPH would limit the rate of biosynthesis. In aerobic conditions the balancing of redox cofactors is normally not a problem due to a functional electron transport chain and unlimited access to the final electron acceptor, oxygen. In the absence of oxygen the electrons are instead delivered to different intracellular metabolites generating the common products of fermentative metabolism: ethanol, glycerol, acetate and succinate. Glycolysis is stoichiometrically balanced with regard to NAD(H) through ethanol formation and excess NADH formed during biosynthesis is oxidised to NAD in the synthesis of glycerol (Fig. 10).

The introduction of the XR/XDH pathway in *S. cerevisiae* increases the need to regenerate NAD (Fig. 10). When the demand for NAD is not fully met, xylitol is secreted as explained in Chapter 1 and the incapacity to reconstitute the NAD(H) balance under anaerobic conditions has been regarded as the main bottleneck in the fermentation of xylose [Bruinenberg *et al.*, 1983; Wahlbom and Hahn-Hägerdal, 2002]. In **Paper II** the NADH/NAD ratio was compared between a XR/XDH-strain and a XI-strain during xylose fermentation and surprisingly the ratio was not significantly different between the two strains (Fig. 15A). The most likely explanation for this result is that the cytosolic and mitochondrial pools of redox cofactors were analysed together as mixing of the two is unavoidable with the boiling ethanol extraction method. If this is the case, it indicates that the balancing of NAD(H) cofactors in yeast cannot be fully evaluated without taking into account the compartmentalization of these metabolites. So far only one method has been reported which address this issue [Canelas *et al.*, 2008b]. The method is based on the heterologous expression of a bacterial mannitol-1-phosphate 5-dehydrogenase (M1PDH) which catalyses the reaction:

$$M1P + NAD \leftrightarrows F6P + NADH + H^+$$

When this exogenous reaction is active in yeast the cytosolic free NAD/NADH ratio can be calculated from the measured F6P/M1P ratio and the equilibrium constant of the reaction. However, since protons are involved in the reaction, the cytosolic pH needs to be measured, or assumed, as well. The intracellular pH can be estimated by measurements of the fluorescence from GFP-reporter constructs [Orij *et al.*, 2009] but only in cells cultivated aerobically due to the oxygen requirement by GFP. The cytosolic free NAD/NADH ratio was determined in

glucose-limited steady-state cultures of a yeast strain expressing the exogenous M1PDH enzyme grown under aerobic conditions. The analysis revealed a 10-fold difference between the cytosolic ratio and the average cellular ratio [Canelas *et al.*, 2008b]. In light of these results the field of metabolomics is in great need of methods to quantitate compartment-specific metabolite concentrations. Such techniques should preferably not require genetic modifications and should be applicable to a wide range of cultivation conditions. Even the method described above is not universally applicable since yeast forms mannitol from M1P under anaerobic conditions [Costenoble *et al.*, 2003].

A survey of the average cellular ratios of redox cofactors determined in *S. cerevisiae* actively growing anaerobically on glucose suggest that there is a marked difference between industrial strains and laboratory strains with regard to these ratios (Table 6). The industrial strains tend to have low NADH/NAD ratios and high NADPH/NADP ratios, both in concordance with a well-functioning metabolism. The strains based on the CEN.PK2 background on the other hand show the opposite pattern, which is not beneficial for efficient catabolism and biosynthesis. The other laboratory strain, CEN.PK113, seem to have a good NAD(H) balance but is unable to match the NADPH/NADP ratio of the industrial strains.

Table 6. Reported values of the average cellular NADH/NAD and NADPH/NADP ratios in different *S. cerevisiae* strains actively growing anaerobically on glucose. Numbers are reported mean values and their relative standard deviations.

Strain	Cultivation medium and carbon source(s)	$\frac{\text{NADH}}{\text{NAD}}$	$\frac{\text{NADPH}}{\text{NADP}}$	Ref.
KD2 [a]	YEP medium Glucose: 20 g/L	0.3	–	[Dombek and Ingram, 1988]
TN1 [b]	Mineral medium Glucose: 25 g/L	0.2 ± 7%	5.3 ± 10%	[Nissen *et al.*, 2001]
ATCC 4124 [c]	YEP medium Glucose: 20 g/L	0.4 ± 6%	4.2 ± 14%	[Yang *et al.*, 2008]
CEN.PK113-7D	Mineral medium Glucose: 20 g/L	0.3 ± 38%	0.4 ± 42%	[Klimacek *et al.*, 2010]
TMB3057 [d] (XR/XDH)	Mineral medium Glucose: 20 g/L Xylose: 40 g/L	1.9 ± 26%	0.4 ± 71%	**Paper II**
TMB3359 [d] (XI)	Mineral medium Glucose: 20 g/L Xylose: 40 g/L	1.6 ± 23%	0.6 ± 55%	**Paper II**

[a] Petite mutant of industrial brewing strain CC3; [b] Haploid derivative of industrial strain CBS8066
[c] Industrial strain isolated from a molasses distillery; [d] CEN.PK2-1C strain background

To investigate whether the much higher NADH/NAD ratio in the TMB-strains was due to the heterologous xylose pathways or the presence of xylose in the cultivation medium, this ratio was determined in the auxotrophic parental strain TMB3450 (unpublished results). Strain TMB3450 was cultivated in an anaerobic, glucose-limited chemostat at D = 0.21 h^{-1} and metabolites were extracted from steady state samples using the boiling ethanol method. The cellular content of NAD and NADH was determined using a cycling assay [Bernofsk and Swan, 1973]. At steady state in glucose-limited cultures the NADH/NAD ratio was 0.92±0.26 (mean ± standard deviation of two biological experiments). In another set of experiments, 30 g/L xylose was added to the feed reservoir in addition to glucose. The NADH/NAD ratio in this condition was 0.88±0.25 which is not significantly different from the ratio determined without the presence of xylose. Both measurements are in the same range as the ratio determined by LC-MS/MS in the XI-strain (Table 6). This supports the hypothesis that it is a trait of this particular strain. The ratio measured in the XR/XDH-strain by LC-MS/MS was, however, higher than the ratio measured in the parental strain which suggests that the introduction of this pathway does indeed affect the NAD(H) balance, although to a smaller extent than expected.

The introduction of the XR/XDH pathway in *S. cerevisiae* also increases the demand for NADPH (Fig. 10). The cells meet this demand for NADPH by increasing the expression of genes encoding enzymes that catalyse NADPH-yielding reactions, such as those of the oxidative pentose phosphate pathway [Salusjärvi *et al.*, 2006; Runquist *et al.*, 2009b]. Despite this increased requirement, the XR/XDH-strain investigated in **Paper II** did not exhibit a significant reduction in the NADPH/NADP ratio during the transition from glucose fermentation to xylose fermentation (Fig. 15B). In the XI-strain on the other hand, the ratio was reduced 9-fold during the same transition. These results show once more the importance of a high sugar uptake rate, which in this case was needed to sustain a flux through the oxidative PPP where NADPH is formed. As mentioned earlier, NADPH is required to provide electrons for the biosynthetic reactions but having a stable NADPH/NADP ratio was not adequate for stimulating continued growth on xylose. Based on these results the introduction of the XR/XDH pathway does not seem to disturb the redox balance in the recombinant strain to a large extent contrary to the common conception. However, without the knowledge of compartment-specific ratios the redox balance cannot be fully evaluated.

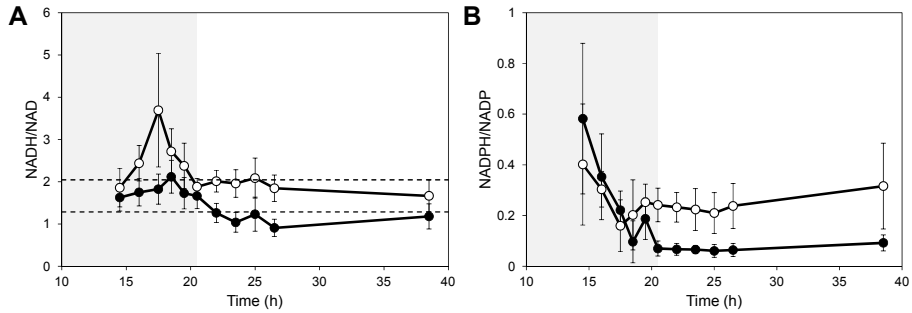

Figure 15. Dynamics in intracellular redox cofactor ratios
Dynamics in the NADH/NAD (A) and NADPH/NADP (B) ratios during anaerobic batch fermentation of 20 g/L glucose and 40 g/L xylose using strains TMB3057 (XR/XDH, white markers) and TMB3359 (XI, black markers). Dotted lines in A) represent the 95% confidence interval of the value in TMB3057 at time point 38.5 h. Errors are given as 95% confidence intervals of the means calculated from duplicate experiments for each strain ($4 \leq n \leq 10$). The shaded area indicates the period until glucose depletion.

Another redox couple is FAD/$FADH_2$ which exist both as free metabolites and as prosthetic groups, bound to certain proteins. These so called flavoproteins often play essential roles in the metabolism (e.g. in the electron transport chain shown in Fig. 12) and the prosthetic group also needs constant reconstitution. The role of the FAD/$FADH_2$ couple is described in more detail in Chapter 3.5.

3.4. Commitment to the cell division cycle

Before a yeast cell commits to start the cell division cycle two criteria need to be fulfilled: accumulation of cell mass to reach a critical size [Johnston *et al.*, 1979] and establishment of a critical rate of protein synthesis [Moore, 1988]. This occurs during the G_1 phase of the cycle in which the cell evaluates the nutritional condition of the environment (Fig. 10). The guanine nucleotides have been implicated as important regulatory factors in both these processes. Recent studies have shown that an imbalance in the guanine nucleotide pool can have detrimental effects on nitrogen metabolism, protein synthesis, viability and proliferation of yeast cells [Yalowitz and Jayaram, 2000; Rudoni *et al.*, 2001; Breton *et al.*, 2008; Saint-Marc *et al.*, 2009; Iglesias-Gato *et al.*, 2011].

The cAMP/PKA pathway plays a central role in the commitment to start the cell division cycle and entry into the M-phase (Fig. 10) [Thevelein and de Winde, 1999]. The activity of this pathway depends on the levels of GTP-bound Ras2p and Gpa2p which are the active forms that can bind to adenylate cyclase and

trigger the production of cAMP [Toda *et al.*, 1985; Rolland *et al.*, 2000]. The joint disruption of the corresponding genes generates a mutant with a very slow-growing phenotype [Xue *et al.*, 1998]. The cAMP molecules formed by adenylate cyclase interact with the regulatory subunits of PKA (Bcy1p) and promotes the release of the catalytic subunits Tpk1p, Tpk2p and Tpk3p [Toda *et al.*, 1987a; Toda *et al.*, 1987b]. These subunits activate glycolysis and utilisation of storage carbohydrates and initiate the biosynthetic machinery by increasing the expression of genes involved in ribosome and cyclin biogenesis [Thevelein, 1992] (Fig. 13). An active PKA pathway is thus required in order for the cell to reach the size threshold and start the cell cycle [Thevelein, 1992]. The level of GTP-bound Ras2p has been reported to be directly correlated with the cytosolic GTP/GDP ratio [Rudoni *et al.*, 2001]. The synthesis of proteins is also highly dependent on GTP availability, both for the initiation of translation and during the whole elongation process [Kapp and Lorsch, 2004]. The initiation factor eIF2α is a GTP-binding protein responsible for delivering the methionyl-tRNA initiator to the 40S ribosome. Upon delivery the bound GTP is hydrolysed and eIF2α-GDP dissociates from the ribosome. To start another round of initiation the GTP-bound eIF2α is restored by the action of the guanine exchange factor eIF2B. As both eIF2α and eIF2B have a higher affinity for GDP than GTP a proper balance between these two metabolites is required for a high rate of protein synthesis [Yalowitz and Jayaram, 2000; Iglesias-Gato *et al.*, 2011].

In contrast to adenylate nucleotides, the concentrations of the guanine nucleotides GMP and GDP change significantly during the transition from glucose fermentation to xylose fermentation [**Paper II**]. The GTP/GDP ratio was reduced 3-fold in the XI-strain (Fig. 16A) which correlates very well with the response observed during carbon starvation [Rudoni *et al.*, 2001]. The low GTP/GDP ratio in this strain on xylose could result in reduced stimulation of cAMP formation and a low rate of protein synthesis leading to an arrest in the G_0 phase of the cell cycle (Fig. 10). This is consistent with the hypothesis that xylose is not sensed as a fermentable carbon source and does not activate the biosynthetic machinery efficiently in the cells. However, the GTP/GDP ratio did not change significantly in the XR/XDH-strain during the transition to xylose fermentation (Fig. 16A). These results suggest that the GTP/GDP ratio rather responds to the rate of carbon supply than to what type of carbon source is actually taken up [**Paper II**]. The receptor complex Gpr1p-Gpa2p is unable to sense extracellular xylose [Rolland *et al.*, 2000] and thus the activation of adenylate cyclase on this carbon source has to occur through GTP-bound Ras2p.

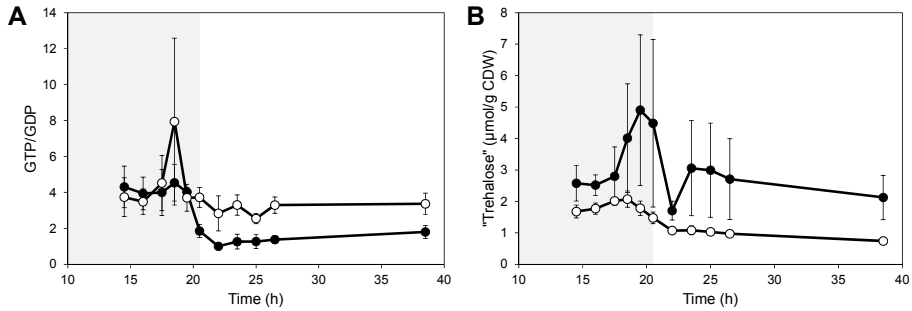

Figure 16. Dynamics in the GTP/GDP ratio and a compound putatively identified as trehalose.
Dynamics in **A**) the GTP/GDP ratio and **B**) the concentration of a compound with the same molecular weight as trehalose during anaerobic batch fermentation of 20 g/L glucose and 40 g/L xylose using strains TMB3057 (XR/XDH, white markers) and TMB3359 (XI, black markers). Errors are given as 95% confidence intervals of the means calculated from duplicate experiments for each strain ($5 \leq n \leq 11$). The shaded area indicates the period until glucose depletion.

The binding of GTP to Ras2p is highly stimulated by intracellular acidification, possibly due to a low activity of Ras-GTPase enzymes under such conditions [Rolland *et al.*, 2000]. The protons responsible for such acidification are mainly formed during the incorporation of ammonium during biosynthesis and the generation of reduced redox cofactors (i.e. when metabolism is active). One of the hallmarks of an active cAMP/PKA pathway is the utilization of trehalose and glycogen [Uno *et al.*, 1983; Lin *et al.*, 1995]. The targeted metabolite analysis in **Paper II** detected a compound with a monoisotopic mass of 342.1162 g/mol which corresponds to that of trehalose. The level of this compound dropped nearly 2-fold in the XR/XDH-strain during the transition from glucose to xylose whereas it did not change markedly in the XI-strain (Fig. 16B). The data from the latter strain is, however, very uncertain making it difficult to draw any conclusions. Still, if this compound is trehalose it would indicate that trehalase activity is induced in the XR/XDH-strain, either through the Ras/cAMP/PKA pathway or the fermentable growth medium-induced pathway [Crauwels *et al.*, 1997]. In future studies on the regulation of xylose metabolism the utilization of storage carbohydrates should be measured more accurately to obtain further information regarding this process. However, before initiating such investigations one should be aware of the presence of a mutation in the gene encoding adenylate cyclase in the CEN.PK2 strain background which renders it insensitive to stimulation by both Gpa2p and Ras2p [Vanhalewyn *et al.*, 1999]. Consequently the activity of PKA is lower in this strain compared to other strains under normal growth conditions [Rützler *et al.*, 2004]. During a screening for suppressors of the slow growing phenotype of *ras2Δ gpa2Δ* mutants, the gene *SUT2* was identified as a modulator of PKA-activity [Rützler *et al.*,

2004]. In a CEN.PK2 *ras2Δ gpa2Δ* mutant a high *SUT2* gene dosage led to increased PKA activity while the opposite effect was observed in a strain background with inherently high PKA activity. Hence, the presence of *SUT2* can both activate and inhibit the action of PKA depending on the basal activity. Transcription data from TMB3415, a xylose-fermenting strain based on the CEN.PK2 background, indicate a 3.5-fold lower expression of *SUT2* (P = 0.01) during anaerobic xylose fermentation compared to aerobic conditions [Runquist *et al.*, 2009b]. In contrast, the expression remained constant during growth on glucose after a switch from aerobic to anaerobic conditions suggesting that the expression of *SUT2* is inhibited during anaerobic xylose fermentation. Sut2p is a homologue of the transcription factor Sut1p which controls the uptake and synthesis of sterols (see Chapter 3.1) [Ness *et al.*, 2001]. Hence, there seems to be a link between two essential processes for anaerobic growth: supply of sterols and high PKA activity. It might therefore be worth investigating the role of Sut2p in xylose fermentation further.

3.5. Biosynthesis and protein folding

Of all the processes required for growth, biosynthesis can be regarded as the central process where it all comes together: the assimilated carbon, the energy conserved in ATP and the electrons stored in NADPH are utilized to form the macromolecules needed for the cells to reach the size threshold and commit to the cell division cycle.

3.5.1. Precursor metabolites and amino acids

There are twelve essential precursor metabolites that are required for biosynthesis of macromolecular building blocks (Table 7) [Stephanopoulos *et al.*, 1998]. All of them are produced in glycolysis, the PPP and the TCA-cycle which is why this is called central carbon metabolism (see Paper II: Fig. 1A). The analysis of intracellular metabolites related to biosynthesis revealed a cellular response similar to carbon starvation during xylose fermentation [**Paper II**]. This response was manifested through the following observations:

1. The concentrations of nearly all the measured precursor metabolites decrease during xylose fermentation, especially in the XI-strain (Table 7).
2. PEP seemed to accumulate in the XI-strain during xylose fermentation (Table 7). Increased concentration of PEP is a generic response to carbon starvation in bacteria [Evans *et al.*, 1981] and has also been observed in

carbon limited or starved yeast cells [Brauer *et al.*, 2006; Kresnowati *et al.*, 2006; Walther *et al.*, 2010].

3. Significant accumulation of the aromatic amino acids phenylalanine (PHE-L), tyrosine (TYR-L) and tryptophan (TRP-L) during xylose fermentation. This particular response has previously not been associated with carbon starvation but the results correlate well with other studies carried out under such conditions (Fig. 17).

In addition the XI-strain displayed two other traits of carbon starvation, which have already been mentioned in the previous sections: depletion of NADPH and a reduced GTP/GDP ratio. Despite the signs of carbon starvation, both strains maintained a high and stable energy charge during the transition to xylose, indicating that neither strain is energy limited. Xylose fermentation thus seems to present a unique condition for *S. cerevisiae* where the energy metabolism is uncoupled from carbon metabolism.

Table 7. The twelve essential precursor metabolites and the fold change between glucose and xylose fermentation. Data is taken from Paper II.

Precursor metabolite	Building block	TMB3057 (XR/XDH)	TMB3359 (XI)
G6P	Glycogen	-8	-40
F6P	Chitin	-3	-33
GAP	Phospholipids	–	–
3PG	Amino acids serine, cysteine and glycine	-4 [a]	-4 [a]
PEP	Amino acids tyrosine, tryptophan and phenylalanine	-1.7	+1.2
E4P	Amino acids tyrosine, tryptophan and phenylalanine	–	–
R5P	Nucleotides (for DNA and RNA) and amino acid histidine	-1.6	-9
PYR	Amino acids alanine, valine and leucine	–	–
Acetyl-CoA	Fatty acids	No change	-3.2
OAA	Amino acids aspartate, asparagine, methionine, threonine and isoleucine	–	–
AKG	Amino acids arginine, glutamate, glutamine, lysine and proline	No change	No change
Succinyl-CoA	Heme	–	–

[a] Measured as the total sum of 3PG and 2PG

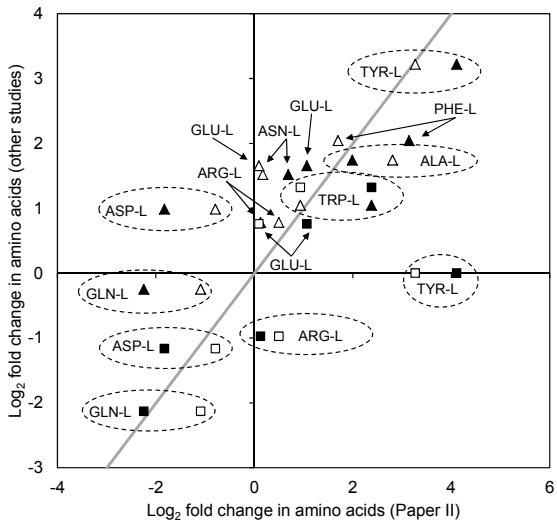

Figure 17. Correlation analysis of amino acid concentrations between studies.
Comparison of $\log_2$-fold change in the concentrations of amino acids between **Paper II** and [Klimacek *et al.*, 2010] (squares) and [Brauer *et al.*, 2006] (triangles). White markers: TMB3057 (XR/XDH), black markers: TMB3359 (XI). The grey line represents a perfect correlation.

3.5.2. Maturation of secretory proteins

Proteins are, like metabolites, located in different cellular compartments. Most proteins therefore contain a built-in signal which directs it to the correct location. Approximately one third of the yeast proteome is directed to the secretory pathway [Barlowe and Miller, 2013]. Here the proteins destined to be inserted into membranes and secreted to the extracellular environment a matured through a series of biochemical modifications (Fig. 19). This pathway constitutes an essential cellular process that ensures a constant provision of lipids and proteins required for expansion of the cell wall and membranes. Hence, cellular growth is directly dependent on the function of this pathway. A short overview of the pathway is given below in order to provide context and background. For more detailed information the reader is referred to [Barlowe and Miller, 2013] and references cited therein.

For most secretory proteins the first step in the maturation process is translocation into the endoplasmic reticulum (ER). This can occur both co-translationally and post-translationally. Nascent polypeptides that contain a hydrophobic signal sequence or transmembrane sequence are recognised by the signal-recognition particle (SRP) during translation. The SRP directs the ribosome complex to a SRP receptor on the ER membrane in a GTP-dependent mechanism, and the polypeptide enters the compartment via the Sec61 complex

(Route A in Fig. 18) [Ogg *et al.*, 1998; Wild *et al.*, 2004]. Peptides that are fully synthesized in the cytosol become coated with chaperone proteins that recognise the hydrophobic signal sequence [Rapoport, 2007]. The chaperones maintain the polypeptide in an unfolded conformation, a process which requires the expenditure of ATP, until delivered to the Sec63 complex on the ER membrane and transferred via the Sec61 complex (Route B in Fig. 18). Hence, the sec61 complex is in common with both co-translational and post-translational translocation routes and current knowledge classifies this complex as an aqueous channel for polypeptides. The third route is independent of the Sec61 and Sec63 complexes and instead uses the Get1p/Get2p complex for translocation (Route C in Fig. 18) [Shao and Hegde, 2011]. This route is specific for short integral membrane proteins and C-terminal tail-anchored proteins whose transmembrane segments are only included by the ribosome after translation is complete. The current understanding of this mechanism suggests that a Sgt2p-Get4p-Get5p subcomplex directs the polypeptide to Get3p which delivers it to the Get1p/Get2p complex. When Get3p associates with the complex the hydrophobic segment of the peptide is inserted into the membrane at the expense of ATP.

Once inside the ER lumen the maturation process begins. For secretory proteins which contain a N-terminal signal sequence the first step is removal of this domain by the signal peptidase complex (SPC) [Antonin *et al.*, 2000]. This occurs during translocation via the Sec61 complex by proteolytic cleavage at a specific target site. The removal of this sequence is regarded essential for the maturation of this type of proteins. The addition of oligosaccharides to glycoproteins also occurs during translocation via the Sec61 complex. The consensus sites Asn-X-Ser/Thr are recognised by the oligosaccharyltransferase (OST) enzyme which catalyses the glycosylation process [Kelleher and Gilmore, 2006]. The role of N-linked glycosylation inside the ER is not fully understood but is believed to assist in protein folding and management of misfolded glycoproteins [Schwarz and Aebi, 2011]. Nearly all secretory proteins contain disulphide bonds which are formed inside the ER. This process is catalysed by Ero1p and Pdi1p which form the major pathway for shuttling of electrons from substrate proteins [Sevier *et al.*, 2007]. This pathway is covered in more detail below. The folding process operates in an iterative cycle where the coordinated actions of glucosidase I, glucosidase II, UDP-glucose:glycoprotein glucosyl-transferase (UGGT) and calnexin trim terminal glucose residues and monitor peptide status [Helenius and Aebi, 2004]. The process is facilitated by molecular chaperones of which Kar2p is the most important [Steel *et al.*, 2004]. This chaperone protein binds to hydrophobic parts of the polypeptide (at the expense of ATP) which become inaccessible for the enzymes in the folding cycle. Kar2p remains bound until nucleotide exchange factors release ADP from the chaperone. Kar2p also plays an important role in the ER-associated degradation

(ERAD) of misfolded proteins [Nishikawa *et al.*, 2001]. The ERAD fulfils a key role in maintaining ER homeostasis and cellular function by diverting non-functional proteins from their intended destinations [Vembar and Brodsky, 2008].

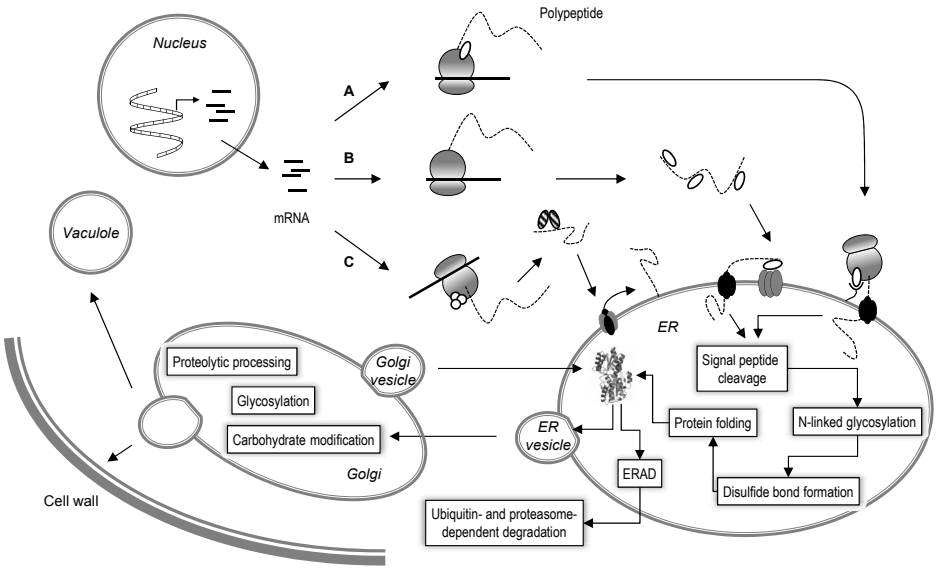

Figure 18. The protein secretory pathway.
The ER is the central organelle of the secretory pathway. It regulates protein translation, protein translocation across the membrane, protein folding and post-translational modification, protein quality control and directs the transport of both lipids and proteins to other organelles via vesicles that bud off the ER membrane. The translocation of nascent peptides into the ER occurs through three routes: co-translational insertion (A), post-translational insertion (B) or GET-mediated insertion (C).

Many of the maturation processes taking place in the ER are regulated by a mechanism referred to as the unfolded protein response (UPR) [Bernales *et al.*, 2006]. The ER contains a transmembrane protein encoded by *IRE1* which has a cytosolic ribonuclease domain and a luminal sensor domain. This sensor detects rising levels of unfolded proteins inside the ER and activates the cytosolic domain. This activity removes an intron from *HAC1* pre-mRNA and the fragments formed are ligated by Trl1p ligase to form mature *HAC1* mRNA. Hac1p is a potent transcriptional activator of UPR target genes which include *PDI1* and *ERO1* (disulphide formation), *KAR2* (folding) and dozens of genes related to translocation, glycosylation and degradation (ERAD) [Travers *et al.*, 2000]. The UPR thus balances the biosynthetic rate of secretory proteins and fine tunes the ER capacity to meet cellular demands.

The transcript levels of *IRE1* and *HAC1* in recombinant XR/XDH-strain TMB3415 are ~65% and ~50% higher (P = 0.02 and P = 0.05, respectively) in cells growing anaerobically on xylose compared to cells growing aerobically [Runquist *et al.*, 2009b]. However, the transcript level of *TRL1*, encoding the ligase, is 50% lower (P = 0.02), suggesting that *HAC1* is present as pre-mRNA rather than the mature form. In fact, very few of the known UPR target genes [Travers *et al.*, 2000] are up-regulated on xylose when the conditions change from aerobic to anaerobic (Fig. 19).

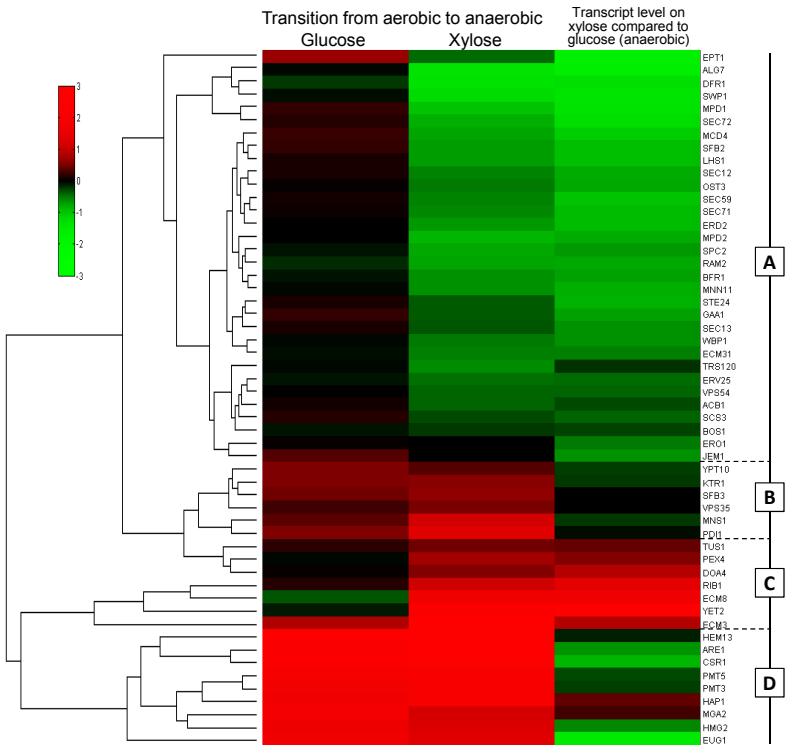

Figure 19. Transcriptional response of genes induced by the UPR.
The heat map was generated using transcriptional data from [Runquist *et al.*, 2009b] and shows the $\log_2$-fold change between exponential growth under aerobic and anaerobic conditions with either glucose or xylose as carbon source. The difference in transcript level between cultures growing anaerobically on xylose and glucose and is also shown.

The cluster analysis illustrated in Figure 19 actually show the opposite pattern: 61% of the genes included in the analysis were down-regulated during the transition from aerobic to anaerobic conditions while no change was observed during the same transition on glucose (Group A). The genes belonging to this group represent functions taking place in all steps of the maturation process:

translocation, glycosylation, disulphide bond formation, protein folding, vesicle budding and vesicle transport to the cell membrane. The smallest group contains those genes which are regulated equally on glucose and xylose, with only small differences in abundance between the two carbon sources (Group B). A small number of genes were up-regulated on xylose while remaining largely unchanged on glucose (Group C). These genes are related to peroxisome biogenesis (*PEX4*), ubiquitin recycling (*DOA4*) and the cell integrity signalling pathway (*TUS1*). The three genes *ECM3*, *ECM8* and *YET2* encode proteins with largely unknown functions. *RIB1* encodes GTP-cyclohydrolase II which catalyses the first step of the riboflavin (FAD and FMN) biosynthesis pathway. Up-regulation of *RIB1* could be related to the up-regulation of the genes encoding components of the flavin-requiring complexes in the electron transport chain (see Fig. 12 in Chapter 3.2). The fourth group contains genes which are strongly up-regulated in response to anaerobiosis in both conditions (Group D). However, in contrast to the genes in Group B, the transcript levels of these genes are in general much lower on xylose compared to glucose. This analysis shows that the UPR responds differently to xylose than to glucose and the repression of a majority of the target genes suggest there is a limited capacity of the secretory pathway during xylose fermentation. If this response is due to the reduced growth rate or the cause of it remains to be investigated.

The analysis of metabolite concentrations in the XR/XDH-strain revealed an accumulation of intracellular malate and fumarate during xylose fermentation [**Paper II**]. These metabolites are involved in the balancing of NAD(H) inside the mitochondria (see Paper II: Fig. 1A). Under anaerobic conditions the TCA-cycle operates as a branched pathway with an oxidative path and a reductive path [Camarasa *et al.*, 2003]. The oxidative path serves to produce α-ketoglutarate and glutamate from oxaloacetate for amino acid synthesis. ATP can also be produced in this pathway if α-ketoglutarate is converted to succinate; however, the ATP formed through these reactions is relatively little on glucose [Camarasa *et al.*, 2003]. The reductive path is used to regenerate NAD from NADH formed in the oxidative path and begins with the conversion of oxaloacetate to L-malate by NAD-dependent malate dehydrogenase (MDH). L-malate is then equilibrated with fumarate by fumarate hydratase (FUMase). In the final step fumarate is converted to succinate by $FADH_2$-dependent fumarate reductase [Rossi *et al.*, 1964]. *S. cerevisiae* possesses two genes, *FRD1* and *OSM1*, encoding the cytosolic and mitochondrial fumarate reductase enzymes, respectively (see Paper II: Fig 1A) [Enomoto *et al.*, 1996; Muratsubaki and Enomoto, 1998]. Deletion of any single gene does not affect anaerobic growth, but a double deletion mutant cannot grow under such conditions unless an external electron acceptor (e.g. oxygen, menadione or phenazine methosulphate) is supplied [Arikawa *et al.*, 1998; Enomoto *et al.*, 2002; Camarasa *et al.*, 2007]. It has thus been proposed that, the fumarate reductase provides the only way for yeast to regenerate the FAD/FMN

prosthetic group of flavin enzymes under anaerobiosis. The ability of *S. cerevisiae* to grow under strict anaerobic conditions has been attributed to the soluble nature of the fumarate reductase enzymes, which in most other species are membrane bound [Camarasa *et al.*, 2007]. Due to the soluble nature of the fumarate reductase enzymes also membrane bound flavoproteins can be included in this regeneration process. In particular, two essential flavin-containing oxidases which otherwise use oxygen as a final electron acceptor for FAD regeneration have been suggested to be dependent on the action of fumarate reductase: Ero1p and Erv1p. Erv1p is located in the mitochondrial intermembrane space and is required for the maturation of Fe/S proteins in the mitochondria and for retaining proteins imported into this compartment [Herrmann *et al.*, 2007]. Ero1p is a thiol oxidase [Frand and Kaiser, 1998; Pollard *et al.*, 1998] which operates together with Pdi1p [Freedman, 1989] in the ER. Both proteins are essential for the formation of disulphide bonds and together they form a classical proteinaceous electron relay system in which electrons are passed from the substrate polypeptide, via Pdi1p and membrane-bound Ero1p, to eventually react with oxygen (see Paper III: Fig 1B) [Frand and Kaiser, 1999; Tu *et al.*, 2000; Tu and Weissman, 2002]. Previous experiments have shown that the activity of fumarate reductase decreases when *S. cerevisiae* enters stationary phase [Camarasa *et al.*, 2007]. Such a decrease would explain the observed accumulation of fumarate during xylose fermentation [**Paper II**]. With regard to the essential function of fumarate reductase under anaerobic conditions a possible explanation for the slow anaerobic growth on xylose could be inadequate regeneration of FAD prosthetic groups. This hypothesis was evaluated by over-expressing either *FRD1* or *OSM1*, alone or in combination with *ERO1*, in a XR/XDH-strain [**Paper III**]. However, the over-expression of *FRD1*, alone or in combination with *ERO1*, did not have any significant effect on xylose fermentation, neither in minimal medium nor in rich medium. The over-expression of *OSM1*, on the other hand, led to a diversion of carbon from glycerol to acetate and a decrease in growth rate by 25%-50% during xylose fermentation. This phenotype could be the outcome of an interaction between Osm1p and FAD-dependent glycerol 3-phosphate dehydrogenase in the mitochondria [**Paper III**].

These results suggest that fumarate reductase is not limiting in the recombinant strains used for the evaluations. This conclusion is supported by the fact that Osm1p can substitute for the function of Frd1p [Camarasa *et al.*, 2007]. Hence, reduced expression of *FRD1* should not have a drastic effect on cellular function since the expression of *OSM1* does not change significantly between glucose fermentation and xylose fermentation [Runquist *et al.*, 2009b]. Furthermore, the yield of succinate during xylose fermentation is actually 4.5-fold higher than the yield obtained during glucose fermentation (Fig. 20). Consequently, succinate production is not directly coupled with cell growth under such conditions. This suggests that xylose conversely stimulates hyper-

oxidation of protein substrates or other reactions forming succinate or providing $FADH_2$ for the fumarate reductase. As mentioned in Chapter 2, proteome analysis of a mutant strain with improved xylose-fermenting capability identified Pdi1p as significantly more abundant in the improved strain compared with the wild-type [Karhumaa *et al.*, 2009]. This strongly indicates that there indeed is a need for a higher capacity in the protein folding mechanism for efficient xylose fermentation. Whether this capacity is for regulation of disulphide bond formation [Kim *et al.*, 2012], reduction of non-native disulphide bonds [Laboissiere *et al.*, 1995] or targeting unfolded glycoproteins for degradation [Gauss *et al.*, 2011] remains to be investigated.

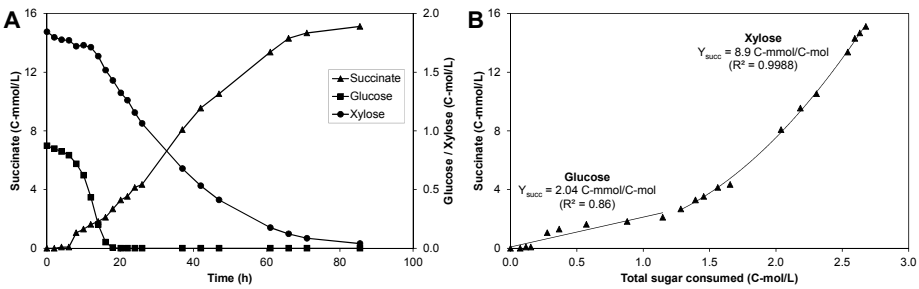

Figure 20. Succinate formation during fermentation of a glucose/xylose mixture.
The volumetric rate of succinate production by XR/XDH-strain TMB3492 [Paper II] is ~65% higher during xylose fermentation than during glucose fermentation (**A**) and the yield increases by 4.5-fold on xylose compared to glucose (**B**). The yield coefficient on xylose is given as an average since it is not constant but follows a 2nd degree polynomial (**B**).

In light of the results presented in **Paper III**, the accumulation of malate and fumarate is most likely a consequence of the poor repressive capability of xylose [**Paper II**]. This trait leads to an increased expression of *MDH2* which encodes the cytosolic malate dehydrogenase. This gives the cells an enhanced NADH-oxidizing capability and could therefore aid in the balancing of redox cofactors. However, this reaction would direct carbon away from oxaloacetate, one of the precursor metabolites needed for amino acid synthesis (see Paper II: Fig. 1A). This includes methionine (Table 7) which is required for the initiation of translation of all mRNA molecules. Another consequence could be a reduced flux through both the oxidative and reductive branches of the TCA-cycle thus affecting the synthesis of more amino acids. From this reasoning it is clear that the poor repressive capability of xylose has to be addressed. This is the topic of Chapter 4.

3.6. Uncharted potential indicators of metabolic status

3.6.1. The flavin adenine nucleotides

The current model of the role of fumarate reductase implies that the Osm1p protein is able to translocate from the mitochondria to the ER and interact with $FADH_2$ covalently bound to Ero1p. Such translocation has not yet been reported and seems an unlikely event given that Osm1p already is assigned to a specific compartment. A simpler description of the function of the fumarate reductases is that they act on free $FADH_2$ in the cytosol and the mitochondria, respectively. One study demonstrated that the activity of Ero1p is very sensitive to the level of free FAD possibly due to additional weak-affinity binding sites [Tu and Weissman, 2002]. This interaction was interpreted as a regulatory coupling between the metabolic and nutritional status of the cell and the processing of secretory proteins. In conditions when cells are no longer able to actively produce biomass, the cellular level of free FAD would decrease which in turn reduces the activity of Ero1p. Hence, fumarate reductase would be responsible for conveying the correct signal to Ero1p by balancing the ratio of free FAD:$FADH_2$. However, a more recent study could not corroborate the activation of Ero1p by free FAD [Gross *et al.*, 2006]. The discrepancy was attributed to the use of a thermo sensitive Ero1p variant in the former study. This variant has a mutation close to the FAD-binding site that could affect the coupling of catalytic activity with co-factor binding. Nevertheless, *S. cerevisiae* possesses one gene encoding a mitochondrial FAD transporter (*FLX1*) and three genes encoding putative transporters associated with the ER (*FLC1-3*) suggesting that FAD-exchange between compartments is possible [Tzagoloff *et al.*, 1996; Protchenko *et al.*, 2006]. Furthermore, Ero1p has been shown to use free FAD as electron acceptor *in vitro* under anaerobic conditions [Gross *et al.*, 2006], which is in line with the essential nature of the fumarate reductases under such conditions. The much higher yield of succinate on xylose suggest that the fumarate reductases are actively trying to maintain a high level of free FAD and some process is providing substrate for this reaction. It is possible that glutathione plays a major role in this behaviour as it was seen to accumulate significantly during xylose fermentation [**Paper II**]. Little is known about the interactions between these components and further experiments are needed to elucidate the precise mechanism of this process. Although it has not been directly quantified, these results highlight the FAD/$FADH_2$ ratio as a potential indicator of metabolic status, especially under anaerobic conditions.

3.6.2. The guanine nucleotides

In Chapter 3.4 it was suggested that the GTP/GDP ratio could be an indicator of sugar uptake rate due to the different responses in two recombinant strains with significantly different xylose uptake rates. In contrast, the concentration of GMP increased in both these strains [**Paper II**]. This response was also observed in an independent study of anaerobic xylose fermentation [Klimacek *et al.*, 2010]. The concentration of this metabolite was between 5- and 32-fold higher during xylose fermentation compared to glucose fermentation, the highest increase being measured in the XI-strain analysed in **Paper II**. Concomitantly, a 10-fold decrease in the GTP/GMP ratio was reported in both studies (Fig. 21A). Hence, this relationship might serve as a quite sensitive indicator of the metabolic status. However, so far there have been no studies on how and to what extent the GTP/GMP ratio affects or controls metabolic processes. The observed accumulation of GMP is most likely due to endogenous production by a mechanism that remains to be identified.

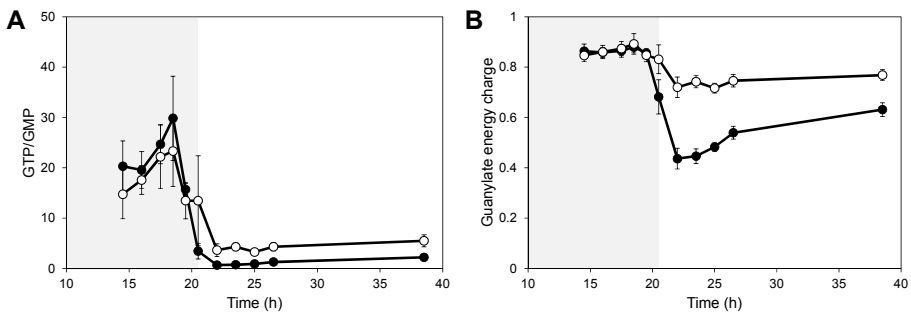

Figure 21. Dynamics in the GTP/GMP ratio and the GEC.
Dynamics in **A**) the GTP/GMP ratio and **B**) the GEC during anaerobic batch fermentation of 20 g/L glucose and 40 g/L xylose using strains TMB3057 (XR/XDH, white markers) and TMB3359 (XI, black markers). The GEC was calculated according to (GTP + ½GDP)/(GTP + GDP+ GMP). Errors are given as 95% confidence intervals of the means calculated from duplicate experiments for each strain ($5 \leq n \leq 11$). The shaded area indicates the period until glucose depletion.

Another relationship that could serve as an indicator of metabolic status is the guanylate energy charge (GEC). It is calculated analogous to the AEC and showed a fast and distinct response to the transition from glucose fermentation to xylose fermentation (Fig. 21B) [**Paper II**]. However, yeast lacks an enzyme equivalent to adenylate kinase that can catalyse the conversion of two molecules of GDP to GTP and GMP. Thus, the GEC is not related to any biological process. Even so, the pools of the adenine and guanine nucleotides are directly

interconnected as GTP is used as a phosphate donor in the *de novo* synthesis of AMP and vice versa (Fig. 22) [Henderson and Paterson, 1973].

Even though the role of the guanine nucleotides in yeast metabolism has been less explored than that of the adenine nucleotides, it is clear that the biochemical processes in which these nucleotides participate are required for both growth and survival [Varma *et al.*, 1985; Rudoni *et al.*, 2001; Saint-Marc *et al.*, 2009]. Further systematic investigations of the response in the guanine nucleotide pools under different conditions are still needed to understand the role they play in the physiology of yeast. Such knowledge could very well be the key information needed to design more efficient xylose fermenting strains.

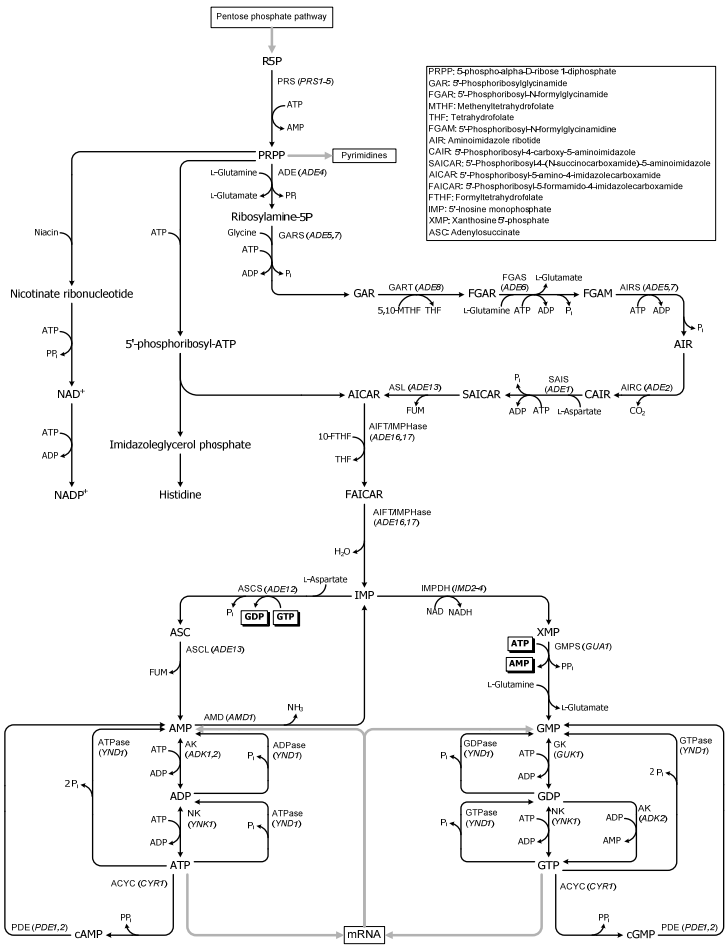

Figure 22. *De novo* synthesis pathway of purine nucleotides in *S. cerevisiae*.
The interconnection between the synthesis of AMP and GMP is indicated by the metabolites in shadowed boxes. Source: SGD (www.yeastgenome.org)

4. Hexokinase 2 - A Global Glycolytic Regulator

4.1. Glucose signalling circuits

When yeast cells growing on a non-fermentable carbon source are subjected to glucose, a fast and comprehensive modulation of the transcriptional organization occurs [Wang *et al.*, 2004; Zaman *et al.*, 2009]. Within minutes the cell enhances the capacity of its metabolism by inducing expression of genes encoding enzymes in glycolysis, sugar transporters and those needed for ribosome biogenesis. At the same time, transcription of genes related to respiration, gluconeogenesis and stress responses become repressed [Wang *et al.*, 2004; Slattery *et al.*, 2008; Zaman *et al.*, 2009]. This response is commonly termed glucose repression. More than 90% of these changes are mediated through the Ras/cAMP/PKA pathway [Wang *et al.*, 2004; Zaman *et al.*, 2009]. Apart from PKA, three additional pathways are required for complete signal transduction: Rgt2p/Snf3p-Rgt1p, Snf1p and the Hap2p/3p/4p/5p complex (Fig. 23) [Zaman *et al.*, 2009]. Each pathway controls the expression of a distinct group of target genes through mechanisms that are briefly explained below. For more detailed information the reader is referred to recent reviews on the topic [Schuller, 2003; Gancedo, 2008; Zaman *et al.*, 2008; Busti *et al.*, 2010].

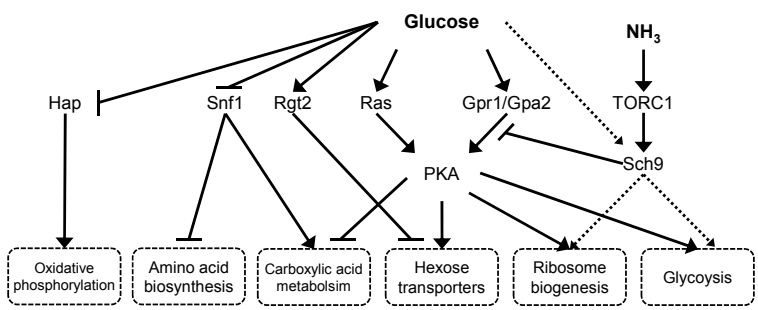

Figure 23. The interconnections between glucose signalling pathways.
Glucose repression operates through four main pathways: PKA, Rgt2p/Snf3p, Snf1p and the Hap2p/3p/4p/5p complex. The Sch9p pathway provides a minor, parallel circuit should activation of PKA fail (indicated by dotted lines).

4.1.1. The Snf1p pathway

The Snf1p pathway controls the expression of genes required for growth on less preferred fermentable carbon sources (e.g. galactose, sucrose and maltose) and non-fermentable carbon sources like glycerol and ethanol [Schuller, 2003]. Snf1p is activated upon glucose depletion through phosphorylation by three kinases: Sak1p, Elm1p and Tos3p (Fig. 23A). The activated Snf1p remains in the cytosol until it forms a complex with the two subunits Snf4p and Gal83p. The Gal83p subunit directs the complex to the nucleus where it phosphorylates Mig1p. Mig1p is the transcription factor responsible for the repression of genes needed for utilization of alternative fermentable carbon sources. When Mig1p is phosphorylated by Snf1p it loses the ability to form the repressing complex with Cyc8p and Tup1p and leaves the nucleus. Inactivation of Mig1p releases the repression on Cat8p, a transcription factor which, together with Sip4p, induces the expression of genes related to respiratory metabolism, gluconeogenesis and the glycoxylate cycle. One of the genes controlled by Cat8p is *ADH2* which enables growth on ethanol. Transcription of this gene is also controlled by Adr1p which additionally induces the expression of genes involved in fatty acid oxidation. Cat8p, Sip4p and Adr1p are all activated by Snf1p. Addition of glucose effectively inactivates Snf1p by inhibiting the phosphorylation catalysed by Sak1p, Elm1p and Tos3p and by stimulating the activity of the Glc7p/Reg1p phosphatase in the cytosol [Jiang and Carlson, 1996; Sanz *et al.*, 2000] (Fig. 24A). The number of genes transcriptionally controlled by Snf1p independently of the PKA pathway is rather small, only 39 have been identified so far (Fig 24B) [Zaman *et al.*, 2009]. The genes induced by Snf1p are mainly those regulated by Cat8p (including *MDH2* which was discussed in Chapter 3.5) while the set of genes repressed by Snf1p are primarily related to amino acid biosynthesis. The genes induced by Snf1p in concert with PKA are in general related to fatty acid metabolism but also include *ACS1* (Acetyl-CoA synthetase), *RKI1* (Ribose-5-phosphate isomerase of the PPP) and *HXT5* (hexose transporter). None of these reported sets of genes contain *ADH2*, perhaps due to the absence of ethanol which is also needed

(See figure on the next page).

Figure 24. Regulatory circuits in the main glucose signalling pathways and the response of target genes in recombinant XR/XDH-strain TMB3415

A) The mechanism of transcriptional control by the Snf1p and Rgt2p/Snf3p-Rgt1p pathways and their target gene-groups. The influence of the PKA pathway and its main targets are also shown. See text for details. **B**) Specific genes that change at least two-fold by Snf1p-inactivation or Rgt2p-activation [Zaman *et al.*, 2009]. The heat maps were generated using transcriptional data from [Runquist *et al.*, 2009b] and shows the $\log_2$-fold change due to transition from glucose to xylose or from aerobic to anaerobic conditions. 75% of all the comparisons are statistically significant at $P \leq 0.1$ or $P \geq 0.90$ indicating that the general pattern is likely due to biological factors and not caused by random errors. The groups of genes are indicated in the figure according to [Zaman *et al.*, 2009].

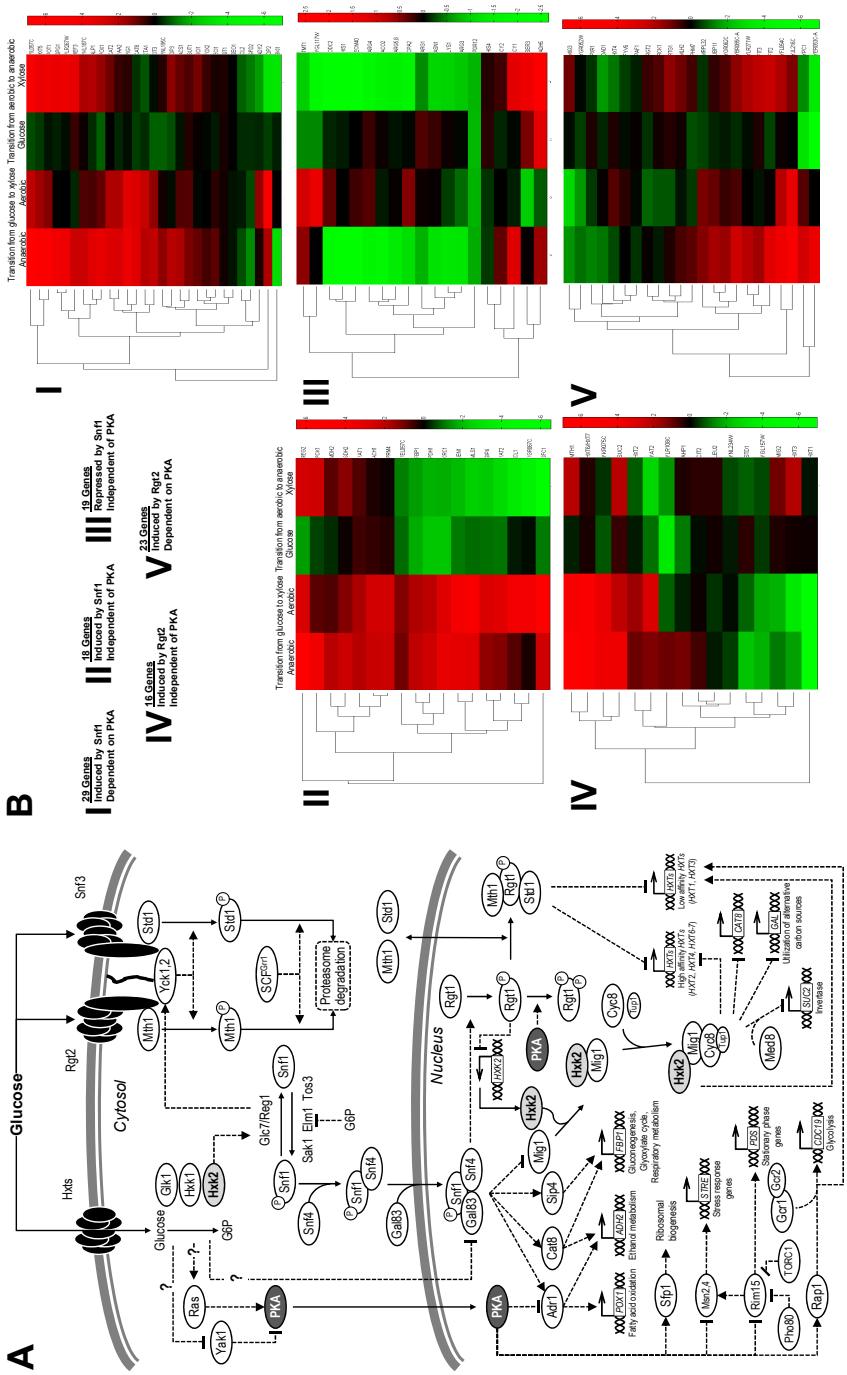

Figure 24. (See legend on the previous page).

to induce expression [Denis *et al.*, 1981]. Nevertheless, the majority of these genes follow a pattern of derepression when comparing transcript levels between glucose-grown and xylose-grown cells of an XR/XDH-strain (Fig. 24B). The response was more distinct in anaerobic than in aerobic conditions. This clearly indicates that xylose is unable to induce deactivation of Snf1p. As expected, only a few genes exhibit a transcriptional change due to a shift from aerobic to anaerobic conditions with glucose as the carbon source. The same transition on xylose, however, caused distinct induction and repression responses that correlate with a high Snf1p-activity. The exception to this pattern was repression of several genes encoding mitochondrial proteins.

4.1.2. The Rgt2p/Snf3p-Rgt1p pathway

The Rgt2p/Snf3p-Rgt1p pathway mainly controls the expression of genes encoding hexose transporters. It operates in parallel with the PKA pathway and in conjunction with the Snf1p pathway [Kaniak *et al.*, 2004; Slattery *et al.*, 2008] but is probably more sensitive to low concentrations of glucose than the other two [Zaman *et al.*, 2009]. The importance of the two glucose-sensors Rgt2p and Snf3p in controlling the growth rate was discussed in Chapter 1.3. Rgt2p and Snf3p interact with extracellular glucose at the plasma membrane. Upon binding of glucose the two sensors attain a higher affinity for the two co-repressors Mth1p and Std1p which are subsequently recruited from the cytosol. At the plasma membrane Mth1p and Std1p become targets for phosphorylation by membrane-bound casein kinases Yck1p and Yck2p. Following phosphorylation, the co-repressors are ubiquinated by SCF^{Grr1} and degraded by the proteasome. With the removal of Mth1p and Std1p, the nuclear transcription factor Rgt1p becomes exposed to phosphorylation by PKA after which it is incapable of binding to recognition sites near target genes (Fig. 24A). Rgt1p functions as a transcriptional repressor of all hexose transporters and of *HXK2* (hexokinase 2) [Kim and Johnston, 2006; Palomino *et al.*, 2006]. The targets of Rgt1p have been reported to correlate with the genes induced by artificial activation of Rgt2p (Fig. 24B) [Kaniak *et al.*, 2004; Zaman *et al.*, 2009]. The transcriptional response of these genes in a XR/XDH-strain to a transition from glucose to xylose in anaerobic conditions is also characteristic of glucose derepression: up-regulation of high-affinity transporters (*HXT2,6-7*) and *SUC2* (invertase), and down-regulation of low-affinity hexose transporters (*HXT1*,*3*). The expression of transcription regulators *MTH1*, *STD1*, *MIG2* and *MIG3* also changed during this transition. Mig2p and possibly Mig3p operate together with Mig1p to repress expression of both *SUC2* and *MTH1*; hence it is not surprising that these genes become induced due to the absence of at least two important repressors.

4.1.3. The cAMP/PKA pathway

The components of the cAMP/PKA pathway are shown in Figure 13 in Chapter 3.2 and the importance of the guanine nucleotides GTP and GDP for the operation of the pathway was discussed in Chapter 3.4. As indicated in Figure 23 there are two parallel branches that can induce cAMP production and activate PKA. This has been shown in studies using *gpr1Δ* mutants in which the glucose-mediated transcriptional response is largely unaffected [Zaman *et al.*, 2009]. The ability of the Gpr1p/Gpa2p-branch to induce the transcriptional response via PKA is, however, weaker than the Ras-dependent branch [Wang *et al.*, 2004]. Hence, the latter is regarded as the major pathway through which the cells mediate regulatory glucose signals. The genes induced due to activation of PKA are those belonging to the Ribi and RP regulons [Warner, 1999]. The Ribi regulon consists of 236 genes encoding the enzymes needed for ribosome assembly and high translational activity such as RNA polymerases I and III, tRNA synthetases, rRNA processing and modifying enzymes. The RP regulon consists of 138 genes encoding the ribosomal protein components and rRNA molecules [Zaman *et al.*, 2008]. Rapidly growing cells synthesises ~2000 ribosomes per min, a process that uses a substantial fraction of the total cellular resources and is thus strictly regulated according to nutrient availability [Warner, 1999]. Accordingly, several transcription factors are involved in the regulation of RP and Ribi genes, the most central being Sfp1p, Rap1p, Fhl1p and Ifh1p. The precise mechanism for the regulation of ribosome biogenesis still remains to be characterised. However, a cross-talk between the secretory pathway (Chapter 3.5) and the ribosome biosynthesis pathway has been established [Nierras and Warner, 1999]. In response to a defect in the secretory pathway, indicating that the cells are not able to synthesise membrane-constituents, Pkc1p (protein kinase C) and Wsc1p initiate a signal transduction mechanism that effectively repress rRNA- and RP-genes, halting ribosome biogenesis.

Activation of PKA enables it to phosphorylate Rap1p which enhances the interaction with the Gcr1p/Gcr2p-complex resulting in increased transcription of the majority of the glycolytic genes (Fig. 24A) [Chambers *et al.*, 1995]. This ensures the high rate of ATP production needed for driving the ribosome biogenesis machinery. In addition to activating a large part of the metabolic machinery, PKA also inhibits the expression of stress related genes. Rim15p is a regulator of entry into quiescence and negatively controlled by PKA through phosphorylation. In fact, the activity of Rim15p is controlled by three independent nutrient-related pathways: PKA (carbon), TORC1 (nitrogen) and the Pho80p/Pho85p complex (phosphate) [Wanke *et al.*, 2005]. The expression of stress-related genes is controlled by transcription factors Msn2p and Msn4p. Both factors are inactivated by PKA through phosphorylation which expels them from the nucleus. As in the case of Rim15p, several nutrient signalling pathways

control the activity of Msn2p/Msn4p by preventing the complex from entering the nucleus or binding to the STRE sites on target genes. Yak1p is another protein kinase that inhibits growth and is repelled from the nucleus to the cytosol in the presence of glucose [Moriya *et al.*, 2001]. However, PKA does not seem to be the only kinase acting on this regulator since Yak1p can be phosphorylated in a *tpk1Δ tpk2Δ tpk3Δ* mutant [Garrett *et al.*, 1991]. The glucose-mediated phosphorylation of Yak1p thus seems to be a pathway parallel to PKA yet to be defined. In the absence of glucose Yak1p enters the nucleus where it phosphorylates Pop2p [Moriya *et al.*, 2001]. In this form Pop2p induces the expression of glucose-repressed genes and those needed to arrest in the G_1-phase before entering stationary phase. Yak1p might also influence the activity of PKA by phosphorylating the regulatory subunit Bcy1p upon which it is relocated from the nucleus to the cytosol where it can bind to the catalytically active subunits Tpk1p-3p [Griffioen *et al.*, 2001].

4.1.4. The perception of xylose

The transcriptional status of recombinant *S. cerevisiae* on xylose indicates a high activity of Snf1p and Rgt1p due to increased expression of *CAT8* and *ADR1* and reduced expression of *HXK2* (Fig. 25). The transcription of genes encoding positive regulators of ribosome biogenesis and glycolysis show no clear pattern (Fig. 25). However, it has previously been reported that the glycolytic genes having sites for both Rap1p and Gcr1p are consistently down-regulated on xylose, whereas those genes lacking one or both of these sites are consistently up-regulated [Runquist, 2010]. This would be indicative of a low PKA-activity, which is supported by increased transcription of *RIM15* and *MSN4* encoding regulators negatively controlled by PKA (Fig. 25). These are the main transcription factors that induce the expression of STRE related genes [Gasch *et al.*, 2000] which have been shown to correlate negatively with growth rate, i.e. a high expression of these genes occurs at low growth rates [Brauer *et al.*, 2008]. Also the transcript levels of *YAK1*, encoding the protein kinase working antagonistically to PKA, are higher on xylose compared to glucose. Hence, both *RIM15* and *YAK1*, the two genes directly related to inhibiting growth by arresting cells in the G_1 or G_0 phase of the cell cycle, are significantly up-regulated on xylose. As the analysis of intracellular metabolites in central carbon metabolism could not reveal a clear reason for the slow-growth phenotype on xylose (see Chapter 3 and **Paper II**), the most likely explanation is a limitation in the perception of xylose.

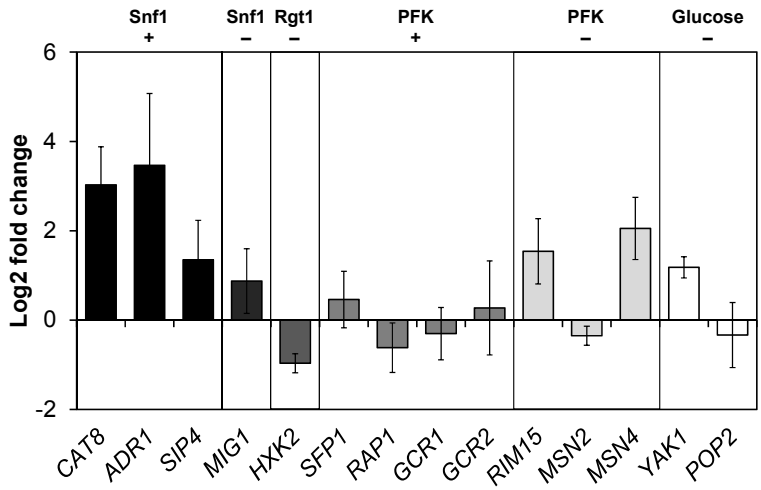

Figure 25. Transcriptional response of key regulators in glucose repression
Data shows the $\log_2$-fold change of transcript levels in XR/XDH-strain TMB3415 due to a transition from glucose to xylose in anaerobic conditions. Genes are grouped according the controlling signalling pathway and whether they are induced (plus-sign) or repressed (minus-sign). Error bars show the 90% confidence interval of the mean (df = 2). The data was taken from [Runquist *et al.*, 2009b].

Several studies have highlighted the importance of nutrient perception on the growth phenotype. Youk *et al.* [2009] showed that cells without the ability to control the expression of specific *HXT* genes according to the extracellular glucose concentration display severe growth defects. They developed a phenomenological model of growth in which the perception of glucose, modelled as function of the extracellular glucose concentration, was a crucial parameter for describing the experimental data. Slattery *et al.* [2008] showed that the transcriptional induction mediated by the cAMP/PKA pathway is not dependent on the rate of metabolism. The addition of cAMP to a culture of a *cyr1Δ* mutant strain in a quiescent state generated the same up-regulation in a nutrient depleted medium as in a fresh medium. However, the correlation of repressed genes between the two conditions was very low indicating that other signals are required in this process. Zaman *et al.* [2009] performed a similar experiment using a different approach. By controlling the expression of $RAS2^{G19V}$, an activated variant of Ras2p, using the galactose inducible promoter of *GAL10*, the addition of galactose to glycerol-grown *gal1Δ* mutants mediated nearly all the transcriptional changes observed when adding glucose. However, there was a drastic difference in the resulting growth rate. 20 min after addition of glucose the growth rate increased by 55% whereas the addition of galactose efficiently halted cell proliferation. This shows that a mismatch between the cells perception of the environment and the actual nutritional condition can be detrimental for growth.

4.2. Metabolic consequences of xylose-induced inactivation of Hexokinase 2

S. cerevisiae possesses three structural genes that encode enzymes which can catalyse the phosphorylation of glucose to glucose 6-phosphate: *HXK1*, *HXK2* and *GLK1* [Lobo and Maitra, 1977]. *HXK1* and *HXK2* encode hexokinases which, in addition to glucose, also can phosphorylate fructose and mannose [Barnard, 1975]. These two proteins share an identity of 77%. *GLK1* encodes a glucokinase which has an identity of 38% with the two hexokinases and lacks the ability to phosphorylate fructose [Maitra, 1970]. During growth on fermentable carbon sources the *HXK2* gene is predominantly expressed and thus the main substrate-phosphorylating capability is provided by Hxk2p [Gancedo *et al.*, 1977; Fernandez *et al.*, 1984]. In conditions with high glucose, expression of *HXK2* is induced by the degradation of Mth1p and Std1p which exposes Rgt1p to hyper-phosphorylation by PKA and loss of repressive control as a result (Fig. 24A) [Palomino *et al.*, 2006].

Hexokinase 2 is a bi-functional protein. In addition to its catalytic function it also fulfils important regulatory functions in several glucose signalling mechanisms (Fig 24A) [Gancedo, 1998; Bisson and Kunathigan, 2003; Moreno *et al.*, 2005]. Early studies on glucose catabolite repression revealed that xylose can induce a decrease in the glucose phosphorylating activity [Fernandez *et al.*, 1984]. Experiments *in vitro* confirmed that Hxk2p becomes irreversibly inactivated by xylose through an autophosphorylation mechanism in the presence of ATP [DelaFuente, 1970; Menezes and Pudles, 1977; Fernandez *et al.*, 1986]. The target residue for the autophosphorylation was later identified as Ser158[2] and attempts to exchange this amino acid indeed abolished the autophosphorylation but also severely reduced the catalytic activity [Heidrich *et al.*, 1997]. The induced inactivation by xylose also caused an increase in invertase activity (encoded by *SUC2*), demonstrating that both the catalytic and regulatory functions of Hxk2p are affected by the modification [Fernandez *et al.*, 1984]. Recently it has been shown that these two functions can operate independently through different parts of the protein [Pelaez *et al.*, 2010], suggesting that the phosphorylation of Ser158 has a profound influence on its functions.

[2] Here the amino acid residues are numbered according to the translated mRNA sequence. Other communications may take into account that the initial methionine residue is cleaved of during post-translational processing, lowering all numbers by one.

The precise role of Hxk2p in glucose signalling was for long unknown but in the last 5-10 years several groups have contributed to define the mechanism by which Hxk2p acts as a transcriptional regulator (Fig. 26). In short, Hxk2p is an essential Snf1p-antagonist and co-repressor of Mig1p.

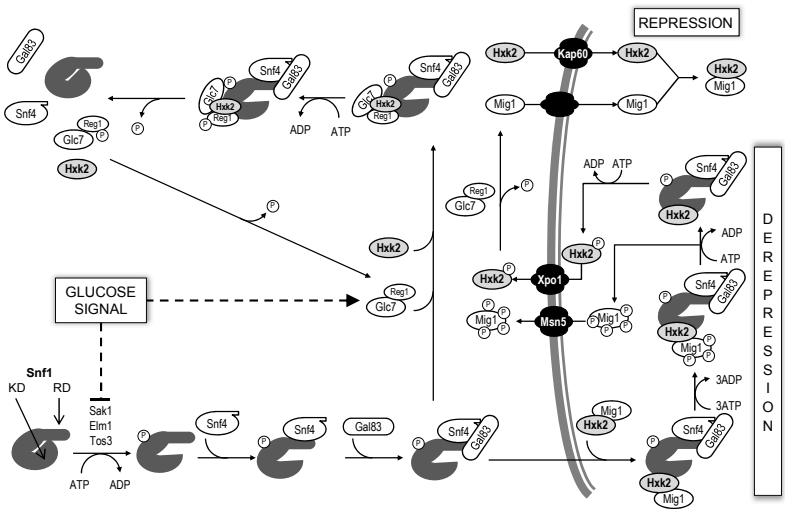

Figure 26. Mechanism of Hxk2p-mediated transcriptional repression.
In the absence of glucose Snf1p is phosphorylated by three protein kinases, although mainly by Sak1p. This induces a conformational change in which the catalytic kinase domain (KD) moves away from the regulatory domain (RD). This allows the regulatory subunit Snf4p to bind to the RD and promote binding of a second subunit. Upon recruitment of Gal83p the complex is able to move into the nucleus. There it phosphorylates both Mig1p and Hxk2p which targets them for transport out from the nucleus and leads to derepression of Mig1p-responsive genes. Upon a glucose signal the Snf1 complex is inactivated through the coordinated actions of Glc7p/Reg1p and Hxk2p. All three components are essential in this process. Glc7p/Reg1p also dephosphorylates Mig1p and Hxk2p allowing them to enter the nucleus and repress expression of target genes. See text for further details.

Hxk2p is constitutively bound to Snf1p, both in the presence of high and low glucose concentration [Ahuatzi *et al.*, 2007; Fernandez-Garcia *et al.*, 2012]. In repressing conditions this interaction facilitates binding of the Glc7p/Reg1p complex to Snf1p, which in turn phosphorylates Reg1p [Sanz *et al.*, 2000]. The phosphorylation of Reg1p probably induces a small conformational change which places Glc7p in a position so that Snf1p is dephosphorylated. This destabilises the open, active, conformation of Snf1p and moves the catalytic domain towards the regulatory domain. In this closed conformation the regulatory subunits Snf4p and Gal83p can no longer stay bound and are released [Sanz *et al.*, 2000]. Hxk2p is essential in this deactivation-mechanism by preventing Glc7p from

dephosphorylating Reg1p instead of Snf1p. Hence, in a *hxk2Δ* mutant, Snf1p never becomes dephosphorylated and consequently Snf1p and Snf4p are constitutively bound, even at high concentrations of glucose [Ludin *et al.*, 1998; Treitel *et al.*, 1998]. The same constitutive interaction is displayed in a *reg1Δ* mutant showing that both Hxk2p and Reg1p are required for the inactivation of Snf1p [Ludin *et al.*, 1998].

When the glucose concentration becomes low, Snf1p is activated through phosphorylation by Sak1p, Elm1p or Tos3p. Active Snf1p can phosphorylate Hxk2p at residue Ser15 which prevents Hxk2p from entering the nucleus [Fernandez-Garcia *et al.*, 2012]. However, a small fraction is dephosphorylated by Glc7p/Reg1p [Alms *et al.*, 1999] which promotes interaction with the karyopherin α/β carrier complex Kap60p/Kap95p [Fernandez-Garcia *et al.*, 2012; Pelaez *et al.*, 2012]. This complex in turn facilitates the transport into the nucleus. The transport requires a lysine-rich nuclear localisation sequence (NLS) located between Lys7 and Lys13 [Herrero *et al.*, 1998; Ahuatzi *et al.*, 2004; Pelaez *et al.*, 2012]. Inside the nucleus, Hxk2p interacts with Mig1p and forms a repressor complex that binds to DNA. This interaction requires the sequence located between Lys7 and Met16 in Hxk2p and Ser311 in Mig1p [Ahuatzi *et al.*, 2007; Pelaez *et al.*, 2010]. In de-repressing conditions active Snf1p is transported into the nucleus and bind the Hxk2p/Mig1p complex. There are three sites (Ser222, 278 and 311) that probably have to be phosphorylated by Snf1p before Ser311 becomes accessible [Ahuatzi *et al.*, 2007]. Phosphorylation of Ser311 induces a release of Mig1p from Hxk2p and is an essential modification for transport of Mig1p out from the nucleus to the cytosol through karyopherin carrier Msn5p [DeVit and Johnston, 1999]. Without Mig1p, Hxk2p is phosphorylated at Ser15 and transported to the cytosol through Xpo1p (Crm1p) [Pelaez *et al.*, 2009]. This interaction involves two nuclear export sequences (NESs) located between Leu23 and Ile33 (NES1) and Leu310 and Leu318 (NES2) [Fernandez-Garcia *et al.*, 2012]. Without the presence of Hxk2p, Mig1p is constitutively phosphorylated in the nucleus and transported out with loss of repressive capacity as a result.

The Hxk2p/Mig1p complex binds to the Mig1p-recognition sites upstream target genes and recruits the co-repressors Cyc8p and Tup1p [Treitel and Carlson, 1995]. In the case of *SUC2* repression Hxk2p also interacts with Med8p which supposedly hinders the activation of RNA polymerase [de la Cera *et al.*, 2002; Moreno and Herrero, 2002; Gancedo and Flores, 2008]. Further transcriptional analysis of an *hxk2Δ* strain showed significant upregulation of genes with binding sites for Mig1p and/or Cat8p (e.g. *FBP1*, *MDH2*, *MDH3, MLS1*, *ICL1*, *IDP2* and *PCK1*) [Schuurmans *et al.*, 2008b]. This confirms the significant role of Hxk2p in the Snf1p circuit of the glucose signalling mechanism.

The role of Hxk2p in the control of sugar transporters has been quite firmly established using *hxk2Δ* mutants [Özcan and Johnston, 1995; Schuurmans *et al.*, 2008a; Schuurmans *et al.*, 2008b]. The presence of Hxk2p is required to fully induce *HXT1* at high glucose concentrations and *HXT2* and *HXT4* at low concentrations. Hxk2p is also needed to repress the expression of *HXT2* and *HXT4* at high glucose concentration [Özcan and Johnston, 1995]. In glucose-limited chemostat cultures of a *hxk2Δ* mutant the expression of *HXT4-7* was found significantly higher and *HXT1*-expression was lower compared to the wild-type; *HXT2* was however unaffected under those conditions [Schuurmans *et al.*, 2008a]. Kinetic modelling of glucose and xylose transport highlighted the need for high-capacity transporters (e.g. *HXT1* or *HXT3*) for efficient xylose transport at low glucose concentrations [Bertilsson *et al.*, 2008] (see Chapter 1.3). Hence, the xylose-induced inactivation of Hxk2p may severely hamper xylose uptake due to the absence of *HXT1* induction.

Furthermore, a functional hexokinase is required to stimulate the Ras/cAMP signal [Rolland *et al.*, 2002] and alteration of Ser158 in Hxk2p significantly reduces this ability [Kraakman *et al.*, 1999]. A specific role for Hxk2p in modulating mitochondrial cytochrome content and respiratory activity has also been suggested [Noubhani *et al.*, 2009]. This is supported by a diminished Crabtree effect in *hxk2Δ* mutants, resulting in a nearly complete respiratory metabolism at high glucose concentration [Schuurmans *et al.*, 2008a]. In light of these findings, the Hxk2p protein can be regarded as a global glycolytic regulator that is essential for mediating the complete glucose repression signal.

4.3. Finding improved Hexokinase 2 variants

Due to the high correlation between the transcriptional state of recombinant strains growing on xylose and *hxk2Δ* mutants, it is possible that the inactivation of Hxk2p by xylose leads to a reduced capability to regulate expression of genes involved in sugar transport and fermentative metabolism. If Hxk2p was made immune to autophosphorylation by xylose, such an enzyme could potentially increase the sugar consumption rate during fermentation of a glucose/xylose mixture by restoring the repressive capability closer to its nominal level and thus increase the ethanol productivity.

To investigate this we constructed a condensed, rationally designed combinatorial library targeting the active-site in Hxk2p, the first reported for this enzyme, and screened the library for beneficial mutations (Fig. 27) [**Paper IV**]. After analysing the three-dimensional structure of the protein, 13 amino acid residues were chosen for mutagenesis. The location of these residues in relation to other features can be found in the Appendix. The theoretical combinatorial

protein library was calculated to contain 16,384 variants and in practice we obtained an estimated 97% coverage of this library. In order to couple the screening of the library to the growth capacity of the yeast cells, the quadruple deletion strain TMB3463 (*hxk2Δ hxk1Δ1 glk1Δ hxk1Δ2*) was constructed [**Paper IV**]. This strain lacked all genes encoding glucose phosphorylating enzymes and was thus unable to grow on glucose. Hence, those transformants of TMB3463 with a functional Hxk2p in the presence of xylose would be able to utilize glucose and grow faster than other transformants in the population. Selection of the fastest growing transformants was thus performed in an anaerobic carbon-limited chemostat with 5 g/L glucose and 50 g/L xylose in the feed reservoir. After establishing a steady state at a low dilution rate (D = 0.07 h^{-1}) the flow rate was increased high enough to initiate a washout of all cells (D = 0.40 h^{-1}).

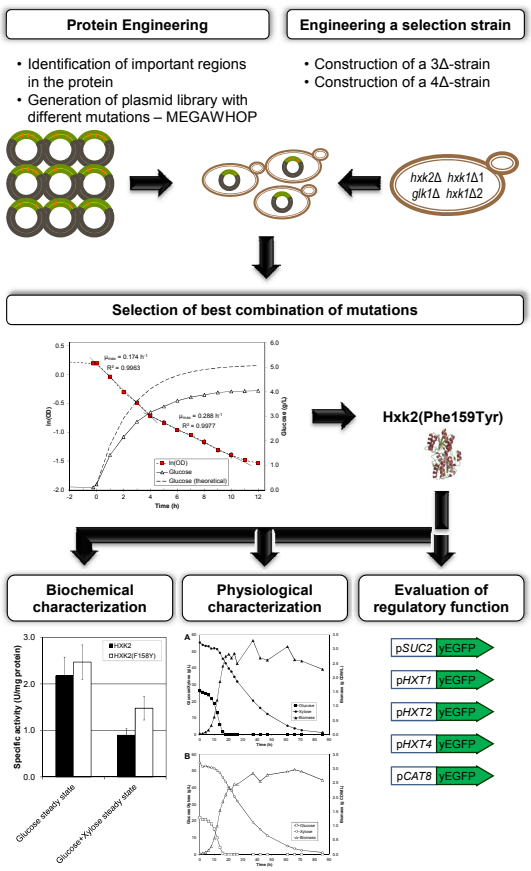

Figure 27. Identification and evaluation of Hxk2p(F159Y).
By combing methods for protein engineering and genetic engineering with fermentation technology a new variant of Hxk2p was identified with higher catalytic activity in the presence of xylose. See text and **Paper IV** for details.

Immediately upon increasing the flow rate the population was able to grow at a rate of 0.17 h^{-1} (Fig. 27). After 4 h the concentration of glucose had increased above 3 g/L which was enough to inhibit the transport of xylose into the cells and as a consequence the growth rate increased to 0.29 h^{-1} (Fig. 27). After 12 h the OD had decreased by 83% and the *HXK2* gene from ten random colonies was analysed for mutations [**Paper IV**]. The majority of these sequences had mutations corresponding to a single amino acid substitution: Phe159Tyr. The gene carrying these mutations was introduced into TMB3463 under the control of *TDH3*-promoter and the enzymatic activity was evaluated in steady-state cultures with and without xylose (Fig. 27) [**Paper IV**]. The Hxk2p(F159Y) variant had 64% higher activity in the presence of xylose compared to the wild-type and the mutation had no detrimental effect on the catalytic efficiency in the absence of xylose. The strain expressing the Hxk2p(F159Y) also had a 15% higher specific glucose consumption rate in the presence of xylose in chemostat cultures. To investigate if the variant could improve xylose fermentation the gene was introduced into strain TMB3490 which lacks the native *HXK2* gene and harbours an XR/XDH pathway [**Paper IV**]. The performance was evaluated in anaerobic batch fermentation with 20 g/L glucose and 50 g/L xylose, but no obvious difference was observed compared with the native gene (Fig. 27) [**Paper IV**]. Hence, other components of the Hxk2p/Mig1p pathway are most likely missing. There are three obvious candidates that are essential for the function of this pathway: Glc7p, Reg1p and the carrier complex Kap60p/Kap95p. Future efforts should be to investigate whether these proteins are missing in the pathway during xylose fermentation.

In an attempt to evaluate the regulatory function of the Hxk2p(F159Y) variant we constructed a set of five GFP-reporter plasmids (Fig. 27; see Appendix for plasmid maps). The upstream regions (ca. 1 kb) of five genes believed to be controlled by Hxk2p were fused to yEGFP (yeast enhanced GFP) [Cormack *et al.*, 1997] and introduced in a *hxk2Δ* mutant together with either *HXK2*(F159Y) or native *HXK2* under the control of the *TDH3* promoter. In total were 12 strains constructed, including two control strains without the gene encoding GFP. All strains were pre-grown in YNB 2% glucose for 12 h and then transferred to fresh medium containing 2% glucose and 5% xylose. Control experiments were also performed without xylose. The fluorescence of GFP was followed over time using flow cytometry. However, the experiments were unsuccessful; in the case of the Hxk2p(F159Y) variant we did not detect a fluorescence different from the negative control with any construct. The results with the strains expressing the native gene were inconclusive and did not correspond with the expected behaviour. It is possible that the use of the *TDH3*-promoter altered the behaviour of the system more than expected. Nevertheless, the constructed plasmids can be used in the future to generate reporter-strains which are responsive to Snf1p/Hxk2p-mediated regulation.

The noblest pleasure is the joy of understanding.

Leonardo da Vinci

5. Conclusions and Future Perspectives

The development of efficient xylose-fermenting strains of *S. cerevisiae* has certainly come very far, from the first generation of strains that were only able to produce xylitol from xylose, to the current strains that are able to grow anaerobically on xylose as the sole carbon source. Increased fermentation efficiency of glucose/xylose mixtures is, however, still needed. The work presented in this thesis aimed to increase the ethanol productivity by improving the growth rate during fermentation of such a substrate mixture. The work resulted in a comprehensive evaluation of the processes and mechanisms required for balance microbial growth. The conclusions are summarised below for each process.

Nutrient assimilation: Efficient uptake of xylose and other nutrients is indeed important. Without sufficient carbon uptake several metabolites risk becoming depleted which affect all the downstream processes such as generation of ATP and balancing of redox co-factors. However, the growth rate of current strains does not seem to be limited by the uptake rate of xylose [**Paper I**, **Paper II**]. Hence, there are other processes currently limiting the growth rate. Nevertheless, if glucose and xylose are ever going to be co-consumed, specific xylose transporters are needed and the screening for or engineering of such facilitators is thus of utmost importance. The recently identified xylose-specific transporters encoded by *XYP29* from *S. stipitis* and *An25* from *N. crassa* may confer such co-consumption capability. Xylose uptake will eventually become a limiting step when other, more eminent, bottlenecks have been solved and there is no reason why this development cannot be performed in parallel.

Energy conservation: The ability of the cells to generate and balance the levels of ATP and the other adenine nucleotides is important to drive the biosynthetic reactions, especially the biogenesis of ribosomes, DNA and RNA. However, the targeted metabolite study showed that recombinant xylose-fermenting strains are able to maintain this balance [**Paper II**]. Furthermore, the rate of ATP formation does not seem to be directly related to the growth rate [**Paper III**]. Hence, the adenine nucleotides seem to play a minor role in the regulation of the growth rate. Still, recombinant strains may exhibit futile cycles of ATP which adds an unnecessary metabolic burden to the cells. The Pho13p phosphatase is one example which has been shown to hamper xylose assimilation by dephosphorylating xylulose 5-phosphate.

Redox-balancing: An imbalance in the redox-cofactors can have a detrimental effect on both catabolic and anabolic reactions. For this reason the development of engineered variants of XR and/or XDH is important. The effects of such modifications are both increased ethanol yield and increased growth rate with xylose as the sole carbon source. However, these variants do not confer a faster growth rate on xylose during fermentation of a glucose/xylose mixture. Hence, as with xylose uptake, the balancing of NAD(H) and NADP(H) will only influence the growth rate under such conditions when more severe limitations in other processes have been solved. The analysis of redox co-factors is also complicated by their compartmentalisation within the cells. A significant challenge for the area of metabolomics is therefore to develop methods that will allow quantification of metabolites in specific compartments.

Biosynthesis: The biogenesis of building blocks, such as amino acids, and macromolecules such as proteins, lipids, DNA and RNA is an absolute necessity for balanced growth. The intracellular concentrations of several of the precursor metabolites needed for these processes are significantly reduced during xylose fermentation [**Paper II**]. This response indicates that the rate of supply is lower than the rate of utilization and the limitation is thus located in either sugar transport and/or specific enzymatic reactions. If an increased uptake rate of xylose restores homeostasis of these metabolites remains to be evaluated, but such improvement did not lead to an increased growth rate of these strains [**Paper I**]. The observed accumulation of intracellular malate and fumarate point toward a diversion of carbon away from amino acids through the reaction catalysed by Mdh2. However, the cultivation of these strains in rich medium, containing all the amino acids, did not improve the growth rate [**Paper III**]. Hence, the signal needed for the cells to utilize these nutrients is missing. One such signal is provided by the Hac1 transcription factor which induces expression of several genes involved in the maturation of secretory proteins. Limitations may exist in the splicing and ligation of mature *HAC1* mRNA. The hypothesis that fumarate reductase activity was inadequate during xylose fermentation was shown to be incorrect [**Paper III**]. Further analysis of the available information suggest that xylose causes the process of disulphide bond formation to be hyper-active. The underlying cause of this behaviour and the roles of free FAD, $FADH_2$ and glutathione require further investigations.

Xylose signalling and commitment to the cell division cycle: Xylose is not recognised as a fermentable carbon source by *S. cerevisiae*. As a consequence the PKA pathway is not activated by xylose and the required induction of genes involved in ribosome biogenesis, the translation machinery and glycolysis is absent. Instead xylose induces the expression of factors related to stress response and entry into stationary phase (i.e. *YAK1* and *RIM15*). This response certainly hinders the cells from committing to the cell division cycle because they cannot reach the threshold rate of protein synthesis and cell size. The guanine nucleotides

may play an important role in this mechanism as an imbalance in the pool of these metabolites can have detrimental effects on nitrogen metabolism, protein synthesis, viability and proliferation of yeast cells. Recombinant strains show a clear disturbance in the GTP:GMP ratio during xylose fermentation [**Paper II**]. However, further systematic studies on how and to what extent this ratio can act as a regulatory signal are required. The hexokinase 2 protein is an important part of the glucose signalling mechanism. It acts as a Snf1p-antagonist and Mig1p co-repressor. In the presence of xylose it is inactivated with loss of regulatory function as a result. An engineered variant was developed that has a higher catalytic activity in the presence of xylose [**Paper IV**]. However, it did not markedly change the fermentation performance in a glucose/xylose mixture indicating that other factors are required for full repressive capacity.

This analysis shows that the perception of xylose is the key limitation. Several studies have shown that the cells tune the expression of genes according the perception of the nutritional status. When the perception mechanism fails and the cells are given the wrong information it results in reduced growth or even cell death. *S. cerevisiae* does not perceive xylose as a fermentable carbon source but is still able to use it as an energy source under anaerobic conditions. To alleviate this inconsistency, future strains need to be engineered so that they recognise xylose as a fermentable carbon source.

The results presented in this thesis may provide a starting point for such future work. However, most of these results were generated through detailed studies of the underlying mechanisms. Such an approach is not only time consuming, but the number of interactions is so large that the risk of missing important factors is eminent. Hence, there is a need for mathematical descriptions of these interactions that allow the combination of data from transcriptome, proteome and metabolome analyses. This need has been recognised and tools that combine network reconstructions with kinetic rate equations, thermodynamic properties, mass balances and regulatory interactions are being developed [Thomas *et al.*, 2007; Miskovic and Hatzimanikatis, 2010; Smallbone *et al.*, 2010; Jensen *et al.*, 2011; Soh *et al.*, 2012; Hyduke *et al.*, 2013]. Further analysis of the time-course data set of intracellular metabolite concentrations generated in **Paper II** using such tools may provide new insights of xylose metabolism.

Acknowledgements

These past years have been a journey and an adventure full of challenges. These challenges have tested me and pushed me almost to the limit. Because of that I feel stronger and wiser than I ever thought I could be. But it would not have been possible without the support from my colleagues, friends and family.

Bärbel Hahn-Hägerdal, thank you for giving me the opportunity to live in Brazil and to conduct research there. It was a once-in-a-life-time opportunity that changed me and made me grow as a person. Thank you for accepting me as a PhD student at Applied Microbiology, for believing in me and for your constant support. Your guidance in the art of science and other aspects of life has been invaluable to me.

Ed van Niel, thank you for taking on the role as my main supervisor and for always keeping an open mind about my hypotheses. Those small sessions were important for me to vent some of my many ideas. Also, thank you for your immense support in the writing of papers and this thesis. Your suggestions have made me a much better writer.

Marie-Francoise Gorwa-Grauslund, although our collaboration only began half-way through my studies I believe it has been very fruitful. You have forced me to become more critical toward my own work and that I am very grateful for. Thank you for your guidance during the last months of lab work for it helped me a lot to keep my focus.

Peter Rådström, thank you for showing an interest in my work, for giving me valuable advice on many issues and for sharing your knowledge of teaching with me. I will try to apply your methods whenever possible.

My students: Mégane Cléret, Mirna Sallaku, Tarinee Boonyawan and Celina Borgström, thank you for all your help and efforts in realizing my ideas. You all worked so hard to give me results. Without you this thesis would not have been possible! I had a lot of fun working with you and I learned a lot, not only in science but also about being a supervisor.

My past and present office mates: Nádia, Ahmad and Nikoletta, thank you for creating an excellent working environment where ideas, questions and various

topics of life have been discussed. Nádia, thank you for a very nice collaboration and for being a true friend in moments of need. Ahmad, thank you for sharing your immense knowledge of microbiology with me and your willingness to discuss numerous questions that I have thrown at you. Some problems I don't know how I would have solved if it wasn't for your advice. I hope we get the opportunity the work together again. Nikoletta, thank you for taking the time in your busy schedule to discuss everything from issues in the lab to cooking recipes with me. Your advice and our many laughs, both inside and outside the lab, have meant a lot for me!

My two sisters in arms, Violeta and Valeria, thank you for a great friendship and for always being available to help me with design of experiments, fixing broken equipment etc. Violeta, thank you for tirelessly listening to my ideas and theories, even though it nearly caused you frostbites! Your insights in interpreting experimental data have truly been invaluable to me. Valeria, thank you for giving me critical feedback on my manuscripts. They would not be of this quality if it wasn't for your input.

Maurizio Bettiga, thank you for answering a lot of questions during my initial time at the lab. You also taught me how to analyse a problem by breaking it down in smaller more manageable pieces. That I have applied constantly throughout my studies.

Anders, thank you for a very nice collaboration and for sharing your experience and skills as a researcher with me.

Past and present members of the yeast group: Oskar, João, David, Rosa, Magnus, Nora, Jan, Venkat, Diogo and Alejandro, thank you for creating an inspiring and progressive working environment.

Sudha(nshu), Johannes and Catherine, thank you for keeping me happy! Especially Sudha for always meeting my remarks with laughter and for giving some back at me! I think there is still hope for you, even though you work on the dark side ☺

Jenny, Christer and Birgit, thank you for solving various problems quickly and with great skill.

Professor Fernando Araripe Torres, thank you for giving me the opportunity to work in your laboratory and with your group. The hospitality and the care you took to make me feel welcome is something I will always remember.

All my friends in Brazil: Alexsandro, Viviane, Hugo, Túlio, Camila, Saulo, Rafael, Marciano, Andrelisse, Mauro, Andre, Thiago, Tatiana and Talita, thank you for your great friendship that I hope will last for a long time. You made the time in Brazil the best years of my life!

Finally, I wish to thank everyone from TMB, our visitors and guests who have been joining our coffee breaks. These short moments have been an opportunity for interesting conversations, discussions and reflections. And, more importantly, they have been moments of laughter that for me were invaluable. I will truly miss them.

In honour of these moments I end this thesis with a poem written by the Swedish poet Tomas Tranströmer, whom in 2011 was awarded the Nobel Prize in Literature.

ESPRESSO
Det svarta kaffet på uteserveringen
med stolar och bord granna som insekter.

Det är dyrbara uppfångade droppar
fyllda med samma styrka som Ja och Nej.

Det bärs fram ur dunkla kaféer
och ser in i solen utan att blinka.

I dagsljuset en punkt av välgörande svart
som snabbt flyter ut i en blek gäst.

Det liknar dropparna av svart djupsinne
som ibland fångas upp av själen,

som ger en välgörande stöt: Gå!
Inspiration att öppna ögonen.

Last, but certainly not least, I wish to thank my family for showing a huge understanding for the passion I feel about my work and for what I have tried to accomplish during the past years. I am truly grateful for all the support and encouragement you have given me, whenever I needed it. Thank you!

Appendix

Derivation of the rate equation for sugar transport

The assumptions made for the derivation of the rate equation are to a large extent the same as those made by Rizzi *et al.* [1996], with some additions made to take into account the second substrate. The assumptions are:

1. Passive diffusion of glucose and xylose across the cell membrane can be neglected.
2. The rate limiting step of the transport is the conformation change between the two surfaces. Thus the free, the glucose-loaded and the xylose-loaded carriers permeate the membrane with different rates: γ, α and β, respectively.
3. Equilibrium exists on both sides of the membrane between the carrier and substrate.

$$K_G = \frac{C^e_{Glc}\, C^e_E}{C^e_{E\text{-}Glc}} = \frac{C^i_{Glc}\, C^i_E}{C^i_{E\text{-}Glc}} \qquad K_X = \frac{C^e_{Xyl}\, C^e_E}{C^e_{E\text{-}Xyl}} = \frac{C^i_{Xyl}\, C^i_E}{C^i_{E\text{-}Xyl}} \tag{A1}$$

4. Assuming that the binding of glucose or xylose to the carrier does not change the interaction with glucose 6-phosphate, the equilibria between the free carrier and carrier-substrate complexes with the inhibitor can be formulated as follows:

$$K_I = \frac{C^i_{G6P}\, C^i_E}{C^i_{E\text{-}G6P}} \qquad K_{II} = \frac{C^i_{G6P}\, C^i_{E\text{-}Glc}}{C^i_{E\text{-}Glc\text{-}G6P}} = \frac{C^i_{G6P}\, C^i_{E\text{-}Xyl}}{C^i_{E\text{-}Xyl\text{-}G6P}} \tag{A2}$$

5. Binding of G6P to the free carrier or the substrate-carrier complexes prevents the transporter from changing the conformation to the extracellular medium.

The total concentration of carrier (E_0) is given as the sum of all carrier species

$$E_0 = C^e_E + C^e_{E\text{-}Glc} + C^e_{E\text{-}Xyl} + C^i_E + C^i_{E\text{-}Glc} + C^i_{E\text{-}Xyl} + C^i_{E\text{-}G6P} + C^i_{E\text{-}Glc\text{-}G6P} + C^i_{E\text{-}Xyl\text{-}G6P} \tag{A3}$$

and the steady-state condition for the carrier gives

$$\alpha C^e_{E\text{-}Glc} + \beta C^e_{E\text{-}Xyl} + \gamma C^e_E = \alpha C^i_{E\text{-}Glc} + \beta C^i_{E\text{-}Xyl} + \gamma C^i_E \tag{A4}$$

The net transport of glucose is given by

$$v_{Glc} = \alpha C^e_{E\text{-}Glc} - \alpha C^i_{E\text{-}Glc} \tag{A5}$$

Dividing both sides of Equation A5 by the total carrier concentration gives

$$\frac{v_{Glc}}{E_0} = \frac{\alpha C^e_{E\text{-}Glc} - \alpha C^i_{E\text{-}Glc}}{C^e_E + C^e_{E\text{-}Glc} + C^e_{E\text{-}Xyl} + C^i_E + C^i_{E\text{-}Glc} + C^i_{E\text{-}Xyl} + C^i_{E\text{-}G6P} + C^i_{E\text{-}Glc\text{-}G6P} + C^i_{E\text{-}Xyl\text{-}G6P}} \tag{A6}$$

By using the relationships in Equation A1 in the numerator and at the same time factorizing the denominator with regard to C^e_E and C^i_E, the following expression is obtained

$$\frac{v_{Glc}}{E_0} = \frac{\alpha \frac{C^e_{Glc} C^e_E}{K_G} - \alpha \frac{C^i_{Glc} C^i_E}{K_G}}{C^e_E\left(1 + \frac{C^e_{E\text{-}Glc}}{C^e_E} + \frac{C^e_{E\text{-}Xyl}}{C^e_E}\right) + C^i_E\left(1 + \frac{C^i_{E\text{-}Glc}}{C^i_E} + \frac{C^i_{E\text{-}Xyl}}{C^i_E} + \frac{C^i_{E\text{-}G6P}}{C^i_E} + \frac{C^i_{E\text{-}Glc\text{-}G6P}}{C^i_E} + \frac{C^i_{E\text{-}Xyl\text{-}G6P}}{C^i_E}\right)} \tag{A7}$$

Dividing the numerator and denominator with C^e_E yields

$$\frac{v_{Glc}}{E_0} = \frac{\alpha \frac{C^e_{Glc}}{K_G} - \alpha \frac{C^i_{Glc}}{K_X} \frac{C^i_E}{C^e_E}}{\left(1 + \frac{C^e_{E\text{-}Glc}}{C^e_E} + \frac{C^e_{E\text{-}Xyl}}{C^e_E}\right) + \frac{C^i_E}{C^e_E}\left(1 + \frac{C^i_{E\text{-}Glc}}{C^i_E} + \frac{C^i_{E\text{-}Xyl}}{C^i_E} + \frac{C^i_{E\text{-}G6P}}{C^i_E} + \frac{C^i_{E\text{-}Glc\text{-}G6P}}{C^i_E} + \frac{C^i_{E\text{-}Xyl\text{-}G6P}}{C^i_E}\right)} \tag{A8}$$

The ratio C^i_E / C^e_E can be expressed by rearranging Equation A4 in the following way

$$\frac{C^i_E}{C^e_E} = \frac{\left(\frac{\alpha}{\gamma}\frac{C^e_{E\text{-}Glc}}{C^e_E} + \frac{\beta}{\gamma}\frac{C^e_{E\text{-}Xyl}}{C^e_E} + 1\right)}{\left(\frac{\alpha}{\gamma}\frac{C^i_{E\text{-}Glc}}{C^i_E} + \frac{\beta}{\gamma}\frac{C^i_{E\text{-}Xyl}}{C^i_E} + 1\right)} \tag{A9}$$

Inserting Equation A9 into Equation A8 and multiplying the numerator and denominator with $\left(\frac{\alpha}{\gamma}\frac{C^i_{E\text{-}Glc}}{C^i_E} + \frac{\beta}{\gamma}\frac{C^i_{E\text{-}Xyl}}{C^i_E} + 1\right)$ gives

$$\frac{v_{Glc}}{E_0} = \frac{\frac{\alpha C^e_{Glc}}{K_G}\left(\frac{\alpha}{\gamma}\frac{C^i_{E\text{-}Glc}}{C^i_E} + \frac{\beta}{\gamma}\frac{C^i_{E\text{-}Xyl}}{C^i_E} + 1\right) - \frac{\alpha C^i_{Glc}}{K_G}\left(\frac{\alpha}{\gamma}\frac{C^e_{E\text{-}Glc}}{C^e_E} + \frac{\beta}{\gamma}\frac{C^e_{E\text{-}Xyl}}{C^e_E} + 1\right)}{\left(1 + \frac{C^e_{E\text{-}Glc}}{C^e_E} + \frac{C^e_{E\text{-}Xyl}}{C^e_E}\right)\left(\frac{\alpha}{\gamma}\frac{C^i_{E\text{-}Glc}}{C^i_E} + \frac{\beta}{\gamma}\frac{C^i_{E\text{-}Xyl}}{C^i_E} + 1\right) + \left(1 + \frac{C^i_{E\text{-}Glc}}{C^i_E} + \frac{C^i_{E\text{-}Xyl}}{C^i_E} + \frac{C^i_{E\text{-}G6P}}{C^i_E} + \frac{C^i_{E\text{-}Glc\text{-}G6P}}{C^i_E} + \frac{C^i_{E\text{-}Xyl\text{-}G6P}}{C^i_E}\right)\left(\frac{\alpha}{\gamma}\frac{C^e_{E\text{-}Glc}}{C^e_E} + \frac{\beta}{\gamma}\frac{C^e_{E\text{-}Xyl}}{C^e_E} + 1\right)} \quad \text{(A10)}$$

After expanding the numerator it can be seen that the term $\frac{\alpha C^e_{Glc}}{K_G}\frac{\alpha}{\gamma}\frac{C^i_{Glc}}{K_G}$ will be cancelled and by using the relationships in Equations A1 and A2 and rearranging the numerator the rate equation is obtained.

$$\frac{v_{Glc}}{E_0} = \frac{\frac{\alpha C^e_{Glc}}{K_G}\left(1 + \frac{\beta}{\gamma}\frac{C^i_{Xyl}}{K^X_S}\right) - \frac{\alpha C^i_{Glc}}{K_G}\left(1 + \frac{\beta}{\gamma}\frac{C^e_{Xyl}}{K^X_S}\right)}{\left(1 + \frac{C^e_{Glc}}{K_G} + \frac{C^e_{Xyl}}{K_X}\right)\left(1 + \frac{\alpha}{\gamma}\frac{C^i_{Glc}}{K_G} + \frac{\beta}{\gamma}\frac{C^i_{Xyl}}{K_X}\right) + \left(1 + \frac{C^i_{Glc}}{K_G} + \frac{C^i_{Xyl}}{K_X} + \frac{C^i_{G6P}}{K_I} + \frac{C^i_{Glc}}{K_G}\frac{C^i_{G6P}}{K_{II}} + \frac{C^i_{Xyl}}{K_X}\frac{C^i_{G6P}}{K_{II}}\right)\left(1 + \frac{\alpha}{\gamma}\frac{C^e_{Glc}}{K_G} + \frac{\beta}{\gamma}\frac{C^e_{Xyl}}{K_X}\right)} \quad \text{(A11)}$$

The rate equation for the transport of xylose is derived by performing the same calculations on the net rate of xylose transfer

$$v_{Xyl} = \beta C^e_{E\text{-}Xyl} - \beta C^i_{E\text{-}Xyl} \quad \text{(A12)}$$

Hexokinase 2 protein sequence

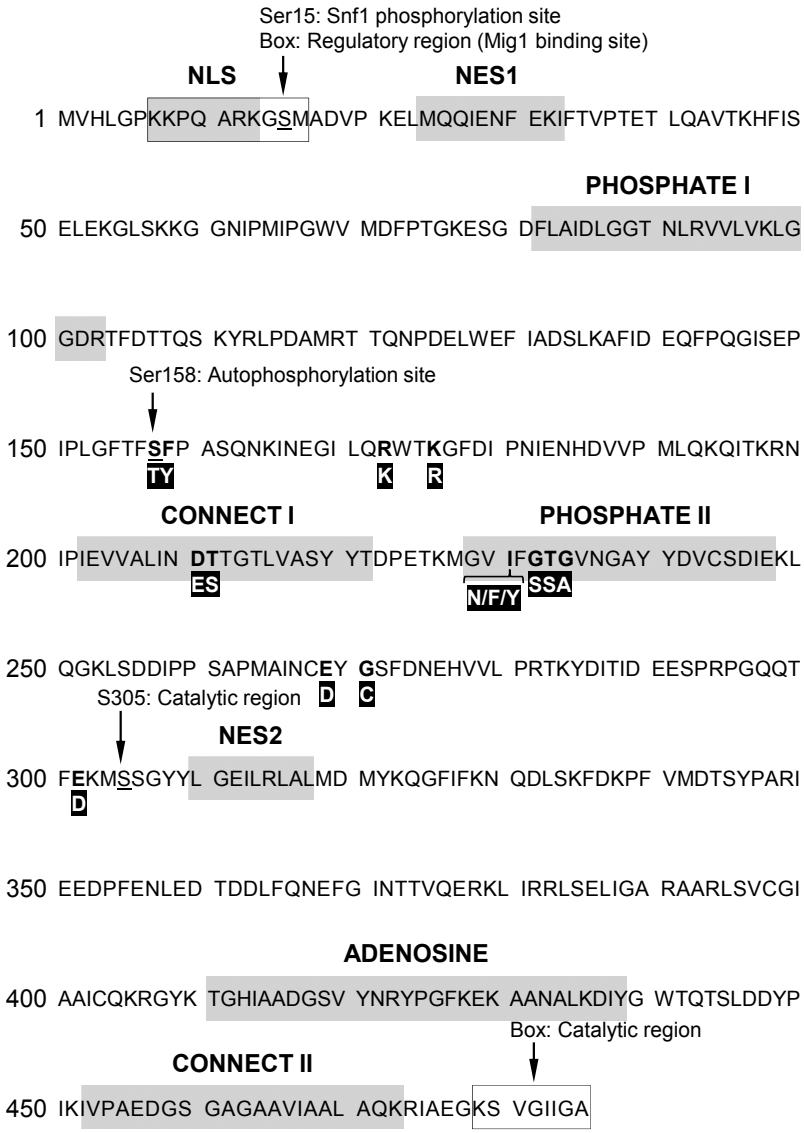

Figure A1. Protein sequence of *S. cerevisiae* Hexokinase 2.
Indicated are regions involved in regulatory function, catalytic activity, ATP binding (see [Bork *et al.*, 1992] for further details) and nuclear-cytosplasmic translocation. Residues in bold were exchanged for the residue(s) highlighted in white-on-black lettering in the gene library. NLS, nuclear localisation signal; NES, nuclear export signal.

Snf1p/Hxk2p GFP-reporter plasmids

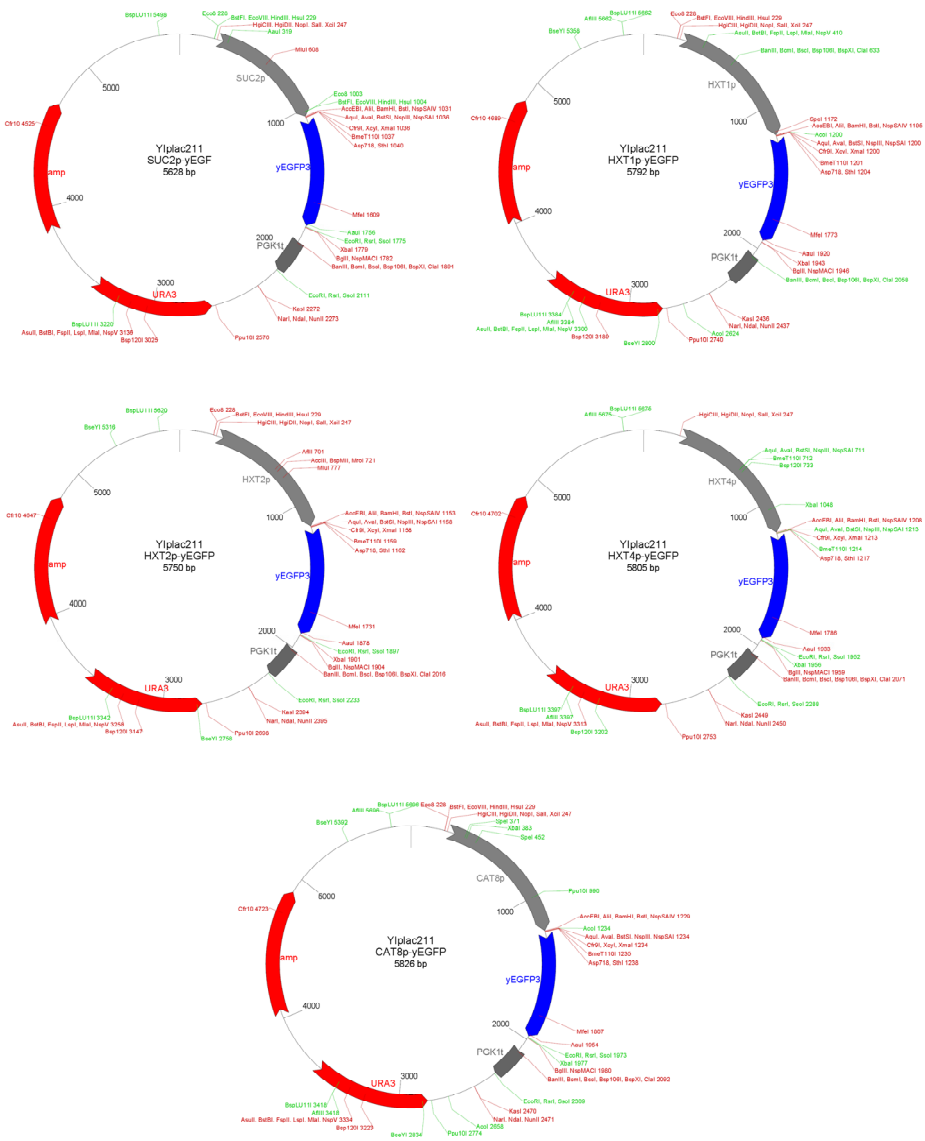

Figure A2. GFP-reporter plasmids containing the promoters of *SUC2*, *HXT1*, *HXT2*, *HXT4* or *CAT8*.

References

1. Ahuatzi D, Herrero P, de la Cera T, Moreno F: **The glucose-regulated nuclear localization of hexokinase 2 in *Saccharomyces cerevisiae* is Mig1-dependent.** *J Biol Chem* 2004, **279**(14):14440-14446.
2. Ahuatzi D, Riera A, Pelaez R, Herrero P, Moreno F: **Hxk2 regulates the phosphorylation state of Mig1 and therefore its nucleocytoplasmic distribution.** *J Biol Chem* 2007, **282**(7):4485-4493.
3. Alms GR, Sanz P, Carlson M, Haystead TAJ: **Reg1p targets protein phosphatase 1 to dephosphorylate hexokinase II in *Saccharomyces cerevisiae*: characterizing the effects of a phosphatase subunit on the yeast proteome.** *EMBO J* 1999, **18**(15):4157-4168.
4. Alvfors P, Arnell J, Berglin N, Björnsson L, Börjesson P, Grahn M, Harvey S, Hoffstedt C, Holmgren K, Jelse K, et al: **Research and development challenges for Swedish biofuel actors – three illustrative examples.** Edited by Grahn M. City: Gothenburg, Sweden, Publisher: The Swedish Centre of Excellence for renewable fuels (F3), 2010.
5. Amore R, Kötter P, Kuster C, Ciriacy M, Hollenberg CP: **Cloning and expression in *Saccharomyces cerevisiae* of the NAD(P)H-dependent xylose reductase-encoding gene (*XYL1*) from the xylose-assimilating yeast *Pichia stipitis*.** *Gene* 1991, **109**(1):89-97.
6. Amore R, Wilhelm M, Hollenberg CP: **The fermentation of xylose - an analysis of the expression of *Bacillus* and *Actinoplanes* xylose isomerase genes in yeast.** *Appl Microbiol Biotechnol* 1989, **30**(4):351-357.
7. Andreasen AA, Stier TJB: **Anaerobic nutrition of *Saccharomyces cerevisiae*. 1. Ergosterol requirement for growth in a defined medium.** *J Cell Comp Physiol* 1953, **41**(1):23-36.
8. Antonin W, Meyer HA, Hartmann E: **Interactions between Spc2p and other components of the endoplasmic reticulum translocation sites of the yeast *Saccharomyces cerevisiae*.** *J Biol Chem* 2000, **275**(44):34068-34072.
9. APEC, Energy Working Group: **A Study of Employment Opportunities from Biofuel Production in APEC Economies** 2010
10. Arikawa Y, Enomoto K, Muratsubaki H, Okazaki M: **Soluble fumarate reductase isoenzymes from *Saccharomyces cerevisiae* are required for anaerobic growth.** *FEMS Microbiol Lett* 1998, **165**(1):111-116.
11. Atkinson DE: **Energy charge of adenylate pool as a regulatory parameter. Interaction with feedback modifiers.** *Biochemistry* 1968, 7(11):4030-4034.
12. Ball WJ, Atkinson DE: **Adenylate energy charge in *Saccharomyces cerevisiae* during starvation.** *J Bacteriol* 1975, **121**(3):975-982.

13. Barlowe CK, Miller EA: **Secretory protein biogenesis and traffic in the early secretory pathway.** *Genetics* 2013, **193**(2):383-410.
14. Barnard EA: **Hexokinases from yeast.** *Methods Enzymol* 1975, **42**:6-20.
15. Barnett JA: **The utilization of sugars by yeasts.** *Adv Carbohydr Chem Biochem* 1976, **32**:125-234.
16. Barwell CJ, Woodward B, Brunt RV: **Regulation of pyruvate kinase by fructose 1,6-diphosphate in *Saccharomyces cerevisiae*.** *Eur J Biochem* 1971, **18**(1):59-64.
17. Bengtsson O, Hahn-Hägerdal B, Gorwa-Grauslund MF: **Xylose reductase from *Pichia stipitis* with altered coenzyme preference improves ethanolic xylose fermentation by recombinant *Saccharomyces cerevisiae*.** *Biotechnol Biofuels* 2009, **2**.
18. Bernales S, Papa FR, Walter P: **Intracellular signaling by the unfolded protein response.** *Annu Rev Cell Dev Biol* 2006, **22**:487-508.
19. Bernofsk C, Swan M: **Improved cycling assay for nicotinamide adenine-dinucleotide.** *Anal Biochem* 1973, **53**(2):452-458.
20. Bertilsson M, Andersson J, Liden G: **Modeling simultaneous glucose and xylose uptake in *Saccharomyces cerevisiae* from kinetics and gene expression of sugar transporters.** *Bioprocess Biosyst Eng* 2008, **31**(4):369-377.
21. Bessou C, Ferchaud F, Gabrielle B, Mary B: **Biofuels, greenhouse gases and climate change. A review.** *Agronomy for Sustainable Development* 2011, **31**(1):1-79.
22. Bisson LF, Coons DM, Kruckeberg AL, Lewis DA: **Yeast sugar transporters.** *Crit Rev Biochem Mol Biol* 1993, **28**(4):259-308.
23. Bisson LF, Kunathigan V: **On the trail of an elusive flux sensor.** *Res Microbiol* 2003, **154**(9):603-610.
24. Boles E, Hollenberg CP: **The molecular genetics of hexose transport in yeasts.** *FEMS Microbiol Rev* 1997, **21**(1):85-111.
25. Boles E, Zimmermann FK, Heinisch J: **Different signals control the activation of glycolysis in the yeast *Saccharomyces cerevisiae*.** *Yeast* 1993, **9**(7):761-770.
26. Bork P, Sander C, Valencia A: **An ATPase domain common to prokaryotic cell-cycle proteins, sugar kinases, actin, and Hsp70 heat-shock proteins.** *Proc Natl Acad Sci U S A* 1992, **89**(16):7290-7294.
27. Bowen BP, Northen TR: **Dealing with the unknown: metabolomics and metabolite atlases.** *J Am Soc Mass Spectrom* 2010, **21**(9):1471-1476.
28. Brauer MJ, Huttenhower C, Airoldi EM, Rosenstein R, Matese JC, Gresham D, Boer VM, Troyanskaya OG, Botstein D: **Coordination of growth rate, cell cycle, stress response, and metabolic activity in yeast.** *Mol Biol Cell* 2008, **19**(1):352-367.
29. Brauer MJ, Yuan J, Bennett BD, Lu W, Kimball E, Botstein D, Rabinowitz JD: **Conservation of the metabolomic response to starvation across two divergent microbes.** *Proc Natl Acad Sci U S A* 2006, **103**(51):19302-19307.
30. Breton A, Pinson B, Coulpier F, Giraud MF, Dautant A, Daignan-Fornier B: **Lethal accumulation of guanylic nucleotides in *Saccharomyces cerevisiae* HPT1-deregulated mutants.** *Genetics* 2008, **178**(2):815-824.

31. Bro C, Regenberg B, Förster J, Nielsen J: **In silico aided metabolic engineering of *Saccharomyces cerevisiae* for improved bioethanol production.** *Metab Eng* 2006, **8**(2):102-111.
32. Bruinenberg PM, de Bot PHM, van Dijken JP, Scheffers WA: **The role of redox balances in the anaerobic fermentation of xylose by yeasts.** *Appl Microbiol Biotechnol* 1983, **18**(5):287-292.
33. Bruinenberg PM, de Bot PHM, van Dijken JP, Scheffers WA: **NADH-linked aldose reductase - the key to anaerobic alcoholic fermentation of xylose by yeasts.** *Appl Microbiol Biotechnol* 1984, **19**(4):256-260.
34. Buscher JM, Czernik D, Ewald JC, Sauer U, Zamboni N: **Cross-platform comparison of methods for quantitative metabolomics of primary metabolism.** *Anal Chem* 2009, **81**(6):2135-2143.
35. Busti S, Coccetti P, Alberghina L, Vanoni M: **Glucose signaling-mediated coordination of cell growth and cell cycle in *Saccharomyces cerevisiae*.** *Sensors* 2010, **10**(6):6195-6240.
36. Börjesson P, Ahlgren S, Berndes G: **The climate benefit of Swedish ethanol: present and prospective performance.** *WIREs Energy Environ* 2012, **1**:81-97.
37. Camarasa C, Faucet V, Dequin S: **Role in anaerobiosis of the isoenzymes for *Saccharomyces cerevisiae* fumarate reductase encoded by *OSM1* and *FRDS1*.** *Yeast* 2007, **24**(5):391-401.
38. Camarasa C, Grivet JP, Dequin S: **Investigation by 13C-NMR and tricarboxylic acid (TCA) deletion mutant analysis of pathways for succinate formation in *Saccharomyces cerevisiae* during anaerobic fermentation.** *Microbiology* 2003, **149**:2669-2678.
39. Canelas AB, Ras C, ten Pierick A, van Dam JC, Heijnen JJ, Van Gulik WM: **Leakage-free rapid quenching technique for yeast metabolomics.** *Metabolomics* 2008a, **4**(3):226-239.
40. Canelas AB, van Gulik WM, Heijnen JJ: **Determination of the cytosolic free NAD/NADH ratio in *Saccharomyces cerevisiae* under steady-state and highly dynamic conditions.** *Biotechnol Bioeng* 2008b, **100**(4):734-743.
41. Chambers A, Packham EA, Graham IR: **Control of glycolytic gene expression in the budding yeast (*Saccharomyces cerevisiae*).** *Curr Genet* 1995, **29**(1):1-9.
42. Chang Q, Griest TA, Harter TM, Petrash JM: **Functional studies of aldo-keto reductases in *Saccharomyces cerevisiae*.** *BBA Molecular Cell Research* 2007, **1773**(3):321-329.
43. Chapman AG, Atkinson DE: **Adenine nucleotide concentrations and turnover rates. Their correlation with biological activity in bacteria and yeast.** In *Advances in Microbial Physiology.* **vol.** 15. Edited by Rose AH, Tempest DW. London: Academic Press; 1977
44. Chen R, Snyder M: **Yeast proteomics and protein microarrays.** *J Proteomics* 2010, **73**(11):2147-2157.

45. Cheng J-S, Qiao B, Yuan Y-J: **Comparative proteome analysis of robust *Saccharomyces cerevisiae* insights into industrial continuous and batch fermentation.** *Appl Microbiol Biotechnol* 2008, **81**(2):327-338.
46. Chu BCH, Lee H: **Genetic improvement of *Saccharomyces cerevisiae* for xylose fermentation.** *Biotechnol Adv* 2007, **25**(5):425-441.
47. Cormack BP, Bertram G, Egerton M, Gow NAR, Falkow S, Brown AJP: **Yeast-enhanced green fluorescent protein (yEGFP): A reporter of gene expression in *Candida albicans*.** *Microbiology* 1997, **143**:303-311.
48. Costenoble R, Adler L, Niklasson C, Liden G: **Engineering of the metabolism of *Saccharomyces cerevisiae* for anaerobic production of mannitol.** *FEMS Yeast Res* 2003, **3**(1):17-25.
49. Crauwels M, Donaton MCV, Pernambuco MB, Winderickx J, deWinde JH, Thevelein JM: **The Sch9 protein kinase in the yeast *Saccharomyces cerevisiae* controls cAPK activity and is required for nitrogen activation of the fermentable-growth-medium-induced (FGM) pathway.** *Microbiology* 1997, **143**:2627-2637.
50. Daran-Lapujade P, Jansen MLA, Daran JM, van Gulik W, de Winde JH, Pronk JT: **Role of transcriptional regulation in controlling fluxes in central carbon metabolism of *Saccharomyces cerevisiae* - A chemostat culture study.** *J Biol Chem* 2004, **279**(10):9125-9138.
51. de la Cera T, Herrero P, Moreno-Herrero F, Chaves RS, Moreno F: **Mediator factor Med8p interacts with the hexokinase 2: Implication in the glucose signalling pathway of *Saccharomyces cerevisiae*.** *J Mol Biol* 2002, **319**(3):703-714.
52. DelaFuente G: **Specific inactivation of yeast hexokinase induced by xylose in the presence of a phosphoryl donor substrate.** *Eur J Biochem* 1970, **16**(2):240-243.
53. Delneri D, Brancia FL, Oliver SG: **Towards a truly integrative biology through the functional genomics of yeast.** *Curr Opin Biotechnol* 2001, **12**(1):87-91.
54. Denis CL, Ciriacy M, Young ET: **A positive regulatory gene is required for accumulation of the functional messenger-RNA for the glucose-repressible alcohol dehydrogenase from *Saccharomyces cerevisiae*.** *J Mol Biol* 1981, **148**(4):355-368.
55. DeVit MJ, Johnston M: **The nuclear exportin Msn5 is required for nuclear export of the Mig1 glucose repressor of *Saccharomyces cerevisiae*.** *Curr Biol* 1999, **9**(21):1231-1241.
56. Di Luccio E, Petschacher B, Voegtli J, Chou H-T, Stahlberg H, Nidetzky B, Wilson DK: **Structural and kinetic studies of induced fit in xylulose kinase from *Escherichia coli*.** *J Mol Biol* 2007, **365**(3):783-798.
57. Dombek KM, Ingram LO: **Intracellular accumulation of AMP as a cause for the decline in rate of ethanol-production by *Saccharomyces cerevisiae* during batch fermentation.** *Appl Environ Microbiol* 1988, **54**(1):98-104.
58. Du J, Li S, Zhao H: **Discovery and characterization of novel D-xylose-specific transporters from *Neurospora crassa* and *Pichia stipitis*.** *Mol Biosyst* 2010, **6**(11):2150-2156.
59. Dudkina NV, Kouřil R, Peters K, Braun H-P, Boekema EJ: **Structure and function of mitochondrial supercomplexes.** *BBA Bioenergetics* 2010, **1797**(6–7):664-670.

60. Dunn WB, Winder CL: **Sample preparation related to the intracellular metabolome of yeast: methods for quenching, extraction, and metabolite quantitation.** *Methods Enzymol* 2011, **500:**277-297.
61. Ehrenreich A: **DNA microarray technology for the microbiologist: an overview.** *Appl Microbiol Biotechnol* 2006, **73**(2)**:**255-273.
62. Eliasson A, Hofmeyr JHS, Pedler S, Hahn-Hägerdal B: **The xylose reductase/xylitol dehydrogenase/xylulokinase ratio affects product formation in recombinant xylose-utilising *Saccharomyces cerevisiae*.** *Enzyme Microb Technol* 2001, **29**(4-5)**:**288-297.
63. Enomoto K, Arikawa Y, Muratsubaki H: **Physiological role of soluble fumarate reductase in redox balancing during anaerobiosis in *Saccharomyces cerevisiae*.** *FEMS Microbiol Lett* 2002, **215**(1)**:**103-108.
64. Enomoto K, Ohki R, Muratsubaki H: **Cloning and sequencing of the gene encoding the soluble fumarate reductase from *Saccharomyces cerevisiae*.** *DNA Res* 1996, **3**(4)**:**263-267.
65. EU, European Commission: **The Fuel Quality Directive 2009/30/EC**. 2009a [http://eur-lex.europa.eu/en/index.htm]
66. EU, European Commission: **The Renewable Energy Directive 2009/28/EC**. 2009b [http://eur-lex.europa.eu/en/index.htm]
67. Evans PR, Farrants GW, Hudson PJ: **Phosphofructokinase - structure and control.** *Philos Trans R Soc Lond B Biol Sci* 1981, **293**(1063)**:**53-62.
68. Fernandez-Garcia P, Pelaez R, Herrero P, Moreno F: **Phosphorylation of yeast hexokinase 2 regulates its nucleocytoplasmic shuttling.** *J Biol Chem* 2012, **287**(50)**:**42151-42164.
69. Fernandez R, Herrero P, Fernandez MT, Moreno F: **Mechanism of inactivation of hexokinase PII of *Saccharomyces cerevisiae* by D-xylose.** *J Gen Microbiol* 1986, **132:**3467-3472.
70. Fernandez R, Herrero P, Gascon S, Moreno F: **Xylose-induced decrease in hexokinase PII activity confers resistance to carbon catabolite repression of invertase synthesis in *Saccharomyces carlsbergensis*.** *Arch Microbiol* 1984, **139**(2-3)**:**139-142.
71. Ferreira C, van Voorst F, Martins A, Neves L, Oliveira R, Kielland-Brandt MC, Lucas C, Brandt A: **A member of the sugar transporter family, Stl1p is the glycerol/H+ symporter in *Saccharomyces cerevisiae*.** *Mol Biol Cell* 2005, **16**(4)**:**2068-2076.
72. Festel GW: **Biofuels - Economic aspects.** *Chemical Engineering & Technology* 2008, **31**(5)**:**715-720.
73. Fiehn O: **Metabolomics - the link between genotypes and phenotypes.** *Plant Mol Biol* 2002, **48**(1-2)**:**155-171.
74. Francois J, Vanschaftingen E, Hers HG: **The mechanism by which glucose increases fructose 2,6-bisphosphate concentration in *Saccharomyces cerevisiae* - A cyclic-AMP-dependent activation of phosphofructokinase-2.** *Eur J Biochem* 1984, **145**(1)**:**187-193.

75. Frand AR, Kaiser CA: **The *ERO1* gene of yeast is required for oxidation of protein dithiols in the endoplasmic reticulum.** *Mol Cell* 1998, **1**(2):161-170.
76. Frand AR, Kaiser CA: **Ero1p oxidizes protein disulfide isomerase in a pathway for disulfide bond formation in the endoplasmic reticulum.** *Mol Cell* 1999, **4**(4):469-477.
77. Freedman RB: **Protein disulfide isomerase - multiple roles in the modification of nascent secretory proteins.** *Cell* 1989, **57**(7):1069-1072.
78. Frick O, Wittmann C: **Characterization of the metabolic shift between oxidative and fermentative growth in *Saccharomyces cerevisiae* by comparative C-13 flux analysis.** *Microb Cell Fact* 2005, **4**.
79. Fujitomi K, Sanda T, Hasunuma T, Kondo A: **Deletion of the *PHO13* gene in *Saccharomyces cerevisiae* improves ethanol production from lignocellulosic hydrolysate in the presence of acetic and formic acids, and furfural.** *Bioresour Technol* 2012, **111**:161-166.
80. Gad A: **Stimulation of yeast phosphofructokinase activity by Fructose 2,6-bisphosphate.** *Biochem Biophys Res Commun* 1981, **102**(3):985-991.
81. Galbe M, Zacchi G: **Pretreatment of lignocellulosic materials for efficient bioethanol production.** In *Adv Biochem Eng Biotechnol: Biofuels*. **vol.** 108. Edited by Olsson L; Berlin: Springer-Verlag Berlin; 2007: 41-65.
82. Gallezot P: **Conversion of biomass to selected chemical products.** *Chem Soc Rev* 2012, **41**(4):1538-1558.
83. Gancedo C, Flores CL: **Moonlighting proteins in yeasts.** *Microbiol Mol Biol Rev* 2008, **72**(1):197-210.
84. Gancedo JM: **Yeast carbon catabolite repression.** *Microbiol Mol Biol Rev* 1998, **62**(2):334-361.
85. Gancedo JM: **The early steps of glucose signalling in yeast.** *FEMS Microbiol Rev* 2008, **32**(4):673-704.
86. Gancedo JM, Clifton D, Fraenkel DG: **Yeast hexokinase mutants.** *J Biol Chem* 1977, **252**(13):4443-4444.
87. Gancedo JM, Lagunas R: **Contribution of the pentose-phosphate pathway to glucose metabolism in *Saccharomyces cerevisiae*: A critical analysis on the use of labelled glucose.** *Plant Science Letters* 1973, **1**(5):193-200.
88. Gardonyi M, Hahn-Hägerdal B: **The *Streptomyces rubiginosus* xylose isomerase is misfolded when expressed in *Saccharomyces cerevisiae*.** *Enzyme Microb Technol* 2003, **32**(2):252-259.
89. Garrett S, Menold MM, Broach JR: **The *Saccharomyces cerevisiae YAK1*-gene encodes a protein-kinase that is induced by arrest early in the cell-cycle.** *Mol Cell Biol* 1991, **11**(8):4045-4052.
90. Gasch AP, Spellman PT, Kao CM, Carmel-Harel O, Eisen MB, Storz G, Botstein D, Brown PO: **Genomic expression programs in the response of yeast cells to environmental changes.** *Mol Biol Cell* 2000, **11**(12):4241-4257.

91. Gauss R, Kanehara K, Carvalho P, Ng DTW, Aebi M: **A complex of Pdi1p and the mannosidase Htm1p initiates clearance of unfolded glycoproteins from the endoplasmic reticulum.** *Mol Cell* 2011, **42**(6):782-793.
92. Geck P: **Properties of a carrier model for transport of sugars by human erythrocytes.** *Biochim Biophys Acta* 1971, **241**(2):462-&.
93. Girio FM, Fonseca C, Carvalheiro F, Duarte LC, Marques S, Bogel-Lukasik R: **Hemicelluloses for fuel ethanol: A review.** *Bioresour Technol* 2010, **101**(13):4775-4800.
94. Goldberg R, Tewari Y, Bhat T: **Thermodynamics of enzyme-catalyzed reactions - a database for quantitative biochemistry.** *Bioinformatics* 2004, **20**(16):2874-2877.
95. Grahn M, Hansson J: **Möjligheter för förnybara drivmedel i Sverige till år 2030 - En rapport utförd på uppdrag av Svenska Petroleum Institutet (SPI).** 2009.
96. Greenbaum D, Colangelo C, Williams K, Gerstein M: **Comparing protein abundance and mRNA expression levels on a genomic scale.** *Genome Biol* 2003, **4**(9).
97. Griffin TJ, Gygi SP, Ideker T, Rist B, Eng J, Hood L, Aebersold R: **Complementary profiling of gene expression at the transcriptome and proteome levels in *Saccharomyces cerevisiae*.** *Mol Cell Proteomics* 2002, **1**(4):323-333.
98. Griffioen G, Branduardi P, Ballarini A, Anghileri P, Norbeck J, Baroni MD, Ruis H: **Nucleocytoplasmic distribution of budding yeast protein kinase A regulatory subunit Bcy1 requires Zds1 and is regulated by Yak1-dependent phosphorylation of its targeting domain.** *Mol Cell Biol* 2001, **21**(2):511-523.
99. Gross E, Sevier CS, Heldman N, Vitu E, Bentzur M, Kaiser CA, Thorpe C, Fass D: **Generating disulfides enzymatically: Reaction products and electron acceptors of the endoplasmic reticulum thiol oxidase Ero1p.** *Proc Natl Acad Sci U S A* 2006, **103**(2):299-304.
100. Grotkjaer T, Christakopoulos P, Nielsen J, Olsson L: **Comparative metabolic network analysis of two xylose fermenting recombinant *Saccharomyces cerevisiae* strains.** *Metab Eng* 2005, 7(5-6):437-444.
101. Gygi SP, Rochon Y, Franza BR, Aebersold R: **Correlation between protein and mRNA abundance in yeast.** *Mol Biol Cell* 1999, **19**(3):1720-1730.
102. Hamacher T, Becker J, Gardonyi M, Hahn-Hägerdal B, Boles E: **Characterization of the xylose-transporting properties of yeast hexose transporters and their influence on xylose utilization.** *Microbiology* 2002, **148**(Pt 9):2783-2788.
103. Hansen R, Pearson SY, Brosnan JM, Meaden PG, Jamieson DJ: **Proteomic analysis of a distilling strain of *Saccharomyces cerevisiae* during industrial grain fermentation.** *Appl Microbiol Biotechnol* 2006, **72**(1):116-125.
104. Hector RE, Qureshi N, Hughes SR, Cotta MA: **Expression of a heterologous xylose transporter in a *Saccharomyces cerevisiae* strain engineered to utilize xylose improves aerobic xylose consumption.** *Appl Microbiol Biotechnol* 2008, **80**(4):675-684.

105. Heidrich K, Otto A, Behlke J, Rush J, Wenzel KW, Kriegel T: **Autophosphorylation-inactivation site of hexokinase 2 in *Saccharomyces cerevisiae*.** *Biochemistry* 1997, **36**(8):1960-1964.
106. Helenius A, Aebi M: **Roles of N-linked glycans in the endoplasmic reticulum.** *Annu Rev Biochem* 2004, **73**:1019-1049.
107. Henderson JF, Paterson ARP: **Nucleotide metabolism: An introduction**. New York: Academic Press; 1973.
108. Herrero P, Martinez-Campa C, Moreno F: **The hexokinase 2 protein participates in regulatory DNA-protein complexes necessary for glucose repression of the *SUC2* gene in *Saccharomyces cerevisiae*.** *FEBS Letters* 1998, **434**(1-2):71-76.
109. Herrgård MJ, Swainston N, Dobson P, Dunn WB, Arga KY, Arvas M, Bluethgen N, Borger S, Costenoble R, Heinemann M, et al: **A consensus yeast metabolic network reconstruction obtained from a community approach to systems biology.** *Nat Biotechnol* 2008, **26**(10):1155-1160.
110. Herrmann JM, Bihlmaier K, Mesecke N: **The role of the Mia40-Erv1 disulfide relay system in import and folding of proteins of the intermembrane space of mitochondria.** In *The Enzymes: Molecular machines involved in protein transport across cellular membranes*. **vol.** XXV: Academic Press; 2007.
111. Hirasawa T, Furusawa C, Shimizu H: ***Saccharomyces cerevisiae* and DNA microarray analyses: what did we learn from it for a better understanding and exploitation of yeast biotechnology?** *Appl Microbiol Biotechnol* 2010, **87**(2):391-400.
112. Ho NWY, Chen ZD, Brainard AP: **Genetically engineered *Sacccharomyces* yeast capable of effective cofermentation of glucose and xylose.** *Appl Environ Microbiol* 1998, **64**(5):1852-1859.
113. Hou J, Vemuri GN, Bao X, Olsson L: **Impact of overexpressing NADH kinase on glucose and xylose metabolism in recombinant xylose-utilizing *Saccharomyces cerevisiae*.** *Appl Microbiol Biotechnol* 2009, **82**(5):909-919.
114. Hyduke DR, Lewis NE, Palsson BO: **Analysis of omics data with genome-scale models of metabolism.** *Mol Biosyst* 2013, **9**(2):167-174.
115. Iglesias-Gato D, Martin-Marcos P, Santos MA, Hinnebusch AG, Tamame M: **Guanine nucleotide pool imbalance impairs multiple steps of protein synthesis and disrupts *GCN4* translational control in *Saccharomyces cerevisiae*.** *Genetics* 2011, **187**(1):105-122.
116. Jeffries TW: **Utilization of xylose by bacteria, yeasts, and fungi.** *Adv Biochem Eng Biotechnol* 1983, **27**:1-32.
117. Jeffries TW, Fady JH, Lightfoot EN: **Effect of glucose supplements on the fermentation of xylose by *Pachysolen tannophilus*.** *Biotechnol Bioeng* 1985, **27**(2):171-176.
118. Jensen PA, Lutz KA, Papin JA: **TIGER: Toolbox for integrating genome-scale metabolic models, expression data, and transcriptional regulatory networks.** *BMC Syst Biol* 2011, **5**.

119. Jeppsson M, Bengtsson O, Franke K, Lee H, Hahn-Hägerdal B, Gorwa-Grauslund MF: **The expression of a *Pichia stipitis* xylose reductase mutant with higher Km for NADPH increases ethanol production from xylose in recombinant *Saccharomyces cerevisiae*.** *Biotechnol Bioeng* 2006, **93**(4):665-673.
120. Jeppsson M, Johansson B, Jensen PR, Hahn-Hägerdal B, Gorwa-Grauslund MF: **The level of glucose-6-phosphate dehydrogenase activity strongly influences xylose fermentation and inhibitor sensitivity in recombinant *Saccharomyces cerevisiae* strains.** *Yeast* 2003a, **20**(15):1263-1272.
121. Jeppsson M, Träff K, Johansson B, Hahn-Hägerdal B, Gorwa-Grauslund MF: **Effect of enhanced xylose reductase activity on xylose consumption and product distribution in xylose-fermenting recombinant *Saccharomyces cerevisiae*.** *FEMS Yeast Res* 2003b, **3**(2):167-175.
122. Jia J, Schorken U, Lindqvist Y, Sprenger GA, Schneider G: **Crystal structure of the reduced Schiff-base intermediate complex of transaldolase B from *Escherichia coli*: Mechanistic implications for class I aldolases.** *Protein Sci* 1997, **6**(1):119-124.
123. Jiang R, Carlson M: **Glucose regulates protein interactions within the yeast Snf1 protein kinase complex.** *Genes Dev* 1996, **10**(24):3105-3115.
124. Jin YS, Jeffries TW: **Changing flux of xylose metabolites by altering expression of xylose reductase and xylitol dehydrogenase in recombinant *Saccharomyces cerevisiae*.** *Appl Biochem Biotechnol* 2003, **105**:277-285.
125. Jin YS, Laplaza JM, Jeffries TW: ***Saccharomyces cerevisiae* engineered for xylose metabolism exhibits a respiratory response.** *Appl Environ Microbiol* 2004, **70**(11):6816-6825.
126. Johansson B, Christensson C, Hobley T, Hahn-Hägerdal B: **Xylulokinase overexpression in two strains of *Saccharomyces cerevisiae* also expressing xylose reductase and xylitol dehydrogenase and its effect on fermentation of xylose and lignocellulosic hydrolysate.** *Appl Environ Microbiol* 2001, **67**(9):4249-4255.
127. Johansson B, Hahn-Hägerdal B: **The non-oxidative pentose phosphate pathway controls the fermentation rate of xylulose but not of xylose in *Saccharomyces cerevisiae* TMB3001.** *FEMS Yeast Res* 2002, **2**(3):277-282.
128. Johnston GC, Ehrhardt CW, Lorincz A, Carter BLA: **Regulation of cell-size in the yeast *Sacchaormyces cerevisiae*.** *J Bacteriol* 1979, **137**(1):1-5.
129. Joubert R, Brignon P, Lehmann C, Monribot C, Gendre F, Boucherie H: **Two-dimensional gel analysis of the proteome of lager brewing yeasts.** *Yeast* 2000, **16**(6):511-522.
130. Jönsson L, Alriksson B, Nilvebrant N-O: **Bioconversion of lignocellulose: inhibitors and detoxification.** *Biotechnol Biofuels* 2013, **6**(1):16.
131. Kaniak A, Xue Z, Macool D, Kim JH, Johnston M: **Regulatory network connecting two glucose signal transduction pathways in *Saccharomyces cerevisiae*.** *Eukaryot Cell* 2004, **3**(1):221-231.
132. Kapp LD, Lorsch JR: **The molecular mechanics of eukaryotic translation.** *Annu Rev Biochem* 2004, **73**:657-704.
133. Karhumaa K, Fromanger R, Hahn-Hägerdal B, Gorwa-Grauslund MF: **High activity of xylose reductase and xylitol dehydrogenase improves xylose**

fermentation by recombinant *Saccharomyces cerevisiae*. *Appl Microbiol Biotechnol* 2007, **73**(5):1039-1046.
134. Karhumaa K, Hahn-Hägerdal B, Gorwa-Grauslund MF: **Investigation of limiting metabolic steps in the utilization of xylose by recombinant *Saccharomyces cerevisiae* using metabolic engineering.** *Yeast* 2005, **22**:359-368.
135. Karhumaa K, Påhlman A-K, Hahn-Hägerdal B, Levander F, Gorwa-Grauslund M-F: **Proteome analysis of the xylose-fermenting mutant yeast strain TMB3400.** *Yeast* 2009, **26**(7):371-382.
136. Katahira S, Ito M, Takema H, Fujita Y, Tanino T, Tanaka T, Fukuda H, Kondo A: **Improvement of ethanol productivity during xylose and glucose co-fermentation by xylose-assimilating *S. cerevisiae* via expression of glucose transporter Sut1.** *Enzyme Microb Technol* 2008, **43**(2):115-119.
137. Kelleher DJ, Gilmore R: **An evolving view of the eukaryotic oligosaccharyltransferase.** *Glycobiology* 2006, **16**(4):47R-62R.
138. Kim J-H, Johnston M: **Two glucose-sensing pathways converge on Rgt1 to regulate expression of glucose transporter genes in *Saccharomyces cerevisiae*.** *J Biol Chem* 2006, **281**(36):26144-26149.
139. Kim S, Sideris DP, Sevier CS, Kaiser CA: **Balanced Ero1 activation and inactivation establishes ER redox homeostasis.** *J Cell Biol* 2012, **196**(6):713-725.
140. Kim SR, Skerker JM, Kang W, Lesmana A, Wei N, Arkin AP, Jin Y-S: **Rational and evolutionary engineering approaches uncover a small set of genetic changes efficient for rapid xylose fermentation in *Saccharomyces cerevisiae*.** *PLoS One* 2013, **8**(2):e57048.
141. Klimacek M, Krahulec S, Sauer U, Nidetzky B: **Limitations in xylose-fermenting *Saccharomyces cerevisiae*, made evident through comprehensive metabolite profiling and thermodynamic analysis.** *Appl Environ Microbiol* 2010, **76**(22):7566-7574.
142. Knowles CJ: **Microbial metabolic regulation by adenine nucleotide pools.** In *Microbial Energetics: Twenty-Seventh Symposium of the Society for General Microbiology.* **vol.** 27. Edited by Haddock BA, Hamilton WA. Cambridge: Cambridge University Press; 1977
143. Kobi D, Zugmeyer S, Potier S, Jaquet-Gutfreund L: **Two-dimensional protein map of an "ale"-brewing yeast strain: proteome dynamics during fermentation.** *FEMS Yeast Res* 2004, **5**(3):213-230.
144. Kraakman LS, Winderickx J, Thevelein JM, De Winde JH: **Structure-function analysis of yeast hexokinase: structural requirements for triggering cAMP signalling and catabolite repression.** *Biochem J* 1999, **343 Pt 1**:159-168.
145. Krahulec S, Klimacek M, Nidetzky B: **Engineering of a matched pair of xylose reductase and xylitol dehydrogenase for xylose fermentation by *Saccharomyces cerevisiae*.** *Biotechnol J* 2009, **4**(5):684-694.
146. Krahulec S, Petschacher B, Wallner M, Longus K, Klimacek M, Nidetzky B: **Fermentation of mixed glucose-xylose substrates by engineered strains of**

***Saccharomyces cerevisiae*: Role of the coenzyme specificity of xylose reductase, and effect of glucose on xylose utilization.** *Microb Cell Fact* 2010, **9**.

147. Kresnowati MTAP, van Winden WA, Almering MJH, ten Pierick A, Ras C, Knijnenburg TA, Daran-Lapujade P, Pronk JT, Heijnen JJ, Daran JM: **When transcriptome meets metabolome: fast cellular responses of yeast to sudden relief of glucose limitation.** *Mol Syst Biol* 2006, **2**.
148. Krishnan P, Kruger NJ, Ratcliffe RG: **Metabolite fingerprinting and profiling in plants using NMR.** *J Exp Bot* 2005, **56**(410):255-265.
149. Krogan NJ, Cagney G, Yu HY, Zhong GQ, Guo XH, Ignatchenko A, Li J, Pu SY, Datta N, Tikuisis AP, et al: **Global landscape of protein complexes in the yeast *Saccharomyces cerevisiae*.** *Nature* 2006, **440**(7084):637-643.
150. Kurtzman C, Suzuki M: **Phylogenetic analysis of ascomycete yeasts that form coenzyme Q-9 and the proposal of the new genera *Babjeviella*, *Meyerozyma*, *Millerozyma*, *Priceomyces*, and *Scheffersomyces*.** *Mycoscience* 2010, **51**(1):2-14.
151. Kuyper M, Harhangi HR, Stave AK, Winkler AA, Jetten MSM, de Laat W, den Ridder JJJ, Op den Camp HJM, van Dijken JP, Pronk JT: **High-level functional expression of a fungal xylose isomerase: the key to efficient ethanolic fermentation of xylose by *Saccharomyces cerevisiae*?** *FEMS Yeast Res* 2003, **4**(1):69-78.
152. Kuyper M, Hartog MMP, Toirkens MJ, Almering MJH, Winkler AA, van Dijken JP, Pronk JT: **Metabolic engineering of a xylose-isomerase-expressing *Saccharomyces cerevisiae* strain for rapid anaerobic xylose fermentation.** *FEMS Yeast Res* 2005a, **5**(4-5):399-409.
153. Kuyper M, Toirkens MJ, Diderich JA, Winkler AA, van Dijken JP, Pronk JT: **Evolutionary engineering of mixed-sugar utilization by a xylose-fermenting *Saccharomyces cerevisiae* strain.** *FEMS Yeast Res* 2005b, **5**(10):925-934.
154. Kuyper M, Winkler AA, van Dijken JP, Pronk JT: **Minimal metabolic engineering of *Saccharomyces cerevisiae* for efficient anaerobic xylose fermentation: a proof of principle.** *FEMS Yeast Res* 2004, **4**(6):655-664.
155. Kötter P, Amore R, Hollenberg CP, Ciriacy M: **Isolation and characterization of the *Pichia stipitis* xylitol dehydrogenase gene, *XYL2*, and construction of a xylose-utilizing *Saccharomyces cerevisiae* transformant.** *Curr Genet* 1990, **18**(6):493-500.
156. Kötter P, Ciriacy M: **Xylose fermentation by *Saccharomyces cerevisiae*.** *Appl Microbiol Biotechnol* 1993, **38**(6):776-783.
157. Laboissiere MCA, Sturley SL, Raines RT: **The essential function of protein-disulfide isomerase is to unscramble nonnative disulfide bonds.** *J Biol Chem* 1995, **270**(47):28006-28009.
158. Lai L-C, Kosorukoff AL, Burke PV, Kwast KE: **Metabolic-state-dependent remodeling of the transcriptome in response to anoxia and subsequent reoxygenation in *Saccharomyces cerevisiae*.** *Eukaryot Cell* 2006, **5**(9):1468-1489.
159. Leandro MJ, Goncalves P, Spencer-Martins I: **Two glucose/xylose transporter genes from the yeast *Candida intermedia*: first molecular characterization of a yeast xylose-H+ symporter.** *Biochem J* 2006, **395**:543-549.

160. Lee TH, Kim MD, Park YC, Bae SM, Ryu YW, Seo JH: **Effects of xylulokinase activity on ethanol production from D-xylulose by recombinant *Saccharomyces cerevisiae*.** *J Appl Microbiol* 2003, **95**(4):847-852.
161. Lin K, Hwang PK, Fletterick RJ: **Mechanism of regulation in yeast glycogen phosphorylase.** *J Biol Chem* 1995, **270**(45):26833-26839.
162. Lobo Z, Maitra PK: **Physiological role of glucose-phosphorylating enzymes in *Saccharomyces cerevisiae*.** *Arch Biochem Biophys* 1977, **182**(2):639-645.
163. Ludin K, Jiang R, Carlson M: **Glucose-regulated interaction of a regulatory subunit of protein phosphatase 1 with the Snf1 protein kinase in *Saccharomyces cerevisiae*.** *Proc Natl Acad Sci U S A* 1998, **95**(11):6245-6250.
164. Maaheimo H, Fiaux J, Çakar ZP, Bailey JE, Sauer U, Szyperski T: **Central carbon metabolism of *Saccharomyces cerevisiae* explored by biosynthetic fractional ^{13}C labeling of common amino acids.** *Eur J Biochem* 2001, **268**(8):2464-2479.
165. Madhavan A, Tamalampudi S, Ushida K, Kanai D, Katahira S, Srivastava A, Fukuda H, Bisaria VS, Kondo A: **Xylose isomerase from polycentric fungus *Orpinomyces*: gene sequencing, cloning, and expression in *Saccharomyces cerevisiae* for bioconversion of xylose to ethanol.** *Appl Microbiol Biotechnol* 2009, **82**(6):1067-1078.
166. Maitra PK: **A glucokinase from *Saccharomyces cerevisiae*.** *J Biol Chem* 1970, **245**(9):2423-2431.
167. Mashego MR, Wu L, Van Dam JC, Ras C, Vinke JL, Van Winden WA, Van Gulik WM, Heijnen JJ: **MIRACLE: mass isotopomer ratio analysis of U-C-13-labeled extracts. A new method for accurate quantification of changes in concentrations of intracellular metabolites.** *Biotechnol Bioeng* 2004, **85**(6):620-628.
168. Menezes LC, Pudles J: **Specific phosphorylation of yeast hexokinase induced by xylose and ATPMg. Properties of the phosphorylated form of the enzyme.** *Arch Biochem Biophys* 1977, **178**(1):34-42.
169. Metzger MH, Hollenberg CP: **Amino-acid substitutions in the yeast *Pichia stipitis* xylitol dehydrogenase coenzyme-binding domain affect the coenzyme specificity.** *Eur J Biochem* 1995, **228**(1):50-54.
170. Miskovic L, Hatzimanikatis V: **Production of biofuels and biochemicals: in need of an ORACLE.** *Trends Biotechnol* 2010, **28**(8):391-397.
171. Mo M, Palsson B, Herrgard M: **Connecting extracellular metabolomic measurements to intracellular flux states in yeast.** *BMC Syst Biol* 2009, **3**(1):37.
172. Moore SA: **Kinetic evidence for a critical rate of protein synthesis in the *Saccharomyces cerevisiae* yeast cell cycle.** *J Biol Chem* 1988, **263**(20):9674-9681.
173. Moreno F, Ahuatzi D, Riera A, Palomino CA, Herrero P: **Glucose sensing through the Hxk2-dependent signalling pathway.** *Biochem Soc Trans* 2005, **33**:265-268.
174. Moreno F, Herrero P: **The hexokinase 2-dependent glucose signal transduction pathway of *Saccharomyces cerevisiae*.** *FEMS Microbiol Rev* 2002, **26**(1):83-90.
175. Moriya H, Johnston M: **Glucose sensing and signaling in *Saccharomyces cerevisiae* through the Rgt2 glucose sensor and casein kinase I.** *Proc Natl Acad Sci U S A* 2004, **101**(6):1572-1577.

176. Moriya H, Shimizu-Yoshida Y, Omori A, Iwashita S, Katoh M, Sakai A: **Yak1p, a DYRK family kinase, translocates to the nucleus and phosphorylates yeast Pop2p in response to a glucose signal.** *Genes Dev* 2001, **15**(10):1217-1228.
177. Muratsubaki H, Enomoto K: **One of the fumarate reductase isoenzymes from *Saccharomyces cerevisiae* is encoded by the *OSM1* gene.** *Arch Biochem Biophys* 1998, **352**(2):175-181.
178. Ness F, Bourot S, Regnacq M, Spagnoli R, Berges T, Karst F: ***SUT1* is a putative Zn II 2Cys6-transcription factor whose upregulation enhances both sterol uptake and synthesis in aerobically growing *Saccharomyces cerevisiae* cells.** *Eur J Biochem* 2001, **268**(6):1585-1595.
179. Nicholson JK, Lindon JC: **Systems biology: Metabonomics.** *Nature* 2008, **455**(7216):1054-1056.
180. Nierras CR, Warner JR: **Protein kinase C enables the regulatory circuit that connects membrane synthesis to ribosome synthesis in *Saccharomyces cerevisiae*.** *J Biol Chem* 1999, **274**(19):13235-13241.
181. Nilsson U, Meshalkina L, Lindqvist Y, Schneider G: **Examination of substrate binding in thiamin diphosphate-dependent transketolase by protein crystallography and site-directed mutagenesis.** *J Biol Chem* 1997, **272**(3):1864-1869.
182. Nishikawa SI, Fewell SW, Kato Y, Brodsky JL, Endo T: **Molecular chaperones in the yeast endoplasmic reticulum maintain the solubility of proteins for retrotranslocation and degradation.** *J Cell Biol* 2001, **153**(5):1061-1070.
183. Nissen TL, Anderlund M, Nielsen J, Villadsen J, Kielland-Brandt MC: **Expression of a cytoplasmic transhydrogenase in *Saccharomyces cerevisiae* results in formation of 2-oxoglutarate due to depletion of the NADPH pool.** *Yeast* 2001, **18**(1):19-32.
184. Noubhani A, Bunoust O, Bonini BM, Thevelein JM, Devin A, Rigoulet M: **The trehalose pathway regulates mitochondrial respiratory chain content through hexokinase 2 and cAMP in *Saccharomyces cerevisiae*.** *J Biol Chem* 2009, **284**(40):27229-27234.
185. Ogg SC, Barz WP, Walter P: **A functional GTPase domain, but not its transmembrane domain, is required for function of the SRP receptor beta-subunit.** *J Cell Biol* 1998, **142**(2):341-354.
186. Oldiges M, Lutz S, Pflug S, Schroer K, Stein N, Wiendahl C: **Metabolomics: current state and evolving methodologies and tools.** *Appl Microbiol Biotechnol* 2007, **76**(3):495-511.
187. Oliveira AP, Ludwig C, Picotti P, Kogadeeva M, Aebersold R, Sauer U: **Regulation of yeast central metabolism by enzyme phosphorylation.** *Mol Syst Biol* 2012, **8**.
188. Oliver SG, Winson MK, Kell DB, Baganz F: **Systematic functional analysis of the yeast genome.** *Trends Biotechnol* 1998, **16**(9):373-378.
189. Olofsson K, Bertilsson M, Liden G: **A short review on SSF - an interesting process option for ethanol production from lignocellulosic feedstocks.** *Biotechnol Biofuels* 2008, **1**.

190. Orij R, Postmus J, Ter Beek A, Brul S, Smits GJ: ***In vivo*** **measurement of cytosolic and mitochondrial pH using a pH-sensitive GFP derivative in *Saccharomyces cerevisiae* reveals a relation between intracellular pH and growth.** *Microbiology* 2009, **155**:268-278.
191. Palomino A, Herrero P, Moreno F: **Tpk3 and Snf1 protein kinases regulate Rgt1 association with *Saccharomyces cerevisiae HXK2* promoter.** *Nucleic Acids Res* 2006, **34**(5):1427-1438.
192. Pao SS, Paulsen IT, Saier MH: **Major facilitator superfamily.** *Microbiol Mol Biol Rev* 1998, **62**(1):1-34.
193. Pelaez R, Fernandez-Garcia P, Herrero P, Moreno F: **Nuclear import of the yeast hexokinase 2 protein requires alpha/beta-Importin-dependent pathway.** *J Biol Chem* 2012, **287**(5):3518-3529.
194. Pelaez R, Herrero P, Moreno F: **Nuclear export of the yeast hexokinase 2 protein requires the Xpo1 (Crm1)-dependent pathway.** *J Biol Chem* 2009, **284**(31):20548-20555.
195. Pelaez R, Herrero P, Moreno F: **Functional domains of yeast hexokinase 2.** *Biochem J* 2010, **432**(1):181-190.
196. Pollard MG, Travers KJ, Weissman JS: **Ero1p: A novel and ubiquitous protein with an essential role in oxidative protein folding in the endoplasmic reticulum.** *Mol Cell* 1998, **1**(2):171-182.
197. Potthast F, Ocenasek J, Rutishauser D, Pelikan M, Schlapbach R: **Database independent detection of isotopically labeled MS/MS spectrum peptide pairs.** *J Chromatogr B Analyt Technol Biomed Life Sci* 2005, **817**(2):225-230.
198. Protchenko O, Rodriguez-Suarez R, Androphy R, Bussey H, Philpott CC: **A screen for genes of heme uptake identifies the *FLC* family required for import of FAD into the endoplasmic reticulum.** *J Biol Chem* 2006, **281**(30):21445-21457.
199. Rapoport TA: **Protein translocation across the eukaryotic endoplasmic reticulum and bacterial plasma membranes.** *Nature* 2007, **450**(7170):663-669.
200. Reifenberger E, Boles E, Ciriacy M: **Kinetic characterization of individual hexose transporters of *Saccharomyces cerevisiae* and their relation to the triggering mechanisms of glucose repression.** *Eur J Biochem* 1997, **245**(2):324-333.
201. Reifenberger E, Freidel K, Ciriacy M: **Identification of novel *HXT* genes in *Saccharomyces cerevisiae* reveals the impact of individual hexose transporters on glycolytic flux.** *Mol Microbiol* 1995, **16**(1):157-167.
202. Richard P, Toivari MH, Penttilä M: **The role of xylulokinase in *Saccharomyces cerevisiae* xylulose catabolism.** *FEMS Microbiol Lett* 2000, **190**(1):39-43.
203. Rizzi M, Erlemann P, Bui-Thanh N-A, Dellweg H: **Xylose fermentation by yeasts. Purification and kinetic-studies of xylose reductase from *Pichia stipitis*.** *Appl Microbiol Biotechnol* 1988, **29**(2):148-154.
204. Rizzi M, Harwart K, Bui-Thanh N-A, Dellweg H: **A kinetic study of the NAD+-xylitol-dehydrogenase from the yeast *Pichia stipitis*.** *J Ferment Bioeng* 1989, **67**(1):25-30.

205. Rizzi M, Theobald U, Querfurth E, Rohrhirsch T, Baltes M, Reuss M: ***In vivo*** **investigations of glucose transport in *Saccharomyces cerevisiae*.** *Biotechnol Bioeng* 1996, **49**(3):316-327.
206. Rolland F, de Winde JH, Lemaire K, Boles E, Thevelein JM, Winderickx J: **Glucose-induced cAMP signalling in yeast requires both a G-protein coupled receptor system for extracellular glucose detection and a separable hexose kinase-dependent sensing process.** *Mol Microbiol* 2000, **38**(2):348-358.
207. Rolland F, Winderickx J, Thevelein JM: **Glucose-sensing and -signalling mechanisms in yeast.** *FEMS Yeast Res* 2002, **2**(2):183-201.
208. Rosenfeld E, Beauvoit B: **Role of the non-respiratory pathways in the utilization of molecular oxygen by *Saccharomyces cerevisiae*.** *Yeast* 2003, **20**(13):1115-1144.
209. Rossi C, Hauber J, Singer TP: **Mitochondrial and cytoplasmic enzymes for the reduction of fumarate to succinate in yeast.** *Nature* 1964, **204**(4954):167-170.
210. Rudoni S, Colombo S, Coccetti P, Martegani E: **Role of guanine nucleotides in the regulation of the Ras/cAMP pathway in *Saccharomyces cerevisiae*.** *BBA Molecular Cell Research* 2001, **1538**(2-3):181-189.
211. Runquist D: **Metabolic Control Points in Ethanolic Fermentation of Xylose by *Saccharomyces cerevisiae*.** *Doctoral Thesis.* Lund University, Department of Chemistry, Division of Applied Microbiology; 2010.
212. Runquist D, Fonseca C, Rådstrom P, Spencer-Martins I, Hahn-Hägerdal B: **Expression of the Gxf1 transporter from *Candida intermedia* improves fermentation performance in recombinant xylose-utilizing *Saccharomyces cerevisiae*.** *Appl Microbiol Biotechnol* 2009a, **82**(1):123-130.
213. Runquist D, Hahn-Hägerdal B, Bettiga M: **Increased expression of the oxidative pentose phosphate pathway and gluconeogenesis in anaerobically growing xylose-utilizing *Saccharomyces cerevisiae*.** *Microb Cell Fact* 2009b, **8**.
214. Runquist D, Hahn-Hägerdal B, Bettiga M: **Increased ethanol productivity in xylose-utilizing *Saccharomyces cerevisiae* via a randomly mutagenized xylose reductase.** *Appl Environ Microbiol* 2010a, **76**(23):7796-7802.
215. Runquist D, Hahn-Hägerdal B, Rådstrom P: **Comparison of heterologous xylose transporters in recombinant *Saccharomyces cerevisiae*.** *Biotechnol Biofuels* 2010b, **3**:5.
216. Rützler M, Reissaus A, Budzowska M, Bandlow W: ***SUT2*** **is a novel multicopy suppressor of low activity of the cAMP/protein kinase A pathway in yeast.** *Eur J Biochem* 2004, **271**(7):1284-1291.
217. Saint-Marc C, Pinson B, Coulpier F, Jourdren L, Lisova O, Daignan-Fornier B: **Phenotypic consequences of purine nucleotide imbalance in *Saccharomyces cerevisiae*.** *Genetics* 2009, **183**(2):529-538.
218. Saloheimo A, Rauta J, Stasyk OV, Sibirny AA, Penttila M, Ruohonen L: **Xylose transport studies with xylose-utilizing *Saccharomyces cerevisiae* strains expressing heterologous and homologous permeases.** *Appl Microbiol Biotechnol* 2007, **74**(5):1041-1052.

219. Salusjärvi L, Kankainen M, Soliymani R, Pitkanen JP, Penttilä M, Ruohonen L: **Regulation of xylose metabolism in recombinant *Saccharomyces cerevisiae*.** *Microb Cell Fact* 2008, **7**.
220. Salusjärvi L, Pitkanen JP, Aristidou A, Ruohonen L, Penttilä M: **Transcription analysis of recombinant *Saccharomyces cerevisiae* reveals novel responses to xylose.** *Appl Biochem Biotechnol* 2006, **128**(3):237-261.
221. Salusjärvi L, Poutanen M, Pitkanen JP, Koivistoinen H, Aristidou A, Kalkkinen N, Ruohonen L, Penttilä M: **Proteome analysis of recombinant xylose-fermenting *Saccharomyces cerevisiae*.** *Yeast* 2003, **20**(4):295-314.
222. Sanz P, Alms GR, Haystead TAJ, Carlson M: **Regulatory interactions between the Reg1-Glc7 protein phosphatase and the Snf1 protein kinase.** *Mol Cell Biol* 2000, **20**(4):1321-1328.
223. Sarthy AV, McConaughy BL, Lobo Z, Sundström JA, Furlong CE, Hall BD: **Expression of the *Escherichia coli* xylose isomerase gene in *Saccharomyces cerevisiae*.** *Appl Environ Microbiol* 1987, **53**(9):1996-2000.
224. Sassner P, Galbe M, Zacchi G: **Techno-economic evaluation of bioethanol production from three different lignocellulosic materials.** *Biomass Bioenergy* 2008, **32**(5):422-430.
225. SCB, Statistics Sweden: **Utvärdering av Sveriges status med EU:s hållbarhetsindikatorer – En genomgång utförd av SCB på uppdrag av Miljödepartementet**. 2012
226. SCB, Statistics Sweden: **Månatlig bränsle-, gas- och lagerstatistik**. 2013a [http://www.scb.se]
227. SCB, Statistics Sweden: **Årliga energibalanser**. 2013b [http://www.scb.se/]
228. Scholz M, Gatzek S, Sterling A, Fiehn O, Selbig J: **Metabolite fingerprinting: detecting biological features by independent component analysis.** *Bioinformatics* 2004, **20**(15):2447-2454.
229. Schuller HJ: **Transcriptional control of nonfermentative metabolism in the yeast *Saccharomyces cerevisiae*.** *Curr Genet* 2003, **43**(3):139-160.
230. Schuurmans JM, Boorsma A, Lascaris R, Hellingwerf KJ, de Mattos MJT: **Physiological and transcriptional characterization of *Saccharomyces cerevisiae* strains with modified expression of catabolic regulators.** *FEMS Yeast Res* 2008a, **8**(1):26-34.
231. Schuurmans JM, Rossell SL, van Tuijl A, Bakker BM, Hellingwerf KJ, Teixeira de Mattos MJ: **Effect of *hxk2* deletion and *HAP4* overexpression on fermentative capacity in *Saccharomyces cerevisiae*.** *FEMS Yeast Res* 2008b, **8**(2):195-203.
232. Schwarz F, Aebi M: **Mechanisms and principles of N-linked protein glycosylation.** *Curr Opin Struct Biol* 2011, **21**(5):576-582.
233. Sedlak M, Ho NWY: **Characterization of the effectiveness of hexose transporters for transporting xylose during glucose and xylose co-fermentation by a recombinant *Saccharomyces* yeast.** *Yeast* 2004, **21**(8):671-684.

234. Senac T, Hahn-Hägerdal B: **Intermediary metabolite concentrations in xylulose-fermenting and glucose-fermenting *Saccharomyces cerevisiae* cells.** *Appl Environ Microbiol* 1990, **56**(1)**:**120-126.
235. Sevier CS, Qu H, Heldman N, Gross E, Fass D, Kaiser CA: **Modulation of cellular disulfide-bond formation and the ER redox environment by feedback regulation of Ero1.** *Cell* 2007, **129**(2)**:**333-344.
236. Shao S, Hegde RS: **Membrane protein insertion at the endoplasmic reticulum.** *Annu Rev Cell Dev Biol* 2011, **27:**25-56.
237. Slattery MG, Liko D, Heideman W: **Protein kinase A, TOR, and glucose transport control the response to nutrient repletion in *Saccharomyces cerevisiae*.** *Eukaryot Cell* 2008, 7(2)**:**358-367.
238. Smallbone K, Simeonidis E, Swainston N, Mendes P: **Towards a genome-scale kinetic model of cellular metabolism.** *BMC Syst Biol* 2010, 4.
239. Smedsgaard J, Nielsen J: **Metabolite profiling of fungi and yeast: from phenotype to metabolome by MS and informatics.** *J Exp Bot* 2005, **56**(410)**:**273-286.
240. Soccol CR, Faraco V, Karp S, Vandenberghe LPS, Thomaz-Soccol V, Woiciechowski A, Pandey A: **Lignocellulosic bioethanol: Current status and future perspectives.** In *Biofuels: Alternative feedstocks and conversion processes*. Oxford, UK: Elsevier Ltd; 2011: 101-122.
241. Soh KC, Miskovic L, Hatzimanikatis V: **From network models to network responses: integration of thermodynamic and kinetic properties of yeast genome-scale metabolic networks.** *FEMS Yeast Res* 2012, **12**(2)**:**129-143.
242. Sonderegger M, Schumperli M, Sauer U: **Metabolic engineering of a phosphoketolase pathway for pentose catabolism in *Saccharomyces cerevisiae*.** *Appl Environ Microbiol* 2004, **70**(5)**:**2892-2897.
243. Song H-S, Morgan JA, Ramkrishna D: **Towards Increasing the Productivity of Lignocellulosic Bioethanol: Rational Strategies Fueled by Modeling.** In *Bioethanol.* Edited by Prof. Lima MAP. InTech; 2012
244. Steel GJ, Fullerton DM, Tyson JR, Stirling CJ: **Coordinated activation of Hsp70 chaperones.** *Science* 2004, **303**(5654)**:**98-101.
245. Stephanopoulos G, Aristidou A, Nielsen J: **Metabolic Engineering: Principles and Methodologies**. San Diego, CA, USA: Elsevier Academic Press; 1998.
246. Steuer R: **On the analysis and interpretation of correlations in metabolomic data.** *Brief Bioinform* 2006, 7(2)**:**151-158.
247. Steuer R, Morgenthal K, Weckwerth W, Selbig J: **A gentle guide to the analysis of metabolomic data.** In *Methods Mol Biol*. **vol.** 358; 2007: 105-126.
248. Suga H, Matsuda F, Hasunuma T, Ishii J, Kondo A: **Implementation of a transhydrogenase-like shunt to counter redox imbalance during xylose fermentation in *Saccharomyces cerevisiae*.** *Appl Microbiol Biotechnol* 2013, **97**(4)**:**1669-1678.
249. Teusink B, Walsh MC, van Dam K, Westerhoff HV: **The danger of metabolic pathways with turbo design.** *Trends Biochem Sci* 1998, **23**(5)**:**162-169.

250. Tewari YB, Steckler DK, Goldberg RN: **Thermodynamics of the conversion of aqueous xylose to xylulose.** *Biophys Chem* 1985, **22**(3):181-185.
251. Thevelein JM: **The Ras-adenylate cyclase pathway and cell cycle control in *Saccharomyces cerevisiae*.** *Antonie Van Leeuwenhoek* 1992, **62**(1-2):109-130.
252. Thevelein JM, de Winde JH: **Novel sensing mechanisms and targets for the cAMP-protein kinase A pathway in the yeast *Saccharomyces cerevisiae*.** *Mol Microbiol* 1999, **33**(5):904-918.
253. Thomas R, Paredes CJ, Mehrotra S, Hatzimanikatis V, Papoutsakis ET: **A model-based optimization framework for the inference of regulatory interactions using time-course DNA microarray expression data.** *BMC Bioinformatics* 2007, **8**.
254. Toda T, Cameron S, Sass P, Zoller M, Scott JD, McMullen B, Hurwitz M, Krebs EG, Wigler M: **Cloning and characterization of *BCY1*, a locus encoding a regulatory subunit of the cyclic AMP-dependent protein-kinase in *Saccharomyces cerevisiae*.** *Mol Cell Biol* 1987a, 7(4):1371-1377.
255. Toda T, Cameron S, Sass P, Zoller M, Wigler M: **Three different genes in *Saccharomyces cerevisiae* encode the catalytic subunits of the cAMP-dependent protein-kinase.** *Cell* 1987b, **50**(2):277-287.
256. Toda T, Uno I, Ishikawa T, Powers S, Kataoka T, Broek D, Cameron S, Broach J, Matsumoto K, Wigler M: **In yeast, Ras proteins are controlling elements of adenylate cyclase.** *Cell* 1985, **40**(1):27-36.
257. Toivari MH, Salusjärvi L, Ruohonen L, Penttilä M: **Endogenous xylose pathway in *Saccharomyces cerevisiae*.** *Appl Environ Microbiol* 2004, **70**(6):3681-3686.
258. Toivola A, Yarrow D, Vandenbosch E, Vandijken JP, Scheffers WA: **Alcoholic fermentation of D-xylose by yeasts.** *Appl Environ Microbiol* 1984, **47**(6):1221-1223.
259. Travers KJ, Patil CK, Wodicka L, Lockhart DJ, Weissman JS, Walter P: **Functional and genomic analyses reveal an essential coordination between the unfolded protein response and ER-associated degradation.** *Cell* 2000, **101**(3):249-258.
260. Treitel MA, Carlson M: **Repression by Ssn6-Tup1 is directed by Mig1, a repressor activator protein.** *Proc Natl Acad Sci U S A* 1995, **92**(8):3132-3136.
261. Treitel MA, Kuchin S, Carlson M: **Snf1 protein kinase regulates phosphorylation of the Mig1 repressor in *Saccharomyces cerevisiae*.** *Mol Cell Biol* 1998, **18**(11):6273-6280.
262. Träff KL, Cordero RRO, van Zyl WH, Hahn-Hägerdal B: **Deletion of the *GRE3* aldose reductase gene and its influence on xylose metabolism in recombinant strains of *Saccharomyces cerevisiae* expressing the *xylA* and *XKS1* genes.** *Appl Environ Microbiol* 2001, **67**(12):5668-5674.
263. Träff KL, Jönsson LJ, Hahn-Hägerdal B: **Putative xylose and arabinose reductases in *Saccharomyces cerevisiae*.** *Yeast* 2002, **19**(14):1233-1241.
264. Tu BP, Ho-Schleyer SC, Travers KJ, Weissman JS: **Biochemical basis of oxidative protein folding in the endoplasmic reticulum.** *Science* 2000, **290**(5496):1571-1574.

265. Tu BP, Weissman JS: **The FAD- and O2-dependent reaction cycle of Ero1-mediated oxidative protein folding in the endoplasmic reticulum.** *Mol Cell* 2002, **10**(5):983-994.
266. Tzagoloff A, Jang J, Glerum DM, Wu M: ***FLX1* codes for a carrier protein involved in maintaining a proper balance of flavin nucleotides in yeast mitochondria.** *J Biol Chem* 1996, **271**(13):7392-7397.
267. Uno I, Matsumoto K, Adachi K, Ishikawa T: **Genetic and biochemical evidence that trehalase is a substrate of cAMP-dependent protein kinase in yeast.** *J Biol Chem* 1983, **258**(18):867-872.
268. Wahlbom CF, Hahn-Hägerdal B: **Furfural, 5-hydroxymethyl furfural, and acetoin act as external electron acceptors during anaerobic fermentation of xylose in recombinant *Saccharomyces cerevisiae*.** *Biotechnol Bioeng* 2002, **78**(2):172-178.
269. Wahlbom CF, Otero RRC, van Zyl WH, Hahn-Hägerdal B, Jönsson LJ: **Molecular analysis of a *Saccharomyces cerevisiae* mutant with improved ability to utilize xylose shows enhanced expression of proteins involved in transport, initial xylose metabolism, and the pentose phosphate pathway.** *Appl Environ Microbiol* 2003, **69**(2):740-746.
270. Walfridsson M, Bao XM, Anderlund M, Lilius G, Bulow L, Hahn-Hägerdal B: **Ethanolic fermentation of xylose with *Saccharomyces cerevisiae* harboring the *Thermus thermophilus xylA* gene, which expresses an active xylose (glucose) isomerase.** *Appl Environ Microbiol* 1996, **62**(12):4648-4651.
271. Walther T, Novo M, Roessger K, Letisse F, Loret M-O, Portais J-C, Francois J-M: **Control of ATP homeostasis during the respiro-fermentative transition in yeast.** *Mol Syst Biol* 2010, **6**.
272. van Maris AJA, Winkler AA, Kuyper M, de Laat W, van Dijken JP, Pronk JT: **Development of efficient xylose fermentation in *Saccharomyces cerevisiae*: Xylose isomerase as a key component.** In *Adv Biochem Eng Biotechnol: Biofuels*. **vol.** 108. Edited by Olsson L; Berlin: Springer-Verlag Berlin; 2007: 179-204.
273. Van Vleet JH, Jeffries TW, Olsson L: **Deleting the para-nitrophenyl phosphatase (pNPPase), *PHO13*, in recombinant *Saccharomyces cerevisiae* improves growth and ethanol production on D-xylose.** *Metab Eng* 2008, **10**(6):360-369.
274. Wang Y, Pierce M, Schneper L, Guldal CG, Zhang X, Tavazoie S, Broach JR: **Ras and Gpa2 mediate one branch of a redundant glucose signaling pathway in yeast.** *PLoS Biol* 2004, **2**(5):E128.
275. Vanhalewyn M, Dumortier F, Debast G, Colombo S, Ma PS, Winderickx J, Van Dijck P, Thevelein JM: **A mutation in *Saccharomyces cerevisiae* adenylate cyclase, Cyr1(K1876M), specifically affects glucose- and acidification-induced cAMP signalling and not the basal cAMP level.** *Mol Microbiol* 1999, **33**(2):363-376.
276. Wanke V, Pedruzzi I, Cameroni E, Dubouloz F, De Virgilio C: **Regulation of G(0) entry by the Pho80-Pho85 cyclin-CDK complex.** *EMBO J* 2005, **24**(24):4271-4278.
277. Varma A, Freese EB, Freese E: **Partial deprivation of GTP initiates meiosis and sporulation in *Saccharomyces cerevisiae*.** *Mol Gen Genet* 1985, **201**(1):1-6.

278. Warner JR: **The economics of ribosome biosynthesis in yeast.** *Trends Biochem Sci* 1999, **24**(11):437-440.
279. Watanabe S, Abu Saleh A, Pack SP, Annaluru N, Kodaki T, Makino K: **Ethanol production from xylose by recombinant *Saccharomyces cerevisiae* expressing protein-engineered NADH-preferring xylose reductase from *Pichia stipitis*.** *Microbiology* 2007a, **153**:3044-3054.
280. Watanabe S, Abu Saleh A, Pack SP, Annaluru N, Kodaki T, Makino K: **Ethanol production from xylose by recombinant *Saccharomyces cerevisiae* expressing protein engineered NADP(+)-dependent xylitol dehydrogenase.** *J Biotechnol* 2007b, **130**(3):316-319.
281. Weierstall T, Hollenberg CP, Boles E: **Cloning and characterization of three genes (*SUT1-3*) encoding glucose transporters of the yeast *Pichia stipitis*.** *Mol Microbiol* 1999, **31**(3):871-883.
282. Vembar SS, Brodsky JL: **One step at a time: endoplasmic reticulum-associated degradation.** *Nat Rev Mol Cell Biol* 2008, **9**(12):944-957.
283. Wenger JW, Schwartz K, Sherlock G: **Bulk segregant analysis by high-throughput sequencing reveals a novel xylose utilization gene from *Saccharomyces cerevisiae*.** *PloS Genetics* 2010, **6**(5).
284. Verho R, Londesborough J, Penttilä M, Richard P: **Engineering redox cofactor regeneration for improved pentose fermentation in *Saccharomyces cerevisiae*.** *Appl Environ Microbiol* 2003, **69**(10):5892-5897.
285. Werner E, Heilier JF, Ducruix C, Ezan E, Junot C, Tabet JC: **Mass spectrometry for the identification of the discriminating signals from metabolomics: Current status and future trends.** *J Chromatogr B Analyt Technol Biomed Life Sci* 2008, **871**(2):143-163.
286. Wieczorke R, Krampe S, Weierstall T, Freidel K, Hollenberg CP, Boles E: **Concurrent knock-out of at least 20 transporter genes is required to block uptake of hexoses in *Saccharomyces cerevisiae*.** *FEBS Letters* 1999, **464**(3):123-128.
287. Wilcox LJ, Balderes DA, Wharton B, Tinkelenberg AH, Rao G, Sturley SL: **Transcriptional profiling identifies two members of the ATP-binding cassette transporter superfamily required for sterol uptake in yeast.** *J Biol Chem* 2002, **277**(36):32466-32472.
288. Wild K, Halic M, Sinning I, Beckmann R: **SRP meets the ribosome.** *Nat Struct Mol Biol* 2004, **11**(11):1049-1053.
289. Villas-Boas SG, Mas S, Akesson M, Smedsgaard J, Nielsen J: **Mass spectrometry in metabolome analysis.** *Mass Spectrom Rev* 2005, **24**(5):613-646.
290. Wisselink HW, Cipollina C, Oud B, Crimi B, Heijnen JJ, Pronk JT, van Maris AJA: **Metabolome, transcriptome and metabolic flux analysis of arabinose fermentation by engineered *Saccharomyces cerevisiae*.** *Metab Eng* 2010, **12**(6):537-551.
291. Wisselink HW, Toirkens MJ, Wu Q, Pronk JT, van Maris AJA: **Novel evolutionary engineering approach for accelerated utilization of glucose, xylose, and arabinose**

mixtures by engineered *Saccharomyces cerevisiae* strains. *Appl Environ Microbiol* 2009, **75**(4):907-914.
292. Xue Y, Batlle M, Hirsch JP: ***GPR1* encodes a putative G protein-coupled receptor that associates with the Gpa2p G(alpha) subunit and functions in a Ras-independent pathway.** *EMBO J* 1998, **17**(7):1996-2007.
293. Yablochkova EN, Bolotnikova OI, Mikhailova NP, Nemova NN, Ginak AI: **The activity of xylose reductase and xylitol dehydrogenase in yeasts.** *Microbiology* 2003, **72**(4):414-417.
294. Yalowitz JA, Jayaram HN: **Molecular targets of guanine nucleotides in differentiation, proliferation and apoptosis.** *Anticancer Res* 2000, **20**(4):2329-2338.
295. Yang WC, Sedlak M, Regnier FE, Mosier N, Ho N, Adamec J: **Simultaneous Quantification of Metabolites Involved in Central Carbon and Energy Metabolism Using Reversed-Phase Liquid Chromatography-Mass Spectrometry and in Vitro ^{13}C Labeling.** *Anal Chem* 2008, **80**(24):9508-9516.
296. Yokoyama SI, Suzuki T, Kawai K, Horitsu H, Takamizawa K: **Purification, characterization and structure-analysis of NADPH-dependent D-xylose reductases from *Candida tropicalis*.** *J Ferment Bioeng* 1995, **79**(3):217-223.
297. Youk H, van Oudenaarden A: **Growth landscape formed by perception and import of glucose in yeast.** *Nature* 2009, **462**(7275):875-U865.
298. Young E, Poucher A, Comer A, Bailey A, Alper H: **Functional survey for heterologous sugar transport proteins, using *Saccharomyces cerevisiae* as a host.** *Appl Environ Microbiol* 2011, **77**(10):3311-3319.
299. Young EM, Comer AD, Huang H, Alper HS: **A molecular transporter engineering approach to improving xylose catabolism in *Saccharomyces cerevisiae*.** *Metab Eng* 2012, **14**(4):401-411.
300. Zaman S, Lippman SI, Schneper L, Slonim N, Broach JR: **Glucose regulates transcription in yeast through a network of signaling pathways.** *Mol Syst Biol* 2009, **5**.
301. Zaman S, Lippman SI, Zhao X, Broach JR: **How *Saccharomyces* responds to nutrients.** *Annu Rev Genet* 2008, **42**:27-81.
302. Zhang G-C, Liu J-J, Ding W-T: **Decreased xylitol formation during xylose fermentation in *Saccharomyces cerevisiae* due to overexpression of water-forming NADH oxidase.** *Appl Environ Microbiol* 2012, **78**(4):1081-1086.
303. Zuzuarregui A, Monteoliva L, Gil C, del Olmo ML: **Transcriptomic and proteomic approach for understanding the molecular basis of adaptation of *Saccharomyces cerevisiae* to wine fermentation.** *Appl Environ Microbiol* 2006, **72**(1):836-847.
304. Öhgren K, Bengtsson O, Gorwa-Grauslund MF, Galbe M, Hahn-Hägerdal B, Zacchi G: **Simultaneous saccharification and co-fermentation of glucose and xylose in steam-pretreated corn stover at high fiber content with *Saccharomyces cerevisiae* TMB3400.** *J Biotechnol* 2006, **126**(4):488-498.
305. Özcan S, Johnston M: **Three different regulatory mechanisms enable yeast hexose transporter (*HXT*) genes to be induced by different levels of glucose.** *Mol Cell Biol* 1995, **15**(3):1564-1572.

Paper I

Metabolic Engineering 13 (2011) 508–517

Contents lists available at ScienceDirect

Metabolic Engineering

journal homepage: www.elsevier.com/locate/ymben

Kinetic modelling reveals current limitations in the production of ethanol from xylose by recombinant *Saccharomyces cerevisiae*

Nádia Skorupa Parachin, Basti Bergdahl, Ed W.J. van Niel, Marie F. Gorwa-Grauslund *

Department of Applied Microbiology, Center for Chemistry and Chemical Engineering, Lund University, P.O. Box 124, SE-221 00 Lund, Sweden

ARTICLE INFO

Article history:
Received 1 December 2010
Received in revised form
16 May 2011
Accepted 19 May 2011
Available online 27 May 2011

Keywords:
Saccharomyces cerevisiae
Xylose
Ethanol
Kinetic model
Xylitol
Xylulokinase

ABSTRACT

Saccharomyces cerevisiae lacks the ability to ferment the pentose sugar xylose that is the second most abundant sugar in nature. Therefore two different xylose catabolic pathways have been heterologously expressed in *S. cerevisiae*. Whereas the xylose reductase (XR)-xylitol dehydrogenase (XDH) pathway leads to the production of the by-product xylitol, the xylose isomerase (XI) pathway results in significantly lower xylose consumption. In this study, kinetic models including the reactions ranging from xylose transport into the cell to the phosphorylation of xylulose to xylulose 5-P were constructed. They were used as prediction tools for the identification of putative targets for the improvement of xylose utilization in *S. cerevisiae* strains engineered for higher level of the non-oxidative pentose phosphate pathway (PPP) enzymes, higher xylulokinase and inactivated *GRE3* gene encoding an endogenous NADPH-dependent aldose reductase. For both pathways, the *in silico* analyses identified a need for even higher xylulokinase (XK) activity. In a XR-XDH strain expressing an integrated copy of the *Escherichia coli* XK encoding gene *xylB* about a six-fold reduction of xylitol formation was confirmed under anaerobic conditions. Similarly overexpression of the *xylB* gene in a XI strain increased the aerobic growth rate on xylose by 21%. In contrast to the *in silico* predictions, the aerobic growth also increased 24% when the xylose transporter gene *GXF1* from *Candida intermedia* was overexpressed together with *xylB* in the XI strain. Under anaerobic conditions, the XI strains overexpressing *xylB* gene and the combination of *xylB* and *GFX1* genes consumed 27% and 37% more xylose than the control strain.

© 2011 Elsevier Inc. All rights reserved.

1. Introduction

Xylose is the second most abundant sugar in nature and its utilization by baker's yeast *Saccharomyces cerevisiae* would significantly decrease the production cost of bioethanol from a wide range of lignocellulosic biomass (Rudolf et al., 2009). Therefore two different pathways have been introduced in *S. cerevisiae* (Fig. 1) enabling xylose utilization (Eliasson et al., 2000; Karhumaa et al., 2007; Kuyper et al., 2003). The reductive/oxidative pathway, consisting of xylose reductase (XR), EC1.1.1.21 and xylitol dehydrogenase (XDH), EC1.1.1.175, usually from *Pichia stipitis*, converts xylose to xylulose with xylitol as intermediate. The other pathway is an isomerization most frequently encountered in bacteria but also present in some fungi. In this case, xylose is directly converted to xylulose by xylose isomerase (XI), EC5.3.1.5. In both pathways, xylulose enters the pentose phosphate pathway (PPP) by its conversion to xylulose-5-phosphate catalyzed by the enzyme xylulokinase (XK) EC2.7.1.17. In both pathways, the overexpression of the non-oxidative part of PPP encoding genes (Karhumaa et al., 2005; Kuyper et al., 2005) and deletion of *GRE3* gene encoding an endogenous NADPH-dependent aldose reductase (Träff et al., 2001) have been shown to benefit xylose fermentation.

A recent study has compared the two xylose catabolic pathways in an isogenic *GRE3* deleted strain overexpressing the genes encoding the non-oxidative PPP enzymes and the endogenous XK (Karhumaa et al., 2007). Heterologous expression of XR and XDH encoding genes from *P. stipitis* gave higher specific ethanol productivity as a result of a significantly higher xylose consumption rate. However xylitol formation arising from the cofactor imbalance between XR and XDH was higher for XR-XDH strain than for the strain expressing the XI encoding gene, where ethanol yields close to theoretical were achieved (Karhumaa et al., 2007). Enzyme engineering of both XR and XDH have aimed to neutralize the redox balance between these two enzymes (Bengtsson et al., 2009; Jeppsson et al., 2006; Matsushika et al., 2008; Petschacher and Nidetzky, 2008; Runquist et al., 2010a; Watanabe et al., 2007; Zeng et al., 2009). Although this has reduced xylitol formation significantly, still about 15% of the consumed xylose is secreted as xylitol

* Corresponding author.
E-mail address: Marie-Francoise.Gorwa@tmb.lth.se (M.F. Gorwa-Grauslund).

1096-7176/$ - see front matter © 2011 Elsevier Inc. All rights reserved.
doi:10.1016/j.ymben.2011.05.005

Nomenclature

α	relative mobility between bound and unbound transport (dimensionless)
A_{cell}	specific surface area of the cell (m^2/g CDW)
C_x	cell concentration (g/L)
r_x	rate of cell death (/h)
P_x	mass density of cells (g CDW/(L cell volume))
P_{xyt}	permeability coefficient for xylitol (m/s)
CDW	cell dry weight (g/L)
rt_{xyt}	xylitol diffusion rate (mmol/g CDW/h)
$V_{max}^{Xi,f}$	xylose isomerase forward (mM/h)
$V_{max}^{Xi,r}$	xylose isomerase reverse (mM/h)
K_i	inhibition constant (mM)
XDH	xylose dehydrogenase (dimensionless)
V_{max}	maximum velocity (mM/h)
K_m	Michaelis constant (mM)
[XR]	concentration of xylose reductase (U/mg)
XYL_e	xylose extracellular (g/L)
XYL	xylose intracellular (mM)
XYLU	xylulose (mM)
XYT	xylitol intracellular (mM)
XYT_e	xylitol extracellular (g/L)

by the most successful mutants (Bengtsson et al., 2009; Petschacher and Nidetzky, 2008; Runquist et al., 2010a). In the XI pathway, heterologous overexpression of XI encoding genes in *S. cerevisiae* has proved to be a challenging task marked by low enzyme activity in yeast (Amore and Hollenberg, 1989; Gárdonyi and Hahn-Hägerdal, 2003; Moes et al., 1996; Sarthy et al., 1987; Walfridsson et al., 1996). Among the numerous investigated XI encoding genes, only three have been so far reported to result in aerobic (Brat et al., 2009; Kuyper et al., 2003; Madhavan et al., 2008) or anaerobic (Kuyper et al., 2004) growth on xylose.

Mainly confirmatory results have been obtained when metabolic flux analysis (MFA) has been used to describe pentose conversion into metabolic intermediates and to predict fluxes towards product formation (Bengtsson et al., 2009; Pitkanen et al., 2003; Sonderegger et al., 2004; Wahlbom et al., 2001; Wisselink et al., 2010). In the present study kinetics for the enzymes of the two xylose catabolic pathways were used to identify targets for increasing the flux of either pathway at the enzyme level. First kinetic parameters were estimated by fitting the two kinetic models to literature data for xylose fermentation by XR-XDH and XI recombinant *gre3*-deleted strains overexpressing the non-oxidative PPP and the endogenous XK genes. Then the XR-XDH and XI models were used to *in silico* simulate minimal xylitol formation and maximum xylose uptake, respectively. Finally genetically modified strains were constructed in the same strain background and used to *in vivo* validate the *in silico* predictions.

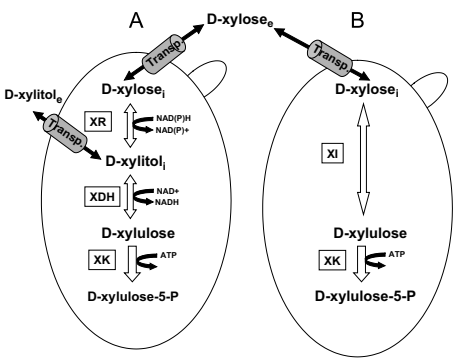

Fig. 1. Initial steps of xylose utilization via reductive/oxidative (A) or isomerization pathway (B). Xylose$_e$ and xylose$_i$ are extracellular and intracellular xylose, respectively.

2. Material and methods

2.1. Kinetic model

Two kinetic models were constructed in Matlab version R2006b within the Systems Biology Toolbox[2] (Schmidt and Jirstrand, 2006). Experimental data were obtained from previously described fermentations for parameter estimation (Karhumaa et al., 2007). Briefly 5 g/L cell dry weight (CDW) of *S. cerevisiae* recombinant *gre3*-deleted strains that have the endogenous XK encoding gene and non-oxidative PPP genes overexpressed, thereby only differing in their initial xylose catabolic pathway (XI or XR/XDH) were utilized in anaerobic batch fermentations containing 50 g/L xylose (Karhumaa et al., 2007).

Kinetic parameters of XR (Rizzi et al., 1988), XDH (Eliasson et al., 2001) and XI (Brat et al., 2009; Vanbastelaere et al., 1991) were taken from studies using pure enzymes. In addition, kinetic parameters for transport was previously determined (Runquist et al., 2010b) in the exact same background as the strains used for the construction of the model and the strains later constructed for its validation. Finally cell parameters including specific cell surface area (A_{cell}) (Tochampa et al., 2005), cell mass density (p_X) (Tochampa et al., 2005) and permeability coefficient for xylitol (P_{xyt}) (Tochampa et al., 2005) were taken from *Candida mogii* and validated by fitting the models to fermentation data (Karhumaa et al., 2007) (Supplementary Fig. 1A and B).

The first model had XR/XDH and the second had XI as first step in xylose conversion. Table 1 summarizes biochemical reactions and enzymes considered in this study. Based on these reactions a set of ordinary differential equations was used to describe the time dependence of metabolite concentrations. For the strain with the XR/XDH pathway the following equations were used:

$$\frac{d(XYL_e)}{dt} = (-V_{trsp,in} + V_{trsp,out})C_x \quad (1)$$

$$\frac{d(XYL)}{dt} = (V_{trsp,in} - V_{trsp,out})P_x - V_{XR} \quad (2)$$

Table 1
Biochemical reactions used in the construction of the kinetic models. (↔) reversible; (→) irreversible. e=extracellular.

Reaction	Name	Enzymes	Reactant	Product
1 (↔)	Transport	Transporter	Xylose$_e$	Xylose
2 (↔)	XR	Xylose reductase	Xylose	Xylitol
3 (↔)	XDH	Xylitol dehydrogenase	Xylitol	Xylulose
4 (→)	XK	Xylulokinase	Xylulose	Xylulose-5-P
5 (↔)	XYT diff	Transporter	Xylitol	Xylitol$_e$
6 (↔)	XI	Xylose isomerase	Xylose	Xylulose

$$\frac{d(XYT)}{dt} = V_{XR} - V_{XDH} - P_x rt_{xyt} \quad (3)$$

$$\frac{d(XYT_e)}{dt} = rt_{xyt} C_x \quad (4)$$

$$\frac{d(XYLU)}{dt} = V_{XDH} - V_{XK} \quad (5)$$

$$\frac{dC_x}{dt} = -C_x r_x \quad (6)$$

For XI strain the equations were:

$$\frac{d(XYL_e)}{dt} = (-V_{trsp,in} + V_{trsp,out}) C_x \quad (7)$$

$$\frac{d(XYL)}{dt} = (V_{trsp,in} - V_{trsp,out}) P_x - V_{XI} \quad (8)$$

$$\frac{d(XYLU)}{dt} = V_{XI} - V_{XK} \quad (9)$$

$$\frac{dC_x}{dt} = -C_x r_x \quad (10)$$

All enzymatic rate expressions with their respective kinetic parameters are listed in supplementary Table 1. In both models a differential equation that defines cell inactivation over time was added (Eq. (6) for the XR/XDH model and Eq (10) for the XI model). All maximum velocities (V_{max}) were calculated based on the values of enzyme activities in crude extracts. The activities (mmol/h) were multiplied by the total protein content per cell dry weight (CDW) according to Teusink et al. (2000) and by the specific cell volume as previously described (de Koning and van Dam, 1992). For the model of the XR/XDH pathway a reaction for xylitol excretion was included as previously described (Tochampa et al., 2005) and it was validated by fitting xylose consumption and xylitol production to fermentation data from a previously published study using a XR/XDH strain carrying *gre3* deletion and overexpression of the non-oxidative PPP and XK genes (Karhumaa et al., 2007). The simulation correlated with experimental data with an $R^2 = 0.962$ (Supplementary Fig. 1A). Some assumptions were also made to simplify the kinetic analysis:

(I) Initial biomass was 5 g/L (CDW) and it was considered constant since no changes in OD was observed during the experiments.

(II) Intracellular concentrations of ATP and relevant co-factors were assumed to be constant with the following values measured elsewhere under usual fermentation conditions (Hynne et al., 2001; Satrustegui et al., 1983): ATP = 0.534 mM, NADPH = 0.487 mM, $NADP^+$ = 0.0657 mM, NADH = 0.553 mM, NAD^+ = 2.767 mM.

(III) Xylitol production resulting from endogenous yeast reductases (Träff et al., 2002) was disregarded in both models.

(IV) In the XR/XDH model, the xylose reductase reaction (XR) was considered only NADPH dependent even though it also utilizes NADH as cofactor (Eliasson et al., 2001). This is due to the fact that the affinity for NADH is much lower than the affinity for NADPH (Bengtsson et al., 2009) so when both cofactors are present the contribution to the total rate of xylitol formation by the NADH-dependent reaction can be neglected. By assuming that the XR cannot use NADH the complexity of the rate equation could be significantly reduced with only a small underestimation of the reaction rate.

(V) The phosphorylation of xylulose into xylulose-5P coupled with ATP hydrolysis was considered unidirectional and the rate of conversion was assumed to be dependent on the concentrations of xylulose and ATP only.

(VI) In the XI model, the rate equation for the XI reaction was described as a reversible Michaelis–Menten reaction with the following relationship between the forward and reverse reaction velocities: $V_{max}^{XI,r} = 1.3 \times V_{max}^{XI,f}$ as formerly observed (Vanbastelaere et al., 1991). Consequently, an increase in the V_{max} of the forward reaction would give an increase in the maximum velocity of the reverse reaction.

Evaluation of the effect of changing the level of individual enzymes was done by manually increasing or decreasing the activity values (V_{max}) by an order of magnitude of 10, *i.e.* an average value of what can be achieved by gene overexpression/deletion.

2.2. Plasmids, strains and cultivation conditions

Plasmids and strains used in this study are listed in Table 2. *Escherichia coli* DH5α (Life Technologies, Rockville, MD, USA) was used for subcloning prior to yeast transformation. All strains were stored as 20% glycerol stocks in liquid media at −80 °C.

S. cerevisiae strains were plated on YNB-media plates (6.7 g/L YNB w/o amino acids, Difco, Becton, Dickinson and Company,

Table 2
Plasmids and strains used in this study.

Plasmid/strain	Relevant genotype	Reference
Plasmids		
p426TEF	*URA3*, *TEF*p-*CYC1*t	Mumberg et al. (1995)
YIplac128	*LEU2*	Gietz and Sugino (1988)
YIplac204	*TRP1*	Gietz and Sugino (1988)
YIpOB9	*URA3*, *TDH3*p-*XYL1*(K270R)-*CYC1*t, *PGK1*p-*XYL2*-*PGK1*t	Bengtsson (2008)
p426TEF-XiPiromyces	p426, *URA3*, *TEF*p-*xylA*-*CYC1*t	This study
YIpDR1	YIplac128, *TDH3*p-*GXF1*-*CYC1*t, *LEU2*	Runquist et al. (2009)
YIpXKEC	YIplac128, *TDH3*p-*xylB*-*CYC1*t, *LEU2*	This study
YIpGXF1	YIplac204, *TDH3*p- *GXF1*-*CYC1*t, *TRP1*	
Strains		
TMB3042	CEN.PK 2-1C Δ*gre3*, *his3*::*PGK1*p-*XKS1*-*PGK1*t, *TAL1*::*PGK1*p-*TAL1*-*PGK1*t, *TKL1*::*PGK1*p-*TKL1*-*PGK1*t, *RKI1*::*PGK1*p-*RKI1*-*PGK1*t, *RPE1*::*PGK1*p-*RPE1*-*PGK1*t, *trp1, leu2, ura3*.	Karhumaa et al. (2005)
TMB3367	TMB 3042, *trp1*::YIplac204, *leu2*::YIplac128, *ura3*::YIpOB9	This study
TMB3368	TMB 3042, *trp1*::YIplac204, *leu2*::YIpXKEC, *ura3*::YIpOB9	This study
TMB3359	TMB3042, *trp1*::YIplac204, *leu2*::YIplac128, *ura3*:: p426TEFXi	This study
TMB3360	TMB 3042, *trp1*::YIplac204, *leu2*::YIpDR1, *ura3*:: p426TEFXi	This study
TMB3361	TMB 3042, *trp1*::YIplac204, *leu2*::YIpXKEC, *ura3*::p426TEFXi	This study
TMB3362	TMB 3042, *trp1*::YIpGXF1, *leu2*::YIpXKEC, *ura3*::p426TEFXi	This study

Sparks, MD, USA) supplemented with 20 g/L glucose and 20 g/L agar. The amino acids L-tryptophan, L-leucine as well as uracil were added to a final concentration of 76 mg/L when needed. *S. cerevisiae* strains were pre-grown in 1 L Erlenmeyer flasks containing 100 mL YNB-medium (6.7 g/L YNB w/o amino acids, 20 g/L glucose) at 180 rpm and 30 °C for approximately 12 h. Cells were subsequently inoculated at $OD_{620\ nm}$=0.2 in 100 mL YNB-medium supplemented with 50 g/L xylose in 1-L Erlenmeyer flasks and grown at 180 rpm and 30 °C. In anaerobic fermentations 400 mg/L Tween 80 and 10 mg/L ergosterol were added to twice concentrated YNB.

2.3. Strain construction

Standard techniques for DNA manipulation were used as previously described (Sambrook et al., 1989). Restriction and ligation enzymes were purchased from Fermentas (St. Leon-Rot, Germany). Primers were purchased from Eurofins MWG Operon (Ebersberg, Germany). DNA extraction from agarose gels and purification of PCR products were performed with the QIAquick extraction kit (Qiagen, Hilder, Germany). Plasmid DNA was prepared with the Biorad miniprep kit (Hercules, CA, USA). Sequencing was performed at Eurofins MWG Operon (Ebersberg, Germany). Yeast transformation was performed as previously described (Gietz et al., 1995).

The XK encoding gene *xylB* from *E. coli* was amplified by PCR using genomic DNA from strain DH5α (Life Technologies, Rockville, MD, USA), primer forward: 5′ TCC*ACTAGT*ATGTATATCGGGATAGATCTTGGCACC 3′ and reverse: 5′ CCG*GTCGAC*TTACGCCATTAATGGCAGAAGTTGCTG 3′. Restriction sites for *Spe*I and *Sal*I are underlined in primers forward and reverse, respectively. Plasmid YIpDR1 (Runquist et al., 2009) (Table 2) was restricted with the same enzymes used for the PCR product restriction. The fragment of 5.2 kb corresponding to the vector without *GXF1* was purified from agarose gel and used as backbone for the ligation with the restricted PCR-amplified XK gene. After insert confirmation, by sequencing, plasmid YIpXKEC (Table 2) was linearized with *Bbs*I, which cuts in *LEU2* gene prior to plasmid integration.

For construction of YIpGXF1, plasmid YIpDR1 was restricted with *Pst*I and *BamH*I. The fragment of approximately 2.6 kb containing the *TDH3* promoter, the glucose/xylose facilitator *GFX1* gene from *Candida intermedia* and the *CYC1* terminator (Runquist et al., 2009) was ligated into YIplac204 previously restricted with the same enzymes. The resulting plasmid YIpGXF1 (Table 2) was linearized with *Eco*RV, which cuts inside *TRP1* gene, prior to integration into yeast.

XI gene from *Piromyces sp.* was amplified by PCR utilizing plasmid YeplacHXT-XI as template (Karhumaa et al., 2005), primer forward: 5′GGA*GGATCC*ATGGCTAAGGAATATTTTCCACAAATTC 3′ and reverse: 5′ TTG*GAATTC*TTACTGATACATTGCAACAATAGCTTCG 3′. Restriction sites for *BamH*I and *Eco*RI are underlined in primers forward and reverse, respectively. Plasmid p426TEF (Mumberg et al., 1995) and the PCR product were restricted with *BamH*I and *Eco*RI and then ligated. Clones with insert were sequenced prior to yeast transformation.

Construction of recombinant *S. cerevisiae* strains for model validation were done using strain TMB3042 that has the same background as the strain utilized for the model construction, *i.e.* overexpressed genes encoding the non-oxidative PPP enzymes and XK and deleted *GRE3* gene (Table 2). Construction of recombinant strain TMB3368 containing XR/XDH pathway and an extra copy of XK was done by sequential integration of linearized YIplac204 (Gietz and Sugino, 1988), YIpXKEC and plasmid YIpOB09 carrying the XR and XDH genes (Bettiga et al., 2009) . The control strain for the XR/XDH pathway, TMB3367, was constructed by integration of linearized YIplac128 (Gietz and Sugino, 1988) instead of YIpXKEC.

The control strain carrying the XI pathway, TMB3359, was obtained by sequential integration of linearized YIplac204 (Gietz and Sugino, 1988), linearized YIpXKEC and the multicopy plasmid p426TEFXI. For the strains carrying the XI pathway in combination with only transport, or an extra copy of XK, TMB3042 was sequentially transformed with YIplac204, YIpDR1 (TMB3360) or YIpXKEC (TMB3361). Finally both strains were transformed with the multicopy plasmid p426TEFXi. Strain TMB3362, carrying both transport and an extra copy of XK was constructed by sequential yeast transformation with YIpGXF1, YIpXKEC and p426TEFXi.

2.4. Enzyme activities

For enzymatic activity measurements, strains were cultivated in YNB medium with 20 g/L glucose and harvested at stationary phase. Cells were washed twice with distilled water and treated with yeast protein extract solution Y-PER (Pierce, Rockford, IL, USA). XI activity was determined using sorbitol dehydrogenase as previously described (Kuyper et al., 2003) at 30 °C. XK activity was measured by coupling ADP production to NADH oxidation via pyruvate kinase as earlier described (Di Luccio et al., 2007). Variations of XK activity, when compared to previous studies (Karhumaa et al., 2005), may be attributed to the fact that the XK assay is usually not performed at V_{max}, due to the cost of pure xylulose. As a consequence, large differences in protein concentrations will impact the final result. Assays were performed using a spectrophotometer U-2000 (Hitachi, Tokyo, Japan). Protein concentration of cell extracts was determined with Coomassie protein assay reagent (Pierce, Rockford, USA) according to the manufacturer's instructions. Enzyme assays were performed in three biological replicates.

2.5. Anaerobic xylose fermentation

Pre-cultures were grown aerobically in 100 mL of YNB medium with 20 g/L glucose. Cells were harvested in late exponential phase and washed twice in sterile water. Anaerobic fermentation was performed in 50 mL bottles containing 48 mL YNB medium with 50 g/L xylose, 0.01 g/L ergosterol, 0.4 g/L Tween 80, 5 g/L CDW and a layer of sterile mineral oil to reduce oxygen transfer. Bottles were supplied with rubbers stoppers containing cannulae for gas outlet and sampling. The temperature was 30 °C and magnetic stirrers provided agitation. Substrate consumption and product formation were monitored by sampling during 100 h. Experiments were performed in biological triplicates.

2.6. Aerobic growth on xylose

Pre-cultures were grown in YNB medium with 20 g/L glucose and harvested in late exponential phase. Cells were washed twice in sterile water and inoculated in YNB medium containing 50 g/L xylose to a starting OD_{620} of 0.2. Specific aerobic growth rates were determined in 50 mL culture in 500 mL baffled shake flasks at 30 °C and 200 rpm (Gallenkamp INR200, Leicester, UK). Growth rates were determined in triplicate.

2.7. Analysis of fermentation products

Substrate and product concentrations were determined by high-performance liquid chromatography (HPLC; waters, Milford, MA, USA) with Aminex HPX-87 H ion exchange column (Bio-Rad, Hercules, CA, USA) using 5 mM H_2SO_4 as mobile phase and refractive index detection (RID-6A, Shimadzu, Kyoto, Japan). The temperature and flow rate were 45 °C and 0.6 mL/min, respectively.

In addition to ethanol, only xylitol, glycerol and acetate were detected as products. Dry weight was determined in triplicates. Nitrocellulose filters with 0.45 μm pore size were dried in a microwave oven for 3 min and left to cool down in a dessicator. Filters were weighed prior to filtering a known volume of cell culture. Dry weight was the difference between the dried filter with and without cells.

3. Results

3.1. Kinetic model

Kinetic models were constructed for the two xylose catabolic pathways. The models included the steps from xylose transport to the phosphorylation of xylulose (Fig. 1, Table 1 and supplementary Table 1) thus reflecting the only metabolic differences between the otherwise isogenic strains (Karhumaa et al., 2007). The models for the XR-XDH and XI pathway were constructed using available cell parameters including specific cell surface area (A_{cell}) (Tochampa et al., 2005), cell mass density (p_X) (Tochampa et al., 2005), permeability coefficient for xylitol (P_{xyt}) (Tochampa et al., 2005) and maximum velocity (V_{max}) for xylose transport (Runquist et al., 2010b). Those were validated concomitant with calculated V_{max} for XR, XDH, XI and XK by fitting the models to fermentation data (Karhumaa et al., 2007) (Supplementary Fig. 1A and B).The calculated values as well as the fitted ones for V_{max} of transport, XR, XDH, XK and XI are listed in the supplementary Table 1.

The XR/XDH model was used to *in silico* simulate minimal xylitol formation with 10-fold changes of individual V_{max} values, which were assumed to correspond to an equal change of protein level (Fig. 2A). The maximum velocity of XDH (V_{max}^{XDH}) did not affect xylitol formation in the range of activities investigated. In contrast xylitol formation was reduced both when the maximum velocity of the transporter (V_{max}^{trsp}) and the maximum velocity of XR (V_{max}^{XR}) were decreased (Fig. 2A), but this also reduced the overall xylose consumption (Fig. 2B). The most significant effect was observed when changing the maximum velocity of XK (V_{max}^{XK}): xylitol production, decreased by 90% when V_{max}^{XK} was increased 10 fold (Fig. 2A), without affecting the total xylose consumption (Fig. 2B).

When using the XI model to simulate how V_{max} of xylose transport and XI, respectively, influenced the total xylose consumption, it was found that neither reaction had a significant effect on xylose consumption (Fig. 2C). In fact, V_{max}^{XI} only affected the total xylose consumption when it decreased below 20% of the fitted value (data not shown). However, similar to the XR-XDH model the largest increase of the total xylose consumption, 63%, was observed when the maximum activity of *XK* (V_{max}^{XK}) was increased 10 fold.

3.2. "in vivo" validation of the XR-XDH model

The predictions of the *in silico* simulations were validated by constructing a number of recombinant *S. cerevisiae* strains having exactly the same background (*gre3* deletion, overexpressed non-oxidative PPP genes and overexpressed XK gene) as the ones utilized for *in silico* simulations (Karhumaa et al., 2007). The only difference concerned XR that carried the K270R mutation resulting in increased affinity for NADH (Bengtsson et al., 2009). Thus the control strain, TMB3367 had overexpressed endogenous XK encoding gene, non-oxidative PPP genes and mutated XR(K270R) in addition to deletion of *GRE3* gene. TMB3368 had exactly the same background than TMB3367 but with an additional copy of a XK encoding gene integrated on the genome (Table 2). The *xylB* gene encoding *E. coli* XK was chosen for the integration because the reported turnover number (k_{cat}) for *S. cerevisiae* XK is only 0.64/s (Richard et al., 2000), whereas that of *E. coli* is 255/s (Di Luccio et al., 2007) despite similar K_m values for both xylulose and ATP. In addition changing the source of XK encoding gene have been shown beneficial in *E. coli* recombinant strains growing on

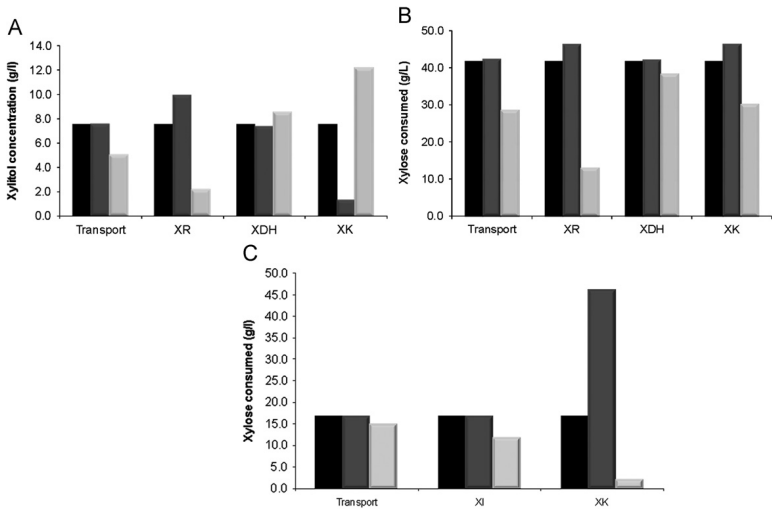

Fig. 2. *In silico* evaluation of individual V_{max} on xylitol formation (A) and total xylose consumption (B) in the XR/XDH kinetic model and total xylose consumption in the XI model (C). Black bars represent values given by the kinetic model; Grey and white bars represent tenfold increased and decreased enzyme activity, respectively.

xylose (Akinterinwa and Cirino, 2009). A doubling of the XK activity (Supplementary Table 2) confirmed the correct expression of *xylB* in *S. cerevisiae*.

The influence of overexpressing *E. coli* XK encoding gene was assessed by aerobic growth and by anaerobic batch fermentation (Fig. 3, Table 3). The aerobic growth rate of the strain overexpressing *xylB* increased 35%. Under anaerobic conditions *xylB* overexpression reduced the xylose consumption rate slightly, resulting in 14% less xylose being consumed at the end of the fermentation than for the control strain, TMB3367 (Fig. 3A). But at the end of the fermentation the final ethanol concentration for the two strains was similar (Fig. 3B), which corresponded to an increased ethanol yield by about 7% for the XK overexpressing strain when calculated on consumed xylose. The major difference between the strains was xylitol and glycerol formation. Overexpressing the *E. coli* XK gene led to a 6-fold reduction of xylitol formation corresponding to about 1% of total xylose consumed (Fig. 3C). The reduced xylitol formation translated into increased glycerol formation by strain TMB3368, two times more than what was produced by the control strain, TMB3367 (Fig. 3D and Table 3).

3.3. In vivo validation of the XI model

Similar to the XR-XDH model the XI model identified the XK reaction as limiting rather than xylose transport and XI. However, for the *in vivo* validation of the XI model we investigated both the XK reaction and the xylose transport in order to test the robustness of the model. It was not technically possible to *in vivo* corroborate that higher XI level does not positively affect xylose utilization because the XI encoding gene was already cloned into a multicopy plasmid and under the regulation of a strong promoter.

Four recombinant strains, all harbouring the *Piromyces sp.* XI gene overexpressed in the same strain background as the one used for the validation of the XR-XDH model, were constructed: (i) the control strain TMB3359, (ii) strain TMB3360 where the xylose transport capacity was increased by overexpressing the heterologous transporter gene *GFX1* from *C. intermedia* (Runquist

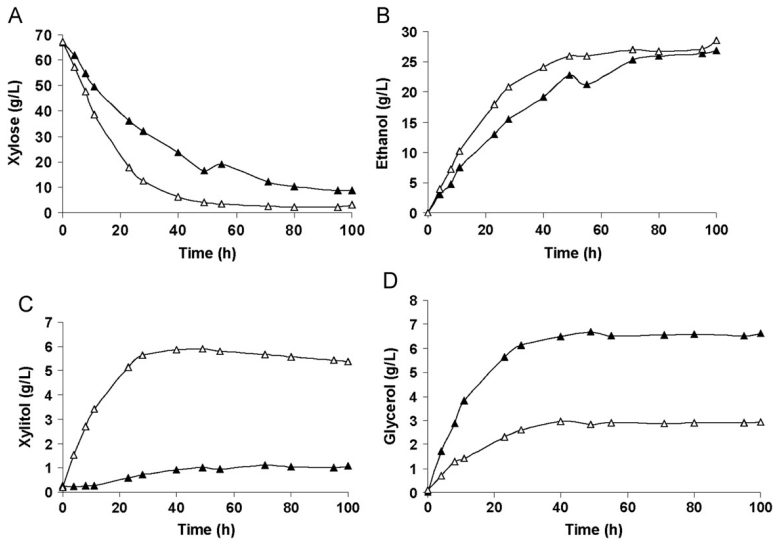

Fig. 3. Anaerobic xylose batch fermentation with the control strain TMB3367 (△) and strain TMB3368 overexpressing *E. coli* XK encoding gene *xylB* (▲) showing xylose consumption (A) (g L h^{-1}) as well as ethanol (B), xylitol (C) and glycerol (D) formation (g L^{-1}). Experiments were performed in triplicates, with less than 10% variation between replicates.

Table 3
Aerobic maximum specific growth rate on xylose (h^{-1}). Anaerobic substrate consumption (g/L) and product yield (g product/g total consumed xylose) in batch fermentation with YNB medium containing 60 g/L xylose. Aerobic growth rates were determined from independent triplicates ($p < 0.05$).

Strain	Main characteristic	Aerobic	Anaerobic			
		μ_{max} (h^{-1})	Xylose consumed	Xylitol yield	Ethanol yield	Glycerol yield
TMB3367	XR/XDH-CTRL	0.13 ± 0.02	64.4 ± 0.6	0.09 ± 0.01	0.43 ± 0.01	0.075 ± 0.02
TMB3368	XR/XDH+XK *E. coli*	0.20 ± 0.01	56.7 ± 2.1	0.01 ± 0.01	0.46 ± 0.01	0.125 ± 0.006
TMB3359	Xi- CTRL	0.070 ± 0.007	17.5 ± 1.0	0.06 ± 0.01	0.42 ± 0.04	0.045 ± 0.012
TMB3360	Xi+Transport	0.081 ± 0.003	18.7 ± 0.5	0.06 ± 0.01	0.40 ± 0.07	0.086 ± 0.008
TMB3361	Xi+XK *E. coli*	0.089 ± 0.002	24.1 ± 0.8	0.05 ± 0.01	0.41 ± 0.05	0.044 ± 0.016
TMB3362	Xi+transport+XK *E. coli*	0.093 ± 0.008	27.9 ± 0.7	0.03 ± 0.01	0.43 ± 0.07	0.023 ± 0.005

et al., 2009), (iii) strain TMB3361, where the XK activity increased by overexpression of the *E. coli* XK encoding gene and (iv) strain TMB3362 combining high transport capacity and high XK activity (Table 2). We confirmed that all four strains displayed similar levels of XI activity, whereas the XK activity was increased in strains TMB3361 and TMB3362 (Supplementary Table 2).

The *in silico* predictions of the XI model were verified *in vivo* by aerobic growth (Fig. 4) and anaerobic fermentation (Fig. 5) on xylose. The aerobic growth rate increased for the two strains with increased XK activity (Fig. 4). The strain overexpressing the heterologous xylose transporter gene *GXF1*, TMB3360, had a longer lag phase but eventually had a growth rate similar to that of the control strain, TMB3359. The growth rate of the strain overexpressing the *E. coli* XK gene increased 21% ($p_{value}=0.041$) whereas the strain harbouring both the heterologous transporter and the *E. coli* XK gene, TMB3362, had the shortest lag phase and a 24% ($p_{value}=0.008$) higher growth rate than the control strain (Table 3). The final OD of strain TMB3361, harbouring the integrated copy of the *E. coli* XK gene, was the same as for the control strain TMB3359. However, for strains TMB3360 and TMB3362, with increased transport capacity and the combination of increased transport and XK activity, respectively, the final OD was about 20% higher than that of the control strain.

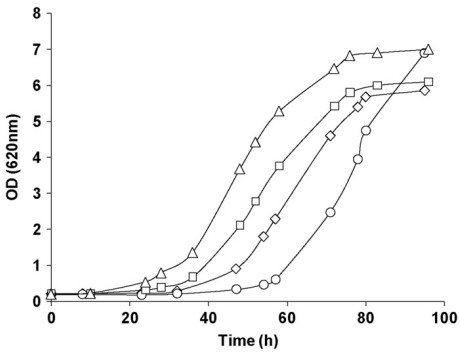

Fig. 4. Aerobic growth of XI strains in mineral media containing 50 g/L xylose. Control strain TMB3359 (⋄), strain TMB3360 overexpressing *GXF1* transporter gene from *C. intermedia* (○), strain TMB3361 overexpressing *E. coli* XK gene *xylB* (□) and strain TMB3362 overexpressing *xylB* and *GXF1* genes (△). Experiments were performed in triplicates, with less than 10% variation between triplicates.

Anaerobic batch fermentation with the recombinant XI-based *S. cerevisiae* strains confirmed that overexpression of the *GXF1* transporter gene *per se* did neither increase xylose consumption nor ethanol formation (Table 3, Fig. 5). In contrast, the total (100 h) xylose consumption increased by 27% and 37% when overexpressing the *E. coli* XK gene, alone or together with the overexpression of the *GXF1* transporter, respectively. The ethanol yield was about the same for the four XI-strains (Table 3). However, since strains TMB3361 (higher XK activity) and TMB3362 (higher XK and transport capacity) consumed more xylose these two strains produced 1.3 and 2 times more ethanol, respectively (Fig. 5).

4. Discussion

The present study demonstrates, for the first time, how *in silico* simulations can be used to identify rate-controlling reactions in the initial xylose catabolic pathways heterologously expressed in recombinant *S. cerevisiae* strains. Kinetic models were constructed for the initial XR-XDH and XI pathways using literature data (Eliasson et al., 2001; Rizzi et al., 1988; Tochampa et al., 2005; Vanbastelaere et al., 1991) and experimental data from xylose fermentation (Karhumaa et al., 2007). Both models identified the XK activity as a rate-controlling step in the recombinant *S. cerevisiae* strains, which have been engineered for xylose utilization with a combination of various traits (increased level of the non-oxidative PPP enzymes, increased level of the endogenous XK, deletion of *GRE3* gene and more balanced cofactor utilization between XR and XDH or high XI level). The rate controlling function of the XK reaction was experimentally verified in strains expressing the two different initial xylose catabolic pathways.

The endogenous XK activity has previously been demonstrated to limit xylose utilization (Ho et al., 1998). Expression of the *S. cerevisiae* XK gene from an episomal multicopy plasmid confirmed the importance of the XK activity (Johansson et al., 2001). It doubled the ethanol yield and reduced xylitol formation by 70%, however, at the expense of a 50% reduction of the xylose consumption rate (Johansson et al., 2001). Subsequently the expression of different levels of *S. cerevisiae* (Lee et al., 2003) and *P. stipitis* (Jin et al., 2003) XK encoding genes corroborated that the xylose consumption rate was reduced when the XK gene was expressed from an episomal multicopy plasmid, whereas the xylulose consumption rate increased almost six times when the

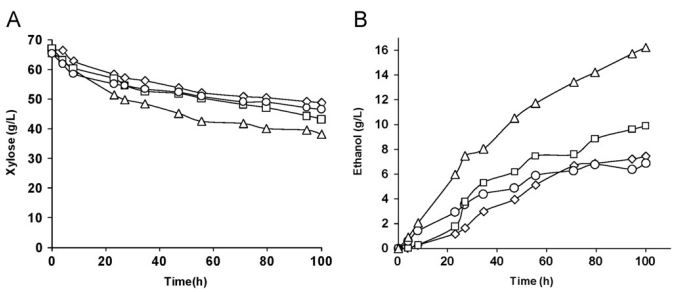

Fig. 5. Anaerobic xylose batch fermentation showing xylose consumption ($g\,L^{-1}$) (A) and ethanol formation ($g\,L^{-1}$) (B). Control strain TMB3359 (⋄), strain TMB3360 overexpressing *GXF1* transporter gene from *C. intermedia* (○), strain TMB3361 overexpressing *E. coli* XK gene *xylB* (□) and strain TMB3362 overexpressing *xylB* and *GXF1* genes (△). Experiments were performed in triplicates, with less than 10% variation between replicates.

S. cerevisiae XK encoding gene was instead chromosomally integrated (Lee et al., 2003). Moreover high levels of endogenous XK have been shown to reduce growth on high concentrations of xylose (Van Vleet et al., 2008). Therefore an integrated copy of the XK encoding gene has been considered sufficient to establish a xylose catabolic pathway in *S. cerevisiae* (Karhumaa et al., 2005; Kuyper et al., 2004). Nonetheless the present study demonstrates that XK is again limiting in the current generation of strains that combine high non-oxidative PPP activity, deletion of the *GRE3* gene and a more balanced cofactor utilization between XR and XDH or a high XI level. In the XR-XDH strain, the overexpression of *E. coli* XK encoding gene led to a reduction of xylitol yield from 0.09 to 0.01 g/g consumed xylose, which is even less than obtained with XI strains (Table 3) (Brat et al., 2009; Karhumaa et al., 2007; Madhavan et al., 2009, 2008).

When the XK encoding gene was overexpressed in the XI strain the total xylose consumption increased by a factor of 27% and when higher XK was combined with higher transport capacity xylose consumption increased by a factor of 37%. This agrees with the fact that the isomerization reaction thermodynamically favors xylose formation at 30 °C (Tewari et al., 1985) and that xylulose must be continuously converted to xylulose-5-P to maintain xylose consumption. Indeed, XI strains with native levels of XK have been reported both to secrete xylulose (van Maris et al., 2007) and to consume only 10% of the available xylose (Madhavan et al., 2008).

Whereas the kinetic models proved to be valuable for the identification of a rate limiting activity, the models were designed only to cover the initial xylose catabolic pathways. This could, for instance, explain why the significantly lower xylitol yield in the XR-XDH strain was not accompanied by a higher ethanol yield. Instead the glycerol yield increased about two fold. Since fermentation experiments were performed with a high cell density, biomass formation was hardly observed and increased glycerol could not result from a need to regenerate the excess of NADH formed during biosynthesis (Van Dijken and Scheffers, 1986). Instead the combination of increased XK activity and higher flux through the non-oxidative part of the PPP may have increased dihydroxyacetone phosphate (DHAP) formation from glyceraldehyde 3-phosphate (GA3P), which increased the flux towards glycerol formation. Moreover, overexpression of an extra copy of XK encoding gene resulted in a slight reduction of the xylose consumption rate in the XR-XDH strain under anaerobic conditions, which was not predicted by the model. This has been previously observed elsewhere (Jin et al., 2003; Johansson et al., 2001; Lee et al., 2003) and it has been explained due to the increase in the rate of ATP required for sugar phosphorylation (Becker and Boles, 2003; Teusink et al., 1998). The current model did not account for any reduction in xylose consumption because ATP levels were fixed and assumed not to be limiting.

The *in vivo* demonstration of control by the xylose transport reaction illustrated another limitation of the constructed kinetic models. Even after the XK level had been up-regulated, *in silico* simulations were not able to identify any rate control of the xylose transport step in the XI strain (data not shown). Xylose transport capacity has been considered limiting only when the intracellular rate of xylose catabolism has already been improved (Gárdonyi et al., 2003; Runquist et al., 2009), which has been experimentally corroborated for strains with increased XK activity (Madhavan et al., 2008) as well as strains constructed in the current study. Moreover discrepancies between the model and the *in vivo* result may be caused by the conditions under which enzyme activities were measured. Enzyme activities were measured in cell extracts under optimal "*in vitro*" conditions and sometimes with in coupled assays, which do not necessarily reflect the "*in vivo*" conditions (Teusink et al., 2000).

The model also predicted levels of XK, not XI, to be rate-controlling. This supports previous experiments from our group (Karhumaa et al., 2007), where a high and similar level of XI activity as reported by others (Kuyper et al., 2003, 2004) did not results in the same high xylose consumption rate in strains that were, in theory, isogenic. Unfortunately the activity levels of XK and PPP enzymes were not reported, so a comparison could not be made. Xylose fermenting XI strains that are considerably better than those constructed in the current investigation have also been generated through extensive adaptation, but so far the molecular bases for the improvement of these strains are also not available in the public domain (Brat et al., 2009; Kuyper et al., 2005; Madhavan et al., 2009). The present rationally engineered XI strains consumed at most half of the available xylose when both XK and the transport capacity had been increased, suggesting that the XK activity in recombinant strain with XI pathway may have to be further increased. Alternatively there may be one or more rate limiting reactions downstream of XK, since these were not included in the kinetic model. The current models could serve as a base for the construction of more extended kinetic models covering xylose catabolism beyond the initial reactions.

5. Conclusion

In this study, kinetic modelling was successfully used as a designing tool for strains with improved xylose utilization. It resulted in the construction of (i) recombinant XR-XDH strains that produced xylitol concentrations equivalent to that of XI strains and (ii) 59% increase total xylose consumption in recombinant XI strains. In both cases, higher levels of XK were necessary, whereas a combination of increased transport and XK activity proved to be the most advantageous in the XI strain. The constructed models may serve as a base for the construction of more complex models that take into account the steps downstream of XK.

Acknowledgments

Bärbel Hahn–Hägerdal and Elke Lohmeier–Vogel are acknowledged for critically reading the manuscript. This work was financed by the Swedish Research Council (VR) and the Swedish Energy Agency (Energimyndigheten).

Appendix A. Supporting information

Supplementary data associated with this article can be found in the online version at doi:10.1016/j.ymben.2011.05.005.

References

Akinterinwa, O., Cirino, P.C., 2009. Heterologous expression of D-xylulokinase from *Pichia stipitis* enables high levels of xylitol production by engineered *Escherichia coli* growing on xylose. Metab. Eng. 11, 48–55.

Amore, R., Hollenberg, C.P., 1989. Xylose isomerase from *Actinoplanes missouriensis*: primary structure of the gene and the protein. Nucl. Acids Res. 17, 7515.

Becker, J., Boles, E., 2003. A modified *Saccharomyces cerevisiae* strain that consumes L-Arabinose and produces ethanol. Appl. Environ. Microbiol. 69, 4144–4150.

Bengtsson, O., 2008. Genetic traits beneficial for xylose utilization by recombinant *Saccharomyces cerevisiae* Doctoral Thesis. Division of Applied Microbiology. Lund University, Lund.

Bengtsson, O., Hahn-Hägerdal, B., Gorwa-Grauslund, M.F., 2009. Xylose reductase from *Pichia stipitis* with altered coenzyme preference improves ethanolic xylose fermentation by recombinant *Saccharomyces cerevisiae*. Biotechnol. Biofuels 2, 9.

Bettiga, M., Bengtsson, O., Hahn-Hägerdal, B., Gorwa-Grauslund, M.F., 2009. Arabinose and xylose fermentation by recombinant *Saccharomyces cerevisiae* expressing a fungal pentose utilization pathway. Microb. Cell Fact. 8, 40.

Brat, D., Boles, E., Wiedemann, B., 2009. Functional expression of a bacterial xylose isomerase in *Saccharomyces cerevisiae*. Appl. Environ. Microbiol. 75, 2304–2311.

de Koning, W., van Dam, K., 1992. A method for the determination of changes of glycolytic metabolites in yeast on a subsecond time scale using extraction at neutral pH. Anal. Biochem. 204, 118–123.

Di Luccio, E., Petschacher, B., Voegtli, J., Chou, H.T., Stahlberg, H., Nidetzky, B., Wilson, D.K., 2007. Structural and kinetic studies of induced fit in xylulose kinase from *Escherichia coli*. J. Mol. Biol. 365, 783–798.

Eliasson, A., Christensson, C., Wahlbom, C.F., Hahn-Hägerdal, B., 2000. Anaerobic xylose fermentation by recombinant *Saccharomyces cerevisiae* carrying XYL1, XYL2, and XKS1 in mineral medium chemostat cultures. Appl. Environ. Microbiol. 66, 3381–3386.

Eliasson, A., Hofmeyr, J.H.S., Pedler, S., Hahn-Hägerdal, B., 2001. The xylose reductase/xylitol dehydrogenase/xylulokinase ratio affects product formation in recombinant xylose-utilising *Saccharomyces cerevisiae*. Enzyme Microbial Technol. 29, 288–297.

Gárdonyi, M., Hahn-Hägerdal, B., 2003. The *Streptomyces rubiginosus* xylose isomerase is misfolded when expressed in *Saccharomyces cerevisiae*. Enzy. Microbial. Technol. 32, 252–259.

Gárdonyi, M., Jeppsson, M., Líden, G., Gorwa-Grauslund, M.F., Hahn-Hägerdal, B., 2003. Control of xylose consumption by xylose transport in recombinant *Saccharomyces cerevisiae*. Biotechnol. Bioeng. 82, 818–824.

Gietz, R.D., Schiestl, R.H., Willems, A.R., Woods, R.A., 1995. Studies on the transformation of intact yeast cells by the LiAc/SS-DNA/PEG procedure. Yeast 11, 355–360.

Gietz, R.D., Sugino, A., 1988. New yeast-*Escherichia coli* shuttle vectors constructed with in vitro mutagenized yeast genes lacking six-base pair restriction sites. Gene 74, 527–534.

Ho, N.W., Chen, Z., Brainard, A.P., 1998. Genetically engineered *Saccharomyces* yeast capable of effective cofermentation of glucose and xylose. Appl. Environ. Microbiol. 64, 1852–1859.

Hynne, F., Dano, S., Sorensen, P.G., 2001. Full-scale model of glycolysis in *Saccharomyces cerevisiae*. Biophys. Chem. 94, 121–163.

Jeppsson, M., Bengtsson, O., Franke, K., Lee, H., Hahn-Hägerdal, B., Gorwa-Grauslund, M.F., 2006. The expression of a *Pichia stipitis* xylose reductase mutant with higher K(M) for NADPH increases ethanol production from xylose in recombinant *Saccharomyces cerevisiae*. Biotechnol. Bioeng. 93, 665–673.

Jin, Y.S., Ni, H., Laplaza, J.M., Jeffries, T.W., 2003. Optimal growth and ethanol production from xylose by recombinant *Saccharomyces cerevisiae* require moderate D-xylulokinase activity. Appl. Environ. Microbiol. 69, 495–503.

Johansson, B., Christensson, C., Hobley, T., Hahn-Hägerdal, B., 2001. Xylulokinase overexpression in two strains of *Saccharomyces cerevisiae* also expressing xylose reductase and xylitol dehydrogenase and its effect on fermentation of xylose and lignocellulosic hydrolysate. Appl. Environ. Microbiol. 67, 4249–4255.

Karhumaa, K., Garcia-Sanchez, R., Hahn-Hägerdal, B., Gorwa-Grauslund, M.F., 2007. Comparison of the xylose reductase-xylitol dehydrogenase and the xylose isomerase pathways for xylose fermentation by recombinant *Saccharomyces cerevisiae*. Microb. Cell Fact 6, 5.

Karhumaa, K., Hahn-Hägerdal, B., Gorwa-Grauslund, M.F., 2005. Investigation of limiting metabolic steps in the utilization of xylose by recombinant *Saccharomyces cerevisiae* using metabolic engineering. Yeast 22, 359–368.

Kuyper, M., Harhangi, H.R., Stave, A.K., Winkler, A.A., Jetten, M.S., de Laat, W.T., den Ridder, J.J., Op den Camp, H.J., van Dijken, J.P., Pronk, J.T., 2003. High-level functional expression of a fungal xylose isomerase: the key to efficient ethanolic fermentation of xylose by *Saccharomyces cerevisiae*? FEMS Yeast Res. 4, 69–78.

Kuyper, M., Hartog, M.M., Toirkens, M.J., Almering, M.J., Winkler, A.A., van Dijken, J.P., Pronk, J.T., 2005. Metabolic engineering of a xylose-isomerase-expressing *Saccharomyces cerevisiae* strain for rapid anaerobic xylose fermentation. FEMS Yeast Res. 5, 399–409.

Kuyper, M., Winkler, A.A., van Dijken, J.P., Pronk, J.T., 2004. Minimal metabolic engineering of *Saccharomyces cerevisiae* for efficient anaerobic xylose fermentation: a proof of principle. FEMS Yeast Res. 4, 655–664.

Lee, T.H., Kim, M.D., Park, Y.C., Bae, S.M., Ryu, Y.W., Seo, J.H., 2003. Effects of xylulokinase activity on ethanol production from D-xylulose by recombinant *Saccharomyces cerevisiae*. J. Appl. Microbiol. 95, 847–852.

Madhavan, A., Tamalampudi, S., Srivastava, A., Fukuda, H., Bisaria, V.S., Kondo, A., 2009. Alcoholic fermentation of xylose and mixed sugars using recombinant *Saccharomyces cerevisiae* engineered for xylose utilization. Appl. Microbiol. Biotechnol. 82, 1037–1047.

Madhavan, A., Tamalampudi, S., Ushida, K., Kanai, D., Katahira, S., Srivastava, A., Fukuda, H., Bisaria, V.S., Kondo, A., 2008. Xylose isomerase from polycentric fungus *Orpinomyces*: gene sequencing, cloning, and expression in *Saccharomyces cerevisiae* for bioconversion of xylose to ethanol. Appl. Microbiol. Biotechnol. 82, 1067–1078.

Matsushika, A., Watanabe, S., Kodaki, T., Makino, K., Inoue, H., Murakami, K., Takimura, O., Sawayama, S., 2008. Expression of protein engineered $NADP^+$-dependent xylitol dehydrogenase increases ethanol production from xylose in recombinant *Saccharomyces cerevisiae*. Appl. Microbiol. Biotechnol. 81, 243–255.

Moes, C.J., Pretorius, I.S., vanZyl, W.H., 1996. Cloning and expression of the *Clostridium thermosulfurogenes* D-xylose isomerase gene (xylA) in *Saccharomyces cerevisiae*. Biotechnol. Lett. 18, 269–274.

Mumberg, D., Müller, R., Funk, M., 1995. Yeast vectors for the controlled expression of heterologous proteins in different genetic backgrounds. Gene 156, 119–122.

Petschacher, B., Nidetzky, B., 2008. Altering the coenzyme preference of xylose reductase to favor utilization of NADH enhances ethanol yield from xylose in a metabolically engineered strain of *Saccharomyces cerevisiae*. Microb. Cell Fact 7, 9.

Pitkanen, J.P., Aristidou, A., Salusjarvi, L., Ruohonen, L., Penttila, M., 2003. Metabolic flux analysis of xylose metabolism in recombinant *Saccharomyces cerevisiae* using continuous culture. Metabolic Eng. 5, 16–31.

Richard, P., Toivari, M.H., Penttila, M., 2000. The role of xylulokinase in *Saccharomyces cerevisiae* xylulose catabolism. FEMS Microbiol. Lett. 190, 39–43.

Rizzi, M., Erlemann, P., Buithanh, N.A., Dellweg, H., 1988. Xylose Fermentation by Yeasts .4. Purification and Kinetic-Studies of Xylose Reductase from *Pichia-Stipitis*. Appl. Microbiol. Biotechnol. 29, 148–154.

Rudolf, A., Karhumaa, K., Hahn-Hägerdal, B., 2009. Ethanol production from traditional and emerging raw materials. In: Satyanarayana, T., Kunze, G. (Eds.), Yeast Biotechnology: Diversity and Applications. Springer, Netherlands.

Runquist, D., Fonseca, C., Rådström, P., Spencer-Martins, I., Hahn-Hägerdal, B., 2009. Expression of the Gxf1 transporter from *Candida intermedia* improves fermentation performance in recombinant xylose-utilizing *Saccharomyces cerevisiae*. Appl. Microbiol. Biotechnol. 82, 123–130.

Runquist, D., Hahn-Hägerdal, B., Bettiga, M., 2010a. Increased ethanol productivity in xylose-utilizing *Saccharomyces cerevisiae* via a randomly mutagenized xylose reductase. Appl. Environ. Microbiol. 76, 7796–7802.

Runquist, D., Hahn-Hägerdal, B., Rådström, P., 2010b. Comparison of heterologous xylose transporters in recombinant *Saccharomyces cerevisiae*. Biotechnol. Biofuels 3, 5.

Sambrook, J., Fritch, E., Maniatis, T., 1989. Molecular Cloning: A Laboratory Manual, 2nd ed. Cold Spring harbor Laboratory Press, Cold Spring Harbor, New York.

Sarthy, A.V., McConaughy, B.L., Lobo, Z., Sundstrom, J.A., Furlong, C.E., Hall, B.D., 1987. Expression of the *Escherichia coli* xylose isomerase gene in *Saccharomyces cerevisiae*. Appl. Environ. Microbiol. 53, 1996–2000.

Satrustegui, J., Bautista, J., Machado, A., 1983. NADPH/$NADP^+$ ratio: regulatory implications in yeast glyoxylic acid cycle. Mol. Cell Biochem. 51, 123–127.

Schmidt, H., Jirstrand, M., 2006. Systems biology toolbox for MATLAB: a computational platform for research in systems biology. Bioinformatics 22, 514–515.

Sonderegger, M., Jeppsson, M., Hahn-Hägerdal, B., Sauer, U., 2004. Molecular basis for anaerobic growth of *Saccharomyces cerevisiae* on xylose, investigated by global gene expression and metabolic flux analysis. Appl. Environ. Microbiol. 70, 2307–2317.

Teusink, B., Passarge, J., Reijenga, C.A., Esgalhado, E., van der Weijden, C.C., Schepper, M., Walsh, M.C., Bakker, B.M., van Dam, K., Westerhoff, H.V., Snoep, J.L., 2000. Can yeast glycolysis be understood in terms of in vitro kinetics of the constituent enzymes? Testing biochemistry. Eur. J. Biochem. 267, 5313–5329.

Teusink, B., Walsh, M.C., van Dam, K., Westerhoff, H.V., 1998. The danger of metabolic pathways with turbo design. Trends Biochem. Sci. 23, 162–169.

Tewari, Y.B., Steckler, D.K., Goldberg, R.N., 1985. Thermodynamics of the Conversion of Aqueous Xylose to Xylulose. Biophys. Chem. 22, 181–185.

Tochampa, W., Sirisansaneeyakul, S., Vanichsriratana, W., Srinophakun, P., Bakker, H.H.C., Chisti, Y., 2005. A model of xylitol production by the yeast *Candida mogii*. Bioproc. Biosys. Eng. 28, 175–183.

Träff, K.L., Jönsson, L.J., Hahn-Hägerdal, B., 2002. Putative xylose and arabinose reductases in *Saccharomyces cerevisiae*. Yeast 19, 1233–1241.

Träff, K.L., Otero Cordero, R.R., van Zyl, W.H., Hahn-Hägerdal, B., 2001. Deletion of the GRE3 aldose reductase gene and its influence on xylose metabolism in recombinant strains of *Saccharomyces cerevisiae* expressing the xylA and XKS1 genes. Appl. Environ. Microbiol. 67, 5668–5674.

van Maris, A.J., Winkler, A.A., Kuyper, M., de Laat, W.T., van Dijken, J.P., Pronk, J.T., 2007. Development of efficient xylose fermentation in *Saccharomyces cerevisiae*: xylose isomerase as a key component. Adv Biochem. Eng. Biotechnol. 108, 179–204.

Van Vleet, J.H., Jeffries, T.W., Olsson, L., 2008. Deleting the para-nitrophenyl phosphatase (pNPPase), PHO13, in recombinant *Saccharomyces cerevisiae* improves growth and ethanol production on D-xylose. Metabolic Eng. 10, 360–369.

Vanbastelaere, P., Vangrysperre, W., Kerstershilderson, H., 1991. Kinetic-studies of Mg^{2+}-activated, Co^{2+}-activated and Mn^{2+}-activated D-xylose isomerases. Biochem. J. 278, 285–292.

Van Dijken, J.P., Scheffers, W.A., 1986. Redox balances in the metabolism of sugars by yeasts. Fems Microbiol. Rev. 32, 199–224.

Wahlbom, C.F., Eliasson, A., Hahn-Hägerdal, B., 2001. Intracellular fluxes in a recombinant xylose-utilizing *Saccharomyces cerevisiae* cultivated anaerobically at different dilution rates and feed concentrations. Biotechnol. Bioeng. 72, 289–296.

Walfridsson, M., Bao, X., Anderlund, M., Lilius, G., Bülow, L., Hahn-Hägerdal, B., 1996. Ethanolic fermentation of xylose with *Saccharomyces cerevisiae* harboring the *Thermus thermophilus* xylA gene, which expresses an active xylose (glucose) isomerase. Appl. Environ. Microbiol. 62, 4648–4651.

Watanabe, S., Abu Saleh, A., Pack, S.P., Annaluru, N., Kodaki, T., Makino, K., 2007. Ethanol production from xylose by recombinant *Saccharomyces cerevisiae* expressing protein-engineered NADH-preferring xylose reductase from *Pichia stipitis*. Microbiology 153, 3044–3054.

Wisselink, H.W., Cipollina, C., Oud, B., Crimi, B., Heijnen, J.J., Pronk, J.T., van Maris, A.J., 2010. Metabolome, transcriptome and metabolic flux analysis of arabinose fermentation by engineered Saccharomyces cerevisiae. Metab. Eng. 12, 537–551.

Zeng, Q.K., Du, H.L., Wang, J.F., Wei, D.Q., Wang, X.N., Li, Y.X., Lin, Y., 2009. Reversal of coenzyme specificity and improvement of catalytic efficiency of *Pichia stipitis* xylose reductase by rational site-directed mutagenesis. Biotechnol. Lett. 31 (7), 1025–1029.

Paper II

Bergdahl et al. Biotechnology for Biofuels 2012, 5:34
http://www.biotechnologyforbiofuels.com/content/5/1/34

Biotechnology for Biofuels

RESEARCH Open Access

Dynamic metabolomics differentiates between carbon and energy starvation in recombinant *Saccharomyces cerevisiae* fermenting xylose

Basti Bergdahl[1*], Dominik Heer[2], Uwe Sauer[2], Bärbel Hahn-Hägerdal[1] and Ed WJ van Niel[1]

Abstract

Background: The concerted effects of changes in gene expression due to changes in the environment are ultimately reflected in the metabolome. Dynamics of metabolite concentrations under a certain condition can therefore give a description of the cellular state with a high degree of functional information. We used this potential to evaluate the metabolic status of two recombinant strains of *Saccharomyces cerevisiae* during anaerobic batch fermentation of a glucose/xylose mixture. Two isogenic strains were studied, differing only in the pathways used for xylose assimilation: the oxidoreductive pathway with xylose reductase (XR) and xylitol dehydrogenase (XDH) or the isomerization pathway with xylose isomerase (XI). The isogenic relationship between the two strains ascertains that the observed responses are a result of the particular xylose pathway and not due to unknown changes in regulatory systems. An increased understanding of the physiological state of these strains is important for further development of efficient pentose-utilizing strains for bioethanol production.

Results: Using LC-MS/MS we determined the dynamics in the concentrations of intracellular metabolites in central carbon metabolism, nine amino acids, the purine nucleotides and redox cofactors. The general response to the transition from glucose to xylose was increased concentrations of amino acids and TCA-cycle intermediates, and decreased concentrations of sugar phosphates and redox cofactors. The two strains investigated had significantly different uptake rates of xylose which led to an enhanced response in the XI-strain. Despite the difference in xylose uptake rate, the adenylate energy charge remained high and stable around 0.8 in both strains. In contrast to the adenylate pool, large changes were observed in the guanylate pool.

Conclusions: The low uptake of xylose by the XI-strain led to several distinguished responses: depletion of key metabolites in glycolysis and NADPH, a reduced GTP/GDP ratio and accumulation of PEP and aromatic amino acids. These changes are strong indicators of carbon starvation. The XR/XDH-strain displayed few such traits. The coexistence of these traits and a stable adenylate charge indicates that xylose supplies energy to the cells but does not suppress a response similar to carbon starvation. Particular signals may play a role in the latter, of which the GTP/GMP ratio could be a candidate as it decreased significantly in both strains.

Keywords: Metabolomics, Yeast metabolism, Xylose fermentation, Metabolic status, Starvation, Bioethanol

* Correspondence: basti.bergdahl@tmb.lth.se
[1]Applied Microbiology, Lund University, PO Box 124, SE-221 00 Lund, Sweden
Full list of author information is available at the end of the article

BioMed Central

© 2012 Bergdahl et al.; licensee BioMed Central Ltd. This is an Open Access article distributed under the terms of the Creative Commons Attribution License (http://creativecommons.org/licenses/by/2.0), which permits unrestricted use, distribution, and reproduction in any medium, provided the original work is properly cited.

Background

The yeast *Saccharomyces cerevisiae* has been the organism of choice in the food and beverage industry due to its excellent growth and fermentation capabilities under anaerobic conditions. These characteristics combined with high tolerance to low pH and high sugar and ethanol concentrations yields a production organism, which is very robust in industrial processes. Thus, *S. cerevisiae* has also become the preferred organism for the production of biofuels and fine chemicals [1]. An important step towards the replacement of fossil raw materials is the efficient utilization of renewable lignocellulose. This raw material is generated in the forest and agricultural sectors, and contains carbohydrates which can be converted into fuel-grade ethanol by fermentation [2]. The pentose sugar xylose constitutes a major fraction of the sugar monomers obtained after hydrolysis of certain lignocellulose materials [3,4] and complete utilization of xylose is therefore necessary to obtain competitive process economics [5].

S. cerevisiae cannot naturally utilize xylose and has therefore been extensively engineered to acquire this trait as summarized in several recent reviews [6-9]. To enable xylose utilization and fermentation to ethanol by *S. cerevisiae*, one of two heterologous pathways have been introduced: the oxido-reductive pathway or the isomerisation pathway [10] (Figure 1A). The oxido-reductive pathway is found in fungi and consists of two enzymes, a NAD(P)H-dependent xylose reductase (XR) and a NAD-dependent xylitol dehydrogenase (XDH). Some XR enzymes can use both NADH and NADPH as cofactor although with a preference for the latter [11]. This causes a cofactor imbalance between the XR and XDH reactions and leads to xylitol formation and reduced ethanol yields [12-14]. This does not occur in the isomerisation pathway, which only consists of a cofactor-independent xylose isomerase (XI). The XI with highest activity when expressed in *S. cerevisiae* originates from the fungus *Piromyces sp*. Even so, the activity of this XI is too low to enable anaerobic growth on xylose without further evolution or adaptation of the recombinant strain [10,15].

The rational design of industrially applicable microorganisms requires an understanding of the cellular processes that give rise to a certain phenotype. The functional information about a cellular phenotype is found in the biochemical processes that occur in response to environmental conditions and is commonly viewed as the connection between the three major 'omes in the cell: transcriptome, proteome and metabolome [16,17]. Both proteins and metabolites are directly involved in the cellular biochemistry and thereby closely dictate the function of the organism [18]. The functional role of intracellular metabolites is eminent as they can influence the conversion rate by an enzyme, either as substrate, product or allosteric effector, act as signalling molecules and even influence the direction of enzymatic reactions through their thermodynamic properties [19]. The concerted effect of changes in gene expression in response to environmental variation is thus ultimately reflected in the metabolome. The dynamic changes in metabolite concentrations under a certain perturbation can therefore provide a description of the phenotype and the cellular state with a higher degree of functional information than a snap-shot of either the transcriptome or the proteome. We used this potential to evaluate the metabolic status of two isogenic recombinant strains of *S. cerevisiae* harbouring either the XR/XDH or the XI pathway during anaerobic batch fermentation of a glucose/xylose mixture. A recently developed method for quantification of intracellular concentrations of metabolites by LC-MS/MS [20] was used to determine the dynamic response of targeted metabolites in these recombinant strains when the carbon and energy source changed from glucose to xylose. The difference in xylose uptake rate between the XI-strain and the XR/XDH-strain allows us to propose responses in metabolite concentrations expected to occur during starvation for carbon and energy. The results suggest that xylose is primarily used as an energy source as both strains maintained a high energy charge during the transition to xylose fermentation while varying signs of carbon starvation were observed.

Results

In this study we determined the dynamics in the concentrations of metabolites in glycolysis, the pentose phosphate pathway (PPP), the TCA cycle, nine amino acids, the purine nucleotides and redox cofactors, in two recombinant strains of *Saccharomyces cerevisiae*. The two strains have identical genetic background but employ two different pathways for xylose utilization; strain TMB 3057 [21] has the oxido-reductive fungal pathway consisting of XR and XDH from *Pichia stipitis* and strain TMB 3359 [22] has the isomerisation pathway consisting of the XI from *Piromyces sp*. Samples for determination of metabolite concentrations were collected at specific time points during anaerobic batch fermentation with 20 g/L glucose and 40 g/L xylose as substrates. Additionally, for the XR/XDH-strain measured intracellular metabolite concentrations were validated by evaluating the simultaneous thermodynamic feasibility of 237 metabolic and transport reactions at each sampling point.

Fermentation performance

Both the XR/XDH-strain and the XI-strain consumed all glucose within 20.5 hours (Figure 2A and B) and in the same time the XR/XDH-strain co-consumed 5.7 ± 0.5 g/L xylose (Figure 2A), whereas the XI-strain only co-consumed 0.6 ± 0.2 g/L xylose (Figure 2B). Until this point the biomass yield per gram sugar consumed was similar for the two strains but higher yield of the by-products glycerol and xylitol were obtained with the XR/XDH-

strain (Additional file 1: Table S1). After glucose depletion, the XR/XDH-strain consumed an additional 10.8 ± 0.1 g/L xylose (r_{xyl} = 0.30 g/g CDW/h) most of which was converted to xylitol and ethanol with a minor amount used for biomass and glycerol (Figure 2A and C). The XI-strain only consumed an additional 0.6 ± 0.1 g/L

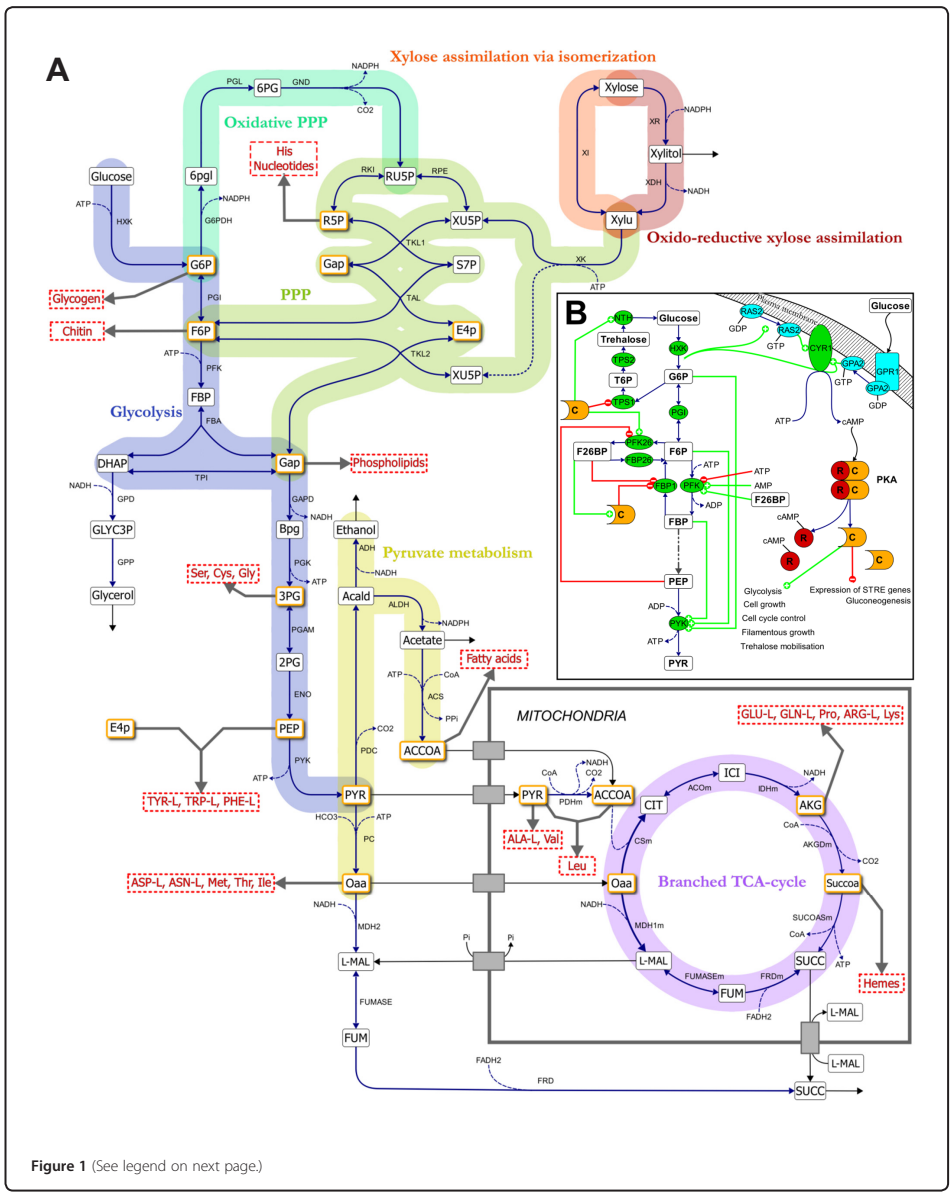

Figure 1 (See legend on next page.)

(See figure on previous page.)

Figure 1 Overview of the main metabolic reactions in central carbon metabolism. A) Xylose can be assimilated through two pathways: the fungal oxidoreductive pathway consisting of XR and XDH or the bacterial isomerization pathway via an XI. The xylulose formed by the two pathways is phosphorylated by XK and channelled through the non-oxidative PPP yielding 2/3 moles F6P and 1/3 moles GAP per mole substrate. These metabolites enter glycolysis to generate ATP in the conversion of PEP to pyruvate and the oxidative PPP to regenerate NADPH. Pyruvate is converted into ethanol, acetate and oxaloacetate, which is transported into the mitochondria for amino acid synthesis. Under anaerobic conditions succinate dehydrogenase is not operational which results in a branched TCA-cycle with succinate as the end product. The twelve precursor metabolites which are required for biosynthesis of macromolecules are highlighted in orange colour. Metabolites in capital letters have been measured in the current study. **B**) Glycolysis is activated through the induction of the Ras/cAMP/PKA pathway. cAMP formed by adenylate cyclase (CYR1) interacts with the regulatory subunits (R) of PKA which releases the catalytic subunits (C). The active PKA phosphorylates PFK26 which subsequently produces F26BP from F6P and ATP. F26BP is an essential activator of PFK1 which phosphorylates F6P to FBP. The production of FBP in turn activates PYK and ATP generation. Production of ATP and ethanol depends on a high catalytic activity of PYK which requires the simultaneous presence of G6P, F6P and FBP. PKA and F26BP also efficiently inactivate gluconeogenesis by inhibiting FBP1.

xylose ($r_{xyl} = 0.036$ g/g CDW/h) after glucose depletion (Figure 2B). During the xylose phase the XI-strain produced negligible amounts of xylitol (0.12 ± 0.02 g/L) in contrast to the XR/XDH-strain (6.8 ± 0.01 g/L xylitol) (Figure 2C and D).

Validation of measured metabolite concentrations in the XR/XDH-strain

The metabolic response to a change in carbon source from glucose to xylose was determined by measuring intracellular metabolites at 11 time points during 24 hours of anaerobic batch cultivation. The first samples were collected at mid-exponential growth on glucose while the majority of samples were collected during the transition towards glucose depletion. The last samples were collected 18 hours after glucose exhaustion and represent a state when xylose is the sole carbon and energy source. Quadruplicate samples were collected at each time point and experiments were performed in duplicate for each strain. The

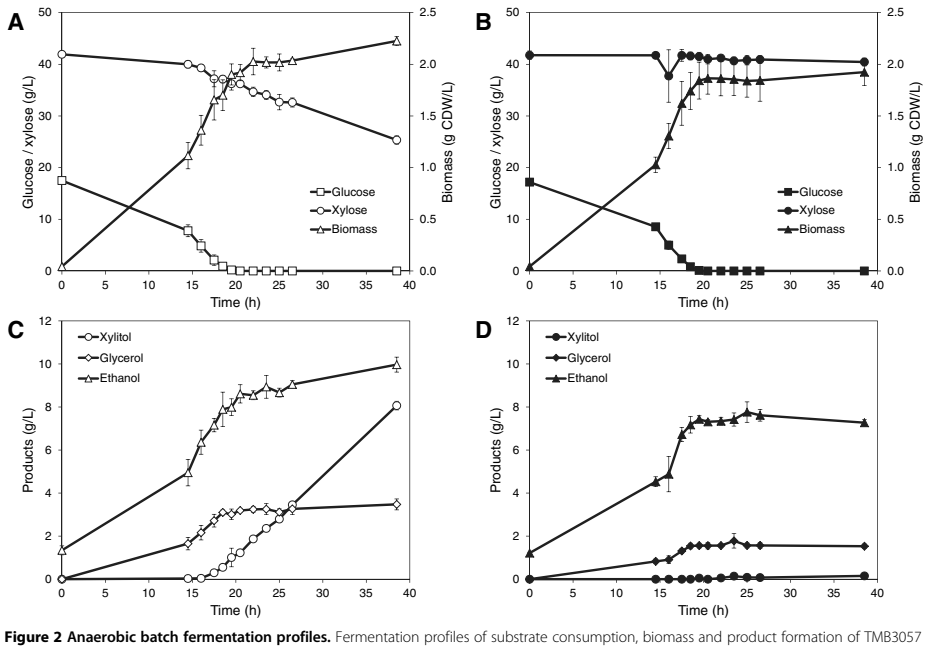

Figure 2 Anaerobic batch fermentation profiles. Fermentation profiles of substrate consumption, biomass and product formation of TMB3057 (XR/XDH) (**A** and **C**) and TMB3359 (XI) (**B** and **D**) Fermentation was performed in 2× YNB medium containing 20 g/L glucose and 40 g/L xylose. Figures show mean values of duplicate experiments and errors are given as the standard deviation of the mean (n = 4).

final data set consisted of 185 samples and 44 measured metabolites.

The thermodynamic feasibility of 38 out of the 44 metabolite ranges measured in the XR/XDH-strain were validated using anNET toolbox [23]. These 38 metabolites were quantified using external standards. The metabolites that could not be quantified, due to lack of standards, were sedoheptulose 7-phosphate (S7P), acetyl-CoA (ACCOA), reduced and oxidized glutathione (GTTred and GTTox), FAD and FMN. All metabolites evaluated, apart from 1,3-bisphosphoglycerate (BPG), glucose 1-phosphate (G1P) and glyceraldehyde 3-phosphate (GAP), were within the feasible ranges in all 11 time points (see Additional file 2 for further details). This means that the measurements of the remaining 35 metabolites are of good quality as they allowed 237 reactions to be thermodynamically feasible simultaneously.

Global analysis of the metabolite responses

Hierarchical clustering of the metabolite data was used to obtain a global overview of the metabolomic response. To avoid performing this and subsequent analyses on metabolite data that might be erroneous and not physiologically relevant, GAP and BPG were removed from the data set (see Additional file 2). The clustering revealed four major groups of metabolites: one group where concentrations increased over time (Group A), one group where few changes occurred (Group B) and two groups where concentrations decreased over time (Group C and D) (Figure 3). In general, the response in metabolite concentrations was the same in both strains. Nearly all the measured amino acids are found in Group A. Specifically, all the aromatic amino acids clearly cluster in the top of this group. The nucleotide profiles displayed few changes and are found in Group B. The exceptions to this pattern were the guanine nucleotides GMP and GDP, which increased markedly in both strains during the fermentation, and GTP which decreased slightly. The redox cofactors NAD, NADH and NADP decreased moderately and are found in Group C. The concentration of NADPH, on the other hand, decreased significantly and is thus designated to Group D. Group D is otherwise dominated by sugar phosphates from both glycolysis and the PPP. The heat map also shows that the greatest shifts in the metabolite profiles were initiated immediately prior to glucose depletion.

Identification of key metabolites and phases during batch fermentation

Principal component analysis (PCA) was used to determine the natural grouping of the sampling points based on quantified and validated concentrations, and to identify which metabolites have the highest influence on the separation of the data. The concentrations of pyruvate were not included in this analysis due to large errors in the measurements from the XI-strain (Additional file 1: Figure S6E). The first and second principal components (PC1 and PC2, respectively) accounted for 76.2% and 10.4% of the variance in the data, respectively (Additional file 1: Figure S1). The data points were separated by sampling time in PC1 and by strain background in PC2. The grouping of the data closely reflects the experimental structure. Samples from the glucose-xylose phase cluster together, illustrating similar metabolite profiles in the two strains during glucose metabolism, which reflects the isogenicity of the strains with the only difference being the xylose pathway. This difference becomes evident when glucose is depleted. Samples collected from the xylose phase clearly form two separate clusters, one for each strain. The grouping of the data from the XI-strain also reveals that there are three distinct phases during the fermentation: a glucose phase between 14.5 h and 18.5 h, a transition phase between 18.5 h and 22 h and a xylose phase between 22 h and 38.5 h. Among the 20 most influential metabolites on PC1 and PC2 the distribution was as follows: nine amino acids, five sugar phosphates, three carboxylic acids, two nucleotides and one redox cofactor (Additional file 1: Figure S1). This distribution agrees well with the results of the cluster analysis (Figure 3). It is worth noting that several parts of metabolism are represented by these metabolites and most importantly that the adenine nucleotides are not among them.

A two-sided t-test was used to establish whether the average concentration of each quantified metabolite was different between the two strains at each sampling point. This analysis showed that the number of metabolites that were significantly different between the strains (at a significance level of $\alpha = 0.05$) increased from between 16 and 23 in the mixed sugar phase to between 29 and 33 in the xylose phase (Additional file 1: Table S2), which confirms the general pattern of the PCA analysis. The majority of the quantified metabolites (81%) were significantly different in more than half of the time points, including all the metabolites in Figure S1 (Additional file 1). The remaining metabolites that showed few differences between the two strains were the nucleotides and intermediates of the TCA cycle which are in Group B of the cluster analysis (Figure 3).

Dynamic changes in sugar phosphates, precursor metabolites and amino acids

The concentrations of sugar phosphates and amino acids showed the largest changes in concentration during the fermentation (Figure 3) and also had a high influence on the separation of the collected data (Additional file 1: Figure S1). Xylulose 5-phosphate (XU5P), ribulose 5-phosphate (RU5P) and ribose 5-phosphate (R5P) had a high influence on the separation of the two strains in

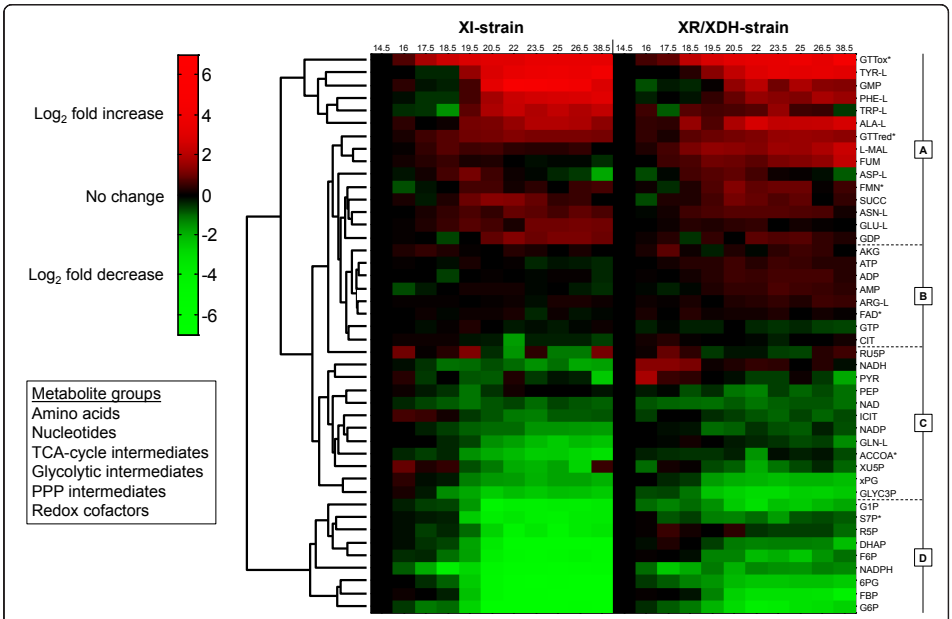

Figure 3 Hierarchical clustering of time course profiles during fermentation of glucose and xylose. The heat map was generated using either quantified metabolite concentrations or normalized areas of the chromatographic peaks (indicated by *) and shows the $\log_2$ fold change relative to the first sampling point (t = 14.5 h) which represents exponential growth on a mixture of glucose and xylose. The hierarchical clustering of metabolite profiles yields four major clusters: Cluster A contains 15 metabolites which increase in either of the two strains; Cluster B contains 8 metabolites which show little change during the fermentation; Cluster C contains 12 metabolites which decrease moderately in at least one strain; Cluster D contains 9 metabolites which decrease markedly in both the XR/XDH-strain and the XI-strain.

the PCA analysis and the concentrations were also consistently lower in the XI-strain compared to the XR/XDH-strain (Figure 4A and B). The concentrations of these metabolites were rather stable in the XR/XDH-strain during the fermentation whereas the concentrations decreased in the XI-strain during the transition phase. The largest change was observed in the concentration of R5P which decreased by 9-fold (Figure 4B). The same change was observed in the level of S7P (Figure 4C). During the same period the level of S7P decreased only slightly (1.2-fold) in the XR/XDH-strain. S7P was not included in the PCA analysis due to the lack of quantitative data but the relative change during the transition phase could be calculated from the chromatographic peak areas. 6-phosphogluconate (6PG), the only metabolite measured in the oxidative part of the PPP, decreased significantly in both strains during the glucose- and transition phases (Figure 4D). The concentration decreased 5-fold in the XR/XDH-strain and nearly 75-fold in the XI-strain, leading to an almost depleted pool of 6PG in the latter. In addition to R5P several precursor metabolites in glycolysis and TCA-cycle also decreased during the transition from glucose to xylose fermentation (Figure 5). In the XR/XDH-strain the most significant changes occurred in the concentrations of glucose 6-phosphate (G6P), fructose 6-phosphate (F6P) and the combined pool of 2-phosphoglycerate (2PG) and 3-phosphoglycerate (3PG) which decreased by 8-, 3- and 4-fold, respectively (Figure 5 A-C). In the XI-strain the xPG pool also decreased 4-fold, but the decrease in hexose phosphates was more severe with 40- and 33-fold changes in the concentrations of G6P and F6P, respectively, resulting in near depletion of these pools after glucose exhaustion. In both strains the concentration of fructose 1,6-bisphosphate (FBP) decreased the most with 10- and 88-fold changes in the XR/XDH- and XI-strain, respectively (Additional file 1: Figure S5B). The concentrations of the metabolites in glycolysis generally decreased in both strains and the time course profiles correlated with decreasing concentration of extracellular glucose (Figure 3; Additional file 1: Figure S5). The exception to this pattern was phosphoenolpyruvate (PEP) which transiently increased 2-fold in

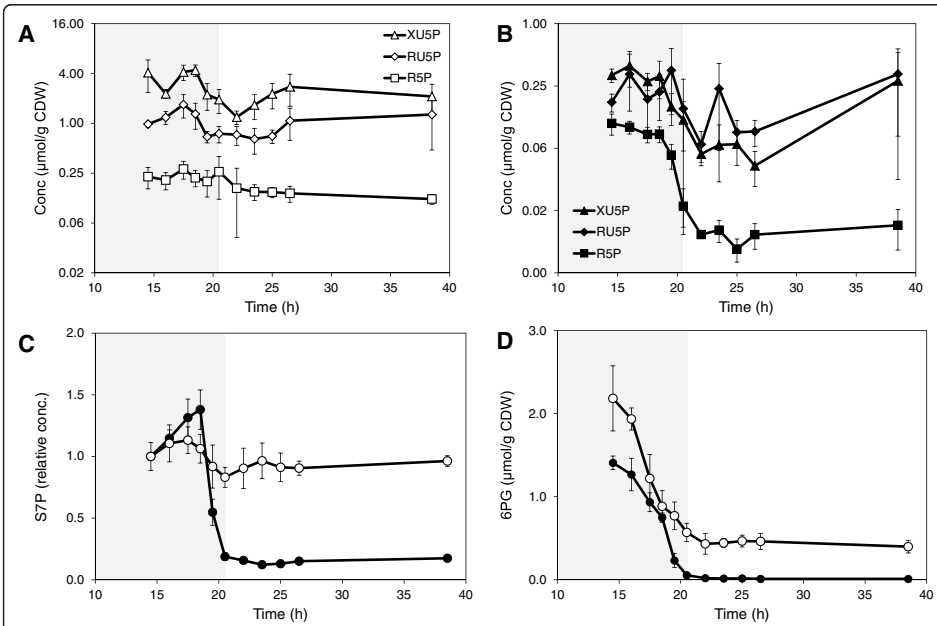

Figure 4 Dynamics of metabolites in the pentose phosphate pathway. Intracellular concentrations of **A**) XU5P, RU5P and R5P in TMB3057 (XR/XDH), **B**) XU5P, RU5P and R5P in TMB3359 (XI), **C**) S7P and **D**) 6PG during anaerobic batch fermentation of 20 g/L glucose and 40 g/L xylose using strains TMB3057 (XR/XDH, white markers) and TMB3359 (XI, black markers). Errors are given as 95% confidence intervals of the means calculated from duplicate experiments for each strain ($5 \leq n \leq 10$). The Y-axis in A and B is in $\log_2$ scale. The levels of S7P are calculated relative to the first time point at 14.5 h. The shaded area indicates the period until glucose depletion.

concentration in the XI-strain after glucose depletion and then returned to the original concentration during the xylose phase (Figure 5D). The dynamic change in the level of ACCOA in the XI-strain followed that of the glycolytic intermediates and decreased by 3.7-fold (Figure 5E). In the XR/XDH-strain on the other hand there were few changes in the ACCOA concentration during the three phases. The concentration of α-ketoglutarate (AKG) varied notably in both strains during the three phases but within a rather small range from 1.5 µmol/g CDW to 2.3 µmol/g CDW on average (Figure 5F).

All the free amino acids measured in the current study, except glutamine (GLN-L), accumulated during the glucose and/or the transition phase (Figure 3; Additional file 1: Figure S7). The largest increase was seen in the pools of the aromatic amino acids phenylalanine (PHE-L), tryptophan (TRP-L) and tyrosine (TYR-L). The response was stronger in the XI-strain where the concentrations of PHE-L, TRP-L and TYR-L increased by 9-, 6- and 17-fold, respectively, while in the XR/XDH-strain the response was more moderate with 4-, 2- and 11-fold increases, respectively (Additional file 1: Figure S2). Concentrations of L-malate and fumarate also increased during the glucose and transition phases by ca. 2.3-fold and 1.4-fold in the XR/XDH-strain and XI-strain, respectively (Additional file 1: Figure S6 C and D). However, in the xylose phase these two carboxylic acids decreased in concentration in the XI-strain, whereas they continued to accumulate in the XR/XDH-strain, reaching around 5-fold higher concentrations compared with the glucose phase.

Dynamic changes in redox cofactors and nucleotides

In contrast to the consistent responses observed within the sugar phosphate and amino acid metabolite groups, the responses in redox cofactors and nucleotides were more diverse. The concentration of redox cofactors decreased similarly in both strains during the glucose- and transition phases, after which they levelled out in the xylose phase (Additional file 1: Figure S3). NADP was the only redox cofactor that appeared among the 20 most influential metabolites in the PCA analysis (Additional file 1: Figure S1) and the concentration was consistently

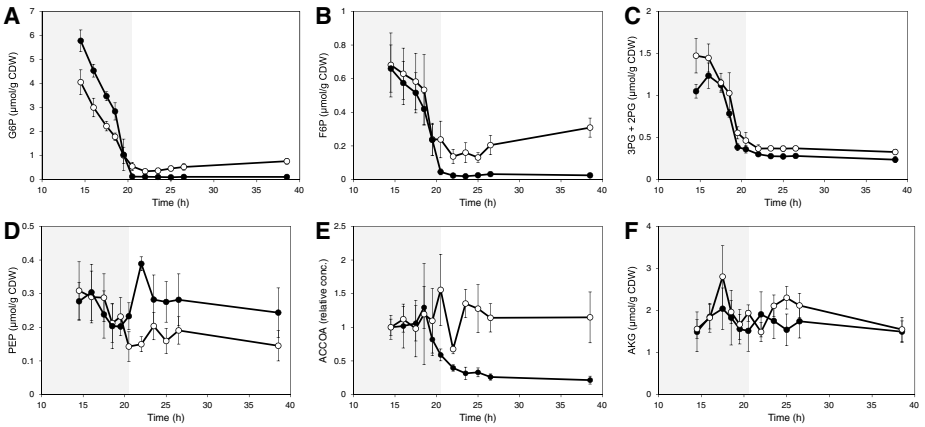

Figure 5 Dynamics of important precursor metabolites. Intracellular concentrations of **A**) G6P, **B**) F6P, **C**) the combined pool of 2PG and 3PG, **D**) PEP, **E**) ACCOA and **F**) AKG during anaerobic batch fermentation of 20 g/L glucose and 40 g/L xylose using strains TMB3057 (XR/XDH, white markers) and TMB3359 (XI, black markers). Errors are given as 95% confidence intervals of the means calculated from duplicate experiments for each strain ($4 \leq n \leq 10$). The shaded area indicates the period until glucose depletion. The levels of ACCOA are calculated relative to the first time point at 14.5 h. The shaded area indicates the period until glucose depletion.

higher in the XR/XDH-strain compared to the XI strain with a difference as high as 3.4-fold in the xylose phase (Additional file 1: Figure S3A). This large difference was due to a 2-fold reduction in concentration in the XI-strain whereas the concentration only changed by 27% in the XR/XDH-strain. During most of the glucose phase the concentration of NADPH was the same in both strains but in the xylose phase the concentration had decreased by 2.8-fold in the XR/XDH-strains and by nearly 22-fold in the XI-strain (Additional file 1: Figure S3B). As with several sugar phosphates this decrease led to a near depletion of the NADPH pool in the XI-strain. This depletion resulted in a 9-fold reduction of the NADPH/NADP ratio from 0.6 to ca. 0.07 (Figure 6A). In the XR/XDH-strain, on the other hand, few significant changes were observed in the NADPH/NADP ratio and the average ratio over all phases was 0.25 ± 0.03 (mean ± 95% CI, n = 79). In contrast to NADP, the concentration of NAD was on average 26% lower in the XR/XDH-strain compared to the XI-strain during all three phases and the change during the first two phases was almost 2-fold in both strains (Additional file 1: Figure S3C). There were few significant differences in NADH concentration between the XR/XDH-strain and the XI-strain (Additional file 1: Table S2) and the average concentration in the two strains during all three phases was 2.10 ± 0.20 μmol/g CDW (mean ± 95% CI, n = 85) and 1.91 ± 0.18 μmol/CDW (mean ± 95% CI, n = 85), respectively. This high consistency between the two strains in NAD(H) cofactors led to very few significant differences in the NADH/NAD ratio when comparing time point by time point (Figure 6B). However, there was a significant difference in the average ratio during the xylose phase which was 1.93 ± 0.15 (mean ± 95% CI, n = 41) in the XR/XDH-strain and 1.14 ± 0.11 (mean ± 95% CI, n = 39) in the XI-strain.

The dynamic response of the adenine nucleotides was the same in both the XR/XDH-strain and the XI-strain. Furthermore, we found very few significant differences in the concentrations between the two strains (Additional file 1: Figure S4 A and B; Table S2). This was also reflected in the adenylate energy charge (AEC) which was nearly identical in both strains and remained at 0.82 during exponential growth on glucose and xylose fermentation (Figure 7A). This level of the AEC agrees very well with previously reported values for *S. cerevisiae* growing on glucose [36-38]. In contrast to adenylate nucleotides, the concentrations of the guanine nucleotides GMP and GDP changed significantly in the transition phase (Additional file 1: Figure S4C). In the XI-strain the concentrations increased 32- and 2.6-fold, respectively. In the XR/XDH-strain the concentrations also increased but to a lesser extent, i.e. 5- and 1.6-fold of GMP and GDP, respectively. The concentration of GTP decreased in the XR/XDH-strain throughout the three experimental phases, whereas in the XI-strain it gradually returned to a level close to the initial concentration (Additional file 1: Figure S4D). During the glucose phase both strains had nearly identical values of the guanylate energy charge (GEC) around 0.86,

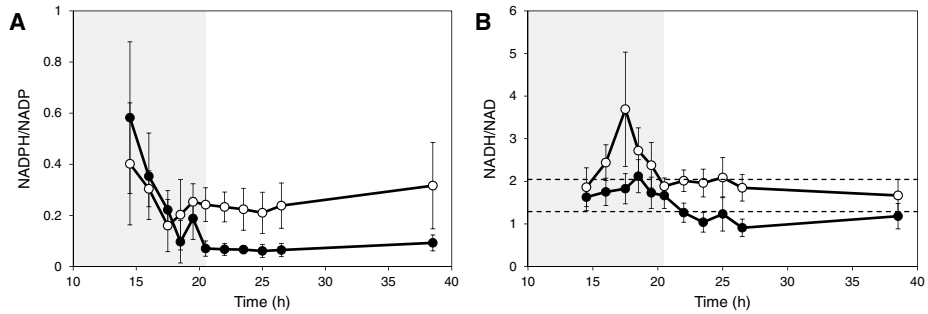

Figure 6 Dynamics in redox cofactor ratios. Dynamics in the NADPH/NADP (**A**) and NADH/NAD (**B**) ratios during anaerobic batch fermentation of 20 g/L glucose and 40 g/L xylose using strains TMB3057 (XR/XDH, white markers) and TMB3359 (XI, black markers). Dotted lines in B) represent the 95% confidence interval of the value in TMB3057 at time point 38.5 h. Errors are given as 95% confidence intervals of the means calculated from duplicate experiments for each strain ($4 \leq n \leq 10$). The shaded area indicates the period until glucose depletion.

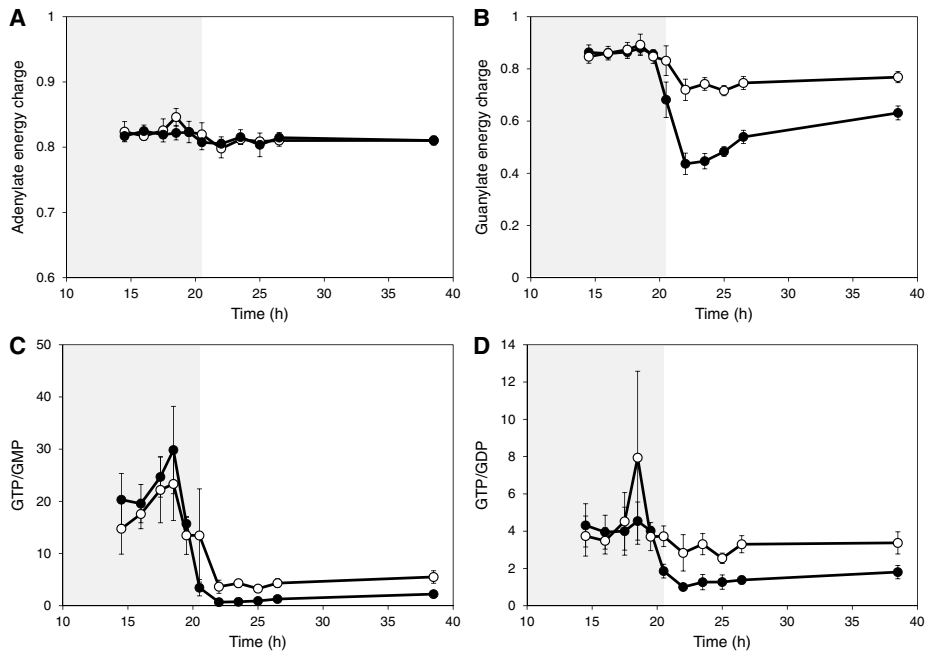

Figure 7 Dynamics in different purine nucleotide ratios. Dynamics in **A**) the adenylate energy charge, **B**) the guanylate energy charge, **C**) the GTP/GMP ratio and **D**) the GTP/GDP ratio during anaerobic batch fermentation of 20 g/L glucose and 40 g/L xylose using strains TMB3057 (XR/XDH, white markers) and TMB3359 (XI, black markers). The adenylate energy charge and the guanylate energy charge were calculated according to (ATP + ½ADP)/(ATP + ADP + AMP) and (GTP + ½GDP)/(GTP + GDP + GMP) , respectively. Errors are given as 95% confidence intervals of the means calculated from duplicate experiments for each strain ($5 \leq n \leq 11$). The shaded area indicates the period until glucose depletion.

but during the transition phase the GEC dropped by almost 50% in the XI-strain to 0.44 whereas it stabilized at 0.72 in the XR/XDH-strain (Figure 7B). During the xylose phase the GEC recovered to 0.63 and 0.77 in the XI-strain and XR/XDH-strain, respectively. In addition to a drop in the GEC, the changes in GMP and GDP concentrations also resulted in altered GTP/GDP and GTP/GMP ratios. The dynamic response in the GTP/GMP ratio was similar in the two strains with decreases of 3- and 9-fold in the XR/XDH-strain and XI-strain, respectively (Figure 7C). The response in the GTP/GDP ratio was on the other hand different in the two strains (Figure 7D). The average GTP/GDP ratio was around 3.70 ± 0.34 (mean ± 95% CI, n = 81) in the XR/XDH-strain throughout the three experimental phases whereas it dropped from around 4.2 to ca 1.4 in the XI-strain.

Discussion

For a culture of microorganisms to obtain balanced growth a careful coordination between nutrient assimilation, transformation of energy to generate ATP, redox balancing, biosynthesis and progression through the cell division cycle is required. In this study we determined the time-dependent changes of targeted metabolites in two recombinant strains of *S. cerevisiae*, harbouring either the XR/XDH- or the XI-pathway. This data allows us to evaluate the status of the five cellular processes required for balanced growth, from a metabolic perspective, when the cells shift from glucose to xylose fermentation.

Carbon assimilation is not the main limitation of growth on xylose

When the carbon source changed from glucose to xylose there was a significant decrease in sugar uptake rate (Figure 2). Both strains had the same specific uptake rate of glucose, but that of xylose was 60% and 94% lower in the XR/XDH-strain and the XI-strain, respectively. These results agree well with previously reported performance data for both the XR/XDH-strain [39] and the XI-strain [22]. The results for the XI-strain also compare well with data from a related strain with the same genetic background, but with a different promoter controlling the expression of the XI-encoding gene [10]. The XI-strain used in the current study does not perform as well as other yeast strains harbouring an XI but which have also undergone extensive evolutionary engineering [40]. However, for the current investigation rationally designed strains were deliberately chosen to ensure isogenicity, except for the two initial xylose assimilating pathways, so that it can be reasonably assumed that the metabolism of the strains is controlled by the same regulatory system. The isogenic relationship between the two strains thus ensures that the observed responses are primarily a consequence of the metabolic impact of the adopted xylose assimilation pathway. When xylose is the sole carbon source mainly the high affinity glucose transporters are expressed [41] which have a $K_m \approx 130$ mM for xylose [42]. Since the concentration of xylose during our experiments was on average double the K_m the transporters would be operating at 2/3 of the maximum velocity, which corresponds to approximately 0.26 g/g CDW/h (assuming a single transporter with $V_{max} = 110$ nmol/min/mg protein [42] and a cellular protein content of 40%). This value is probably an underestimation since more than one transporter is actually present, but the magnitude can be considered reasonable as it is close to the measured uptake rate in the XR/XDH-strain (0.3 g/g CDW/h). In the XI-strain on the other hand the measured uptake rate is several folds lower than the potential capacity, indicating that other factors downstream sugar transport is limiting the uptake of xylose. From this calculation it is difficult to evaluate whether transport is limiting in the XR/XDH-strain, but even though the uptake rate is 10-fold higher than in the XI-strain it is not able to grow on xylose. Attempts to improve the uptake of xylose in other XR/XDH-strains by introducing a heterologous glucose/xylose facilitator only had an effect at low xylose concentrations and the increased uptake did not improve biomass or ethanol yield from xylose [43]. This suggests that also in the XR/XDH-strain there are other limitations in addition to sugar uptake.

A carbon starvation response is displayed in biosynthetic metabolites

In this study we measured 16 metabolites that are related to biosynthesis. Seven of these were precursor metabolites [44] required for biosynthesis of macromolecular building blocks (i.e. G6P, F6P, R5P, PEP, 3PG, AKG and ACCOA) (Figure 4; Figure 5) and the remaining nine were amino acids (Figure 3; Additional file 1: Figure S2 and S7). In total there are twelve essential precursor metabolites which are all produced in glycolysis, PPP and the TCA-cycle (Figure 1A). Hence, the rate of their formation is closely linked to the carbon uptake rate.

Concentrations of PPP intermediates reflect the xylose uptake rate

The measured concentrations of the metabolites in the non-oxidative PPP were markedly higher in the XR/XDH-strain compared to the XI-strain, even during growth on glucose (Figure 4A and B). This is most likely caused by the difference in xylose uptake. Between 14.5 h and 18.5 h the specific glucose uptake rate differed by less than 9% between the two strains (data not shown), however, when the uptake of xylose is also taken into account the difference in total sugar uptake rate is 45% (data not shown). The small difference with regard to glucose is consistent

with the isogenic relationship between the two strains. Also the large difference in total sugar uptake rate, caused by a higher uptake of xylose by the XR/XDH-strain, agrees well with the higher concentrations of pentose sugar phosphates measured in this strain. The carbon channelled through the PPP during fermentative growth of natural *S. cerevisiae* is only around 15% of the glucose utilized [45] and the PEP generated by employing the PPP has been estimated to be less than 4% [46,47]. The role of PPP has thus been suggested as exclusively anabolic and not catabolic [47]. Native *S. cerevisiae* accumulates intracellular S7P during xylulose fermentation which was interpreted as insufficient activity of subsequent PPP enzymes [48]. This hypothesis seemed to be confirmed when overexpression of the four genes of the non-oxidative PPP led to increased fermentation of xylulose [49] and xylose [21]. Many recombinant xylose fermenting strains of *S. cerevisiae*, like the two strains used in the current investigation, currently carry this trait [50]. Nevertheless, recent metabolomics studies continue to point out overexpression of the non-oxidative PPP enzymes as targets for improved pentose utilization [37,38]. Based on the dynamics of the PPP intermediates in the current investigation with two isogenic strains, the limitation rather seems to have been shifted toward the initial xylose assimilating steps. This appears to be the case with the XI pathway in particular. One consequence of this limitation is that the XI-strain is unable to sustain a flux towards 6PG formation (Figure 4D). 6PG is formed and consumed in two irreversible reactions catalysed by 6-phosphogluconolactonase (PGL; EC 3.1.1.31) and 6-phosphogluconate dehydrogenase (GND; EC 1.1.1.44), respectively (Figure 1A). Hence, the concentration of 6PG depends on the ratio between the rates of formation and consumption. The depletion of 6PG in the XI-strain after glucose exhaustion indicates a much slower rate of 6PG formation than consumption and consequently a lower flux through the oxidative PPP. The flux through the oxidative PPP depends on the formation of G6P, which during xylose assimilation can only occur via the non-oxidative PPP and phosphoglucoisomerase (PGI; EC 5.3.1.9) (Figure 1A). The depletion of 6PG in the XI-strain is therefore most likely caused by a reduced flux through the non-oxidative PPP during xylose assimilation.

Significant decrease of hexose phosphates influences metabolite homeostasis in lower glycolysis

The concentration of the hexose phosphates in glycolysis decreased significantly in both strains during the transition from glucose to xylose fermentation (Figure 5; Additional file 1: Figure S5B). This was a general response in all glycolytic metabolites except for PEP. In bacteria, increased concentration of PEP is a generic response to carbon starvation [51]. Elevated levels of PEP have also been reported in carbon limited or starved yeast cells under aerobic conditions [52-54] but not under anaerobic conditions [37]. In mutant strains it was shown, using traditional biochemical methods, that the hexose phosphates in upper glycolysis play an important role for the activation of the enzymes in lower glycolysis [55,56]. ATP generation and production of ethanol depends on a high activity of pyruvate kinase (PYK; EC 2.7.1.40) which catalyses the last reaction in glycolysis where PEP is converted to pyruvate (PYR) (Figure 1A). This enzyme requires both G6P and F6P for induction [55] and FBP for activation [57] (Figure 1B). FBP is formed from F6P and ATP in the reaction catalysed by 6-phosphofructo kinase (PFK; EC 2.7.1.11) whose activity significantly increases in the presence of fructose 2,6-bisphosphate (F26BP) [58] (Figure 1B). The formation of F26BP is activated through phosphorylation of 6-phosphofructo-2-kinase (PFK26; EC 2.7.1.105) by protein kinase A (PKA) [59] which is most active in the presence of glucose [60] (Figure 1B). This series of metabolic interactions could be the underlying mechanism of the stimulating effect low glucose concentration has on xylose uptake [61-63]. However, it does not explain why xylose is not taken by the engineered yeast cells in a medium with this compound in excess. The accumulation of PEP in the XI-strain suggests a reduced activity of PYK which is consistent with the depletion of FBP. This is most likely connected with the low uptake of xylose by this strain as FBP was not depleted in the XR/XDH-strain (Additional file 1: Figure S5B).

Accumulation of aromatic amino acids is a general response to carbon starvation

Increased concentrations of alanine (ALA-L), asparagine (ASN-L), glutamate (GLU-L) and the aromatic amino acids has been observed in yeast when starved for carbon under aerobic conditions [52]. Similar results for GLU-L and the aromatic amino acids PHE-L and TRP-L have also been reported for anaerobic conditions [37]. Thus the currently observed accumulation of amino acid pools (Figure 3) corresponds well with previously reported response to carbon starvation, both qualitatively and in many cases also quantitatively (Figure S2D). Aromatic amino acids are the most "expensive" amino acids to synthesize, in terms of ATP requirement [64]. It is therefore unlikely that the observed accumulation is a result of continued synthesis. Instead it is more a reflection of protein degradation with subsequent accumulation of aromatic amino acids, whose aromatic ring is energetically "expensive" or unfavourable to break open. This hypothesis is supported by a measured decrease in total protein content from 0.5 ± 0.05 g protein/g CDW to 0.4 ± 0.03 g protein/g CDW in

the XR/XDH-strain when the carbon source changed from glucose to xylose (data not shown).

The XR/XDH pathway has no apparent effect on the redox balance

Declining concentrations of redox cofactors have been observed in cells entering stationary phase [65] and during carbon starvation [37,52]. The introduction of the XR/XDH pathway in *S. cerevisiae* increases the demand for NADPH and the need to re-oxidize NADH (Figure 1A). The increased demand for NADPH is met by increased expression of genes encoding enzymes which catalyse NADPH-yielding reactions, such as those of the oxidative pentose phosphate pathway [24,66]. During xylose assimilation NADPH generation in the oxidative PPP depends on the flux from the non-oxidative PPP via F6P to G6P. The current study shows that the XR/XDH-strain, despite its increased demand for NADPH, is able to maintain a low but constant concentration throughout the xylose phase (Figure S3B). In contrast, the XI-strain is depleted of NADPH already at the beginning of the xylose phase which coincides with the depletion of 6PG after glucose exhaustion (Figure 4D). The depletion of NADPH supports the previous suggestion that the flux through the non-oxidative PPP is low in the XI-strain and it also indicates that this strain suffers from significant carbon limitation.

When the demand for oxidized NADH, i.e. NAD, is not fully met xylitol is secreted as was observed during the transition and xylose phases for the XR/XDH-strain only (Figure 2). The incapacity of both native and recombinant xylose-utilizing XR/XDH yeast strains to reconstitute the NAD/NADH balance under anaerobic conditions has frequently been suggested to be the most important bottleneck in the fermentation of xylose [13,67] and has been the major incentive to develop XI-strains [15]. However, the current targeted metabolite analysis recorded little significant difference between the XR/XDH-strain and the XI-strain in NADH concentration (Figure S3D) and NADH/NAD ratio (Figure 6B). Furthermore, no accumulation of NADH was observed in the XR/XDH-strain during the xylose phase. Although unexpected, it is most likely a result of mixing the cytosolic and mitochondrial pools of redox cofactors which is unavoidable with the extraction method used. If this is the case, it indicates that it is necessary to take into account the compartmentalization of metabolites when evaluating the balancing of redox cofactors in yeast. Another aspect of the redox balance is that several genes associated with respiratory metabolism become derepressed, regardless of oxygenation level, when xylose is the sole carbon source [24,66,68,69]. This specifically leads to increased transcript levels of the three genes coding for malate dehydrogenase (MDH): *MDH1* (mitochondrial), *MDH2* (cytosolic) and *MDH3* (peroxisomal). Under anaerobic conditions Mdh1p converts oxaloacetate to L-malate and is required for reoxidizing the NADH formed during amino acid synthesis inside the mitochondria [70] (Figure 1A). The physiological role of Mdh2p is to generate oxaloacetate for G6P-synthesis during growth on non-fermentable carbon sources and is thus repressed by glucose [71]. The increased expression of both *MDH1* and *MDH2* on xylose gives the cells an enhanced NADH-oxidizing capability. This capability seems to be utilized by the XR/XDH-strain as the concentration of L-malate, the product of the MDH-catalysed reaction, accumulated intracellularly during xylose consumption (Figure 3; Additional file 1: Figure S6D). Even though this path can aid in the balancing of redox cofactors it does not appear to be sufficient as a significant amount of xylitol is still being formed (Figure 2). Instead this path might actually be detrimental for the cells, rather than beneficial, since oxaloacetate is an important precursor metabolite for synthesis of several amino acids, including methionine (Figure 1A). A diversion of flux from these reactions towards L-malate production could result in depletion of these amino acids. Unfortunately we cannot confirm this hypothesis due to lack of measurements of these amino acids and oxaloacetate. However, some support is given by the fact that yeast cells with high Mdh2p-activity only grow half as fast on glucose as the wild-type cells, thus illustrating its negative effect [71].

Both yeast strains are able to maintain high energy charge on xylose

The most commonly used measure to assess the energetic status of cells is the adenylate energy charge (AEC) [72]. It is defined as the ratio between the total adenine nucleotide pool and the sum of the ATP pool and half the ADP pool: (ATP + ½ADP)/(ATP + ADP + AMP). The adenine nucleotides are balanced by adenylate kinase (AK) which catalyses the reaction ATP + AMP ↔ 2 ADP with the ADP pool serving as energy reserve to be used when ATP levels decrease. The AEC has been suggested as an important regulatory signal for controlling the energy balance by directly modulating enzyme activities [73-75]. In *S. cerevisiae* the AEC drops sharply from 0.8 to around 0.5 in response to glucose depletion and continues to fall during prolonged glucose starvation [36,37]. It would therefore have been expected that the low uptake rate of xylose by the two strains (Figure 2) would lead to a decrease in the AEC and ATP concentration, especially in the XI-strain. However, the results show that there is a remarkable consistency between the adenine nucleotide pools in the two strains, clearly demonstrated by the very small confidence intervals in the energy charge (Figure 7A). This implies that the regulatory signal the AEC provides is the same during xylose fermentation as during glucose fermentation.

Furthermore, it may reflect an ability of the cells to sense the surplus of external xylose even at very low uptake rates. The observed consistency could thus be the outcome of a mechanism to prevent depletion of ATP which is required to phosphorylate whatever small amount of carbon source is taken up. Therefore the cells do not respond with an energy starvation but only a carbon starvation phenotype. However, the absence of growth despite a high and stable AEC strongly indicates that it is not the required signal for continued growth on xylose.

Role of guanine nucleotides in cell division cycle control

Before a yeast cell commits to start the cell division cycle two criteria need to be fulfilled: accumulation of cell mass to reach a critical size [76] and establishment of a critical rate of protein synthesis [77]. This occurs during the G1 phase of the cycle in which the cell evaluates the nutritional condition of the environment. The guanine nucleotides have been implicated as important regulatory factors in both these processes [78-80]. Rudoni *et al.* [78] reported a value for the GTP/GDP ratio in exponentially growing yeast cells of ca. 4 which is reduced to below one in stationary phase and during glucose starvation. Furthermore, they found a correlation between the cytosolic GTP/GDP ratio and the level of GTP-bound Ras2, which is the active form of this protein. In this form it can bind to adenylate cyclase and trigger the production of cAMP [81] (Figure 1B). The active Ras/cAMP/PKA pathway initiates the biosynthetic machinery by increasing the expression of genes involved in ribosome biogenesis [60] and is thereby required for the cell to reach the size threshold and start the cell cycle [82]. The synthesis of proteins is highly dependent on GTP availability, not only in the elongation step but also in the initiation of translation [83]. The two initiation factors eIF2α and eIF2B have a higher affinity for GDP than GTP and it is therefore not surprising that an imbalance in the GTP/GDP ratio also can affect the rate of protein synthesis [79,80].

The value of the GTP/GDP ratio during exponential growth on glucose obtained in the current study (Figure 7D) agrees well with the results presented by Rudoni *et al.* [78]. The dynamic change in the XI-strain also corresponds with the reported response to carbon exhaustion. The very low GTP/GDP ratio in this strain on xylose could result in low Ras/cAMP activity and rate of protein synthesis leading to an arrest in the G0 phase of the cell cycle. This would support the idea that xylose is not sensed as a fermentable carbon source by the yeast cells [24,66,69] and does not activate the biosynthetic machinery efficiently. However, the GTP/GDP ratio did not change significantly in the XR/XDH-strain during the transition to xylose fermentation, suggesting that the GTP/GDP ratio rather responds to the rate of carbon supply than to what type of carbon source is actually taken up. Hence, other constituents of the nutrient sensing pathways must be involved, e.g. Snf1 and the Tor kinases which can control the initiation of translation by modulating the phosphorylation of eIF2α [84].

Other indicators of metabolic status

In contrast to the GTP/GDP ratio both the guanylate energy charge (GEC) and the GTP/GMP ratio decreased significantly in the two strains when shifting to xylose fermentation (Figure 7B and C). The fast and distinct response in the GEC indicates that this measure could serve as a more sensitive indicator of metabolic status than the AEC. However, yeast lacks an enzyme equivalent to adenylate kinase that can catalyse the conversion of two molecules of GDP to GTP and GMP. Thus, the GEC can be calculated analogous to the AEC, but it is not related to any biological process. Even so, the pools of the adenine and guanine nucleotides are directly interconnected as GTP is used as a phosphate donor in the *de novo* synthesis of ATP and vice versa [85]. This could explain the similar values of the AEC and the GEC (0.82 and 0.86, respectively) during the glucose phase (Figure 7A and B). A 10-fold decrease in the GTP/GMP ratio, similar to the one reported here, as a response to a change from glucose to xylose fermentation has also been measured in a recent study [41]. This highlights the sensitivity of this ratio and could therefore be a better indicator of metabolic status as it is directly related to metabolic processes. However, there have been no studies on how and to what extent the GTP/GMP ratio affects or controls metabolic processes. Even though the role of the guanine nucleotides in yeast metabolism has been less explored than that of the adenine nucleotides, it is clear that the biochemical processes in which these nucleotides participate are required for both growth and survival [86,87]. Recent studies have shown that an imbalance in the guanine nucleotide pool can have detrimental effects on nitrogen metabolism, protein synthesis, viability and proliferation of yeast cells [78,79,88,89]. Still, more systematic investigations of the response in the guanine nucleotide pools under different conditions are needed to understand the role they play in the physiology of yeast.

Conclusions

In this study we determined the time-dependent changes in a selected part of the metabolome of two recombinant strains of *S. cerevisiae*, harbouring either the XR/XDH or the XI pathway, in response to a transition from glucose to xylose fermentation. A fundamental difference between the two strains was the very low uptake rate of xylose by the XI-strain, which gave rise to larger changes in metabolite concentrations than in the XR/XDH-

strain. However, even though the XR/XDH-strain had a 10-fold higher uptake rate of xylose it did not continue to grow after glucose depletion. This indicates that factors other than sugar transport limit the growth on xylose. Several distinct responses in the XI-strain were not observed in the XR/XDH-strain: depletion of NADPH and several metabolites in glycolysis, accumulation of PEP and a reduced GTP/GDP ratio. These changes in the metabolome typically direct towards carbon starvation, which appears to be the general response of the XI-strain to xylose. Still, both strains maintained a high and stable energy charge during the transition to xylose, indicating that neither strain is energy limited. In fact, the only response observed in both strains was the accumulation of aromatic amino acids. We suggest that this is related to a general decrease in protein concentration. We also suggest that the redox imbalance between XR and XDH, combined with the poor ability of xylose to repress genes associated with respiratory pathways, give rise to reactions unbeneficial for xylose fermentation.

In light of the stable energy charge, xylose fermentation seems to present a unique condition for *S. cerevisiae* where the energy metabolism is uncoupled from carbon metabolism. The observed discrimination between energy and carbon starvation during xylose fermentation has not been reported previously, but is now made visible through metabolomic analysis of isogenic strains. However, the maintenance of a high energy charge does evidently not correlate with the general metabolic status of the cells; hence, other internal signals could be better indicators. Potential candidates are the guanylate energy charge and the GTP/GMP ratio as they decreased significantly in both strains. The importance of these relationships as indicators of metabolic status merits further investigation as the guanine nucleotides have been shown to play an important regulatory role in cell biology and metabolism. Dynamic metabolomics is a suitable method for exposing such underlying metabolic interactions and to unravel the behaviour of rationally designed cell factories and wild type microorganisms.

Methods

Strains and cultivation conditions

In this study, two recombinant strains of *Saccharomyces cerevisiae*, with the same genetic background but with two different pathways for xylose utilization, were used, i.e. TMB 3057 employing the XR/XDH pathway [21] and TMB 3359 utilizing a xylose isomerase from *Piromyces* sp [22]. Liquid cultures were grown in yeast nitrogen base medium (YNB) without amino acids (1.7 g/L; Difco, Becton, Dickinson and Company, Sparks, MD, USA) with 20 g/L glucose and 5 g/L ammonium sulphate. In anaerobic fermentation, double concentration of YNB (2X YNB) with 20 g/L glucose and 40 g/L xylose was used, supplemented with 5 g/L ammonium sulphate, 400 mg/L Tween 80 and 10 mg/L ergosterol.

Batch fermentation

Cells were pre-grown in YNB medium until late exponential phase and inoculated into the bioreactor at a concentration of 0.04 g CDW/L. Anaerobic fermentation was performed in a 3.1 L Benchtop Fermenter Type KLF2000 bioreactor (Bioengineering AG, Switzerland) with a working volume of 2 litres. The temperature was 30°C, stirring was set at 900 rpm and pH was controlled at 5.5 with 3 M KOH and 1.5 M H_2SO_4. Anaerobic conditions were maintained by sparging the culture broth with 0.5 L/min nitrogen gas (Grade 5.0, containing less than 3 ppm oxygen; PanGas AG, Switzerland) controlled by a gas flow controller (Get red-y, Vögtlin Intruments AG, Switzerland). The condenser was connected to a Thermostatic Circulator 2219 (LKB Produkter AB, Sweden) and cooled to 4°C. Foaming was prevented by adding three to four drops of sterile 50% PEG2000. Fermentation experiments were performed in duplicate.

Quantification of extracellular substrates and products

Concentrations of substrates and products in the culture broth were determined by HPLC (Waters, USA) with Aminex HPX-87 H ion exchange column (Bio-Rad, USA) and refractive index detector (RID-6A, Shimadzu, Japan). Mobile phase was 5 mM H_2SO_4, the temperature 45°C and the flow rate 0.6 mL/min. Apart from glucose, xylose, xylitol, glycerol and ethanol, no other compounds were detected in the analysis. Stated concentrations of ethanol are not corrected for losses due to evaporation.

Biomass determination

Optical density was measured in triplicate at each time point at 600 nm. Cell dry weight was determined in triplicate by filtering 10 mL of culture through a dried and pre-weighed nitrocellulose filter with a 0.45 μm pore size. The filters were washed with an equal amount of water and dried at 80°C overnight. The filters were allowed to equilibrate to room temperature before weighed again.

Quenching, extraction of intracellular metabolites and sample preparation

The quenching procedure of cell samples was based on the method developed by de Koning *et al.* [25]. Quenching was achieved by quickly adding 1 mL of cell culture to 4 mL of cold, buffered methanol (60% methanol, 10 mM ammonium acetate, pH 7.5, -40°C). The cells were cooled at −40°C in an ethylene glycol bath (FP40-MC, Julabo, Germany) for maximum 30 seconds and then collected by centrifugation at 5000 rpm and −9°C for 5 min. The supernatant was decanted and any residual

liquid was removed with a pipette. The pellet was then immediately frozen in liquid nitrogen and stored at −80°C until extraction. Quadruplicate samples were quenched at each time point.

Intracellular metabolites were extracted using the boiling ethanol procedure [90]. Frozen cell pellets were briefly thawed at −40°C before extraction. To extract the metabolites, 1 mL of boiling, buffered ethanol (75% ethanol, 10 mM ammonium acetate, pH 7.5, 85°C) was added to the pellet, directly followed by addition of 100 μL of an internal standard (metabolite extract of yeast grown on ^{13}C-labeled glucose) and vortexed quickly. The mixture was incubated 3 min at 85°C with vigorous mixing every 30 seconds. The solution was then shortly cooled back to −40°C and cell debris was spun down by centrifugation at 5000 rpm and −9°C for 3 min. The supernatant was collected in a 1.5 mL tube, frozen in liquid nitrogen and stored at −80°C until further use.

Extracted metabolites were dried by evaporating the solvent at low pressure, 0.01-0.1 mbar, using a Christ Alpha 2–4 LD Plus rotational vacuum concentrator (Adolf Kühner AG, Switzerland) connected to a Chemistry Hybrid Pump RC 6 (Vacuubrand GmbH, Germany) and a Christ AVC 2–33 centrifuge (Adolf Kühner AG, Switzerland). Dried samples were stored at −80°C until further use.

Metabolite analysis by LC-MS/MS

Separation and detection of compounds was achieved on a Waters Acquity UPLC (Waters Corporation, Milford, MA, USA) using a Waters Acquity T3 end-capped reverse phase column with dimensions 150 mm × 2.1 mm × 1.8 mm (Waters Corporation) coupled to a Thermo TSQ Quantum Ultra triple quadrupole mass spectrometer (Thermo Fisher Scientific, Waltham, MA, USA) as previously described [20].

Data normalization, calibration and quantification

Detection and integration of chromatographic peaks was performed using Xcalibur software version 2.0.7 (Thermo Fisher Scientific Inc, USA). The automatic integrations were manually curated to obtain consistent peak boundaries and the results were exported to MATLAB R2008a (The MathWorks, USA) where subsequent data processing was performed.

The signal of each analyte was normalized according to the following equation:

$$\widetilde{X}_{ijk} = X_{ijk}\frac{\langle Z_{i\cdot}\rangle}{Z_{ijk}}$$

where X_{ijk} and $\widetilde{X}_{ijk}$ are the measured and normalized signals of analyte i in sample k of time point j, respectively, Z_{ijk} is the signal of the ^{13}C-labeled analyte i and $\langle Z_{i\cdot}\rangle$ is a robust mean of the internal standard signals of analyte i in all samples. The robust mean was calculated according to an iterative procedure as outlined in Miller & Miller [91] p. 174].

Seven external standards with known concentrations ranging from 0.14 μM to 100 μM were analyzed together with each batch of samples to be quantified. An initial robust linear regression with a logistic estimator was used to identify possible outliers in the calibration data. Data points with a z-score above three were regarded as outliers and removed from the data set [92]. An ordinary least squares (OLS) regression was then performed with the remaining data points to obtain unbiased model and regression parameters [93]. All calibration curves had at least five data points in the final OLS regression and the adjusted coefficients of determination (adjusted R^2) were between 0.90 and 1, with the majority around 0.99. A term for the intercept was included in the equation only if the root mean squared error (RMSE) was lower than the RMSE obtained without including the intercept and if it was statistically significant according to a t-test at the 0.05 probability level.

The intracellular concentration corresponding to an estimated sample concentration was calculated from the sample volume and the measured cell dry weight. All intracellular concentrations stated in this paper are mean values of concentrations from duplicate biological experiments and errors are given as a 95% confidence interval of the calculated mean. Samples collected at a particular time point were analyzed for outliers before calculating the mean. This was done by calculating the ratio between $|c_{ijk} - \text{median}(c_{ij\cdot})|$ and the median absolute deviation (MAD): $\text{median}(|c_{ijk} - \text{median}(c_{ij\cdot})|)$. Measurements with a ratio above four were regarded as outliers and were removed. The total number of replicates at each time point was between four and ten, but the majority of the means were calculated from seven replicates.

Chemometrics

Principal component analysis (PCA) is a statistical method commonly used to analyse data from metabolomics studies [94]. PCA is an unsupervised method used to reduce the dimension of the data by calculating new components which are linear combinations of the original values [95]. The first component is constructed so that it accounts for the highest fraction of the total variance in the data; the second component is constructed to be orthogonal (uncorrelated) to the first component and account for the highest fraction of the variance in this direction. Subsequent components are constructed similarly resulting in a number of components that are fewer than the original number of variables (dimension reduction) and uncorrelated and thus give a unique

description of each sample in the new dimension. PCA is classified as an unsupervised method because no prior grouping of the data is required. The result can therefore give an insight into the natural grouping of the data based on the maximisation of the variance criterion. PCA was performed in MATLAB R2010b (Mathworks, USA) using the *princomp* function on quantified concentrations of 37 metabolites from 185 samples. After removing outliers according to the above mentioned criterion the data matrix contained 5.6% missing data points. If only one data point was missing in a certain sampling point and strain it was replaced by the average value of the measured concentrations. If more than one data point was missing, they were replaced by randomly generated numbers from a t-distribution with the number of degrees of freedom equal to the number of samples at that sampling point minus one. The random numbers were converted to concentrations by multiplication with the standard deviation and addition of the mean of the known concentrations. Each metabolite in the imputed data matrix was normalized to the median concentration measured in both strains at the first sampling point and then converted to $\log_2$ scale.

Hierarchical clustering was performed using the *clustergram* function in MATLAB R2010b with quantified concentrations and normalized chromatographic peak areas of 38 and six metabolites, respectively. The data for the XR/XDH-strain and the XI-strain contained 95 and 90 samples, respectively. Each set of samples was normalized to the corresponding mean concentration or peak area at the first sampling point before converted to $\log_2$ scale. Euclidean distance was used to calculate the distance between the metabolite profiles and average linkage was used to generate the dendrogram. Data used for the PCA and the hierarchical clustering are given as supplementary information in Additional file 3.

Thermodynamic analysis

The thermodynamic analysis of measured metabolite concentrations in the XR/XDH-strain was performed using anNET version 1.1.06 [23]. Detailed information regarding the calculations and discussion of the results is given in Additional file 2. All the data used in the calculations are given as supplementary information in Additional file 4.

Additional files

Additional file 1: Supplementary figures and tables.

Additional file 2: Thermodynamic evaluation of metabolite concentrations [20, 24-35].

Additional file 3: Data used for PCA and cluster analysis.

Additional file 4: Data used for validation of metabolite concentrations.

Abbreviations

AEC: Adenylate energy charge; GEC: Guanylate energy charge; PCA: Principal component analysis; PPP: Pentose phosphate pathway; TCA cycle: Tricarboxylic acid cycle;

Metabolites

2PG: 2-phosphoglycerate; 3PG: 3-phosphoglycerate; 6PG: 6-phosphogluconate; 6pgl: 6-phosphogluconolactonate; Acald: Acetaldehyde; ACCOA: Acetyl-Coenzyme A; ADP: Adenosine 5'-diphosphate; AKG: α-ketoglutarate; ALA-L: Alanine; AMP: Adenosine 5'-monophosphate; ARG-L: Arginine; ASN-L: Asparagine; ASP-L: Aspartate; ATP: Adenosine 5'-triphosphate; BPG, Bpg: 1,3-bisphosphoglycerate; cAMP: Cyclic AMP; CIT: Citrate; CoA: Coenzyme A; Cys: Cysteine; DHAP: Dihydroxy acetone phosphate; E4p: Erythrose 4-phosphate; F26BP: Fructose 2,6-bisphosphate; F6P: Fructose 6-phosphate; FAD: Flavin adenine dinucleotide; FBP: Fructose 1,6-bisphosphate; FMN: Riboflavin 5'-monophosphate; FUM: Fumarate; G1P: Glucose 1-phosphate; G6P: Glucose 6-phosphate; GAP, Gap: Glyceraldehyde 3-phosphate; GDP: Guanosine 5'-diphosphate; GLN-L: Glutamine; GLU-L: Glutamate; Gly: Glycine; GLYC3P: Glycerol 3-phosphate; GMP: Guanosine 5'-monophosphate; GTP: Guanosine 5'-triphosphate; GTTox: Oxidized glutathione; GTTred: Reduced glutathione; His: Histidine; ICIT: Isocitrate; Ile: Isoleucine; Leu: Leucine; L-MAL: L-malate; Lys: lysine; Met: Methionine; NAD: Oxidized nicotinamide adenine dinucleotide; NADH: Reduced nicotinamide adenine dinucleotide; NADP: Oxidized nicotinamide adenine dinucleotide phosphate; NADPH: Reduced nicotinamide adenine dinucleotide phosphate; Oaa: Oxaloacetate; PEP: Phoshoenolpyruvate; PHE-L: Phenylalanine; Pro: Proline; PYR, pyr: Pyruvate; R5P: Ribose 5-phosphate; RU5P: Ribulose 5-phosphate; S7P: Sedoheptulose 7-phosphate; Ser: Serine; SUCC: Succinate; Succoa: Succinyl-Coenzyme A; T6P: Trehalose 6-phosphate; Thr: Threonine; TRP-L: Tryptophane; TYR-L: Tyrosine; Val: Valine; xPG: Combined pool of 2PG and 3PG; XU5P: Xylulose 5-phosphate; Xylu: Xylulose;

Enzymes

ACOm: Aconitase EC 4.2.1.3; ACS: Acetyl-CoA synthetase EC 6.2.1.1; ADH: Alcohol dehydrogenase EC 1.1.1.1; AK: Adenylate kinase EC 2.7.4.3; AKGDm: Alpha-ketoglutarate dehydrogenase EC 1.2.4.2; ALDH: Aldehyde dehydrogenase EC 1.2.1.3; CSm: Citrate synthase EC 2.3.3.1; CYR1: Adenylate cyclase EC 4.6.1.1; ENO: Enolase EC 4.2.1.11; FBA: Fructose 1,6-bisphosphate aldolase EC 4.1.2.13; FBP1: Fructose-1,6-bisphosphatase EC 3.1.3.11; FBP26: Fructose-2,6-bisphosphatase EC 3.1.3.46; FRD, FRDm: Fumarate reductase EC 1.3.1.6; FUMASE, FUMASEm: Fumarase EC 4.2.1.2; G6PDH: Glucose-6-phosphate dehydrogenase EC 1.1.1.49; GAPD: Glyceraldehyde-3-phosphate dehydrogenase EC 1.2.1.12; GND: 6-phosphogluconate dehydrogenase EC 1.1.1.44; GPD: NAD-dependent glycerol 3-phosphate dehydrogenase EC 1.1.1.8; GPP: DL-glycerol-3-phosphatase EC 3.1.3.21; HXK: Hexokinase EC 2.7.1.2; IDHm: Isocitrate dehydrogenase EC 1.1.1.41; MDH2, MDH1m: Malate dehydrogenase EC 1.1.1.37; NTH: Trehalase, EC 3.2.1.28; PC: Pyruvate carboxylase EC 6.4.1.1; PDC: Pyruvate decarboxylase EC 4.1.1.1; PDHm: Pyruvate dehydrogenase complex EC 1.2.4.1; PFK: 6-phosphofructo kinase EC 2.7.1.11; PFK26: 6-phosphofructo-2-kinase EC 2.7.1.105; PGAM: Phosphoglycerate mutase EC 5.4.2.1; PGI: Phosphoglucose isomerase EC 5.3.1.9; PGK: 3-phosphoglycerate kinase EC 2.7.2.3; PGL: 6-phosphogluconolactonase EC 3.1.1.31; PKA: cAMP-dependent protein kinase EC 2.7.11.11; PYK: Pyruvate kinase EC 2.7.1.40; RKI: Ribose-5-phosphate ketol-isomerase EC 5.3.1.6; RPE: D-ribulose-5-phosphate 3-epimerase EC 5.1.3.1; SUCOASm: Succinate-CoA ligase EC 6.2.1.5; TAL: Transaldolase EC 2.2.1.2; TKL1, TKL2: Transketolase EC 2.2.1.1; TPI: Triose phosphate isomerase EC 5.3.1.1; TPS1: Trehalose-6-phosphate synthase EC 2.4.1.15; TPS2: Trehalose-6-phosphate phosphatase EC 3.1.3.12; XDH: Xylitol dehydrogenase EC 1.1.1.9; XI: Xylose isomerase EC 5.3.1.5; XR: Xylose reductase EC 1.1.1.307.

Competing interests

The authors declare that BHH is founder and chairman of the board of C5 Ligno Technologies in Lund AB, Sweden.

Authors' contributions

BB conceived the study, carried out the experimental work, the analysis and interpretation of the data and drafted the manuscript. DH participated in the

design of the study and in the experimental work. BBH and EWJN participated in the design of the study, contributed to the interpretation of the data and critically revised the manuscript. US contributed by critically revising the content of the manuscript. All authors' read and approved the final manuscript.

Acknowledgements
This work was supported by funding from the EU project NILE within the 6th framework programme (Contract N° 019882). BB also received financial support from the Swedish Energy Agency. We wish to thank Professor Marie-Francoise Gorwa-Grauslund for critically reading the manuscript.

Author details
[1]Applied Microbiology, Lund University, PO Box 124, SE-221 00 Lund, Sweden. [2]ETH Zurich, Zurich 8093 Switzerland.

Received: 15 November 2011 Accepted: 23 April 2012
Published: 15 May 2012

References

1. Nevoigt E: **Progress in metabolic engineering of *Saccharomyces cerevisiae*.** *Microbiol Mol Biol Rev* 2008, **72:**379–412.
2. Lin Y, Tanaka S: **Ethanol fermentation from biomass resources: Current state and prospects.** *Appl Microbiol Biotechnol* 2006, **69:**627–642.
3. Wiselogel AE, Agblevor FA, Johnson DK, Deutch S, Fennell JA, Sanderson MA: **Compositional changes during storage of large round switchgrass bales.** *Bioresour Technol* 1996, **56:**103–109.
4. Perez DD, Guillemain A, Berthelot A, N'Guyen-The N, De Morogues F, Gomes C: **Evaluation of forestry biomass quality for the production of second-generation biofuels.** *Cell Chem Technol* 2010, **44:**1–14.
5. Sassner P, Galbe M, Zacchi G: **Techno-economic evaluation of bioethanol production from three different lignocellulosic materials.** *Biomass Bioenerg* 2008, **32:**422–430.
6. Van Vleet JH, Jeffries TW: **Yeast metabolic engineering for hemicellulosic ethanol production.** *Curr Opin Biotechnol* 2009, **20:**300–306.
7. Matsushika A, Inoue H, Kodaki T, Sawayama S: **Ethanol production from xylose in engineered *Saccharomyces cerevisiae* strains: Current state and perspectives.** *Appl Microbiol Biotechnol* 2009, **84:**37–53.
8. Hahn-Hagerdal B, Karhumaa K, Fonseca C, Spencer-Martins I, Gorwa-Grauslund MF: **Towards industrial pentose-fermenting yeast strains.** *Appl Microbiol Biotechnol* 2007, **74:**937–953.
9. Kern A, Tilley E, Hunter IS, Legisa M, Glieder A: **Engineering primary metabolic pathways of industrial micro-organisms.** *J Biotechnol* 2007, **129:**6–29.
10. Karhumaa K, Sanchez RG, Hahn-Hagerdal B, Gorwa-Grauslund MF: **Comparison of the xylose reductase-xylitol dehydrogenase and the xylose isomerase pathways for xylose fermentation by recombinant *Saccharomyces cerevisiae*.** *Microb Cell Fact* 2007, **6:**5. doi:10.1186/1475-2859-6-5.
11. Bengtsson O: **Genetic traits beneficial for xylose utilization by recombinant *Saccharomyces cerevisiae*. *Doctoral Thesis*.** *Lund University, Division of Applied Microbiology* 2008, .
12. Bruinenberg PM, de Bot PHM, van Dijken JP, Scheffers WA: **NADH-linked aldose reductase - the key to anaerobic alcoholic fermentation of xylose by yeasts.** *Appl Microbiol Biotechnol* 1984, **19:**256–260.
13. Bruinenberg PM, de Bot PHM, van Dijken JP, Scheffers WA: **The role of redox balances in the anaerobic fermentation of xylose by yeasts.** *Appl Microbiol Biotechnol* 1983, **18:**287–292.
14. Kotter P, Ciriacy M: **Xylose fermentation by *Saccharomyces cerevisiae*.** *Appl Microbiol Biotechnol* 1993, **38:**776–783.
15. van Maris AJA, Winkler AA, Kuyper M, de Laat W, van Dijken JP, Pronk JT: **Development of efficient xylose fermentation in *Saccharomyces cerevisiae*: Xylose Isomerase as a key component**. In *Biofuels*. Edited by Olsson L. Berlin: Springer-Verlag Berlin; 2007:179–204 [Scheper T (Series Editor): *Advances in Biochemical Engineering/Biotechnology*, vol 108.].
16. Smedsgaard J, Nielsen J: **Metabolite profiling of fungi and yeast: from phenotype to metabolome by MS and informatics.** *J Exp Bot* 2005, **56:**273–286.
17. Delneri D, Brancia FL, Oliver SG: **Towards a truly integrative biology through the functional genomics of yeast.** *Curr Opin Biotechnol* 2001, **12:**87–91.
18. Heinemann M, Sauer U: **Systems biology of microbial metabolism.** *Curr Opin Microbiol* 2010, **13:**337–343.
19. Gerosa L, Sauer U: **Regulation and control of metabolic fluxes in microbes.** *Curr Opin Biotechnol* 2011, **22:**566–575.
20. Buescher JM, Moco S, Sauer U, Zamboni N: **Ultrahigh performance liquid chromatography-tandem mass spectrometry method for fast and robust quantification of anionic and aromatic metabolites.** *Anal Chem* 2010, **82:**4403–4412.
21. Karhumaa K, Hahn-Hägerdal B, Gorwa-Grauslund MF: **Investigation of limiting metabolic steps in the utilization of xylose by recombinant *Saccharomyces cerevisiae* using metabolic engineering.** *Yeast* 2005, **22:**359–368.
22. Parachin NS, Bergdahl B, van Niel EWJ, Gorwa-Grauslund MF: **Kinetic modeling reveals current limitations in the production of ethanol from xylose by recombinant *Saccharomyces cerevisiae*.** *Metab Eng* 2011, **13:**508–517.
23. Zamboni N, Kummel A, Heinemann M, anNET: **A tool for network-embedded thermodynamic analysis of quantitative metabolome data.** *BMC Bioinformatics* 2008, **9:**199.
24. Runquist D, Hahn-Hagerdal B, Bettiga M: **Increased expression of the oxidative pentose phosphate pathway and gluconeogenesis in anaerobically growing xylose-utilizing *Saccharomyces cerevisiae*.** *Microb Cell Fact* 2009, **8:**49.
25. de Koning W, van Dam K: **A method for the determination of changes of glycolytic metabolites in yeast on a subsecond time scale using extraction at neutral pH.** *Anal Biochem* 1992, **204:**118–123.
26. Zamboni N, Kummel A, Heinemann M: **anNET: A tool for networkembedded thermodynamic analysis of quantitative metabolome data.** *BMC Bioinformatics* 2008, **9:**199.
27. Mo M, Palsson B, Herrgard M: **Connecting extracellular metabolomic measurements to intracellular flux states in yeast.** *BMC Syst Biol* 2009, **3:**37.
28. Becker SA, Feist AM, Mo ML, Hannum G, Palsson BO, Herrgard MJ: **Quantitative prediction of cellular metabolism with constraint-based models: the COBRA Toolbox.** *Nat Protocols* 2007, **2:**727–738.
29. Wahlbom CF, Eliasson A, Hahn-Hägerdal B: **Intracellular fluxes in a recombinant xylose-utilizing *Saccharomyces cerevisiae* cultivated anaerobically at different dilution rates and feed concentrations.** *Biotechnol Bioeng* 2001, **72:**289–296.
30. Snitkin E, Dudley A, Janse D, Wong K, Church G, Segre D: **Model-driven analysis of experimentally determined growth phenotypes for 465 yeast gene deletion mutants under 16 different conditions.** *Genome Biol* 2008, **9:**R140.
31. Jankowski MD, Henry CS, Broadbelt LJ, Hatzimanikatis V: **Group contribution method for thermodynamic analysis of complex metabolic networks.** *Biophys J* 2008, **95:**1487–1499.
32. Klimacek M, Krahulec S, Sauer U, Nidetzky B: **Limitations in xylosefermenting *Saccharomyces cerevisiae*, made evident through comprehensive metabolite profiling and thermodynamic analysis.** *Appl Environ Microbiol* 2010, **76:**7566–7574.
33. Cipollina C, ten Pierick A, Canelas AB, Seifar RM, van Maris AJA, van Dam JC, Heijnen JJ: **A comprehensive method for the quantification of the nonoxidative pentose phosphate pathway intermediates in *Saccharomyces cerevisiae* by GC-IDMS.** *J Chromatogr B* 2009, **877:**3231–3236.
34. Hynne F, Dano S, Sorensen PG: **Full-scale model of glycolysis in *Saccharomyces cerevisiae*.** *Biophys Chem* 2001, **94:**121–163.
35. Altintas MM, Eddy CK, Zhang M, McMillan JD, Kompala DS: **Kinetic modeling to optimize pentose fermentation in *Zymomonas mobilis*.** *Biotechnol Bioeng* 2006, **94:**273–295.
36. Ball WJ, Atkinson DE: **Adenylate energy charge in *Saccharomyces cerevisiae* during starvation.** *J Bacteriol* 1975, **121:**975–982.
37. Klimacek M, Krahulec S, Sauer U, Nidetzky B: **Limitations in xylose-fermenting *Saccharomyces cerevisiae*, made evident through comprehensive metabolite profiling and thermodynamic analysis.** *Appl Environ Microbiol* 2010, **76:**7566–7574.
38. Wisselink HW, Cipollina C, Oud B, Crimi B, Heijnen JJ, Pronk JT, van Maris AJA: **Metabolome, transcriptome and metabolic flux analysis of arabinose fermentation by engineered *Saccharomyces cerevisiae*.** *Metab Eng* 2010, **12:**537–551.
39. Karhumaa K, Fromanger R, Hahn-Hagerdal B, Gorwa-Grauslund MF: **High activity of xylose reductase and xylitol dehydrogenase improves xylose fermentation by recombinant *Saccharomyces cerevisiae*.** *Appl Microbiol Biotechnol* 2007, **73:**1039–1046.

40. Kuyper M, Toirkens MJ, Diderich JA, Winkler AA, van Dijken JP, Pronk JT: **Evolutionary engineering of mixed-sugar utilization by a xylose-fermenting Saccharomyces cerevisiae strain.** *Fems Yeast Research* 2005, **5:**925–934.
41. Sedlak M, Ho NWY: **Characterization of the effectiveness of hexose transporters for transporting xylose during glucose and xylose co-fermentation by a recombinant Saccharomyces yeast.** *Yeast* 2004, **21:**671–684.
42. Saloheimo A, Rauta J, Stasyk OV, Sibirny AA, Penttila M, Ruohonen L: **Xylose transport studies with xylose-utilizing Saccharomyces cerevisiae strains expressing heterologous and homologous permeases.** *Appl Microbiol Biotechnol* 2007, **74:**1041–1052.
43. Fonseca C, Olofsson K, Ferreira C, Runquist D, Fonseca LL, Hahn-Hagerdal B, Liden G: **The glucose/xylose facilitator Gxf1 from *Candida intermedia* expressed in a xylose-fermenting industrial strain of *Saccharomyces cerevisiae* increases xylose uptake in SSCF of wheat straw.** *Enzyme Microb Technol* 2011, **48:**518–525.
44. Stephanopoulos G, Aristidou A, Nielsen J: *Metabolic Engineering: Principles and Methodologies*. San Diego, CA, USA: Elsevier Academic Press; 1998.
45. Frick O, Wittmann C: **Characterization of the metabolic shift between oxidative and fermentative growth in *Saccharomyces cerevisiae* by comparative C-13 flux analysis.** *Microb Cell Fact* 2005, **4:**30. doi:10.1186/1475-2859-4-30.
46. Gancedo JM, Lagunas R: **Contribution of the pentose-phosphate pathway to glucose metabolism in *Saccharomyces cerevisiae*: A critical analysis on the use of labelled glucose.** *Plant Science Letters* 1973, **1:**193–200.
47. Maaheimo H, Fiaux J, Çakar ZP, Bailey JE, Sauer U, Szyperski T: **Central carbon metabolism of *Saccharomyces cerevisiae* explored by biosynthetic fractional ^{13}C labeling of common amino acids.** *Eur J Biochem* 2001, **268:**2464–2479.
48. Senac T, Hahn-Hägerdal B: **Intermediary metabolite concentrations in xylulose-fermenting and glucose-fermenting *Saccharomyces cerevisiae* cells.** *Appl Environ Microbiol* 1990, **56:**120–126.
49. Johansson B, Hahn-Hagerdal B: **The non-oxidative pentose phosphate pathway controls the fermentation rate of xylulose but not of xylose in *Saccharomyces cerevisiae* TMB3001.** *Fems Yeast Research* 2002, **2:**277–282.
50. Chu BCH, Lee H: **Genetic improvement of *Saccharomyces cerevisiae* for xylose fermentation.** *Biotechnol Adv* 2007, **25:**425–441.
51. Evans PR, Farrants GW, Hudson PJ: **Phosphofructokinase - structure and control.** *Philos Trans R Soc Lond B Biol Sci* 1981, **293:**53–62.
52. Brauer MJ, Yuan J, Bennett BD, Lu W, Kimball E, Botstein D, Rabinowitz JD: **Conservation of the metabolomic response to starvation across two divergent microbes.** *Proc Natl Acad Sci USA* 2006, **103:**19302–19307.
53. Walther T, Novo M, Roessger K, Letisse F, Loret M-O, Portais J-C, Francois J-M: **Control of ATP homeostasis during the respiro-fermentative transition in yeast.** *Mol Syst Biol* 2010, **6:**344.
54. Kresnowati MTAP, van Winden WA, Almering MJH, ten Pierick A, Ras C, Knijnenburg TA, Daran-Lapujade P, Pronk JT, Heijnen JJ, Daran JM: **When transcriptome meets metabolome: fast cellular responses of yeast to sudden relief of glucose limitation.** *Mol Syst Biol* 2006, **2:**49. doi:10.1038/msb4100083.
55. Boles E, Zimmermann FK, Heinisch J: **Different signals control the activation of glycolysis in the yeast *Saccharomyces cerevisiae*.** *Yeast* 1993, **9:**761–770.
56. Mueller S, Boles E, May M, Zimmermann FK: **Different internal metabolites trigger the induction of glycolytic gene expression in Saccharomyces cerevisiae.** *J Bacteriol* 1995, **177:**4517–4519.
57. Barwell CJ, Woodward B, Brunt RV: **Regulation of pyruvate kinase by fructose 1,6-diphosphate in *Saccharomyces cerevisiae*.** *Eur J Biochem* 1971, **18:**59–64.
58. Gad A: **Stimulation of yeast phosphofructokinase activity by Fructose 2,6-bisphosphate.** *Biochem Biophys Res Commun* 1981, **102:**985–991.
59. Francois J, Vanschaftingen E, Hers HG: **The mechanism by which glucose increases fructose 2,6-bisphosphate concentration in *Saccharomyces cerevisiae* - A cyclic-AMP-dependent activation of phosphofructokinase-2.** *Eur J Biochem* 1984, **145:**187–193.
60. Busti S, Coccetti P, Alberghina L, Vanoni M: **Glucose signaling-mediated coordination of cell growth and cell cycle in *Saccharomyces cerevisiae*.** *Sensors* 2010, **10:**6195–6240.
61. Jeffries TW, Fady JH, Lightfoot EN: **Effect of glucose supplements on the fermentation of xylose by *Pachysolen tannophilus*.** *Biotechnology and Bioengineering* 1985, **27:**171–176.
62. Ohgren K, Bengtsson O, Gorwa-Grauslund MF, Galbe M, Hahn-Hagerdal B, Zacchi G: **Simultaneous saccharification and co-fermentation of glucose and xylose in steam-pretreated corn stover at high fiber content with *Saccharomyces cerevisiae* TMB3400.** *Journal of Biotechnology* 2006, **126:**488–498.
63. Krahulec S, Petschacher B, Wallner M, Longus K, Klimacek M, Nidetzky B: **Fermentation of mixed glucose-xylose substrates by engineered strains of *Saccharomyces cerevisiae*: Role of the coenzyme specificity of xylose reductase, and effect of glucose on xylose utilization.** *Microb Cell Fact* 2010, **10:**9–16.
64. Braus GH: **Aromatic amino acid biosynthesis in the yeast *Saccharomyces-cerevisiae* - a model system for the regulation of a eukaryotic biosynthetic pathway.** *Microbiol Rev* 1991, **55:**349–370.
65. Mauricio JC, Pareja M, Ortega JM: **Changes in the intracellular concentrations of the adenosine phosphates and nicotinamide adenine dinucleotides of *Saccharomyces cerevisiae* during batch fermentation.** *World J Microbiol Biotechnol* 1995, **11:**196–201.
66. Salusjarvi L, Pitkanen JP, Aristidou A, Ruohonen L, Penttila M: **Transcription analysis of recombinant *Saccharomyces cerevisiae* reveals novel responses to xylose.** *Appl Biochem Biotechnol* 2006, **128:**237–261.
67. Wahlbom CF, Hahn-Hagerdal B: **Furfural, 5-hydroxymethyl furfural, and acetoin act as external electron acceptors during anaerobic fermentation of xylose in recombinant *Saccharomyces cerevisiae*.** *Biotechnol Bioeng* 2002, **78:**172–178.
68. Wahlbom CF, Otero RRC, van Zyl WH, Hahn-Hagerdal B, Jonsson LJ: **Molecular analysis of a *Saccharomyces cerevisiae* mutant with improved ability to utilize xylose shows enhanced expression of proteins involved in transport, initial xylose metabolism, and the pentose phosphate pathway.** *Appl Environ Microbiol* 2003, **69:**740–746.
69. Jin YS, Laplaza JM, Jeffries TW: ***Saccharomyces cerevisiae* engineered for xylose metabolism exhibits a respiratory response.** *Appl Environ Microbiol* 2004, **70:**6816–6825.
70. Camarasa C, Grivet JP, Dequin S: **Investigation by 13C-NMR and tricarboxylic acid (TCA) deletion mutant analysis of pathways for succinate formation in *Saccharomyces cerevisiae* during anaerobic fermentation.** *Microbiology* 2003, **149:**2669–2678.
71. Minard KI, McAlisterhenn L: **Glucose-induced degradation of the MDH2 isozyme of malate dehydrogenase in yeast.** *J Biol Chem* 1992, **267:**17458–17464.
72. Atkinson DE: **Energy charge of adenylate pool as a regulatory parameter. Interaction with feedback modifiers.** *Biochemistry* 1968, **7:**4030–4034.
73. Dombek KM, Ingram LO: **Intracellular accumulation of AMP as a cause for the decline in rate of ethanol-production by *Saccharomyces cerevisiae* during batch fermentation.** *Appl Environ Microbiol* 1988, **54:**98–104.
74. Knowles CJ: **Microbial metabolic regulation by adenine nucleotide pools**. In *Microbial Energetics: Twenty-Seventh Symposium of the Society for General Microbiology*. Edited by Haddock BA, Hamilton WA. Cambridge: Cambridge University Press; 1977:241–283.
75. Chapman AG, Atkinson DE: **Adenine nucleotide concentrations and turnover rates. Their correlation with biological activity in bacteria and yeast**. In *Advances in microbial physiology*. Edited by Rose AH, Tempest DW. London: Academic Press; 1977:253–306.
76. Johnston GC, Ehrhardt CW, Lorincz A, Carter BLA: **Regulation of cell-size in the yeast *Sacchaormyces cerevisiae*.** *J Bacteriol* 1979, **137:**1–5.
77. Moore SA: **Kinetic evidence for a critical rate of protein synthesis in the *Saccharomyces cerevisiae* yeast cell cycle.** *J Biol Chem* 1988, **263:**9674–9681.
78. Rudoni S, Colombo S, Coccetti P, Martegani E: **Role of guanine nucleotides in the regulation of the Ras/cAMP pathway in *Saccharomyces cerevisiae*.** *BBA Mol Cell Res* 2001, **1538:**181–189.
79. Iglesias-Gato D, Martin-Marcos P, Santos MA, Hinnebusch AG, Tamame M: **Guanine nucleotide pool imbalance impairs multiple steps of protein synthesis and disrupts GCN4 translational control in *Saccharomyces cerevisiae*.** *Genetics* 2011, **187:**105–122.
80. Yalowitz JA, Jayaram HN: **Molecular targets of guanine nucleotides in differentiation, proliferation and apoptosis.** *Anticancer Res* 2000, **20:**2329–2338.
81. Toda T, Uno I, Ishikawa T, Powers S, Kataoka T, Broek D, Cameron S, Broach J, Matsumoto K, Wigler M: **In yeast, Ras proteins are controlling elements of adenylate cyclase.** *Cell* 1985, **40:**27–36.
82. Thevelein JM: **The Ras-adenylate cyclase pathway and cell cycle control in *Saccharomyces cerevisiae*.** *Antonie Van Leeuwenhoek* 1992, **62:**109–130.

83. Kapp LD, Lorsch JR: **The molecular mechanics of eukaryotic translation.** *Annu Rev Biochem* 2004, **73:**657–704.
84. Cherkasova V, Qiu H, Hinnebusch AG: **Snf1 promotes phosphorylation of the alpha subunit of eukaryotic translation initiation factor 2 by activating Gcn2 and inhibiting phosphatases Glc7 and Sit4.** *Molecular and Cellular Biology* 2010, **30:**2862–2873.
85. Henderson JF, Paterson ARP: *Nucleotide metabolism: an introduction*. New York: Academic Press; 1973.
86. Thompson FM, Atkinson DE: **Response of nucleoside diphosphate kinase to adenylate energy charge.** *Biochem Biophys Res Commun* 1971, **45:**1581.
87. Varma A, Freese EB, Freese E: **Partial deprivation of GTP initiates meiosis and sporulation in *Saccharomyces cerevisiae*.** *Mol Gen Genet* 1985, **201:**1–6.
88. Breton A, Pinson B, Coulpier F, Giraud MF, Dautant A, Daignan-Fornier B: **Lethal accumulation of guanylic nucleotides in *Saccharomyces cerevisiae* HPT1-deregulated mutants.** *Genetics* 2008, **178:**815–824.
89. Saint-Marc C, Pinson B, Coulpier F, Jourdren L, Lisova O, Daignan-Fornier B: **Phenotypic consequences of purine nucleotide imbalance in *Saccharomyces cerevisiae*.** *Genetics* 2009, **183:**529–538.
90. Gonzalez B, Francois J, Renaud M: **A rapid and reliable method for metabolite extraction in yeast using boiling buffered ethanol.** *Yeast* 1997, **13:**1347–1355.
91. Miller JN, Miller JC: *Statistics and Chemometrics for Analytical Chemistry*. 5th edition. Harlow: Pearson Education Limited; 2005.
92. Rousseeuw PJ: **Tutorial to robust statistics.** *J Chemometr* 1991, **5:**1–20.
93. Ortiz MC, Sarabia LA, Herrero A: **Robust regression techniques - A useful alternative for the detection of outlier data in chemical analysis.** *Talanta* 2006, **70:**499–512.
94. Scholz M, Selbig J: **Visualization and analysis of molecular data**. In *Metabolomics*. Totowa, USA: Humana Press; 2007:87–104 [Walker JM (Series Editor): *Methods in Molecular Biology*, vol 358.].
95. Jolliffe IT: *Principal component analysis*. 2nd edition. New York: Springer-Verlag; 2002.

doi:10.1186/1754-6834-5-34
Cite this article as: Bergdahl *et al.*: Dynamic metabolomics differentiates between carbon and energy starvation in recombinant *Saccharomyces cerevisiae* fermenting xylose. *Biotechnology for Biofuels* 2012 **5**:34.

Submit your next manuscript to BioMed Central and take full advantage of:

- **Convenient online submission**
- **Thorough peer review**
- **No space constraints or color figure charges**
- **Immediate publication on acceptance**
- **Inclusion in PubMed, CAS, Scopus and Google Scholar**
- **Research which is freely available for redistribution**

Submit your manuscript at
www.biomedcentral.com/submit

BioMed Central

Additional file 1
Figures

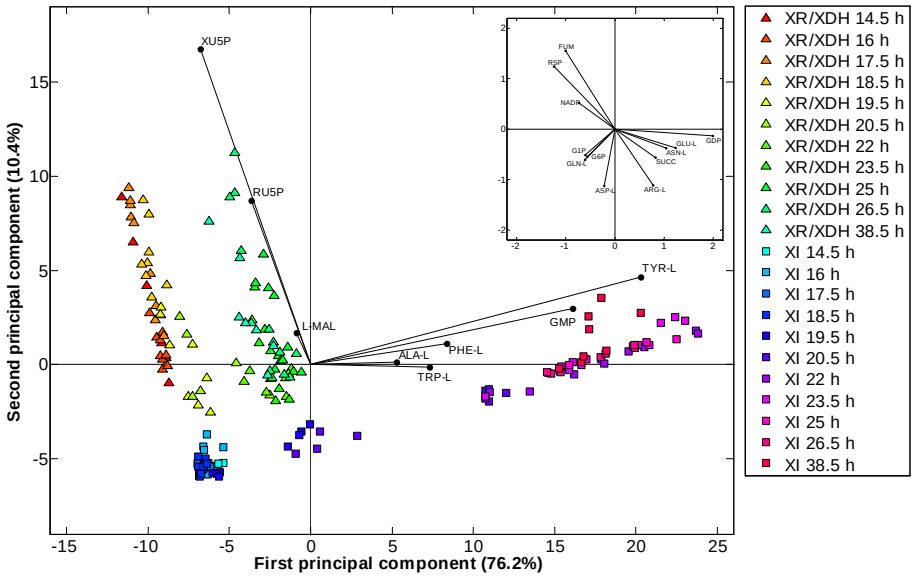

Figure S1 – Global analysis of the data by PCA.
Scores of the data points in the first two dimensions of the PCA analysis and the loadings of the 20 most influential metabolites. The first component accounted for 76.2% of the variance and separated the data by sampling time. The second component accounted for 10.4% of the variance and separated the data by strain background. Three distinct phases were identified during the fermentation: a glucose phase (14.5 h to 18.5 h), a transition phase (18.5 h to 22 h) and a xylose phase (22 h to 38.5 h). The two strains cluster closer together during the glucose phase as compared with the xylose phase. The metabolite loadings were scaled up 30 times in PC1 and 20 times in PC2 to increase readability.

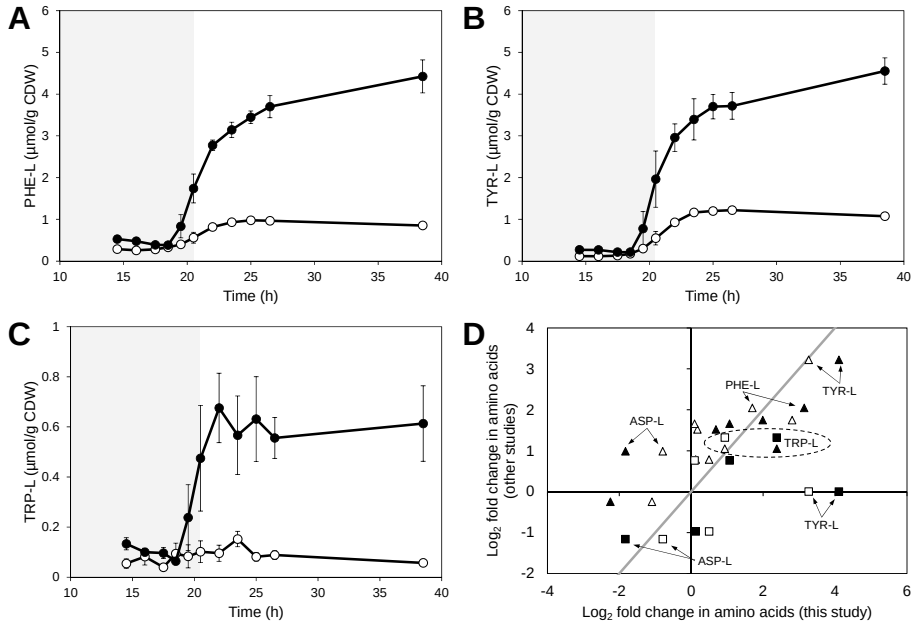

Figure S2 – Accumulation of aromatic amino acids.
Intracellular concentrations of **A**) L-phenylalanine (PHE-L), **B**) L-tyrosine (TYR-L) and **C**) L-tryptophan (TRP-L) during anaerobic batch fermentation of 20 g/L glucose and 40 g/L xylose using strains TMB3057 (XR/XDH, white markers) and TMB3359 (XI, black markers). Errors are given as 95% confidence intervals of the means calculated from duplicate experiments for each strain ($6 \leq n \leq 10$). The shaded area indicates the period until glucose depletion. **D**) Comparison of $\log_2$ fold change in the concentrations of amino acids between this study and Brauer *et al*. [47] (triangles) and Klimacek *et al*. [27] (squares).

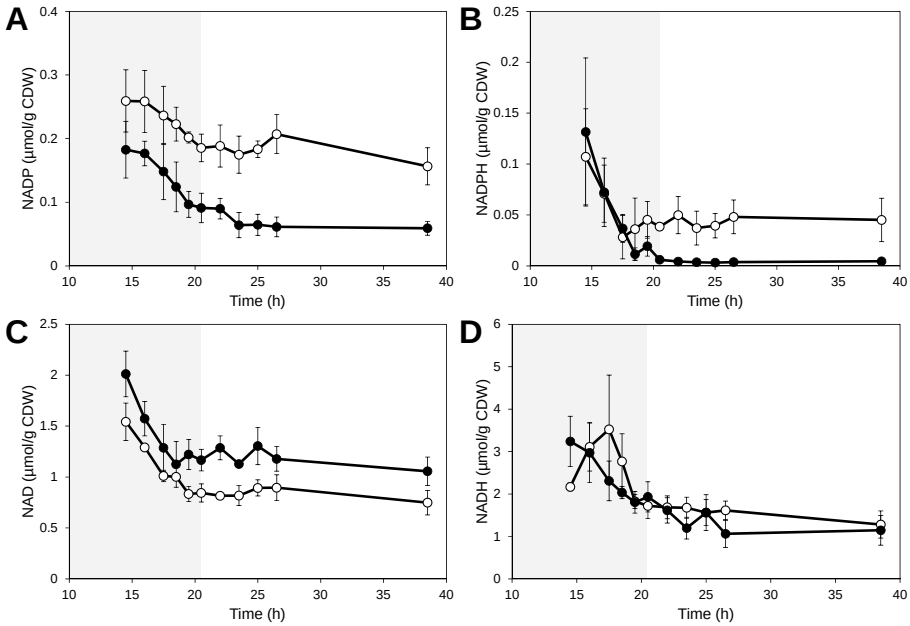

Figure S3 – Dynamics in redox cofactors
Intracellular concentrations of **A**) NADP, **B**) NADPH, **C**) NAD and **D**) NADH during anaerobic batch fermentation of 20 g/L glucose and 40 g/L xylose using strains TMB3057 (XR/XDH, white markers) and TMB3359 (XI, black markers). Errors are given as 95% confidence intervals of the means calculated from duplicate experiments for each strain ($4 \leq n \leq 10$). The shaded area indicates the period until glucose depletion.

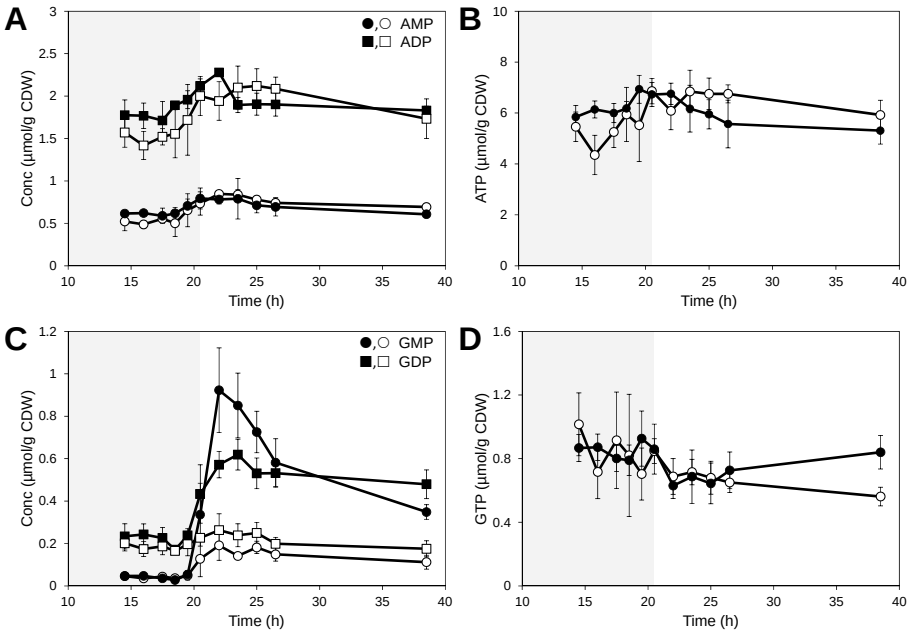

Figure S4 – Dynamics in the purine nucleotide pools
Intracellular concentrations of **A**) AMP and ADP, **B**) ATP, **C**) GMP and GDP and **D**) GTP during anaerobic batch fermentation of 20 g/L glucose and 40 g/L xylose using strains TMB3057 (XR/XDH, white markers) and TMB3359 (XI, black markers). Errors are given as 95% confidence intervals of the means calculated from duplicate experiments for each strain ($5 \leq n \leq 11$). The shaded area indicates the period until glucose depletion.

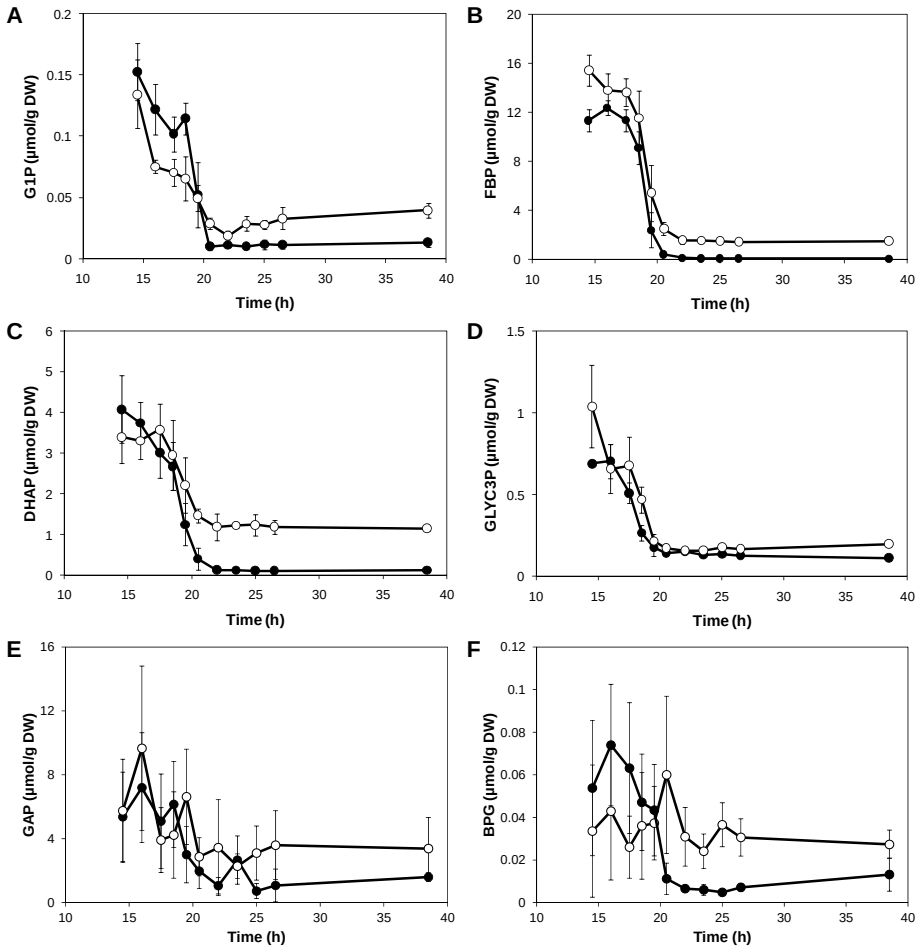

Figure S5 – Additional metabolites in glycolysis.

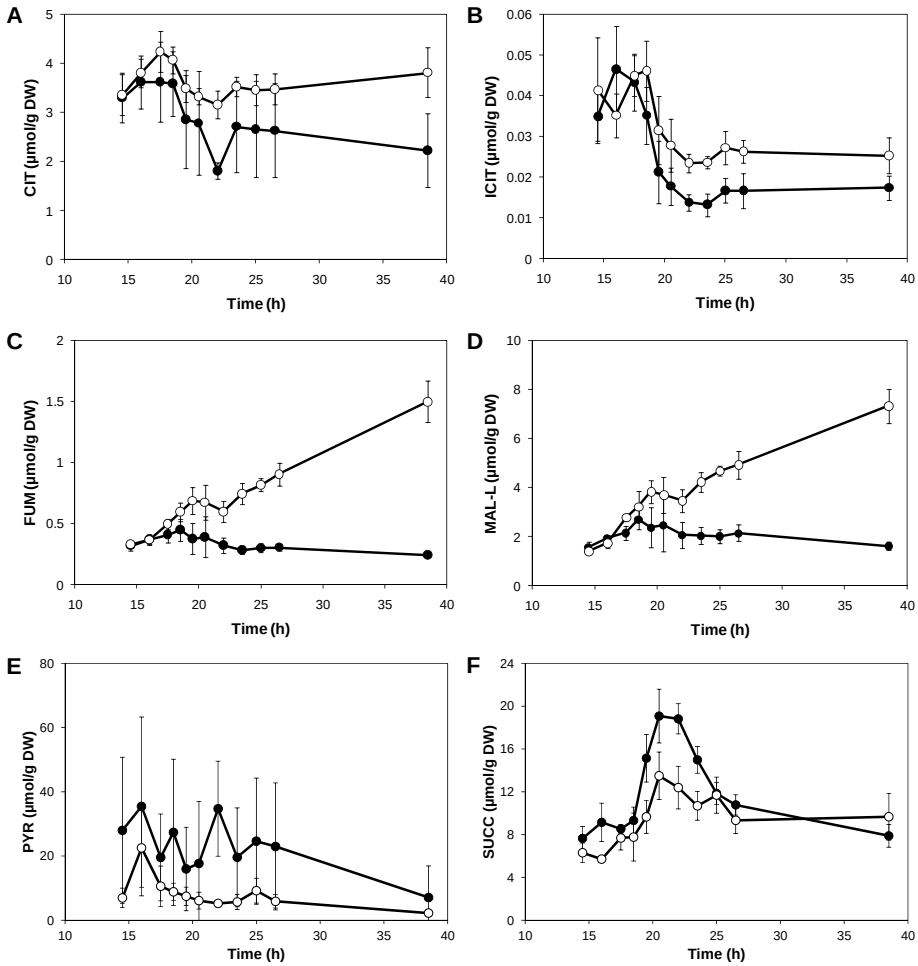

Figure S6 – Additional metabolites in the TCA-cycle.

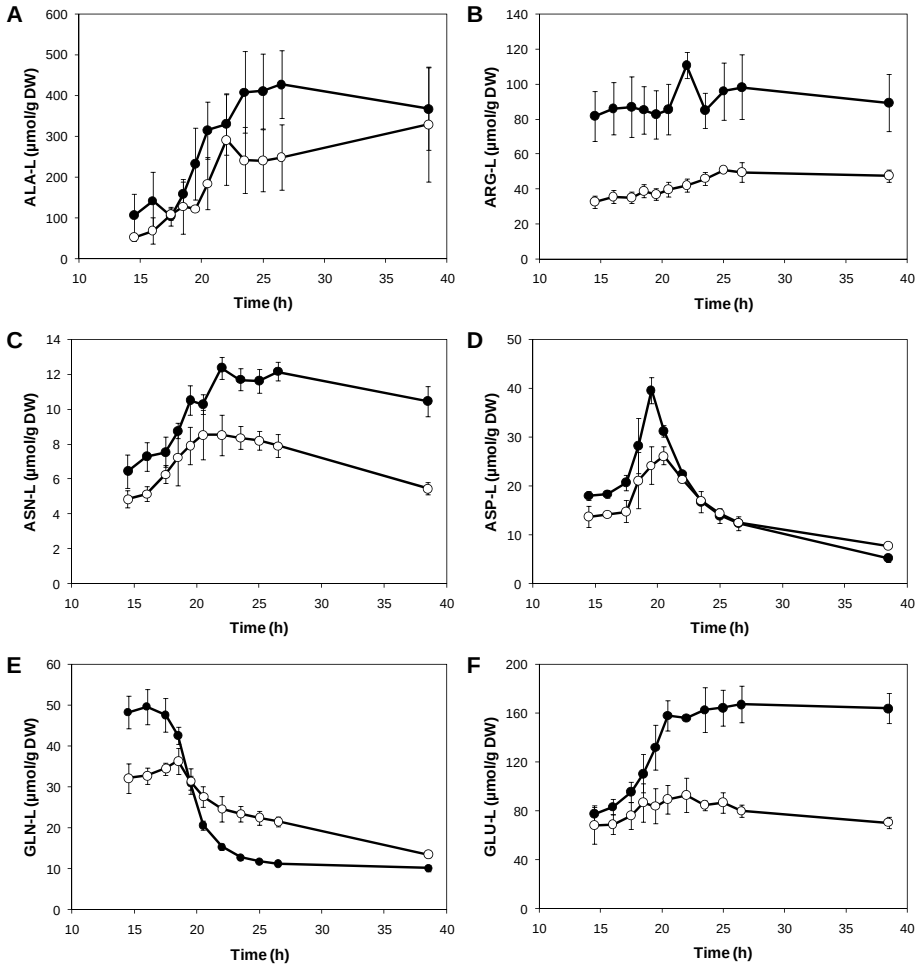

Figure S7 – Additional amino acids.

Tables

Table S1 – Product yields on substrate during anaerobic batch fermentation. Fermentation was performed with the strains TMB 3057 (XR/XDH) and TMB 3359 (XI) using 2X YNB with 20 g L^{-1} glucose and 50 g L^{-1} xylose as substrates.

Yield (g/g)	Mixed sugar		Xylose only		Total sugar	
	TMB 3057	TMB 3359	TMB 3057	TMB 3359	TMB 3057	TMB 3359
Y_{sx}	0.07±0.004	0.08±0.03	0.02±0.003	0.07±0.05	0.05±0.005	0.09±0.02
Y_{se}	0.28±0.03	0.28±0.13	0.13±0.02	-0.06±0.36	0.23±0.02	0.31±0.08
Y_{sg}	0.13±0.01	0.07±0.03	0.03±0.01	0.08±0.17	0.08±0.01	0.08±0.02
Y_{sxylt}	0.09±0.03	0.002±0.003	0.64±0.03	0.17±0.06	0.34±0.06	0.011±0.006

Yields: Y_{sx}, biomass yield on substrate; Y_{se}, ethanol yield on substrate; Y_{sg}, glycerol yield on substrate; Y_{sxylt}, xylitol yield on substrate.

Table S2. Metabolites with significantly different means between the XR/XDH-strain and the XI-strain during anaerobic batch fermentation. Two-sided t-tests were systematically performed for each metabolite and at each sampling point, to determine if there were any significant differences between the two strains. The tests were performed at the 0.05 significance level, assuming equal variance in the two populations. (* $p < 0.01$; ** $p < 0.005$; *** $p < 0.001$)

Time (h)	Number of metabolites	Metabolites			
		Sugar phosphates	Nucleotides and cofactors	Amino acids	TCA-cycle intermediates
14.5	19	G6P(***), R5P(***), GLYC3P(**), Xu5P(**), Ru5P(***), 6PG(***), xPG(***), FBP(***)	NAD(**), NADH, NADP	ARG-L(***), ASN-L(**), GLN-L(***), TYR-L(***), PHE-L(***), ASP-L(***), TRP-L(***)	SUCC
16	23	G6P(***), R5P(***), G1P(***), Xu5P(***), Ru5P(***), 6PG(***)	GMP(**), NAD(**), AMP(***), GDP, NADP(*), ADP(**), ATP(***)	ARG-L(***), ALA-L, ASN-L(***), GLN-L(***), TYR-L(***), GLU-L(*), PHE-L(***), ASP-L(***)	SUCC(***), ICIT
17.5	20	G6P(***), R5P(***), G1P(**), Xu5P(***), Ru5P(***), FBP(**)	GMP, NAD, NADP(*), ATP	ARG-L(***), ASN-L(*), GLN-L(***), TYR-L(***), GLU-L(*), PHE-L(***), ASP-L(***), TRP-L(***)	L-MAL(***), FUM
18.5	16	G6P(***), R5P(***), GLYC3P(***), G1P(***), Xu5P(***), Ru5P(***), xPG, FBP	NADH, NADP(***)	ARG-L(***), GLN-L(**), GLU-L, PHE-L	FUM, ICIT
19.5	22	R5P(***), Xu5P(***), Ru5P(*), DHAP, 6PG(***), xPG(***), FBP	NAD(***), NADP(***), GTP, NADPH(**)	ARG-L(***), ALA-L, ASN-L(***), TYR-L, GLU-L(***), PHE-L(**), ASP-L(***), TRP-L	SUCC(***), L-MAL(**), FUM(***)
20.5	30	G6P(***), R5P(**), F6P(**), GLYC3P, G1P(***), Xu5P(***), Ru5P(***), DHAP(***), 6PG(***), xPG, PEP(**), FBP(***)	GMP, NAD(***), GDP, NADP(***), NADPH(***)	ARG-L(***), ALA-L(*), ASN-L, GLN-L(***), TYR-L(***), GLU-L(***), PHE-L(***), ASP-L(***), TRP-L(**)	SUCC(**), L-MAL, FUM(*), ICIT
22	31	G6P(***), R5P(*), F6P(***), G1P(***), Xu5P(***), Ru5P(***), DHAP(***), 6PG(***), xPG(***), PEP(***), FBP(***)	GMP(***), NAD(***), GDP(***), NADP(***), ADP(**), NADPH(***)	ARG-L(***), ASN-L(***), GLN-L(***), TYR-L(***), GLU-L(***), PHE-L(***), ASP-L, TRP-L(***)	PYR(**), SUCC(***), L-MAL(***), FUM(***), CIT(***), ICIT(***)
23.5	30	G6P(***), R5P(***), F6P(***), GLYC3P(***), G1P(***), Xu5P(***), Ru5P(**), DHAP(***), 6PG(***), xPG(***), PEP, FBP(***)	GMP(***), NAD(***), GDP(***), NADH(*), NADP(***), NADPH(***)	ARG-L(***), ALA-L(*), ASN-L(***), GLN-L(***), TYR-L(***), GLU-L(***), PHE-L(***), TRP-L(***)	SUCC(***), L-MAL(***), FUM(***), ICIT(***)
25	29	G6P(***), R5P(***), F6P(***), GLYC3P(**), G1P(***), Xu5P(***), Ru5P(***), DHAP(***), 6PG(***), xPG(***), PEP(**), FBP(***)	GMP(***), NAD(***), GDP(***), NADP(***), NADPH(***)	ARG-L(***), ALA-L(**), ASN-L(***), GLN-L(***), TYR-L(***), GLU-L(***), PHE-L(***), TRP-L(***)	L-MAL(***), AKG(**), FUM(***), ICIT(***)
26.5	33	G6P(***), R5P(***), F6P(***), GLYC3P(***), G1P(***), Xu5P(**), Ru5P(**), DHAP(***), 6PG(***), xPG(***), PEP, FBP(***)	GMP(***), NAD(**), GDP(***), NADH(**), NADP(***), ADP, NADPH(***), ATP(*)	ARG-L(***), ALA-L(**), ASN-L(***), GLN-L(***), TYR-L(***), GLU-L(***), PHE-L(***), TRP-L(***)	SUCC, L-MAL(***), FUM(***), CIT, ICIT(***)
38.5	31	G6P(***), R5P(***), F6P(***), GLYC3P(***), G1P(***), Xu5P(***), Ru5P, DHAP(***), 6PG(***), xPG(***), PEP, FBP(***)	GMP(***), NAD(**), AMP(**), GDP(***), NADP(***), GTP(***), NADPH(**)	ARG-L(***), ASN-L(***), GLN-L(***), TYR-L(***), GLU-L(***), PHE-L(***), ASP-L(***), TRP-L(***)	L-MAL(***), FUM(***), CIT(***), ICIT(**)

Additional file 2

Thermodynamic evaluation of metabolite concentrations

The thermodynamic analysis of measured metabolite concentrations in the XR/XDH-strain was performed using anNET version 1.1.06 [1]. anNET can evaluate the feasibility of a reaction system constrained by flux directions and ranges of metabolite concentrations. When the system is feasible anNET can calculate the maximum and minimum values of feasible metabolite concentrations.

Calculation of flux distributions

We used the genome scale model iMM904 of *S. cerevisiae* [2] as the reaction network. The reaction network was slightly modified to represent the recombinant XR/XDH-strain: i) the reactions associated with the *GRE*3 gene were deleted except for the NADPH-dependent xylose reductase reaction, ii) a NADH-dependent xylose reductase reaction was added to the model and iii) the xylitol dehydrogenase reaction was made reversible. The glukokinase reaction (GLUK) and the two irreversible alcohol deydrogenase reactions (ALCD2if and ALCD2ir) were also deleted to avoid loops in the flux variability analysis.

The COBRA Toolbox [3] was used to calculate a set of flux directions in the XR/XDH-strain under two conditions. Data from anaerobic chemostat experiments at dilution rate 0.06 h^{-1} with 10 g/L glucose and 10 g/L xylose in the feed [4] was used to simulate the fermentation of a mixed sugar solution. In the case where xylose was the sole carbon source, data from anaerobic batch cultivation of a xylose-growing strain [5] was used to calculate the flux distribution. In both conditions the oxygen uptake rate was set to zero to simulate anaerobic conditions and the maximum uptake rates of sterols, fatty acids, vitamins and trace elements were specified according to Snitkin *et al*. [6]. The objective function was maximisation of biomass formation in both cases. A flux variability analysis was performed to obtain a range of flux directions for each reaction and to identify reactions which never held a flux. Reactions with an absolute flux below 10^{-6} were also regarded as zero and removed from the reaction network. The reduced model consisted of 722 reactions and 590 metabolites.

Input data

To convert measured metabolite concentrations from micro moles per gram cell dry weight (µmol/g CDW) to moles per litre a factor of 1.5 µL cytosolic volume per mg cell dry weight was used [7]. Two measured concentration ranges were not included in the thermodynamic calculations: that of 1,3-bisphosphoglycerate (BPG) which was associated with rather large errors (Fig. S5, Additional file 1) and that of glucose 1-phosphate (G1P) since it only participates in one reaction that could be evaluated. Hence, the concentrations of G1P and BPG were intentionally allowed to vary within the default range (1×10^{-4}-10 mM) in the evaluation. In this study we used the extended set of Gibbs energies of formation supplied with the anNET toolbox for several common biological compounds and complemented these with estimated data for L-arginine, L-ornithine, N(omega)-(L-Arginino)succinate, L-citrulline, acetoin and sedoheptulose-1,7-bisphosphate using the group contribution method [8]. All the data used in the calculations are given as supplementary information in Additional file 4.

Results

The feasibility was evaluated at each sampling point and the measured concentrations of BPG were found to be infeasible in the first four sampling points while all but one measured concentration of G1P fell within the calculated ranges (Table 1). In addition, the measured concentration of glyceraldehyde 3-phosphate (GAP) was found to be thermodynamically infeasible in all time points. The minimum measured concentration of GAP was between 3 and 14 times higher than the maximum calculated concentration (Table 1). Inconsistent concentrations of GAP have previously been identified [1] but the magnitude of the currently obtained concentrations (mM scale) is significantly higher than earlier reported (µM scale) [9-12]. The discrepancy could be due to a combination of the extraction method applied and limitations in the LC-MS/MS method, which yields broad and indistinct chromatographic peaks of GAP with low intensities [13]. This led to inconsistent normalization of GAP peak areas to the internal standard and poor calibration curves for GAP, possibly due to degradation of this compound during the extraction procedure. Apart from BPG, G1P and GAP, all other metabolites evaluated were within the feasible ranges in all 11 time points.

Table 1. Feasibility of measured concentrations of GAP, BPG and G1P. Measured concentration ranges of glyceraldehyde 3-phosphate (GAP), 1,3-bisphospho-D-glycerate (BPG) and glucose 1-phosphate (G1P) based on the 95% confidence intervals compared with thermodynamically feasible ranges calculated using the anNET toolbox.

Time	GAP (mM)		BPG (mM)[a]		G1P (mM)[a]	
(h)	Measured	Calculated	Measured	Calculated	Measured	Calculated
14.5	1.7–6.0	0.005–0.26	0.0017–0.043	0.098–5.5	0.13–0.18	1×10^{-4}–0.18
16	3.0–9.9	0.007–0.25	0.0071–0.050	0.075–2.5	0.11–0.14	1×10^{-4}–0.13
17.5	1.3–4.0	0.010–0.24	0.0077–0.027	0.065–1.7	0.087–0.12	1×10^{-4}–0.095
18.5	1.0–4.6	0.013–0.23	0.0073–0.041	0.045–0.81	0.11–0.13	1×10^{-4}–0.076
19.5	2.4–6.4	0.014–0.18	0.013–0.036	0.023–0.29	0.026–0.079	1×10^{-4}–0.052
20.5	1.1–2.7	0.028–0.11	0.015–0.065	0.027–0.11	0.007–0.013	1×10^{-4}–0.028
22	0.29–4.3	0.028–0.086	0.011–0.030	0.017–0.053	0.009–0.012	1×10^{-4}–0.016
23.5	1.0–2.0	0.042–0.083	0.011–0.021	0.020–0.038	0.008–0.012	1×10^{-4}–0.019
25	0.94–3.2	0.050–0.080	0.018–0.031	0.019–0.031	0.008–0.016	1×10^{-4}–0.022
26.5	0.96–3.8	0.057–0.078	0.015–0.026	0.022–0.030	0.008–0.014	1×10^{-4}–0.026
38.5	0.95–3.6	0.074–0.079	0.014–0.023	0.017–0.019	0.01–0.017	1×10^{-4}–0.035

References

1. Zamboni N, Kummel A, Heinemann M: **anNET: A tool for network-embedded thermodynamic analysis of quantitative metabolome data.** *BMC Bioinformatics* 2008, **9**.
2. Mo M, Palsson B, Herrgard M: **Connecting extracellular metabolomic measurements to intracellular flux states in yeast.** *BMC Syst Biol* 2009, **3:**37.
3. Becker SA, Feist AM, Mo ML, Hannum G, Palsson BO, Herrgard MJ: **Quantitative prediction of cellular metabolism with constraint-based models: the COBRA Toolbox.** *Nat Protocols* 2007, **2:**727-738.
4. Wahlbom CF, Eliasson A, Hahn-Hägerdal B: **Intracellular fluxes in a recombinant xylose-utilizing *Saccharomyces cerevisiae* cultivated anaerobically at different dilution rates and feed concentrations.** *Biotechnol Bioeng* 2001, **72:**289-296.
5. Runquist D, Hahn-Hagerdal B, Bettiga M: **Increased expression of the oxidative pentose phosphate pathway and gluconeogenesis in anaerobically growing xylose-utilizing *Saccharomyces cerevisiae*.** *Microb Cell Fact* 2009, **8**.
6. Snitkin E, Dudley A, Janse D, Wong K, Church G, Segre D: **Model-driven analysis of experimentally determined growth phenotypes for 465 yeast gene deletion mutants under 16 different conditions.** *Genome Biol* 2008, **9:**R140.
7. de Koning W, van Dam K: **A method for the determination of changes of glycolytic metabolites in yeast on a subsecond time scale using extraction at neutral pH.** *Anal Biochem* 1992, **204:**118-123.
8. Jankowski MD, Henry CS, Broadbelt LJ, Hatzimanikatis V: **Group contribution method for thermodynamic analysis of complex metabolic networks.** *Biophys J* 2008, **95:**1487-1499.
9. Klimacek M, Krahulec S, Sauer U, Nidetzky B: **Limitations in xylose-fermenting *Saccharomyces cerevisiae*, made evident through comprehensive metabolite profiling and thermodynamic analysis.** *Appl Environ Microbiol* 2010, **76:**7566-7574.
10. Cipollina C, ten Pierick A, Canelas AB, Seifar RM, van Maris AJA, van Dam JC, Heijnen JJ: **A comprehensive method for the quantification of the non-oxidative pentose phosphate pathway intermediates in *Saccharomyces cerevisiae* by GC-IDMS.** *J Chromatogr B* 2009, **877:**3231-3236.
11. Hynne F, Dano S, Sorensen PG: **Full-scale model of glycolysis in *Saccharomyces cerevisiae*.** *Biophys Chem* 2001, **94:**121-163.
12. Altintas MM, Eddy CK, Zhang M, McMillan JD, Kompala DS: **Kinetic modeling to optimize pentose fermentation in *Zymomonas mobilis*.** *Biotechnol Bioeng* 2006, **94:**273-295.
13. Buescher JM, Moco S, Sauer U, Zamboni N: **Ultrahigh performance liquid chromatography-tandem mass spectrometry method for fast and robust quantification of anionic and aromatic metabolites.** *Anal Chem* 2010, **82:**4403-4412.

Paper III

Physiological effects of over-expressing compartment-specific components of the protein folding machinery in xylose-fermenting *Saccharomyces cerevisiae*

Basti Bergdahl, Marie F. Gorwa-Grauslund and Ed W.J. van Niel

Division of Applied Microbiology, Department of Chemistry,
Lund University, P.O. Box 124, SE-221 00 Lund, Sweden

ABSTRACT

The ability of *S. cerevisiae* to grow under strict anaerobic conditions has been ascribed to the presence of soluble fumarate reductase enzymes. *S. cerevisiae* has two genes, *FRD1* and *OSM1*, encoding the cytosolic and mitochondrial fumarate reductase enzymes, respectively. These enzymes catalyze the reduction of fumarate to succinate while regenerating FAD from $FADH_2$ and have been proposed to provide the only way for yeast to regenerate the FAD/FMN prosthetic group of flavin enzymes that are required for growth under anaerobic conditions. One such enzyme is Ero1p, encoded by *ERO1*, which catalyses the formation of disulphide bonds in polypeptides during the protein folding process in the endoplasmic reticulum. In this study we tested whether an impaired protein folding process was the underlying cause for the very slow growth of recombinant yeast strains on xylose under anaerobic conditions. Four strains over-expressing *FRD1*, *OSM1* and *ERO1* in different combinations were constructed and cultivated anaerobically in defined minimal medium as well as in a complex medium containing both glucose and xylose. Over-expression of *FRD1*, alone or in combination with *ERO1*, did not have any significant effect on xylose fermentation, neither in minimal medium nor in rich medium. Over-expression of *OSM1*, on the other hand, led to a diversion of carbon from glycerol to acetate and a decrease in growth rate by 25%-50% during xylose fermentation. This phenotype might be the outcome of an interaction between Osm1p and FAD-dependent glycerol 3-phosphate dehydrogenase in the mitochondria. This combination that arose due to the poor repressive capability of xylose could be utilized in other strains to reduce glycerol production in favour of succinate.

INTRODUCTION

The yeast *Saccharomyces cerevisiae* is one of few yeast species capable of growth under strict anaerobic conditions [Visser *et al.*, 1990]. This trait together with a high tolerance toward inhibitory compounds, e.g. ethanol, weak acids, phenolics and furaldehydes, has made *S. cerevisiae* the organism of choice for bioethanol production [Nevoigt, 2008; Jönsson *et al.*, 2013]. The development of sustainable processes for biofuel production is an important step in the efforts to reduce greenhouse gas emissions and becoming independent of fossil fuels [Festel, 2008]. The utilization of lignocellulosic raw material for the production of fuel-grade ethanol is one such process currently under development [Girio *et al.*, 2010; Soccol *et al.*, 2011]. These raw materials are currently generated as waste in agricultural, forestry and pulp and paper industries and contain a large fraction of fermentable sugars. The composition of the sugar fraction varies between different materials, but the largest part is often made up of glucose and xylose [Girio *et al.*, 2010]. Efficient utilization of both these sugars is necessary for the ethanol production process to be economically feasible [Jeffries, 1985; Sassner *et al.*, 2008].

S. cerevisiae is well-known for its capability to ferment hexoses, especially glucose. However, *S. cerevisiae* cannot naturally utilize xylose and thus has to be genetically modified [Skoog and Hahn-Hägerdal, 1988]. The simultaneous expression of the *XYL1* and *XYL2* genes from *Scheffersomyces stipitis* (formerly *Pichia stipitis* [Kurtzman and Suzuki, 2010]) encoding xylose reductase (XR) and xylitol dehydrogenase (XDH), respectively, first enabled xylose utilization by *S. cerevisiae* [Kötter *et al.*, 1990]. Many advances have then been made in the development of xylose-fermenting *S. cerevisiae* strains but the efficiency is still far from matching that of glucose [Hahn-Hägerdal *et al.*, 2007; Van Vleet and Jeffries, 2009]. Current rationally designed XR/XDH-strains require 2-3 fold longer time to ferment xylose than the time required to ferment an equal amount of glucose [Bengtsson *et al.*, 2009]. One important inadequacy is the inability of these strains to grow anaerobically on xylose when fermenting a mixture of hexoses and pentoses. Although increased growth might decrease the final product yield by diverting some of the assimilated carbon toward biomass, it would also increase the overall productivity leading to faster output of the product. Even a small reduction of this time would have a strong positive effect on the overall process.

The ability of *S. cerevisiae* to grow under strict anaerobic conditions has been ascribed to the soluble nature of the fumarate reductase enzymes, which in most other species are membrane bound [Arikawa *et al.*, 1998; Camarasa *et al.*, 2007]. *S. cerevisiae* has two genes, *FRD1* and *OSM1*, encoding the cytosolic and mitochondrial fumarate reductase enzymes, respectively [Enomoto *et al.*, 1996;

Muratsubaki and Enomoto, 1998]. These enzymes catalyse the reduction of fumarate to succinate while regenerating FAD from $FADH_2$ [Rossi *et al.*, 1964]. This is the last step of the reductive branch of the TCA-cycle where mitochondrial NAD is regenerated under anaerobic conditions (Fig. 1A) [Camarasa *et al.*, 2003]. Expression of *FRD1* is induced by anoxia by relieve of Rox1-mediated repression whereas expression of *OSM1* is nearly unaffected by the absence of oxygen [Lai *et al.*, 2006; Camarasa *et al.*, 2007]. Hence, Osm1 is believed to provide basal reductase-activity for biosynthesis. Expression of both genes is, however, highest in exponentially growing cells and decrease upon entry into stationary phase and during carbon starvation [Gasch *et al.*, 2000; Camarasa *et al.*, 2007; Bradley *et al.*, 2009]. Expression of both genes is also lower in the presence of non-fermentable carbon sources such as glycerol [Roberts and Hudson, 2006].

Deletion of *FRD1* or *OSM1* has no effect on the cells ability to grow under anaerobiosis, but a double deletion mutant cannot grow under such conditions unless an external electron acceptor (e.g. oxygen, menadione or phenazine methosulphate) is supplied [Arikawa *et al.*, 1998; Enomoto *et al.*, 2002; Camarasa *et al.*, 2007]. It has thus been proposed that, under anaerobiosis, fumarate reductase provides the only way for yeast to regenerate the FAD/FMN prosthetic group of flavin enzymes that are required for growth [Camarasa *et al.*, 2007]. Due to the soluble nature of the fumarate reductase enzymes, membrane bound flavoproteins can also be included in this regeneration process. In particular, two essential flavin-containing oxidases which normally use oxygen as a final electron acceptor for FAD regeneration have been suggested to be dependent on the action of fumarate reductase under anaerobiosis: Ero1p and Erv1p [Camarasa *et al.*, 2007]. Erv1p is a flavin-linked sulfhydryl oxidase capable of catalyzing the formation of disulfide bridges [Lee *et al.*, 2000] and is essential for mitochondrial function and cell viability [Lisowsky, 1992; Lisowsky, 1994; Becher *et al.*, 1999]. Erv1p is located in the mitochondrial intermembrane space (IMS) and together with Mia40p it forms a mitochondrial disulphide relay system [Herrmann *et al.*, 2007]. This pathway is essential for the biogenesis of iron sulphur clusters in the cytosol and for retaining proteins imported into the IMS [Lange *et al.*, 2001; Mesecke *et al.*, 2005; Bien *et al.*, 2010]. Some of these proteins are components of the electron transport chain and others fulfil many important cellular functions e.g. transport of polypeptides, maintenance of ion homeostasis and catalysis of metabolic reactions [Herrmann *et al.*, 2007]. Ero1p is a thiol oxidase [Frand and Kaiser, 1998; Pollard *et al.*, 1998] which operates together with Pdi1p (protein disulphide isomerase) [Freedman, 1989] in the endoplasmic reticulum (ER) where they take part in the maturation of secretory proteins [Barlowe and Miller, 2013]. Both proteins are essential for the formation of disulphide bonds and together they form a classical proteinaceous electron relay system in which electrons are passed from the substrate polypeptide, via Pdi1p and the membrane-bound Ero1p, to eventually react with oxygen (Fig. 1B) [Frand and Kaiser, 1999;

Tu *et al.*, 2000; Tu and Weissman, 2002]. Approximately one third of the yeast proteome is processed in the secretory pathway which makes this mechanism indispensable for cell viability, growth and function [Barlowe and Miller, 2013].

Previous transcriptional analyses of recombinant xylose-fermenting strains have shown that xylose is not recognised as a fermentable carbon source by *S. cerevisiae* [Wahlbom *et al.*, 2003; Jin *et al.*, 2004; Salusjärvi *et al.*, 2006; Runquist *et al.*, 2009b]. Recombinant strains growing on xylose thus display an induction of genes involved in respiratory metabolism, gluconeogenesis and glyoxylate cycle, regardless of the oxygenation level. Consistent with previously reported expression pattern on non-fermentable carbon sources, the expression of both *FRD1* and *ERO1* is repressed on xylose [Runquist *et al.*, 2009b]. Recently we conducted a comprehensive analysis of the dynamic changes in intracellular metabolites that occur during a batch fermentation of a glucose/xylose mixture using a recombinant XR/XDH-strain [Bergdahl *et al.*, 2012]. In that study we observed a marked accumulation of malate and fumarate intracellularly during fermentation of xylose. We thus hypothesized that the activity of fumarate reductase is reduced during xylose fermentation which in turn would affect the capacity to regenerate the FAD required for proper folding of proteins in the ER. Such an impairment of the protein folding process could be the underlying cause for the slow anaerobic growth on xylose. In this study we examined this hypothesis by over-expressing the two genes encoding fumarate reductase, alone and in combination with *ERO1*, and evaluated the effect on fermentation performance in a mixture of glucose and xylose.

EXPERIMENTAL PROCEDURES

Strains and culture conditions

Plasmids and yeast strains used in the study are listed in Table 1. Yeast strains were recovered from 20% glycerol stocks stored at -80 °C on solid YPD plates (10 g/L yeast extract, 20 g/L peptone, 20 g/L glucose, 15 g/L agar) for two days at 30 °C. Yeast cultures were grown in liquid YPD medium for 14-16 h, or less when required, at 30 °C and 180 rpm in an orbital shaker. Transformants were selected on solid Yeast Nitrogen Base (YNB) medium (6.7 g/L YNB without amino acids) with 20 g/L glucose as carbon source. Leucine was supplemented when required at 220 mg/L. Cultivations in shake flasks had a culture volume of 10% or less of the flask volume. YNB medium used in fermentation experiments contained 2X YNB, 20 g/L glucose, 50 g/L xylose and 50 mM potassium hydrogen phthalate buffer at pH 5.5. Rich medium used in fermentation experiments contained 10 g/L yeast extract, 20 g/L glucose, 50 g/L xylose, 50 mM potassium hydrogen phthalate buffer at pH 5.5, 10 g/L $(NH_4)_2SO_4$, 1 g/L $MgSO_4$ and 6 g/L KH_2PO_4.

All media used in anaerobic cultivations were supplemented with Tween 80 (400 mg/L) and ergosterol (10 mg/L).

E. coli strain NEB5-α (New England Biolabs) was used for sub-cloning of plasmid DNA. Transformants were selected on solid LB plates (5 g/L yeast extract, 10 g/L tryptone, 10 g/L NaCl, 15 g/L agar, pH 7.0), supplemented with 100 mg/L of ampicillin, for 16 h at 37°C. Cultures of transformed *E. coli* were recovered from 25% glycerol stocks stored at -80 °C and grown in liquid LB medium, supplemented with ampicillin, for 14-16 h at 37 °C and 180 rpm in an orbital shaker.

Strain construction

Standard molecular biology techniques were used for all cloning procedures [Sambrook *et al.*, 1989]. Plasmid purification was performed using GeneJet Plasmid Mini-prep Kit (Thermo Scientific, USA). DNA fragments digested with restriction enzymes were excised from agarose gel and purified using QIAquick Gel Extraction Kit (Qiagen, Germany) when needed. DNA fragments amplified by PCR were purified using GeneJet PCR Purification Kit (Thermo Scientific, USA). All enzymes for PCR amplifications, ligations and restriction digestions were obtained from Thermo Scientific unless stated otherwise. PCR reaction mixtures (50 µL) contained 1X Buffer, 1.5 mM $MgCl_2$, 0.2 mM of each dNTP, 0.5 mM of forward and reverse primer and 1U High Fidelity Phusion Hotstart II Polymerase, unless stated otherwise. Competent yeast cells were prepared and transformed according to the PEG/LiAc method [Gietz and Schiestl, 2007] and heat shock competent *E. coli* cells were prepared according to the Inoue method [Sambrook *et al.*, 1989] and transformed according to the supplier's instructions.

The gene *FRD1* was amplified from yeast genomic DNA by PCR using primers FRD1-F1-SpeI (5'-GAC TAG TAA ATG TCT CTC TCT CCC GTT G-3') and FRD1-R1-SalI (5'-GTT GTC GAC TTA CTT GCG GTC ATT GGC-3'). The reaction mixture (50 µL) contained 1X Buffer, 1.5 mM $MgCl_2$, 0.2 mM of each dNTP, 0.3 mM of forward and reverse primer, 1.25 U High Fidelity Taq Polymerase Mix (Fermentas, Lithuania). The amplification program was as follows: 1 min denaturation at 94 °C, 30 cycles of 30 s denaturation at 94 °C, 30 s annealing at 60.1 °C (48.6 °C during the first five cycles), 1 min 30 s extension at 72 °C and 1 cycle of 10 min final extension at 72 °C. The gene *OSM1* was amplified from yeast genomic DNA by PCR using primers OSM1-F1-SpeI (5'-GAC TAG TAA AAT GAT TAG ATC TGT GAG-3') and OSM1-R1-SalI (5'-GTT GTC GAC TCA GTA CAA TTT TGC TAT G-3'). The amplification program was as follows: 30 s denaturation at 98 °C, 30 cycles of 10 s denaturation at 98 °C, 30 s annealing at 48.5 °C during the five first cycles and at 62 °C (-0.2 °C/cycle) during the remaining 25 cycles, 1 min extension at 72 °C and 1 cycle of 10 min final extension at 72 °C. The amplified *FRD1* and *OSM1* genes were digested with *Spe*I and *Sal*I and inserted between the *TDH3* promoter

and *CYC1* terminator of the previously constructed vector YIpDR1, yielding the two plasmids YIpBB1 and YIpBB2 (Table 1). The cloned genes were verified by DNA sequencing.

The *ERO1* gene, including a 300 bp downstream sequence, was amplified from yeast genomic DNA by PCR using primers ERO1-F1-BamHI (5'-GAG GAT CCA AAA TGA GAT TAA GAA CCG CCA TTG-3') and ERO1-R1-XhoI (5'-GTC TCG AGC CCT TGA AGA TGG TAC C-3'). The amplification program was as follows: 30 s denaturation at 98 °C, 30 cycles of 10 s denaturation at 98 °C, 30 s annealing at 55.8 °C during the five first cycles and at 70 °C (-0.2 °C/cycle) during the remaining 25 cycles, 1 min extension at 72 °C and 1 cycle of 10 min final extension at 72 °C. The amplified *ERO1* ORF and terminator was digested with *Bam*HI and *Xho*I and inserted between the *TEF1* promoter and *CYC1* terminator of the vector p426TEF (Table 1). The *TEF1*p-*ERO1*-*ERO1*t cassette was amplified from plasmid p426TEF-ERO1 using primers p426TEF-F1-SacI (5'-GGA GCT CAT AGC TTC AAA ATG-3') and p426ERO1t-R1-NdeI (5'-CAT ATG CCC TTG AAG ATG GTA C-3'). The amplification program was as follows: 30 s denaturation at 98 °C, 25 cycles of 10 s denaturation at 98 °C, 30 s annealing at 58.9 °C (-0.2 °C/cycle), 2 min extension at 72 °C and 1 cycle of 10 min final extension at 72 °C. The amplified cassette was digested with *Bam*HI and *Xho*I and ligated into plasmids YIpBB1 and YIpBB2, digested with the same enzymes, yielding vectors YIpBB3 and YIpBB4, respectively (Table 1). The cloned cassette was verified by DNA sequencing.

S. cerevisiae strain TMB3452 was constructed by transforming strain TMB3043 with YIpDR7, linearized with *Eco*RV. The integrative plasmids YIpBB1-4 were linearized with *Eco*RV, *Afl*II, *Eco91*I and *Afl*II, respectively, and used to transform strain TMB 3452, yielding strains TMB3456 (*FRD1*), TMB3457 (*OSM1*), TMB3458 (*FRD1 ERO1*) and TMB3459 (*OSM1 ERO1*) (Table 1). The control strain TMB3455 was constructed by transforming TMB3452 with YIplac128, linearized with *Eco*RV. Correct integration of the vectors was verified by PCR using primer pairs that annealed on the plasmid and on the chromosome outside the homologous regions of *URA3* or *LEU2* loci.

Fumarate reductase activity assay

Yeast strains were grown until late exponential phase in YNB medium with 2% glucose using baffled shake flasks. Strains cultivated anaerobically were inoculated into 50 mL medium in a 250 mL crimp-sealed serum flask at a concentration of 0.2 g cell dry weight/L (CDW/L). Prior to inoculation the headspace was flushed with N_2-gas containing less than 5 ppm oxygen (AGA Gas AB, Sweden) for at least 30 min. Cultivations were carried out for 10-12 h in a 30 °C water bath with continuous stirring at 180 rpm using magnetic stirrers. Cells were harvested by centrifugation at 4000 rpm and 4°C for 10 min. The resulting cell pellets were resuspended in 1X Lysis buffer (20 mM K,Na-PO_4, 20 mM EDTA, 1 mM DTT,

pH 7.0) to obtain a final suspension of 1 g wet cells/mL. Cell extracts were made through homogenization in a bead beater (1 min shaking, 1 min on ice, 1 min shaking) with an equal weight of 0.5 mm glass beads. Cell debris was pelleted by centrifugation at 14,000x g and 4°C for 20 min and the supernatant was transferred to a small glass vial. Before sealing the vial the headspace was replaced with N_2-gas in a vacuum chamber. The cell free extracts were stored at 4 °C until the following day. Protein concentrations were determined with the Coomassie Protein Assay Reagent (Thermo Scientific, USA) using BSA as standard (Thermo Scientific, USA).

Fumarate reductase activity was determined in a 1.2 mL reaction mixture containing: 50 mM K,Na-PO_4 buffer (pH 7.3), 10 mM fumaric acid (pH 7.3), 0.2 mM FMN-Na, 2.4% (w/v) sodium hydrosulfite. All reagents, except protein extract, were added to a rubber-sealed cuvette inside an anaerobic chamber. The assay buffer was prepared by dissolving 2.762 g of KH_2PO_4 and 2.837 g of $Na_2HPO_4 \cdot 2H_2O$ in 50 mL anaerobic water (separately) inside the anaerobic chamber, creating one 10X solution and one 2X solution, respectively. A 200 mM stock solution at the correct pH was made by mixing 5 mL 10X with 25 mL 2X and completing the volume to 50 mL with anaerobic water. A 40 mM stock solution of fumaric acid was prepared by dissolving 0.464 g fumaric acid in 50 mL of 5 mM K,Na-PO_4 buffer at pH 7.3. The pH was adjusted to 7.3 using 5 M NaOH and the volume was completed to 100 mL with anaerobic water inside the anaerobic chamber. Solutions of the cofactor and reducing agent were prepared fresh before each assay. Both compounds were weighed and brought into the anaerobic chamber. The FMN cofactor was dissolved in anaerobic water and sodium hydrosulfite was dissolved in 100 mM K,Na-PO_4 buffer, but only after all other reagents had been added to the cuvette to ensure that FMN becomes completely reduced to $FMNH_2$. The reaction was started by addition of protein extract using a gas-tight syringe. The formation of FMN was measured at 440 nm in cuvettes with light path length of 1 cm using an Ultrospec 2100 Pro spectrophotometer (Amersham Biosciences Corp., USA) controlled by computer software SWIFT Reaction Kinetics v. 2.05 (Biochrom Ltd., Cambridge, UK). The absorbance was converted to concentration units using the molar extinction coefficient of FMN ($\varepsilon_{440\ nm}$ = 12,500 L/mol/cm). The slope was determined within an interval of at least 1 min, using at least three different dilutions of the cell extract. Only the slopes within the range 0.05-0.35 A/min were considered acceptable. One unit is defined as the conversion of 1 μmole of fumarate per minute.

Anaerobic batch fermentations

Yeast strains were pre-grown in YNB medium with 2% glucose until mid-exponential phase and inoculated into 50 mL medium in a 250 mL crimp-sealed serum flask at a concentration of 0.04 g CDW/L. Prior to inoculation the

headspace was flushed with N_2-gas containing less than 5 ppm oxygen (AGA Gas AB, Sweden) for at least 30 min. Cultivations were carried out in a 30 °C water bath with continuous stirring at 180 rpm using magnetic stirrers. To prevent diffusion of oxygen into the culture during sampling, the excess gas was released through a 0.2 µm filter connected to Norprene tubing submerged under water. Cell dry weight was calculated from OD measurements using a pre-determined relationship between OD and cell dry weight. Fermentation experiments were performed in biological duplicates.

Biomass determination and analysis of metabolites

Optical density was measured at 620 nm using an Ultrospec 2100 Pro spectrophotometer (Amersham Biosciences). Cell dry weight was measured in triplicate by filtering a known volume of the culture through a pre-weighed nitrocellulose filter with 0.45 µm pore size. The filters were washed with three volumes of water, dried in a microwave oven and weighed after equilibrating to room temperature in a desiccator.

Concentrations of glucose, xylose, xylitol, glycerol, succinate, acetate and ethanol were analysed by HPLC (Waters, USA). Aminex HPX-87H ion exchange column (Bio-Rad, USA) was used at 45 °C with a mobile phase of 5 mM H_2SO_4 at a flow rate of 0.6 mL/min. All compounds were detected with a RID-10A refractive index detector (Shimadzu, Japan).

Calculation of metabolic rates

In defined minimal medium the volumetric production and consumption rates (q_i and q_s), the maximum specific consumption rates of xylose (r_{xyl}) and glucose (r_{glc}), as well as the biomass yield per consumed substrate ($Y_{x/s}$) were calculated through linear regression according to Equations 1-4. The product yields per consumed substrate ($Y_{i/s}$) were calculated using the determined volumetric rates according to Equation 5. The product yields per biomass ($Y_{i/x}$) were calculated as the ratio between $Y_{i/s}$ and $Y_{x/s}$ when xylose was the carbon source and according to Equation 6 when glucose was the carbon source. Due to the non-exponential growth on xylose, the maximum specific growth rate (μ_{max}) was calculated as the product between r_{xyl} and $Y_{x/s}$ according to Equation 7. For comparative reasons μ_{max} on glucose was calculated in the same way. These values corresponded very well with those calculated through regression of ln(OD) vs. time. The specific production rates were calculated as the product between μ_{max} and $Y_{i/x}$ according to Equation 8.

$$q_i = \frac{dC_i}{dt}\ ,\ q_s = \frac{dC_s}{dt} \qquad (1)$$

$$r_{xyl} = \frac{d\left(C_{xyl}/C_x\right)}{dt} \quad (2)$$

$$r_{glc} = \frac{d\left(dC_{glc}/dt\right)}{dC_x} \quad (3)$$

$$Y_{x/s} = \frac{dC_x}{dC_{s,tot}} \quad (4)$$

$$Y_{i/s} = \frac{q_i}{q_s} \quad (5)$$

$$Y_{i/x} = \frac{dC_i}{dC_x} \quad (6)$$

$$\mu_{\max} = r_s \cdot Y_{x/s} \quad (7)$$

$$r_i = \mu_{\max} \cdot Y_{i/x} \quad (8)$$

In rich, complex medium all calculations were made as described above except for the maximum specific consumption rate of glucose which could not be determined accurately enough. Hence, the $\mu_{\max}$ under these conditions was determined as the slope in a linear regression of ln(OD) vs. time and r_{glc} was calculated using Equation 7. The significance of a difference between two mean values was calculated using a two-tailed t-test assuming equal variance of the two samples with one degree of freedom unless stated otherwise.

RESULTS

Over-expression of fumarate reductase genes

Fumarate reductase activity was compared in all the constructed strains. The control strain TMB3455 exhibited a low fumarate reductase activity (1.8 mU/mg protein) when grown aerobically in a shake flask (Fig. 2). Changing the environment to anaerobic conditions increased the activity by 88% to 3.4 mU/mg protein (Fig. 1). This is consistent with previous observations that the genes encoding fumarate reductase enzymes are induced in the absence of oxygen [Muratsubaki and Katsume, 1982; Lai *et al.*, 2006]. When the genes *FRD1* and *OSM1* were over-expressed under the control of the *TDH3*-promoter the activity increased 48- and 6-fold, respectively, even when the strains were grown aerobically (Fig. 2). This result agrees well with previous activity measurements in

extracts from deletion mutants showing that the Frd1p enzyme contributed the most to the total cellular fumarate reductase activity [Arikawa *et al.*, 1998; Camarasa *et al.*, 2007]. Since expression of both genes is controlled by the same promoter and from the same locus in the nucleus, this may reflect different kinetic properties between the two enzymes. The mitochondrial enzyme (encoded by *OSM1*) might be adapted to an environment with low concentrations of substrates as a low maximum velocity often indicates a high affinity [Cleland, 1982]. The specific activities in strains TMB3458 (*FRD1 ERO1*) and TMB3459 (*OSM1 ERO1*) were 56% and 58% lower, respectively, than the corresponding strains over-expressing only one gene (Fig. 2). As the activities were reduced to the same extent in the two strains it may be that having two strong and constitutive promoters (*TDH3*p and *TEF1*p) close together on the integration fragment causes a high work load on the RNA polymerases which significantly reduces the overall transcription efficiency. Nevertheless, the activity measurements showed that the genes encoding fumarate reductases were over-expressed in all strains and translated into functional enzymes.

Over-expression of cytosolic fumarate reductase has limited impact on xylose fermentation

Due to the higher contribution of the cytosolic fumarate reductase to the total cellular reductase activity the over-expression of *FRD1,* alone or in combination with *ERO1*, was evaluated first. When cultivated in defined mineral medium with 20 g/L glucose and 50 g/L xylose, TMB3456 (*FRD1*) and TMB3458 (*FRD1 ERO1*) consumed glucose within 20 h (Fig. 3). During this time they gave the same yields of ethanol and biomass as the control strain: 2 mol/mol and 10.5 g CDW/mol, respectively (Table 2). No significant physiological differences from the control strain were observed, except slightly lower yields of ethanol (Table 2; Supplementary material: Table S1). The ethanol yields obtained with TMB3456 and TMB3458 were 6% (P = 0.07) and 10% (P = 0.08) lower, respectively, than the control strain (Table 2).

These results suggest that the implemented genetic modifications have no positive effect on the anaerobic growth on xylose. However, the modifications only ensure that the genes required for regeneration of FAD co-factors are present (Fig. 1). If sufficient amounts of substrates are not available, unfolded polypeptide chains in that case, these modifications will not be effective in regenerating the cofactor. It has previously been suggested that the poor repressive capability of xylose leads to unwanted reactions which direct carbon away from amino acid synthesis [Bergdahl *et al.*, 2012]. Reduced synthesis of amino acid could thus hamper the formation of polypeptides and mask the effect of the genetic modifications. To investigate if the strains were limited by amino acid synthesis they were cultivated in a rich, complex medium containing yeast extract. The fermentation profiles under these conditions are shown in Figure 4. Changing

from a minimal medium to a rich medium led to several significant changes in the physiology of all strains (see below). However, despite the rich medium no significant differences were observed between the control strain and TMB3456 and TMB3458 (Fig. 5; Supplementary material: Table S2). The exceptions were reductions in glycerol yields per glucose consumed by 22% (P = 0.07) and 18% (P = 0.11) with TMB3456 and TMB3458, respectively (Table 2).

Although the change from a defined medium to a complex medium led to a general increase in the growth rate on xylose, the over-expression of *FRD1*, alone or in combination with *ERO1*, had little effect on the cellular physiology. One explanation could be that the previously observed accumulation of fumarate [Bergdahl *et al.*, 2012] does not occur in the cytosol, but is restricted to the mitochondria. To investigate this possibility we over-expressed the *OSM1* gene, alone and in combination with *ERO1*, and evaluated the fermentation performance in both defined and complex media.

Over-expression of mitochondrial fumarate reductase disturbs the cellular redox balance and inhibits growth on xylose

In defined mineral medium with 20 g/L glucose and 50 g/L xylose, TMB3457 (*OSM1*) and TMB3459 (*OSM1 ERO1*) also consumed glucose within 20 h (Fig. 3) and gave the same yields of ethanol and biomass as the control strain and *FRD1*-strains (Table 2). The yields of glycerol and acetate per gram biomass produced during this period were on the other hand between 9% and 18% lower (P < 0.10) than the control strain (Table 2). However, the yields per consumed substrate were not statistically significant, below 10% significance level, except for strain TMB3457 which gave an acetate yield 37% lower (P = 0.02) than the control strain (Table 2). This suggests that only the strain efficiency, and not the product distribution, was affected. When xylose became the sole carbon source the pattern changed drastically and the two strains behaved differently. The maximum growth rate of strain TMB3457 was 47% lower (P = 0.03) compared with the control strain and the biomass-specific yields of acetate and ethanol increased by 130% (P = 0.04) and 69% (P = 0.05), respectively (Fig. 5; Supplementary material: Table S1). As a result a smaller fraction of the carbon was distributed to biomass and glycerol formation in favour of acetate and ethanol (Fig. 5). Strain TMB3459 did not display any differences in growth rate on xylose or biomass-specific yield of ethanol compared with the control strain (Fig. 5). The acetate yield per biomass also increased by 44% (P = 0.008) whereas both the glycerol and xylitol yields decreased by 39% (P = 0.08) and 20% (P = 0.002) compared with the control strain (Fig. 5). Hence, this strain diverted the carbon away from glycerol, xylitol and ethanol for a higher production of acetate and maintained biomass yield (Fig. 5).

The performance of TMB3457 and TMB3459 did not differ significantly from the control strain in complex medium during the glucose phase (Table 2).

With xylose as the carbon source, on the other hand, both strains grew significantly slower than the control strain. The growth rates of TMB3457 and TMB3459 on xylose were reduced by 25% (P = 0.09) and 51% (P = 0.12), respectively (Fig. 5). Both strains also increased the biomass-specific yield of acetate by 73% (P = 0.003) and 157% (P = 0.03), respectively (Fig. 5). Although both strains diverted more carbon toward acetate and increased the substrate-specific yield by 67% (P < 0.07), different by-product yields were reduced by each strain, TMB3457 showed a reduced substrate-specific yield of glycerol by 31% (P = 0.09) whereas TMB3458 showed a reduced yield of ethanol by 21% (P = 0.06) (Fig. 5).

The rate of ATP production does not correlate with growth rate

As mentioned previously changing from a minimal medium to a rich medium led to several significant changes in the physiology. Figure 6 shows the relative changes in specific rates and yield coefficients due to this change and treating all the data from the cultivations in defined and rich medium as two distinct groups. Due to the presence of excess nutrients and external electron acceptors in the rich medium the cells require less carbon for biosynthesis and do not need to produce as much glycerol for regenerating NAD. The presence of external electron acceptors also benefits the conversion of xylitol to xylulose which efficiently reduces the excretion of this by-product [Wahlbom and Hahn-Hägerdal, 2002]. Hence, the cells can produce biomass, acetate, ethanol and ATP more efficiently from the carbon taken up. The maximum growth rate on glucose increased by 22% even though the specific consumption rate of substrate decreased and thus also the production rate of ATP. Although ATP is necessary for growth these results indicate that the two rates are not necessarily correlated. This is further illustrated by the measurements from the fermentations of xylose. Under those conditions the rate of ATP production increased by 77% whereas the growth rate was not significantly affected. This is in agreement with previous results from measurements of intracellular metabolites during fermentation of a glucose xylose mixture which indicated a minimal role of adenine nucleotides in the control of growth on xylose [Bergdahl *et al.*, 2012].

DISCUSSION

Fumarate reductase is not limiting the anaerobic growth on xylose

In this study we examined the hypothesis that recombinant xylose-fermenting *S. cerevisiae* strains have a limited fumarate reductase activity during xylose fermentation which would lead to insufficient recycling of the FAD prosthetic group of Ero1p. Without proper reconstitution of this flavo-protein the

formation of disulphide bonds in nascent polypeptides translocated to the ER becomes inefficient and could be one underlying cause of the low anaerobic growth rate on xylose. However, the over-expression of *FRD1*, encoding the cytosolic fumarate reductase, did not improve the growth rate, even when the strain was provided with all amino acids and an additional copy of the *ERO1* gene controlled by a strong promoter. Over-expression of the *OSM1* gene, encoding the mitochondrial fumarate reductase, even had the opposite effect and disturbed the redox balance of the cells significantly leading to a reduced growth rate.

Previous studies have shown that the activity and expression of *FRD1* and *OSM1* decrease upon entry into stationary phase [Gasch *et al.*, 2000; Camarasa *et al.*, 2007] and during carbon starvation [Bradley *et al.*, 2009]. In addition, transcriptional analysis of a recombinant *S. cerevisiae* XR/XDH-strain indicated a reduced expression of *FRD1* during xylose fermentation, but not of *OSM1* [Runquist *et al.*, 2009b]. Although this information indicates that the activity of fumarate reductase could be lower during xylose fermentation compared to glucose fermentation, the results obtained in this study point to a non-limiting activity during xylose fermentation. In that case, the previously observed accumulation of fumarate [Bergdahl *et al.*, 2012] could result from increased production in the reaction catalysed by cytosolic malate dehydrogenase (encoded by *MDH2*) which is significantly up-regulated during xylose fermentation [Runquist *et al.*, 2009b]. This response would thus be unrelated to the protein folding process. Alternatively, the fumarate reductase activity might be kept high by the stress-related transcription factors Msn2p/Msn4p and Yap1p [Horan *et al.*, 2006; Salin *et al.*, 2008; Kelley and Ideker, 2009] in a response to cellular stress. Due to the involvement of Yap1p, an oxidative stress seems most likely in this case [Herrero *et al.*, 2008]. This possibility is supported by much higher intracellular concentrations of both reduced and oxidized glutathione and higher transcript levels of *MSN4* and *YAP1* in recombinant *S. cerevisiae* strains during xylose fermentation compared to glucose fermentation [Runquist *et al.*, 2009b; Bergdahl *et al.*, 2012].

Alternatively, the unsuccessful demonstration of the involvement of the fumarate reductases in the slow anaerobic growth on xylose could mean that other components of the protein folding mechanism are limiting. There are three immediate factors that should be evaluated: i) the functionality and correct localization of Ero1p to the ER-membrane in strains TMB3458 and TMB3459; ii) the level of free FAD and iii) the activity of Pdi1p. The activity of Ero1p has been shown to be very sensitive to the level of free FAD possibly due to additional weak-affinity binding sites [Tu and Weissman, 2002]. This interaction was interpreted as a regulatory coupling between the metabolic and nutritional status of the cell and the processing of secretory proteins. In conditions when cells are no longer able to actively produce biomass the cellular level of free FAD would decrease which in turn reduces the activity of Ero1p. Hence the cell reduces the risk of becoming overoxidised and start forming misfolded proteins. If *S.*

cerevisiae is unable to maintain a high level of free FAD during xylose fermentation it could explain why increasing the fumarate reductase activity did not have an effect. The protein disulphide isomerase (Pdi1p) is, together with Ero1p, essential for disulphide bond formation in the ER [Farquhar *et al.*, 1991]. Although transcriptional analysis did not show any difference in expression of *PDI1* between glucose and xylose fermentation [Runquist *et al.*, 2009b], proteome analysis of a mutant strain with improved xylose-fermenting capability identified Pdi1p as significantly more abundant in the improved strain compared with the wild-type [Karhumaa *et al.*, 2009]. This strongly indicates that there indeed is a need for a higher capacity in the protein folding mechanism for efficient xylose fermentation. Whether this capacity is for regulation of disulphide bond formation [Kim *et al.*, 2012], reduction of non-native disulphide bonds [Laboissiere *et al.*, 1995] or targeting unfolded glycoproteins for degradation [Gauss *et al.*, 2011] remains to be investigated.

Frd1p and Osm1p do not influence regeneration of cytosolic NAD

It has previously been shown that the addition of oxidised methylene blue or phenazine methosulfate, which chemically oxidises NADH to NAD [Sevcik and Dunford, 1991], to cultures of a *frd1Δ osm1Δ* double mutant rescues the non-growing phenotype under anaerobic conditions [Enomoto *et al.*, 2002]. It was thus proposed that the two fumarate reductases are involved in the oxidation of excess NADH formed in the cytosol and the mitochondria under anaerobic conditions. The formation of xylitol during xylose fermentation has been ascribed to an inability of the cells to regenerate the NAD needed for the conversion of xylitol to xylulose by XDH [Hahn-Hägerdal *et al.*, 1996]. The addition of acetoin, a substrate which can be reduced by yeast to 2,3-butanediol using NADH, to cultures fermenting xylose reduces the xylitol yield significantly [Wahlbom and Hahn-Hägerdal, 2002; Sonderegger *et al.*, 2004]. If the fumarate reductases participate in the regeneration of excess NADH an increased reductase activity could confer a reduction of the xylitol yield during xylose fermentation. However, the over-expression of *FRD1* or *OSM1* did not affect the amount of xylitol produced from xylose (Fig. 5). This is in agreement with other studies showing that addition of acetoin to a culture of a *frd1Δ osm1Δ* double mutant does not rescue the non-growing phenotype under anaerobic conditions [Camarasa *et al.*, 2007]. In addition, the proposed mechanism of NADH oxidation requires the presence of an enzyme capable of transferring electrons from NADH to FAD to generate the reduced cofactor used as substrate by fumarate reductase [Enomoto *et al.*, 2002; Camarasa *et al.*, 2007]. As of yet, no such enzyme has been identified in *S. cerevisiae* that is expressed under anaerobic conditions. Based on these results we conclude that the fumarate reductases from *S. cerevisiae* do not influence the regeneration of cytosolic NAD.

Osm1p may interact with mitochondrial FAD-dependent glycerol 3-phosphate dehydrogenase during xylose fermentation

As stated above, the over-expression of *OSM1* caused physiological responses that were not observed in strains over-expressing *FRD1*. This indicates that Osm1 interacts with components specifically located in the mitochondria. One of these responses was a 20% to 40% reduction in glycerol yield per consumed xylose (Fig.5). The *GUT2* gene encodes a FAD-dependent glycerol 3-phosphate dehydrogenase located in the mitochondrial inner membrane [Rønnow and Kielland-Brandt, 1993]. Gut2p is essential for growth on glycerol [Rønnow and Kielland-Brandt, 1993] and operates together with *GUT1*, encoding a glycerol kinase [Pavlik *et al.*, 1993]. Gut1 catalyses the phosphorylation of glycerol to glycerol 3-phosphate (G3P). G3P is subsequently oxidized to dihydroxyacetone phosphate (DHAP) by Gut2p, using FAD as the electron acceptor. DHAP enters gluconeogenesis while the electrons are passed from $FADH_2$ to the electron transport chain and used to generate ATP. Expression of *GUT2* is repressed in the presence of glucose and induced during growth on non-fermentable carbon sources by Snf1p and the Hap2p/3p/4p/5p complex [Grauslund and Rønnow, 2000]. Several studies on the gene expression profile conferred by xylose show that it is not recognised as a fermentable carbon source [Wahlbom *et al.*, 2003; Jin *et al.*, 2004; Salusjärvi *et al.*, 2006; Runquist *et al.*, 2009b]. Recombinant strains growing on xylose thus display an induction of genes involved in respiratory metabolism, gluconeogenesis and glyoxylate cycle, regardless of the oxygenation level. This response also includes the *GUT2* gene which is induced more than 7-fold during xylose fermentation [Runquist *et al.*, 2009b]. The combination of high *GUT2*-expression with *OSM1* over-expression might create a system in which the electrons from NADH are transferred to succinate instead of glycerol, leading to the observed reduction in glycerol production (Fig. 7). The DHAP produced by Gut2p can either be recycled again through Gpd2p (NAD-dependent glycerol 3-phosphate dehydrogenase) or enter glycolysis, depending on cellular needs (NAD regeneration vs. ATP formation). The DHAP directed to glycolysis could be converted to ethanol, but the strains constructed in this study rather preferred to convert it to acetate (Fig. 5). Perhaps the NAD:NADH ratio in these strains is more beneficial for acetate formation by the aldehyde dehydrogenases Ald2, Ald3 and Ald4 (Fig. 7). The genes encoding these enzymes are all up-regulated during xylose fermentation [Runquist *et al.*, 2009b], but the acetate most likely originates from the mitochondria since xylitol formation in the cytosol was unaffected (Fig. 5). This hypothesis can account for the decreased glycerol yield and the increased acetate yield, but the expected increase in succinate yield was not observed (Fig. 5). Due to the poor repressive capability of xylose, several genes encoding components of the electron transport chain are also up-regulated during xylose fermentation [Runquist *et al.*, 2009b]. This includes the succinate dehydrogenase (SDH) complex which could convert the produced succinate back to fumarate creating a new cycle with Osm1p (Fig. 7). SDH

normally transmits the sequestered electrons to oxygen via the electron transport chain, but under anaerobic conditions this is not possible. Hence, the presence of SDH might lead to a depletion of cellular FAD and accumulation of $FADH_2$. This could explain the reduced growth rate of these strains on xylose (Fig. 5). With further genetic modifications, such as deletion of the *SDH1*, *ALD*, and *RHR2* genes, the Gut2p/Osm1p-couple could become a redox sink producing succinate instead of glycerol, provided there is a sufficient supply of fumarate. A higher yield of succinate instead of glycerol during ethanol production would provide more attractive economic benefits as glycerol is becoming widely available from biodiesel production facilities [Yang *et al.*, 2012].

ACKNOWLEDGEMENTS

We wish to acknowledge Tarinee Boonyawan for the amplification and cloning of the *OSM1* and *ERO1* genes. The Swedish National Energy Agency (Energimyndigheten, Project No. P35350-1) is gratefully acknowledged for financial support.

Table 1. Strains and plasmids used in this study

Name	Relevant genotype	Reference
Plasmids		
p426TEF	*URA3*	[Mumberg *et al.*, 1995]
YIplac128	*LEU2*	[Gietz and Sugino, 1988]
YIplac211	*URA3*	[Gietz and Sugino, 1988]
YIpDR1	YIplac128:TDH3p-*GXF1*-CYC1t	[Runquist *et al.*, 2009a]
YIpDR7	YIplac211:TDH3p-*XYL1*(N272D)-ADH1t; PGK1p-*XYL2*-PGK1t	[Runquist *et al.*, 2010]
YIpBB1	YIplac128:TDH3p-*FRD1*-CYC1t	This study
YIpBB2	YIplac128:TDH3p-*OSM1*-CYC1t	This study
YIpBB3	YIplac128:TDH3p-*FRD1*-CYC1t; TEF1-*ERO1*-ERO1t	This study
YIpBB4	YIplac128:TDH3p-*OSM1*-CYC1t; TEF1-*ERO1*-ERO1t	This study
Yeast strains		
TMB3043	CEN.PK2-1C; *gre3*-Δ; *his3*::PGK1p-XKS1-PGK1t, *HIS3*; *tal1*::PGK1p-TAL1-PGK1t; *tkl1*::PGK1p-TKL1-PGK1t; *rki1*::PGK1p-RKI1-PGK1t; *rpe1*::PGK1p-RPE1-PGK1t; *ura3*, *leu2*	[Karhumaa *et al.*, 2005]
TMB3452	TMB 3043; *ura3*::YIpDR7; *leu2*	This study
TMB3455	TMB 3452; *leu2*::YIplac128	This study
TMB3456	TMB 3452; *leu2*::YIpBB1	This study
TMB3457	TMB 3452; *leu2*::YIpBB2	This study
TMB3458	TMB 3452; *leu2*::YIpBB3	This study
TMB3459	TMB 3452; *leu2*::YIpBB4	This study

Table 2. Maximum yields obtained during the glucose phase in anaerobic batch fermentation of 20 g/L glucose and 50 g/L xylose in 2X YNB medium and complex medium containing 10 g/L yeast extract. Values are given as mean ± standard deviation of two independent experiments.

	Defined mineral medium					Medium with yeast extract				
	TMB3455	**TMB3456**	**TMB3457**	**TMB3458**	**TMB3459**	**TMB3455**	**TMB3456**	**TMB3457**	**TMB3458**	**TMB3459**
μ_{max} (1/h)	0.29±0.012	0.33±0.028	0.30±0.019	0.30±0.029	0.32±0.044	0.37±0.003	0.37±0.000	0.38±0.001	0.38±0.004	0.38±0.003
Yields (mol/mol sugar)										
$Y_{xylt/s}$	–	–	–	–	–	–	–	–	–	–
$Y_{glyc/s}$	0.22±0.02	0.24±0.02	0.20±0.02	0.23±0.02	0.20±0.05	0.13±0.01	0.10±0.00	0.11±0.01	0.11±0.00	0.11±0.01
$Y_{ac/s}$	0.020±0.001	0.020±0.004	0.012±0.000	0.019±0.005	0.017±0.005	0.030±0.006	0.019±0.000	0.022±0.000	0.022±0.001	0.025±0.003
$Y_{etoh/s}$	1.87±0.14	2.08±0.06	1.96±0.21	2.00±0.20	1.96±0.37	2.7±0.6	2.8±0.3	2.6±0.2	2.9±0.5	2.6±0.2
$Y_{ATP/s}$	1.66±0.12	1.85±0.08	1.77±0.19	1.80±0.19	1.78±0.33	2.5±0.4	2.7±0.3	2.5±0.2	2.8±0.4	2.5±0.2
$Y_{x/s}$ (g/mol)	10.4±0.5	11.7±0.7	10.5±0.2	10.7±1.1	11.9±0.9	17.5±1.4	19.3±0.5	18.4±0.9	18.3±2.2	19.5±0.6
Yields (mmol/g CDW)										
$Y_{xylt/x}$	–	–	–	–	–	–	–	–	–	–
$Y_{glyc/x}$	20.2±0.8	18.9±0.3	18.3±0.5	18.9±1.6	16.6±0.2	7.3±0.5	6.9±0.6	6.4±0.2	6.8±0.3	6.4±0.0
$Y_{ac/x}$	2.1±0.1	1.8±0.1	1.8±0.1	1.9±0.4	1.8±0.0	1.3±0.4	1.4±0.2	1.3±0.1	1.3±0.0	1.5±0.1
$Y_{etoh/x}$	152.9±8.0	140.3±3.5	152.5±10.6	150.5±0.9	146.9±6.9	94.2±5.0	92.0±6.9	91.3±5.9	93.2±6.0	93.0±3.5
$Y_{ATP/x}$	134.8±7.4	123.2±3.3	136.0±10.3	133.5±0.4	132.1±6.6	87.4±6.9	86.0±6.7	86.6±6.4	87.4±6.1	88.6±4.8

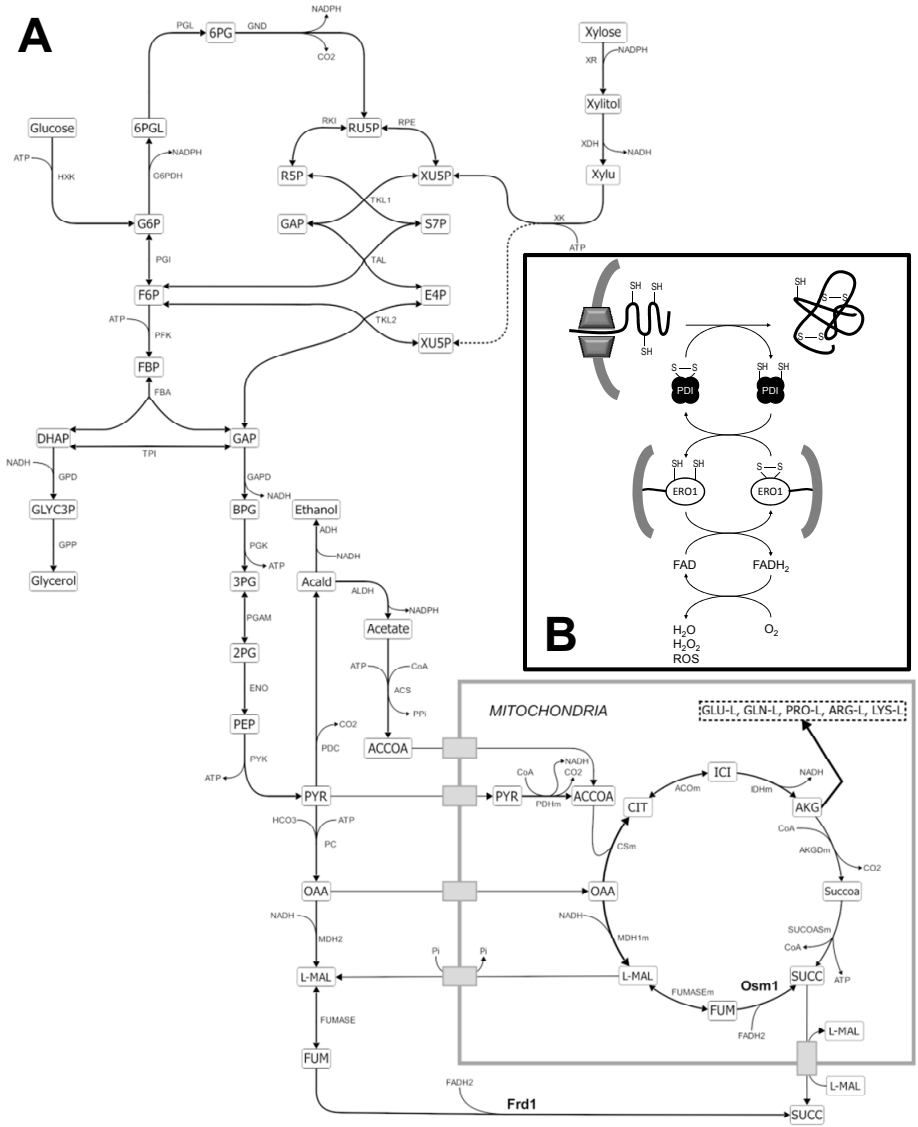

Figure 1. Metabolic pathways in central carbon metabolism (A) and the Pdi1/Ero1-mediated oxidative folding of proteins in the ER (B).

A) Frd1 and Osm1 catalyse the conversion of fumarate to succinate in the last step of the reductive branch of the TCA-cycle. Both enzymes are strictly dependent on $FADH_2$ which is generated inside the ER during the maturation of secretory proteins. **B**) When a nascent polypeptide is translocated into the ER the reduced cysteines are oxidised by Pdi1 giving rise to a disulphide bridge in the protein. The reduced Pdi1 is subsequently oxidised by the membrane bound Ero1 which transfers the electrons to oxygen via covalently bound FAD. In the absence of oxygen the electrons are instead believed to be passed to fumarate in the reaction catalysed by fumarate reductase.

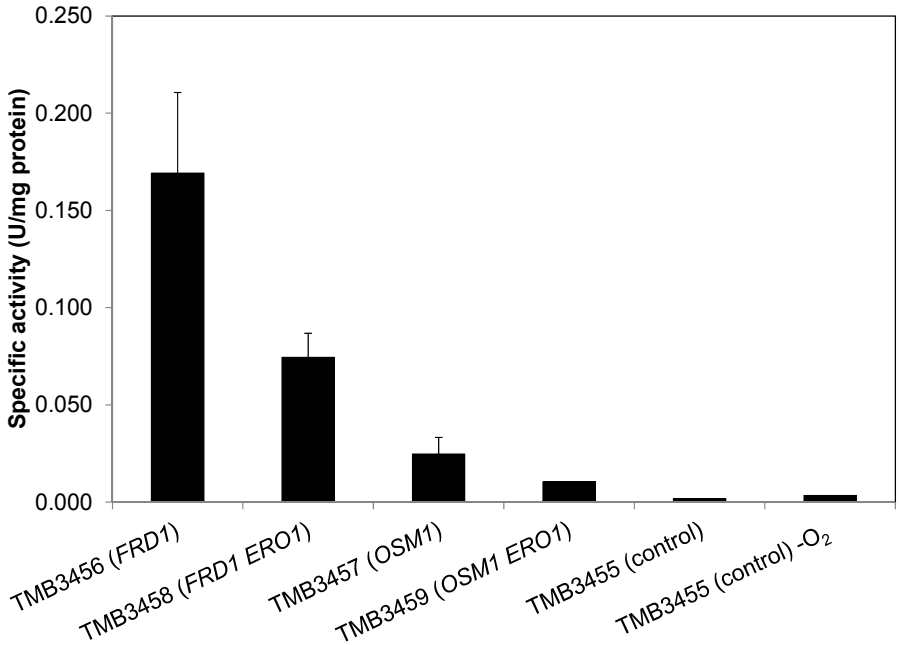

Figure 2. Specific activity of fumarate reductase in the different recombinant strains.
The specific activity was determined in cell-free extracts of cells grown aerobically in defined medium containing glucose as carbon source. Since the genes encoding fumarate reductase enzymes are repressed by oxygen, the activity was also determined in extracts from the control strain grown under anaerobic conditions (far right). Bars showing errors indicate mean ± standard deviation of two independent extracts while those without are single experiments only.

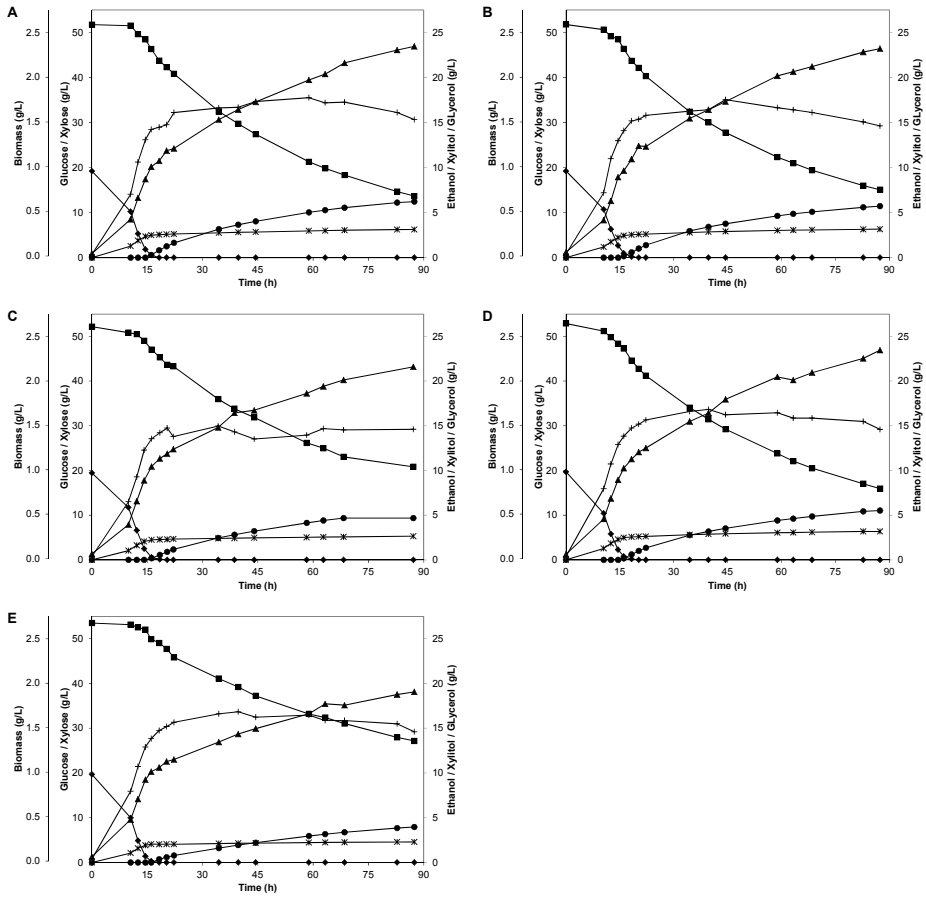

Figure 3. Fermentation of a glucose/xylose mix in defined medium.
A mix of 20 g/L glucose and 50 g/L xylose was fermented in 2X YNB medium by strains **A**) TMB3455 (control), **B**) TMB3456 (*FRD1*), **C**) TMB3457 (*OSM1*), **D**) TMB3458 (*FRD1 ERO1*) and **E**) TMB3459 (*OSM1 ERO1*). Symbols: diamonds, glucose; squares, xylose; plus, biomass; triangles, ethanol; circles, xylitol; stars, glycerol. Figures illustrate one representative experiment out of two biological replicates.

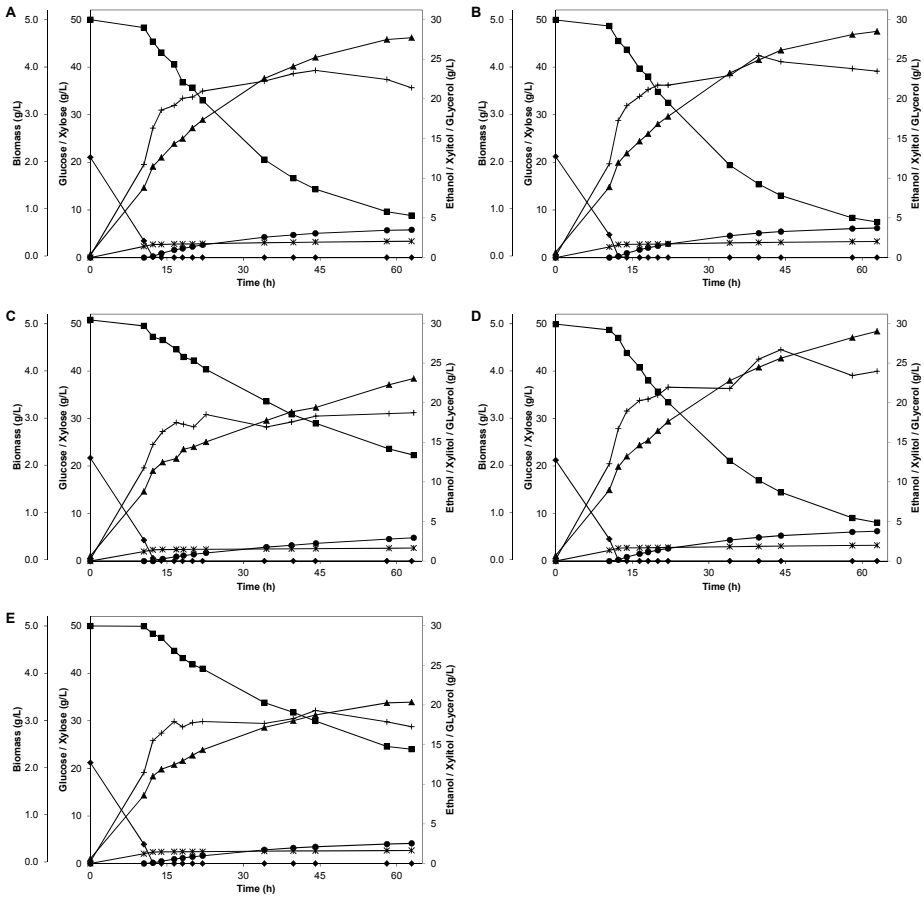

Figure 4. Fermentation of a glucose/xylose mix in rich medium.
A mix of 20 g/L glucose and 50 g/L xylose was fermented in rich medium containing 10 g/L yeast extract by strains **A**) TMB3455 (control), **B**) TMB3456 (*FRD1*), **C**) TMB3457 (*OSM1*), **D**) TMB3458 (*FRD1 ERO1*) and **E**) TMB3459 (*OSM1 ERO1*). Symbols: diamonds, glucose; squares, xylose; plus, biomass; triangles, ethanol; circles, xylitol; stars, glycerol. Figures illustrate one representative experiment out of two biological replicates.

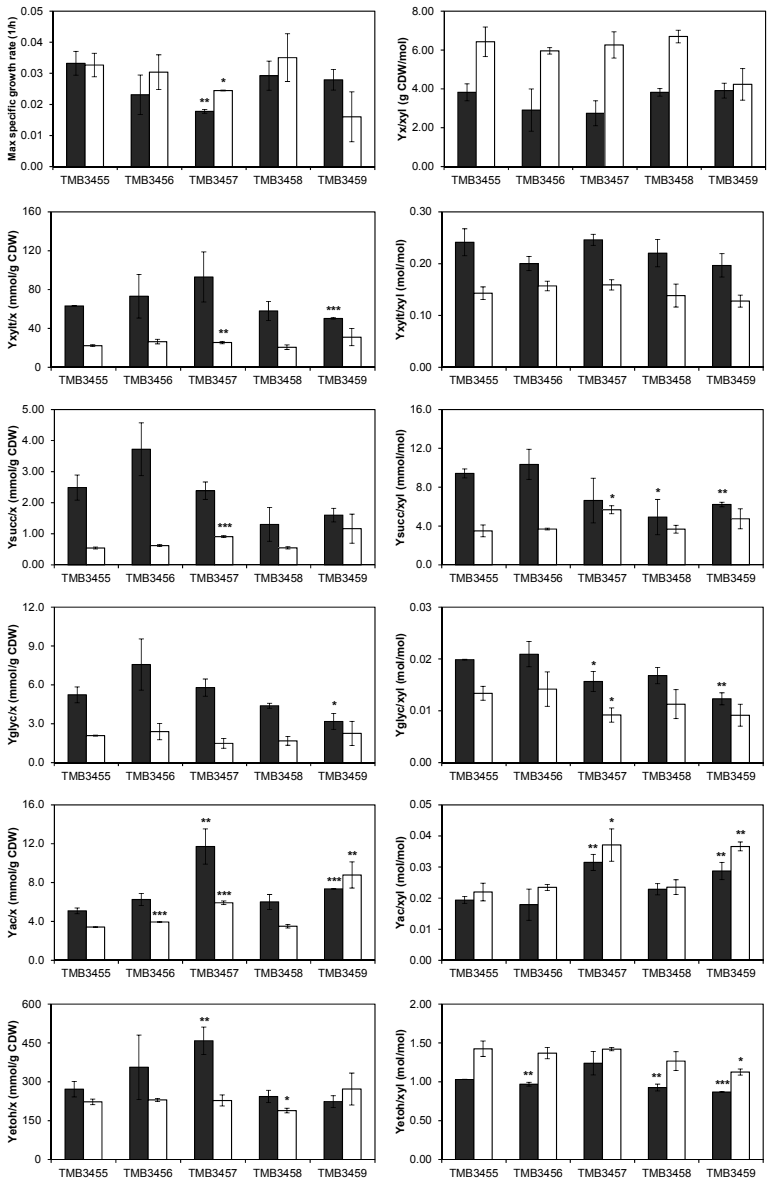

Figure 5. Strain characteristics during the xylose phase in anaerobic batch fermentation of 20 g/L glucose and 50 g/L xylose.

Maximum specific growth rates, product yields per biomass formed and per xylose consumed for strains TMB3455 (control), TMB3456 (*FRD1*), TMB3457 (*OSM1*), TMB3458 (*FRD1 ERO1*) and TMB3459 (*OSM1 ERO1*). Bars show the results obtained from cultivation in defined medium (black) and in rich medium (white). Values represent mean values ± standard deviation of two independent experiments. Asterisks indicate the significance level of a two-sided t-test compared with the control strain: $P < 0.10$ (*), $P < 0.05$ (**) and $P < 0.01$ (***).

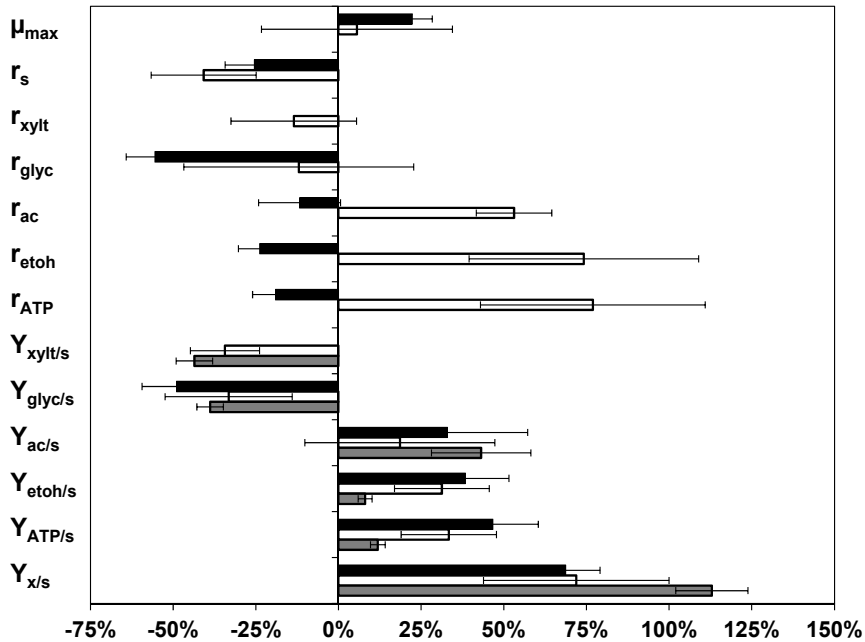

Figure 6. Changes in physiological parameters when changing from defined to rich medium
Treating the data generated from the cultivations in defined and rich medium as two distinct groups, the relative changes in some physiological parameters are shown. The changes refer to a shift from a defined minimal medium (YNB) to a rich, complex medium (yeast extract). Bars indicate parameters determined during glucose fermentation (black), xylose fermentation (white) and total sugar fermentation (grey). Errors show the 95% confidence intervals of the changes (*df* = 18), hence error bars that cross the y-axis indicate a change that is not significant at the 0.05 confidence level. All significant results had *P*-values between $8 \cdot 10^{-15}$ and 0.045. Parameters: μ_{max}, maximum specific growth rate; r, maximum specific consumption or production rate; Y, product yield per consumed substrate. Abbreviations: s, substrate (glucose, xylose or total sugar); xylt, xylitol; glyc, glycerol; ac, acetate; etoh, ethanol.

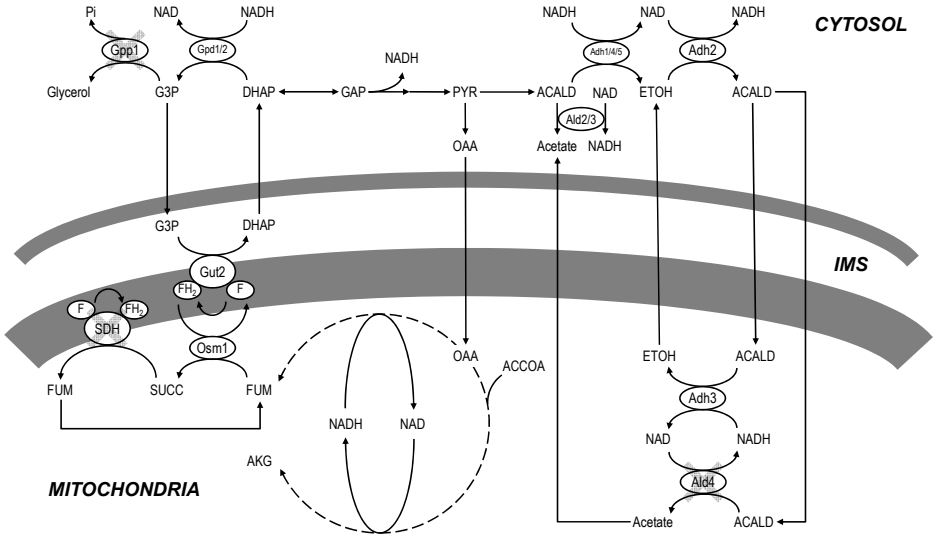

Figure 7. The Gut2/Osm1 redox-couple during xylose fermentation
During xylose fermentation several genes related to respiratory metabolism are derepressed, including *GUT2* which encodes a FAD-dependent glycerol 3-phosphate dehydrogenase. When combined with Osm1 (the mitochondrial fumarate reductase) a cycle is created in which the electrons from cytosolic NADH can be transferred to fumarate instead of DHAP. With further genetic modifications (indicated by grey crosses) it might be possible to form succinate as a major byproduct during alcoholic fermentation instead of glycerol.

REFERENCES

1. Arikawa Y, Enomoto K, Muratsubaki H, Okazaki M: **Soluble fumarate reductase isoenzymes from *Saccharomyces cerevisiae* are required for anaerobic growth.** *FEMS Microbiol Lett* 1998, **165**(1):111-116.
2. Barlowe CK, Miller EA: **Secretory protein biogenesis and traffic in the early secretory pathway.** *Genetics* 2013, **193**(2):383-410.
3. Becher D, Kricke J, Stein G, Lisowsky T: **A mutant for the yeast sc*ERV1* gene displays a new defect in mitochondrial morphology and distribution.** *Yeast* 1999, **15**(12):1171-1181.
4. Bengtsson O, Hahn-Hägerdal B, Gorwa-Grauslund MF: **Xylose reductase from *Pichia stipitis* with altered coenzyme preference improves ethanolic xylose fermentation by recombinant *Saccharomyces cerevisiae*.** *Biotechnol Biofuels* 2009, **2**.
5. Bergdahl B, Heer D, Sauer U, Hahn-Hägerdal B, van Niel EW: **Dynamic metabolomics differentiates between carbon and energy starvation in recombinant *Saccharomyces cerevisiae* fermenting xylose.** *Biotechnol Biofuels* 2012, **5**(1):34.
6. Bien M, Longen S, Wagener N, Chwalla I, Herrmann JM, Riemer J: **Mitochondrial disulfide bond formation is driven by intersubunit electron transfer in Erv1 and proofread by glutathione.** *Mol Cell* 2010, **37**(4):516-528.
7. Bradley PH, Brauer MJ, Rabinowitz JD, Troyanskaya OG: **Coordinated concentration changes of transcripts and metabolites in *Saccharomyces cerevisiae*.** *PLoS Comput Biol* 2009, **5**(1).
8. Camarasa C, Faucet V, Dequin S: **Role in anaerobiosis of the isoenzymes for *Saccharomyces cerevisiae* fumarate reductase encoded by *OSM1* and *FRDS1*.** *Yeast* 2007, **24**(5):391-401.
9. Camarasa C, Grivet JP, Dequin S: **Investigation by 13C-NMR and tricarboxylic acid (TCA) deletion mutant analysis of pathways for succinate formation in *Saccharomyces cerevisiae* during anaerobic fermentation.** *Microbiology* 2003, **149**:2669-2678.
10. Cleland WW: **An analysis of Haldane relationships.** *Methods Enzymol* 1982, **87**:366-369.
11. Enomoto K, Arikawa Y, Muratsubaki H: **Physiological role of soluble fumarate reductase in redox balancing during anaerobiosis in *Saccharomyces cerevisiae*.** *FEMS Microbiol Lett* 2002, **215**(1):103-108.
12. Enomoto K, Ohki R, Muratsubaki H: **Cloning and sequencing of the gene encoding the soluble fumarate reductase from *Saccharomyces cerevisiae*.** *DNA Res* 1996, **3**(4):263-267.
13. Farquhar R, Honey N, Murant SJ, Bossier P, Schultz L, Montgomery D, Ellis RW, Freedman RB, Tuite MF: **Protein disulfide isomerase is essential for viability in *Saccharomyces cerevisiae*.** *Gene* 1991, **108**(1):81-89.

14. Festel GW: **Biofuels - Economic aspects.** *Chemical Engineering & Technology* 2008, **31**(5):715-720.
15. Frand AR, Kaiser CA: **The *ERO1* gene of yeast is required for oxidation of protein dithiols in the endoplasmic reticulum.** *Mol Cell* 1998, **1**(2):161-170.
16. Frand AR, Kaiser CA: **Ero1p oxidizes protein disulfide isomerase in a pathway for disulfide bond formation in the endoplasmic reticulum.** *Mol Cell* 1999, **4**(4):469-477.
17. Freedman RB: **Protein disulfide isomerase - multiple roles in the modification of nascent secretory proteins.** *Cell* 1989, **57**(7):1069-1072.
18. Gasch AP, Spellman PT, Kao CM, Carmel-Harel O, Eisen MB, Storz G, Botstein D, Brown PO: **Genomic expression programs in the response of yeast cells to environmental changes.** *Mol Biol Cell* 2000, **11**(12):4241-4257.
19. Gauss R, Kanehara K, Carvalho P, Ng DTW, Aebi M: **A complex of Pdi1p and the mannosidase Htm1p initiates clearance of unfolded glycoproteins from the endoplasmic reticulum.** *Mol Cell* 2011, **42**(6):782-793.
20. Gietz RD, Schiestl RH: **High-efficiency yeast transformation using the LiAc/SS carrier DNA/PEG method.** *Nat Protoc* 2007, **2**(1):31-34.
21. Gietz RD, Sugino A: **New yeast-*Escherichia coli* shuttle vectors constructed with in vitro mutagenized yeast genes lacking six-base pair restriction sites.** *Gene* 1988, **74**(2):527-534.
22. Girio FM, Fonseca C, Carvalheiro F, Duarte LC, Marques S, Bogel-Lukasik R: **Hemicelluloses for fuel ethanol: A review.** *Bioresour Technol* 2010, **101**(13):4775-4800.
23. Grauslund M, Rønnow B: **Carbon source-dependent transcriptional regulation of the mitochondrial glycerol-3-phosphate dehydrogenase gene, *GUT2*, from *Saccharomyces cerevisiae*.** *Can J Microbiol* 2000, **46**(12):1096-1100.
24. Hahn-Hägerdal B, Hallborn J, Jeppsson H, Meinander N, Walfridsson M, Ojamo H, Penttilä M, Zimmermann FK: **Redox balances in recombinant *Saccharomyces cerevisiae*.** *Ann N Y Acad Sci* 1996, **782**:286-296.
25. Hahn-Hägerdal B, Karhumaa K, Fonseca C, Spencer-Martins I, Gorwa-Grauslund MF: **Towards industrial pentose-fermenting yeast strains.** *Appl Microbiol Biotechnol* 2007, **74**(5):937-953.
26. Herrero E, Ros J, Bellí G, Cabiscol E: **Redox control and oxidative stress in yeast cells.** *BBA General Subjects* 2008, **1780**(11):1217-1235.
27. Herrmann JM, Bihlmaier K, Mesecke N: **The role of the Mia40-Erv1 disulfide relay system in import and folding of proteins of the intermembrane space of mitochondria.** In *The Enzymes: Molecular machines involved in protein transport across cellular membranes*. **vol.** XXV: Academic Press; 2007.
28. Horan S, Bourges I, Meunier B: **Transcriptional response to nitrosative stress in *Saccharomyces cerevisiae*.** *Yeast* 2006, **23**(7):519-535.
29. Jeffries TW: **Emerging technology for fermenting D-xylose.** *Trends Biotechnol* 1985, **3**(8):208-212.

30. Jin YS, Laplaza JM, Jeffries TW: ***Saccharomyces cerevisiae*** **engineered for xylose metabolism exhibits a respiratory response.** *Appl Environ Microbiol* 2004, **70**(11):6816-6825.
31. Jönsson L, Alriksson B, Nilvebrant N-O: **Bioconversion of lignocellulose: inhibitors and detoxification.** *Biotechnol Biofuels* 2013, **6**(1):16.
32. Karhumaa K, Hahn-Hägerdal B, Gorwa-Grauslund MF: **Investigation of limiting metabolic steps in the utilization of xylose by recombinant *Saccharomyces cerevisiae* using metabolic engineering.** *Yeast* 2005, **22**:359-368.
33. Karhumaa K, Påhlman A-K, Hahn-Hägerdal B, Levander F, Gorwa-Grauslund M-F: **Proteome analysis of the xylose-fermenting mutant yeast strain TMB3400.** *Yeast* 2009, **26**(7):371-382.
34. Kelley R, Ideker T: **Genome-wide fitness and expression profiling implicate Mga2 in adaptation to hydrogen peroxide.** *Plos Genetics* 2009, **5**(5).
35. Kim S, Sideris DP, Sevier CS, Kaiser CA: **Balanced Ero1 activation and inactivation establishes ER redox homeostasis.** *J Cell Biol* 2012, **196**(6):713-725.
36. Kurtzman C, Suzuki M: **Phylogenetic analysis of ascomycete yeasts that form coenzyme Q-9 and the proposal of the new genera *Babjeviella*, *Meyerozyma*, *Millerozyma*, *Priceomyces*, and *Scheffersomyces*.** *Mycoscience* 2010, **51**(1):2-14.
37. Kötter P, Amore R, Hollenberg CP, Ciriacy M: **Isolation and characterization of the *Pichia stipitis* xylitol dehydrogenase gene, *XYL2*, and construction of a xylose-utilizing *Saccharomyces cerevisiae* transformant.** *Curr Genet* 1990, **18**(6):493-500.
38. Laboissiere MCA, Sturley SL, Raines RT: **The essential function of protein-disulfide isomerase is to unscramble nonnative disulfide bonds.** *J Biol Chem* 1995, **270**(47):28006-28009.
39. Lai L-C, Kosorukoff AL, Burke PV, Kwast KE: **Metabolic-state-dependent remodeling of the transcriptome in response to anoxia and subsequent reoxygenation in *Saccharomyces cerevisiae*.** *Eukaryot Cell* 2006, **5**(9):1468-1489.
40. Lange H, Lisowsky T, Gerber J, Muhlenhoff U, Kispal G, Lill R: **An essential function of the mitochondrial sulfhydryl oxidase Erv1p/ALR in the maturation of cytosolic Fe/S proteins.** *EMBO Reports* 2001, **2**(8):715-720.
41. Lee JE, Hofhaus G, Lisowsky T: **Erv1p from Saccharomyces cerevisiae is a FAD-linked sulfhydryl oxidase.** *FEBS Letters* 2000, **477**(1-2):62-66.
42. Lisowsky T: **Dual function of a new nuclear gene for oxidative-phosphorylation and vegetative growth in yeast.** *Mol Gen Genet* 1992, **232**(1):58-64.
43. Lisowsky T: ***ERV1*** **is involved in the cell-division cycle and the maintenance of mitochondrial genomes in *Saccharomyces cerevisiae*.** *Curr Genet* 1994, **26**(1):15-20.
44. Mesecke N, Terziyska N, Kozany C, Baumann F, Neupert W, Hell K, Herrmann JM: **A disulfide relay system in the intermembrane space of mitochondria that mediates protein import.** *Cell* 2005, **121**(7):1059-1069.
45. Mumberg D, Muller R, Funk M: **Yeast vectors for the controlled expression of heterologous proteins in different genetic backgrounds.** *Gene* 1995, **156**(1):119-122.

46. Muratsubaki H, Enomoto K: **One of the fumarate reductase isoenzymes from *Saccharomyces cerevisiae* is encoded by the *OSM1* gene.** *Arch Biochem Biophys* 1998, **352**(2):175-181.
47. Muratsubaki H, Katsume T: **Purification and properties of fumarate reductase from Bakers-yeast.** *Agric Biol Chem* 1982, **46**(12):2909-2917.
48. Nevoigt E: **Progress in metabolic engineering of *Saccharomyces cerevisiae*.** *Microbiol Mol Biol Rev* 2008, **72**(3):379-412.
49. Pavlik P, Simon M, Schuster T, Ruis H: **The glycerol kinase (*GUT1*) gene of *Saccharomyces cerevisiae* - cloning and characterization.** *Curr Genet* 1993, **24**(1-2):21-25.
50. Pollard MG, Travers KJ, Weissman JS: **Ero1p: A novel and ubiquitous protein with an essential role in oxidative protein folding in the endoplasmic reticulum.** *Mol Cell* 1998, **1**(2):171-182.
51. Roberts GG, Hudson AP: **Transcriptome profiling of *Saccharomyces cerevisiae* during a transition from fermentative to glycerol-based respiratory growth reveals extensive metabolic and structural remodeling.** *Mol Genet Genomics* 2006, **276**(2):170-186.
52. Rossi C, Hauber J, Singer TP: **Mitochondrial and cytoplasmic enzymes for the reduction of fumarate to succinate in yeast.** *Nature* 1964, **204**(4954):167-170.
53. Runquist D, Fonseca C, Rådstrom P, Spencer-Martins I, Hahn-Hägerdal B: **Expression of the Gxf1 transporter from *Candida intermedia* improves fermentation performance in recombinant xylose-utilizing *Saccharomyces cerevisiae*.** *Appl Microbiol Biotechnol* 2009a, **82**(1):123-130.
54. Runquist D, Hahn-Hägerdal B, Bettiga M: **Increased expression of the oxidative pentose phosphate pathway and gluconeogenesis in anaerobically growing xylose-utilizing *Saccharomyces cerevisiae*.** *Microb Cell Fact* 2009b, **8**.
55. Runquist D, Hahn-Hägerdal B, Bettiga M: **Increased ethanol productivity in xylose-utilizing *Saccharomyces cerevisiae* via a randomly mutagenized xylose reductase.** *Appl Environ Microbiol* 2010, **76**(23):7796-7802.
56. Rønnow B, Kielland-Brandt MC: ***GUT2*, a gene for mitochondrial glycerol 3-phosphate dehydrogenase of *Saccharomyces cerevisiae*.** *Yeast* 1993, **9**(10):1121-1130.
57. Salin H, Fardeau V, Piccini E, Lelandais G, Tanty V, Lemoine S, Jacq C, Devaux F: **Structure and properties of transcriptional networks driving selenite stress response in yeasts.** *BMC Genomics* 2008, **9**.
58. Salusjärvi L, Pitkanen JP, Aristidou A, Ruohonen L, Penttilä M: **Transcription analysis of recombinant *Saccharomyces cerevisiae* reveals novel responses to xylose.** *Appl Biochem Biotechnol* 2006, **128**(3):237-261.
59. Sambrook J, Fritsch EF, Maniatis T: **Molecular cloning: A laboratory manual**. Cold Spring Harbor: Cold Spring Harbor Laboratory Press; 1989.
60. Sassner P, Galbe M, Zacchi G: **Techno-economic evaluation of bioethanol production from three different lignocellulosic materials.** *Biomass Bioenergy* 2008, **32**(5):422-430.

61. Sevcik P, Dunford HB: **Kinetics of the oxidation of NADH by methylene blue in a closed system.** *J Phys Chem* 1991, **95**(6):2411-2415.
62. Skoog K, Hahn-Hägerdal B: **Xylose fermentation.** *Enzyme Microb Technol* 1988, **10**(2):66-80.
63. Soccol CR, Faraco V, Karp S, Vandenberghe LPS, Thomaz-Soccol V, Woiciechowski A, Pandey A: **Lignocellulosic bioethanol: Current status and future perspectives.** In *Biofuels: Alternative feedstocks and conversion processes*. Oxford, UK: Elsevier Ltd; 2011: 101-122.
64. Sonderegger M, Jeppsson M, Hahn-Hägerdal B, Sauer U: **Molecular basis for anaerobic growth of *Saccharomyces cerevisiae* on xylose, investigated by global gene expression and Metabolic Flux Analysis.** *Appl Environ Microbiol* 2004, **70**(4):2307-2317.
65. Tu BP, Ho-Schleyer SC, Travers KJ, Weissman JS: **Biochemical basis of oxidative protein folding in the endoplasmic reticulum.** *Science* 2000, **290**(5496):1571-1574.
66. Tu BP, Weissman JS: **The FAD- and O2-dependent reaction cycle of Ero1-mediated oxidative protein folding in the endoplasmic reticulum.** *Mol Cell* 2002, **10**(5):983-994.
67. Wahlbom CF, Hahn-Hägerdal B: **Furfural, 5-hydroxymethyl furfural, and acetoin act as external electron acceptors during anaerobic fermentation of xylose in recombinant *Saccharomyces cerevisiae*.** *Biotechnol Bioeng* 2002, **78**(2):172-178.
68. Wahlbom CF, Otero RRC, van Zyl WH, Hahn-Hägerdal B, Jönsson LJ: **Molecular analysis of a *Saccharomyces cerevisiae* mutant with improved ability to utilize xylose shows enhanced expression of proteins involved in transport, initial xylose metabolism, and the pentose phosphate pathway.** *Appl Environ Microbiol* 2003, **69**(2):740-746.
69. Van Vleet JH, Jeffries TW: **Yeast metabolic engineering for hemicellulosic ethanol production.** *Curr Opin Biotechnol* 2009, **20**(3):300-306.
70. Visser W, Scheffers WA, Batenburg-van der Vegte WH, van Dijken JP: **Oxygen requirements of yeasts.** *Appl Environ Microbiol* 1990, **56**(12):3785-3792.
71. Yang F, Hanna M, Sun R: **Value-added uses for crude glycerol - a byproduct of biodiesel production.** *Biotechnol Biofuels* 2012, **5**(1):13.

ADDITIONAL FILE 1

Table S1. Maximum specific consumption and production rates and yields in anaerobic batch fermentation of 20 g/L glucose and 50 g/L xylose in 2X YNB medium. Values are given as mean ± standard deviation of two independent experiments.

	Glucose phase					Xylose phase				
	TMB3455	**TMB3456**	**TMB3457**	**TMB3458**	**TMB3459**	**TMB3455**	**TMB3456**	**TMB3457**	**TMB3458**	**TMB3459**
μ_{max} (1/h)	0.29±0.012	0.33±0.028	0.30±0.019	0.30±0.029	0.32±0.044	0.033±0.004	0.023±0.006	0.018±0.001	0.029±0.005	0.028±0.003
Specific rates (mmol/g CDW/h)										
$r_{max,glc}$	-22.4±0.1	-23.4±2.7	-23.6±0.8	-22.5±3.8	-24.0±6.0	–	–	–	–	–
$r_{max,xyl}$	0.76±0.02	0.76±0.19	0.70±0.01	0.88±0.31	0.42±0.06	-9.0±2.0	-8.3±0.8	-6.8±1.8	-7.8±0.9	-7.2±0.0
$r_{max,xylt}$	–	–	–	–	–	2.1±0.3	1.7±0.1	1.7±0.5	1.7±0.0	1.4±0.2
$r_{max,glyc}$	5.9±0.0	6.2±0.6	5. 5±0.2	5.7±1.0	5.3±0.8	0.18±0.04	0.17±0.00	0.11±0.02	0.13±0.03	0.09±0.01
$r_{max,ac}$	0.61±0.01	0.59±0.10	0.53±0.00	0.59±0.17	0.56±0.07	0.17±0.03	0.15±0.03	0.22±0.04	0.18±0.01	0.21±0.02
$r_{max,etoh}$	44.4±0.5	45.8±5.1	45.6±0.3	45.4±4.6	46.7±8.6	9.2±2.0	8.0±0.6	8.3±1.2	7.2±0.4	6.3±0.0
$r_{max,ATP}$	39.1±0.6	40.3±4.5	40.7±0.48	40.3±3.7	42.0±7.9	9.2±2.0	7.9±0.6	8.4±1.2	7.2±0.4	6.4±0.04
Yields (mol/mol sugar)										
$Y_{xylt/s}$	–	–	–	–	–	0.24±0.03	0.20±0.01	0.25±0.01	0.22±0.03	0.20±0.02
$Y_{glyc/s}$	0.22±0.02	0.24±0.02	0.20±0.02	0.23±0.02	0.20±0.05	0.020±0.000	0.021±0.002	0.016±0.002	0.017±0.002	0.012±0.001
$Y_{ac/s}$	0.020±0.001	0.020±0.004	0.012±0.000	0.019±0.005	0.017±0.005	0.019±0.001	0.018±0.005	0.031±0.003	0.023±0.002	0.029±0.003
$Y_{etoh/s}$	1.87±0.14	2.08±0.06	1.96±0.21	2.00±0.20	1.96±0.37	1.03±0.00	0.97±0.03	1.24±0.15	0.93±0.04	0.87±0.00
$Y_{ATP/s}$	1.66±0.12	1.85±0.08	1.77±0.19	1.80±0.19	1.78±0.33	1.03±0.00	0.96±0.03	1.25±0.16	0.93±0.05	0.89±0.00
$Y_{x/s}$ (g/mol)	10.4±0.5	11.7±0.7	10.5±0.2	10.7±1.1	11.9±0.9	3.8±0.4	2.9±1.1	2.7±0.6	3.8±0.2	3.9±0.4
Yields (mmol/g CDW)										
$Y_{xylt/x}$	–	–	–	–	–	63.1±0.3	73.1±22.4	92.9±25.8	57.9±9.8	50.3±0.8
$Y_{glyc/x}$	20.2±0.8	18.9±0.3	18.3±0.5	18.9±1.6	16.6±0.2	5.2±0.6	7.6±1.8	5.8±0.7	4.4±0.2	3.2±0.6
$Y_{ac/x}$	2.1±0.1	1.8±0.1	1.8±0.1	1.9±0.4	1.8±0.0	5.1±0.3	6.3±0.6	11.7±1.8	6.0±0.8	7.3±0.0
$Y_{etoh/x}$	152.9±8.0	140.3±3.5	152.5±10.6	150.5±0.9	146.9±6.9	271.2±29.9	356.1±124.1	458.4±52.7	243.1±24.0	223.4±23.0
$Y_{ATP/x}$	134.8±7.4	123.2±3.3	136.0±10.3	133.5±0.4	132.1±6.6	270.6±29.6	354.0±123.2	463.5±51.7	243.2±25.7	227.4±21.6

Table S2. Maximum specific consumption and production rates and yields in anaerobic batch fermentation of 20 g/L glucose and 50 g/L xylose in rich medium containing 10 g/L yeast extract. Values are given as mean ± standard deviation of two independent experiments.

	Glucose phase					Xylose phase				
	TMB3455	**TMB3456**	**TMB3457**	**TMB3458**	**TMB3459**	**TMB3455**	**TMB3456**	**TMB3457**	**TMB3458**	**TMB3459**
μ_{max} (1/h)	0.37±0.003	0.37±0.000	0.38±0.001	0.38±0.004	0.38±0.003	0.033±0.004	0.030±0.006	0.024±0.000	0.035±0.008	0.016±0.008
Specific rates (mmol/g CDW/h)										
$r_{max,glc}$	-17.5±1.1	-16.3±0.9	-17.6±1.2	-17.0±0.9	-18.1±0.4	–	–	–	–	–
$r_{max,xyl}$	0.59±0.02	0.49±0.06	0.49±0.02	0.45±0.12	0.20±0.01	-5.2±1.2	-5.1±0.8	-3.9±0.4	-5.3±1.4	-3.7±1.2
$r_{max,xylt}$	–	–	–	–	–	0.73±0.11	0.80±0.08	0.62±0.03	0.71±0.08	0.46±0.11
$r_{max,glyc}$	2.7±0.2	2.6±0.2	2.4±0.1	2.6±0.1	2.4±0.0	0.068±0.009	0.071±0.006	0.036±0.009	0.057±0.001	0.032±0.003
$r_{max,ac}$	0.49±0.16	0.51±0.08	0.49±0.03	0.50±0.02	0.55±0.02	0.11±0.01	0.12±0.02	0.15±0.00	0.12±0.02	0.14±0.05
$r_{max,etoh}$	35.3±2.2	34.3±2.6	34.5 ±2.1	35.1±1.2	34.7±1.1	7.3±1.2	7.0±1.5	5.6±0.5	6.6±1.1	4.1±1.2
$r_{max,ATP}$	32.7±2.8	32.1±2.5	32.7±2.3	32.9±1.9	33.4±1.5	7.4±1.1	7.1±1.4	5.7±0.5	6.7±1.1	4.3±1.2
Yields (mol/mol sugar)										
$Y_{xylt/s}$	–	–	–	–	–	0.14±0.01	0.16±0.01	0.16±0.01	0.14±0.02	0.13±0.01
$Y_{glyc/s}$	0.13±0.01	0.10±0.00	0.11±0.01	0.11±0.00	0.11±0.01	0.013±0.001	0.014±0.003	0.009±0.001	0.011±0.003	0.009±0.002
$Y_{ac/s}$	0.030±0.006	0.019±0.000	0.022±0.000	0.022±0.001	0.025±0.003	0.022±0.003	0.023±0.001	0.037±0.005	0.024±0.002	0.037±0.001
$Y_{etoh/s}$	2.7±0.6	2.8±0.3	2.6±0.2	2.9±0.5	2.6±0.2	1.4±0.1	1.4±0.1	1.4±0.0	1.3±0.1	1.1±0.0
$Y_{ATP/s}$	2.5±0.4	2.7±0.3	2.5±0.2	2.8±0.4	2.5±0.2	1.4±0.1	1.4±0.1	1.5±0.0	1.3±0.1	1.2±0.0
$Y_{x/s}$ (g/mol)	17.5±1.4	19.3±0.5	18.4±0.9	18.3±2.2	19.5±0.6	6.4±0.8	6.0±0.2	6.3±0.7	6.7±0.3	4.2±0.8
Yields (mmol/g CDW)										
$Y_{xylt/x}$	–	–	–	–	–	22.3±0.8	26.4±2.3	25.5±1.2	20.6±2.3	31.0±8.7
$Y_{glyc/x}$	7.3±0.5	6.9±0.6	6.4±0.2	6.8±0.3	6.4±0.0	2.1±0.0	2.4±0.6	1.5±0.4	1.7±0.3	2.3±0.9
$Y_{ac/x}$	1.3±0.4	1.4±0.2	1.3±0.1	1.3±0.0	1.5±0.1	3.4±0.0	3.9±0.1	5.9±0.2	3.5±0.2	8.8±1.4
$Y_{etoh/x}$	94.2±5.0	92.0±6.9	91.3±5.9	93.2±6.0	93.0±3.5	222.4±10.8	229.8±5.8	227.9±21.2	188.9±8.8	271.8±61.6
$Y_{ATP/x}$	87.4±6.9	86.0±6.7	86.6±6.4	87.4±6.1	88.6±4.8	224.5±8.9	233.4±4.3	233.9±19.5	192.1±9.4	281.6±64.1

Paper IV

Engineering yeast hexokinase 2 for improved tolerance toward xylose-induced inactivation

Basti Bergdahl, Anders G. Sandström, Ed W.J. van Niel and Marie F. Gorwa-Grauslund

Division of Applied Microbiology, Department of Chemistry, Lund University, P.O. Box 124, SE-221 00 Lund, Sweden

ABSTRACT

Hexokinase 2 from *Saccharomyces cerevisiae* is a bi-functional enzyme; in addition to its catalytic function it also has an important regulatory function in the glucose catabolite repression signalling mechanism. It has been shown that xylose can induce a decrease in the glucose phosphorylating activity through an autophosphorylation mechanism of Ser158. The induced inactivation by xylose also causes a release of glucose repression of some genes, demonstrating that both the catalytic and regulatory functions of Hxk2p are affected. This might lead to a reduced capability to regulate expression of genes involved in sugar transport and fermentative metabolism. The aim of the current study was to select new variants of Hxk2p, immune to autophosphorylation by xylose, which potentially can restore the repressive capability closer to its nominal level. In this study we describe the first condensed, rationally designed combinatorial library targeting the active-site in Hxk2p. The subsequent screening of the library for mutations in the *HXK2* gene, beneficial for resisting xylose-induced inactivation, led to the identification of a new protein variant with a single amino acid substitution: Phe159Tyr. The new variant, designated Hxk2p-Y, had 64% higher catalytic activity compared with the wild type protein in the presence of 30 g/L xylose during glucose limited continuous cultivation at D = 0.21 1/h. In these conditions the strain expressing the Hxk2p-Y variant also had a 15% higher specific glucose consumption rate. When the variant was expressed together with a heterogeneous xylose pathway there were, however, no significant differences compared with the wild type during batch fermentation of a glucose/xylose mixture. The most relevant application of the Hxk2p-Y variant might therefore be in strains designed for fermentation of only the glucose fraction, leaving the pentose fraction unfermented to be used in a subsequent process with another organism.

INTRODUCTION

The yeast *Saccharomyces cerevisiae* has three structural genes which encode enzymes that catalyse the phosphorylation of glucose to glucose 6-phosphate: *HXK1*, *HXK2* and *GLK1* [Lobo and Maitra, 1977]. *HXK1* and *HXK2* encode hexokinases which, in addition to glucose, also can phosphorylate fructose and mannose [Barnard, 1975]. These two proteins share an identity of 77%. *GLK1* encodes a glucokinase which has an identity of 38% with the two hexokinases and lacks the ability to phosphorylate fructose [Maitra, 1970]. During growth on fermentable carbon sources the *HXK2* gene is predominantly expressed and thus the main substrate-phosphorylating capability is provided by hexokinase 2 (Hxk2p) [Gancedo *et al.*, 1977; Fernandez *et al.*, 1984]. When the conditions change to non-fermentable carbon sources the *HXK2* gene becomes repressed and the *HXK1* and *GLK1* genes are rapidly de-repressed.

Hexokinase 2 has a bi-functional role in yeast metabolism; in addition to its catalytic function it also has an important regulatory function in the glucose catabolite repression signalling mechanism [Gancedo, 1998; Bisson and Kunathigan, 2003; Fernandez-Garcia *et al.*, 2012]. In conditions with high glucose Hxk2p enters the nucleus [Herrero *et al.*, 1998; Randez-Gil *et al.*, 1998a] and interacts with two regulatory proteins, Mig1p [Ahuatzi *et al.*, 2004] and Med8p [de la Cera *et al.*, 2002]. The latter complex binds to regulatory regions in the promoter of the *SUC2* gene (encoding the invertase enzyme) which is proposed to hinder the activation of RNA polymerase [Gancedo and Flores, 2008]. Mig1p is a transcriptional repressor protein that binds to the promoters of most glucose-repressible genes [Carlson, 1999; Schuller, 2003]. The interaction between Hxk2p and Mig1p has two functions, one is to prevent both proteins from leaving the nucleus and the other is to prevent phosphorylation of Mig1p by the Snf1p protein kinase complex [Ahuatzi *et al.*, 2007]. It is only in the dephosphorylated form that Mig1p can exert its repressive ability [Treitel *et al.*, 1998; Smith *et al.*, 1999]. A role for Hxk2p in the regulation of hexose transporters has also been demonstrated by transcriptional analysis of a *hxk2-Δ* strain [Schuurmans *et al.*, 2008] as well as mutagenesis of the protein [Randez-Gil *et al.*, 1998b]. The deletion of *HXK2* caused an up-regulation of transporters with low capacity (encoded by *HXT4-7*) and down-regulation of *HXT1* which is normally highly expressed during growth on glucose [Schuurmans *et al.*, 2008]. A similar pattern was observed when Ser15[1] was exchanged for alanine, which rendered the protein unable to undergo (reversible) phosphorylation [Randez-Gil *et al.*, 1998b]. The phosphorylation of Ser15 is essential for repression of *SUC2*, *HXT2* and *HXT4* as well as induction of *HXT1* in conditions with high glucose

[1] Here the amino acid residues are numbered according to the translated mRNA sequence. Other communications may take into account that the initial methionine residue is cleaved of during post-translational processing, lowering all numbers by one.

concentration. In short, the Hxk2p protein can be regarded as a global glycolytic regulator as the deletion of the corresponding gene reduces the Crabtree effect normally observed in *S. cerevisiae*, resulting in an almost fully respiratory metabolism [Schuurmans *et al.*, 2008].

Early studies on glucose catabolite repression revealed that xylose can induce a decrease in the glucose phosphorylating activity [Fernandez *et al.*, 1984]. Experiments *in vitro* confirmed that Hxk2p becomes irreversibly inactivated by xylose through an autophosphorylation mechanism in the presence of ATP [DelaFuente, 1970; Menezes and Pudles, 1977; Fernandez *et al.*, 1986]. The target residue for the autophosphorylation was later identified as Ser158 and attempts to exchange this amino acid indeed abolished the autophosphorylation but also severely reduced the catalytic activity [Heidrich *et al.*, 1997]. The induced inactivation by xylose also caused an increase in invertase activity, demonstrating that both the catalytic and regulatory functions of Hxk2p are affected by the modification [Fernandez *et al.*, 1984]. A recent study has shown that these two functions are not directly correlated and can operate independently through different parts of the protein [Pelaez *et al.*, 2010]. However, it is possible that the phosphorylation of Ser158 alters the conformation of the protein [Bennett and Steitz, 1980; Heidrich *et al.*, 1997] which prevents it from interacting with glucose, MgATP and other proteins such as Mig1p and Med8p, resulting in abolished catalytic ability and a release of repression even in the presence of high glucose concentration.

In the production of bioethanol from lignocellulosic biomass, an efficient conversion of xylose is of great importance to increase the economic feasibility of the process [Sassner *et al.*, 2008]. *S. cerevisiae* lacks the ability to ferment xylose and requires extensive genetic engineering to obtain such a trait [Hahn-Hägerdal *et al.*, 2007; Van Vleet and Jeffries, 2009]. Hence, xylose is not recognised as a fermentable carbon source by this yeast, as shown in several transcription analyses [Wahlbom *et al.*, 2003; Jin *et al.*, 2004; Salusjärvi *et al.*, 2006; Runquist *et al.*, 2009b] and profiling of intracellular metabolite concentrations [Klimacek *et al.*, 2010; Bergdahl *et al.*, 2012].

Due to the distinguished role of Hxk2p in glucose repression signalling we hypothesise that the inactivation by xylose leads to a reduced capability to regulate expression of genes involved in sugar transport and fermentative metabolism. The aim of the current study was to identify a new variant of Hxk2p, immune to autophosphorylation by xylose. Over-expression of such an enzyme could potentially increase the sugar consumption rate during fermentation of a glucose/xylose mixture by restoring the repressive capability closer to its nominal level and thus increase the ethanol productivity.

EXPERIMENTAL PROCEDURES

Strains and culture conditions

Plasmids and yeast strains used in this study are listed in Table 1. Yeast strains were recovered from 20% glycerol stocks stored at -80 °C on solid YPD or YPGal plates (10 g/L yeast extract, 20 g/L peptone, 20 g/L glucose or galactose, 15 g/L agar) for two days at 30 °C. Yeast cultures were grown in liquid YPD or YPGal medium for 14-16 h, or less when required, at 30 °C and 180 rpm in an orbital shaker. Competent yeast cells were prepared and transformed according to the High efficiency protocol [Gietz and Schiestl, 2007a]. Transformants were selected on solid Yeast Nitrogen Base (YNB) medium (6.7 g/L YNB without amino acids) with 20 g/L glucose or galactose as carbon source. When required, uracil and leucine were supplemented at 50 mg/L and 220 mg/L, respectively. When needed, antibiotics geniticin and aureobasidin were supplemented at 200 mg/L and 0.15 mg/L, respectively. In shake flasks the working volume was 10% or less of the total volume. In shake flask cultivations, YNB medium contained 50 mM potassium hydrogen phthalate buffer at pH 5.5. Anaerobic continuous cultivations were made in a defined mineral medium [Verduyn *et al.*, 1992] using 5 g/L glucose and 50 g/L xylose or 15 g/L glucose with or without 30 g/L xylose in the feed reservoir. All media used for anaerobic cultivations were supplemented with Tween 80 (400 mg/L) and ergosterol (10 mg/L).

E. coli strain NEB5α (New England Biolabs, USA) was used for sub-cloning of plasmid DNA. Heat shock competent *E. coli* cells were prepared according to the Inoue method [Sambrook *et al.*, 1989] and transformed according to the supplier's instructions. Transformants were selected from solid LB plates (5 g/L yeast extract, 10 g/L tryptone, 10 g/L NaCl, 15 g/L agar, pH 7.0), supplemented with 100 mg/L of ampicillin, after incubation for 16 h at 37°C. Cultures of transformed *E. coli* were recovered from 25% glycerol stocks stored at -80 °C and grown in liquid LB medium, supplemented with ampicillin, for 14-16 h at 37 °C and 180 rpm in an orbital shaker.

Structural analysis of Hxk2p

A homology model of *S. cerevisiae* Hxk2p was generated based on the closed conformation of the *S. cerevisiae* Hxk1p scaffold with a glucose moiety in the active site (PDB ID 3B8A) [Kuser *et al.*, 2008]. The homology models were generated by SWISS-MODEL [Arnold *et al.*, 2006] by submitting the Hxk2p (GenBank: EIW10681.1) and the later obtained Hxk2p-Y amino acid sequences for automatic homology modelling. Structural analysis of the homology model was done manually using PyMOL. Further information regarding the structural analysis is described in the Results section.

Construction of an *E. coli* library of Hxk2p-variants

The native *HXK2* gene was amplified from genomic DNA of *S. cerevisiae* CEN.PK2-1C using primers HXK2_loc_f (5'-GCT TGC ATG CAC GCC ATA GAA GAG CAA TTT CCG TCC-3') and HXK2_loc_r (5'-CCG GGG ATC CGA GAG GGT TAA AAT TGG CGT GCA ATT TTA TGA AG-3'). This fragment also contained a 700 bp upstream promoter-sequence and a 300 bp downstream terminator-sequence. The locus was amplified using the high fidelity Phusion Hotstart II polymerase (Thermo Scientific, USA) and the following PCR program: 30 s initial denaturation at 98 °C, 30 cycles of 10 s denaturation at 98 °C, 30 s annealing at 65 °C and 1 min elongation at 72 °C, and a final 10 min elongation step at 72 °C. The resulting DNA fragment was digested with *Bam*HI and *Sph*I (FastDigest, Thermo Scientific, USA) at 37°C for 30 min and ligated into YIplac128, linearized with the same restriction enzymes. The ligation system was subsequently used to transform *E. coli* NEB5α. The cloned *HXK2* locus was verified by sequencing and the resulting plasmid was named YIpBB5 (Table 1).

The cloned *HXK2* locus was used as template for introducing specific mutations using six degenerate primer pairs (Table 2). The primers were designed such that the 3'-end of each region overlapped with the 5'-end of the following region, enabling the use of overlap-extension PCR (OE-PCR) [Horton *et al.*, 1989] to link all regions together in a combinatorial manner. In the final round of OE-PCR the missing sequences of the promoter, the non-mutated part of the *HXK2* gene and the terminator were linked to the 5'- and 3'-ends, generating a heterogeneous mix of the complete locus. The plasmid library was generated according to the MEGAWHOP protocol [Miyazaki, 2003] in which the heterogeneous DNA fragments were used as megaprimers and the YIpBB5 plasmid as template. The newly synthesised plasmids, each containing a different variant of the *HXK2* gene, were subsequently cloned in commercial heat shock competent *E. coli* NEB5α (High Efficiency, New England Biolabs, USA). Detailed information on the amplification of all fragments, the OE-PCR programs and the MEGAWHOP procedure can be found in Additional file 1 in the Supplementary material.

Construction of the yeast screening strain TMB3463

The genes *HXK2*, *HXK1* and *GLK1* were deleted sequentially from the background strain TMB3042 (Table 1). The regions used for homologous recombination were amplified from genomic DNA and flanked the intended ORF to ensure complete gene replacement. Three deletion cassettes were created by OE-PCR: *HXK2*(-500 – -1 bp)-*TRP1*-*HXK2*(+1461 – +1960 bp), *HXK1*(-1000 – -451 bp)-*URA3*-*HXK1*(+2040 – +2353 bp) and *GLK1*(-673 – -121 bp)-LoxP-*KanMX*-LoxP-*GLK1*(+1858 – +2359 bp). The selection markers were amplified from plasmids p424, p426 and pUG6 (Table 1) for *TRP1*, *URA3* and LoxP-*KanMX*-LoxP, respectively. Each marker was complete with promoter and terminator regions. Yeasts were transformed using 0.5-1 µg of DNA and selected on solid YNB medium with glucose (*hxk2-Δ* and *hxk1-Δ1*) or galactose (*glk1-Δ*), supplemented with uracil, leucine and geneticin when required. Correct

integration of the cassettes was verified by PCR using primer pairs that anneal inside the marker and on the chromosome, outside the homologous region, and the new strains were named TMB3460 (*hxk2-Δ*), TMB3461 (*hxk2-Δ hxk1-Δ1*) and TMB3462 (*hxk2-Δ hxk1-Δ1 glk1-Δ*) (Table 1). The deletions were also verified using primers specific for each gene. However, this analysis revealed that the *HXK1* gene was still present in the genome even though the deletion cassette was in the correct locus and the strain was expected to be haploid. To delete the second copy of *HXK1* a new deletion vector was constructed based on the pUG6AUR plasmid (Table 1). Additional restriction sites were introduced in the pUG6AUR plasmid by ligating a linker into the *Sal*I/*Nde*I-digested plasmid, generating plasmid pUG62AUR. The linker contained recognition sequences for *Kpn*I, *Sma*I, *Sph*I and *Avr*II. Homologous regions flanking the *HXK1* gene were amplified by PCR from genomic DNA, generating an upstream sequence of 273 bp (-294 – -21 bp) and a downstream sequence of 219 bp (+1780 – +1999 bp). The upstream and downstream fragments were digested with *Sph*I/*Avr*II and *Sph*I/*Kpn*I, respectively, and ligated into pUG62AUR generating the deletion vector pUG62AUR-HXK1USDS. The new deletion vector was linearized with *Sph*I and 1 µg of DNA was used to transform TMB3462. Transformants were selected on solid YNB medium with galactose, supplemented with leucine and aureobasidin. Correct integration of the vector was verified by PCR and enzyme activity measurements confirmed the absence of any glucose phosphorylating activity. The final screening strain was named TMB3463 (Table 1). Detailed information on the amplification of all fragments, the OE-PCR programs and cloning procedures can be found in the Additional file 1 in the Supplementary material.

Large-scale transformation of TMB3463

A single colony of TMB3463 was inoculated in 5 mL YPGal in a 50 mL conical tube and cultivated for 20 h at 30 °C in an orbital shaker at 180 rpm. This pre-culture was used to inoculate 50 mL YPGal in a 500 mL baffled shakeflask at $OD_{620\ nm}$ = 0.1. After 10.5 h of cultivation the cells were in mid-exponential phase and used to inoculate four shake flasks of 1 L containing 100 mL YPGal each at $OD_{620\ nm}$ = 0.02. After 14.5 h of growth the cultures reached an $OD_{620\ nm}$ of 1 and were harvested, washed and transformed according the Large-scale PEG/LiAc protocol [Gietz and Schiestl, 2007b]. The transformation was performed for 90 min at 42 °C in an orbital shaker at 65 rpm, using 300 µg of the plasmid library previously linearized with *Afl*II. After washing the cells, different volumes were spread on solid YNB medium with galactose and incubated at 30 °C. The remaining transformants were inoculated in 1.5 L of defined mineral media [Verduyn *et al.*, 1992] with 20 g/L galactose as carbon source. The propagation was performed in a 2.5 L Braun bioreactor operating at a stirring rate of 800 rpm and a sparging rate of 1 L air/min. The pH was automatically maintained at 5.5 by addition of 3 M KOH. Silicon antifoam (Dow Corning, USA) was added at a concentration of 0.5 mL/L. After four days colonies were counted on the plates and the total size of the yeast library was estimated to 1.4×10^6 ± 3% cfu:s, which

is 6 times larger than the size required for 100% coverage according to [Firth and Patrick, 2005].

Selection of a new Hxk2p-variant

Screening of the yeast Hxk2p-library for variants with increased resistance to autophosphorylation by xylose was performed in anaerobic glucose-limited continuous cultivation. After propagating the yeast library aerobically on galactose in a 2.5 L Braun bioreactor, the culture volume was reduced to 1 L, sparging was changed to N_2 gas at a flow rate of 0.2 L/min and the stirring rate was set to 200 rpm. The feed reservoir, containing 5 g/L glucose and 50 g/L xylose, was supplied at a rate of 1.19 mL/min giving a dilution rate of 0.072 1/h. After 96 h the dilution rate was increased to 0.40 1/h which initiated a washout of all cells. During the washout, samples for OD and HPLC analysis were collected every hour. After 12 h a final sample was collected and diluted to yield single colonies on solid YNB medium with glucose. The plates were incubated for two days at 30 °C and 10 random colonies were selected for genomic DNA extraction. The ten *HXK2* ORFs were amplified from genomic DNA by PCR using primers HXK2_seq_f (5'-GAA AAG ATT GTA GGA ATA TAA TTC TC-3') and HXK2_seq_r (5'-CAC ATA ATT AAA AAA AGG GCA CCT TC-3'). Each reaction mixture (50 µL) contained 1X Buffer, 1.5 mM $MgCl_2$, 0.2 mM of each dNTP, 0.5 mM of forward and reverse primer and 1U High Fidelity Phusion Hotstart II Polymerase (Thermo Scientific, USA). The amplification program was as follows: 30 s denaturation at 98 °C, 30 cycles of 10 s denaturation at 98 °C, 15 s annealing at 58.3 °C, 45 s extension at 72 °C and 1 cycle of 10 min final extension at 72 °C. The PCR-products were purified using GeneJet PCR Purification Kit (Thermo Scientific, USA) and sent for sequencing.

Construction of strains TMB3466, 3467, 3492 and 3493

The native *HXK2* gene was amplified by PCR from plasmid YIpBB5 using primers HXK2-F1-SpeI (5'- CTAGAACTAGTAAATGGTTCATTTAGGTCC AAAAAAACCACAAG-3') and HXK2-R1-SalI (5'- GAGGTCGACTTAAGCA CCGATGATACCAACGG-3'). The gene encoding the selected variant Hxk2p(F159Y) was amplified from genomic DNA of one of the selected clones using the same primers. The amplification program was as follows: 30 s denaturation at 98 °C, 30 cycles of 10 s denaturation at 98 °C, 30 s annealing at 65 °C (-0.5 °C decrease per cycle), 1 min extension at 72 °C and 1 cycle of 10 min final extension at 72 °C. The two amplified *HXK2* genes were digested with *Spe*I and *Sal*I and inserted between the *TDH3* promoter and *CYC1* terminator of the previously constructed vector YIpDR1, yielding the two plasmids YIpBB8 and YIpBB8Y (Table 1). The cloned genes were verified by DNA sequencing.

Strains having only one gene encoding for a hexokinase were constructed by transforming TMB3463 with YIpBB8 or YIpBB8Y, both linearized with *Cla*I. The new strains were named TMB3466 and TMB3467, respectively (Table 1). Xylose fermenting strains were constructed by transforming TMB3460 with

YIpDR7, linearized with *Eco*RV, generating strain TMB3490. This strain was further transformed with YIpBB8 or YIpBB8Y generating the strains TMB3492 and TMB3493, respectively (Table 1).

Carbon limited continuous cultivations

The sensitivity of the native Hxk2p and Hxk2p-Y toward xylose was evaluated in anaerobic glucose-limited continuous cultivations. Strains TMB3466 and TMB3467 (Table 1) were pre-grown in YNB medium with glucose until late exponential phase and inoculated into 3 L stirred-tank bioreactors (Applikon, Schiedam, The Netherlands) equipped with ADI 1025 Bio-Console and ADI 1010 Bio-Controller (Applikon, Schiedam, The Netherlands). Cultivations were performed with a working volume of 1 L of defined mineral medium [Verduyn *et al.*, 1992] at 30 °C. The medium was continuously stirred at 200 rpm and sparged with N_2-gas at a rate of 0.2 L/min. The pH was automatically maintained at 5.5 by addition of 3 M KOH. The condenser was connected to a Heto CBN 8-30 cooling bath (Jouan Nordic A/S, Allerød, Denmark) and cooled to 4 °C. The off-gas was analysed on-line for O_2, CO_2, and ethanol using an INNOVA 1313 Fermentation Monitor (LumaSense Technologies A/S, Denmark). Silicon antifoam (Dow Corning, USA) was added at a concentration of 0.2 mL/L. An initial steady-state was established at D = 0.21 1/h using a feed reservoir with 15 g/L glucose. The cells were then exposed to a gradual increase in xylose concentration by changing to a feed reservoir with 15 g/L glucose and 30 g/L xylose. Samples were collected after 5 and 7.5 volume changes with each feed composition, as well as at different time points during the accumulation of xylose. Cell samples (5 mL) were collected on ice and centrifuged for 5 min at 4000 rpm and 4 °C. Cell pellets for enzyme activity measurements were stored at -80 °C until needed. Fermentation experiments were performed in biological duplicates.

Anaerobic batch fermentations

Cells were pre-grown in YNB medium with glucose until late exponential phase and inoculated into the bioreactor at a concentration of 0.03 g CDW/L. Fermentation experiments were performed in 3 L stirred-tank bioreactors (Applikon, Schiedam, The Netherlands) as described above except that 1 L of 2X YNB with 20 g/L glucose and 50 g/L xylose was used as cultivation medium. Fermentation experiments were performed in biological duplicates.

Enzyme activity assays

Cell-free extracts were prepared by thawing frozen cell pellets on ice and washed once with water. After a centrifugation step of 5 min at 4000 rpm and 4 °C, the cells were treated with 250 µL Y-PER (Thermo Scientific, USA) per 100 mg of wet cell pellet according to the suppliers instructions. Protein concentrations were determined with the Coomassie Protein Assay Reagent (Thermo Scientific, USA) using BSA as standard (Thermo Scientific, USA). Glucose phosphorylating

activity was determined in a 1 mL reaction mixture containing: 20 mM HEPES (pH 7.6), 5 mM glucose, 5 mM $MgCl_2$, 1 mM $NADP^+$, 1 mM ATP and 1.16 U of glucose 6-phosphate dehydrogenase. The formation of NADPH was measured at 340 nm in a cuvette with light path length of 1 cm using a Ultrospec 2100 Pro spectrophotometer (Amersham Biosciences Corp., USA) controlled by computer software SWIFT Reaction Kinetics v. 2.05 (Biochrom Ltd., Cambridge, UK). The absorbance was converted to concentration units using the molar extinction coefficient of NADPH ($\varepsilon_{340\ nm}$ = 6220 L/mol/cm). The slope was determined within an interval of at least 1 min, using at least three different dilutions of the cell extract. Only the slopes within the range 0.05-0.2 A/min were considered acceptable. One unit is defined as the conversion of 1 μmole of glucose per minute.

Biomass determination and analysis of metabolites

Optical density was measured at 620 nm using an Ultrospec 2100 Pro spectrophotometer (Amersham Biosciences Corp., USA). Cell dry weight was measured in triplicate by filtering a known volume of the culture through a pre-weighed nitrocellulose filter with 0.45 μm pore size. The filters were washed with three volumes of water, dried in a microwave oven for eight minutes at 350 W and weighed after equilibrating to room temperature in a desiccator.

Concentrations of glucose, xylose, xylitol, glycerol, acetate and ethanol were analysed by HPLC (Waters, USA). Aminex HPX-87H ion exchange column (Bio-Rad, USA) was used at 45 °C with a mobile phase of 5 mM H_2SO_4 at a flow rate of 0.6 mL/min. All compounds were detected with a RID-10A refractive index detector (Shimadzu, Japan).

Calculation of metabolic rates

Maximum specific consumption rates of glucose and production rates of glycerol, acetate and ethanol were calculated from Equation 1.

$$r_j^{\max} = Y_{j/X} \cdot \mu_{\max} \quad (1)$$

The biomass yield coefficients ($Y_{j/X}$) were calculated as the slope in a linear regression of cumulative consumption or production of metabolite j vs. the biomass concentration. Yield coefficients were calculated from at least eight data points. Maximum specific growth rates on glucose were calculated as the slope in a linear regression of ln(CDW) vs. time from four data points. Due to the non-exponential growth on xylose Equation 1 cannot be used for calculating specific rates. The maximum specific consumption rates of xylose and production rates of xylitol, glycerol, acetate and ethanol during xylose consumption were instead calculated as the slope in linear regression of metabolite concentration divided by biomass concentration vs. time. These rates were calculated using at least four data points from the phase when xylose was the only carbon source. The significance of a difference between two mean values was calculated using a two-

tailed t-test assuming equal variance of the two samples. Comparison of mean values from steady state cultures had a degree of freedom of six (n = 4) whereas all other comparisons had two degrees of freedom (n = 2).

RESULTS

Amino acid residues potentially influencing the xylose-induced inactivation

The aim of the study was to identify a new variant of Hxk2p which: i) is immune to autophosphorylation by xylose, ii) maintains its regulatory capability and iii) has high catalytic activity in the presence of xylose. The Ser158 in the active site is known to be the target for autophosphorylation [Heidrich *et al.*, 1997] and modulation of this residue has been shown to disrupt the catalytic function as well as the regulatory capability [Kraakman *et al.*, 1999]. The active site was thus the natural target for finding other residues that could be substituted to fulfil the above mentioned criteria.

The generated homology model of *S. cerevisiae* Hxk2p was based on the closed conformation of the *S. cerevisiae* Hxk1p scaffold. This was possible due to the high sequence identity between *S. cerevisiae* Hxk2p and Hxk1p (77%). The obtained model contained a glucose moiety in the active site, which allowed the study of the amino acid residues directly involved in substrate binding. Several amino acids in different regions surrounding the active site were assessed for their mutability. This assessment was based on both the structural features of the amino acids and on their orientation towards the glucose moiety. The initial set of residues was within a 6 Å radius volume centred on the C-6 of the β-D-glucopyranose structure. The following residues were removed from the set: Ser162, Leu216, Val217, Phe232, Val236, Asn237, Gly238, Asn267, Tyr270, and Gln299. Most of these residues were within the volume but had a side-chain orientation pointing away from the active site. The final set of potentially mutable positions contained 13 amino acid residues. In each position one or three alternative amino acids were possible in addition to the native amino acid (Table 3). With this approach a condensed library was generated, which might be limited but has been shown to efficiently account for favourable epistatic effects on another enzyme [Sandström *et al.*, 2012]. Often only discreet changes are needed to induce a required adjustment of substrate preference. Thus, the alternative residue(s) were chosen to have chemical properties similar to the wild type residue, while chain length and size of the residue were varied (Table 3). Some substitutions, such as Gly271Cys, were assumed to promote residue-residue interactions and cause slight backbone conformation changes. The isoleucine in position 231 was assumed to be a key residue for distinguishing between the binding of D-glucopyranose and D-xylopyranose [Hoog and Widmalm, 2001] as it is pointing directly at the C-6 of glucose. Hence, four alternative residues (including the wild type residue) were possible in this position (Table 3). The theoretical combinatorial protein library was calculated to contain 16,384

variants. In practice, a total size of 57,000 cfu:s was obtained after transforming *E. coli* with the plasmid library. This corresponds to a 97% coverage of the 16,348 theoretical variants according to [Firth and Patrick, 2005] which represents a real library size of 15,867 variants.

Identification of a new Hxk2p variant with a single amino acid substitution

Strain TMB3463, which is unable to grow on glucose due to the absence of hexokinase activity, was constructed as a vehicle so that the screening of the library could be coupled to survival of the host on this carbon source. Hence, when transformed with the library only those enzyme variants which are catalytically functional could yield strains capable of growing on glucose. To select for a variant immune to inactivation by xylose the population had to be exposed to this sugar and it had to be taken up by the cells. Unfortunately, glucose and xylose are taken up by the same transporters [Hamacher *et al.*, 2002] and due to the much higher affinity for glucose the concentration of this sugar has to be as low as possible to maintain a high xylose-mediated selection pressure. For this reason glucose-limited continuous cultivation was chosen for the screening. Due to the role of Hxk2p in fermentative metabolism, anaerobic conditions were chosen for the screening to generate a selection pressure for a variant with maintained regulatory function.

After transforming strain TMB3463 with the plasmid library the transformants were propagated in aerobic batch cultivation with galactose as carbon source. Galactose was used in order to propagate all variants, including those which might have poor glucose phosphorylating capability. When all the galactose was consumed the conditions were changed to anaerobiosis and the chemostat was initiated by supplying the feed, containing 5 g/L glucose and 50 g/L xylose, at a rate of 1.16 mL/min giving a dilution rate of 0.072 1/h. At this rate it takes ca. 56 h to reach a concentration of 49 g/L of xylose inside the reactor and during this period all variants which are either unable to phosphorylate glucose or significantly inactivated by xylose are washed out from the culture. After 96 h of cultivation the dilution rate was increased to 0.40 1/h and being higher than the maximum growth rate under anaerobic conditions, it initiated a washout of all cells. Hence, the variants with the highest growth rate remain the longest in the culture and could be collected when the optical density was sufficiently low.

Immediately upon increasing the flow rate the population was able to grow at a rate of 0.17 1/h (Fig. 1). After 4 h the concentration of glucose had increased above 3 g/L which was enough to inhibit the transport of xylose into the cells and as a consequence the growth rate increased to 0.29 1/h (Fig. 1). It took 12 h to reduce the OD from 1.2 to 0.2 at which point the culture was diluted and plated on solid medium to yield single colonies. Ten random colonies were selected for sequencing of the *HXK2* gene. Four of these sequences gave inconclusive results due to the detection of more than one nucleotide in some positions and were thus discarded. The remaining six sequences were of good quality and the majority (4

out of 6) had mutations corresponding to a single amino acid substitution: Phe159Tyr. This variant was designated Hxk2p-Y. In Additional file 2 in the Supplementary material another selection experiment is described. That experiment underwent the same screening strategy, but the transformants were propagated differently after the transformation which resulted in the isolation of only the wild type *HXK2* gene (10 out of 10 sequences). The washout profile was therefore quite different from the profile shown in Figure 1 which shows the importance of having a properly designed screening strategy. The large differences in the washout profiles between the two experiments also shows the potential of the library, as the population from the successful screening was capable of having a higher metabolic activity in the presence of xylose (Supplementary material: Additional file 2).

The Phe159Tyr substitution confers higher resistance to xylose-induced inactivation

To evaluate the effect of the Phe159Tyr substitution on the catalytic activity two new yeast strains were constructed: TMB3466 (Hxk2p-wt) and TMB3467 (Hxk2p-Y). Both strains lack other genes coding for hexo- or glucokinase and the expression of the reintroduced gene was controlled by the constitutive *TDH3*-promoter to avoid glucose-control over the expression. Both strains were cultivated in anaerobic, glucose-limited chemostat at D = 0.22±0.01 1/h, first with only glucose in the feed. When steady state had been established the feed was changed to also contain 30 g/L xylose which led to an accumulation of xylose inside the reactor. At steady state on glucose the two strains exhibited nearly the same specific glucose phosphorylating activity (Fig. 2), indicating that the Phe159Tyr substitution has no detrimental effect on the catalytic function. At the second steady state, in the presence of almost 30 g/L xylose, the wild-type enzyme lost 59% of the activity whereas the Hxk2p-Y variant lost 40% (Fig. 2). During the accumulation of xylose there were no statistically significant differences between the two enzymes, although the activity profiles suggest that the wild type enzyme lost the activity more rapidly than the Hxk2p-Y variant. Still, the 64% higher activity of the variant in the presence of xylose at steady state is statistically significant (P = 0.007) which shows that this single mutation indeed confers higher resistance to xylose-induced inactivation without significantly decreasing the non-induced catalytic capability.

Physiological responses of yeast strains harbouring the Hxk2p-Y variant

In the continuous cultivations of strains TMB3466 (Hxk2p-wt) and TMB3467 (Hxk2p-Y) with only glucose there were significant differences in production rates of metabolites involved in balancing redox cofactors. The specific production rates of glycerol and acetate were 26% and 57% faster with TMB3467 compared with the control strain ($P(r_{glyc})$ = 0.008 and $P(r_{ac})$ = 0.12) (Table 4). Nearly the same increases were seen in the yields (23% (P = 0.04) and

55% (P = 0.15) increases of $Y_{glyc/s}$ and $Y_{ac/s}$, respectively) but the most significant difference was a 2.6% higher yield of biomass (P = 0.015) with TMB3467 (Table 4). Yet, in this condition there was no significant difference in the glucose uptake rate, however, in the presence of xylose TMB3466 reduced the glucose consumption rate by 15% ($P = 5 \cdot 10^{-5}$) while TMB3467 only reduced the consumption rate by 5% (P = 0.052). Hence, the Hxk2p-Y variant enabled a 15% higher specific glucose uptake rate in the presence of xylose compared with Hxk2p-wt ($P = 4 \cdot 10^{-4}$). Despite the reduced consumption rate of glucose, TMB3466 did not change its physiology significantly with regard to production rates or product yields when exposed to xylose (Table 4). TMB3467, on the other hand, reduced the yields of glycerol and biomass by 14% (P = 0.11) and 5.8% ($P = 6 \cdot 10^{-5}$), respectively, for the benefit of a 6.5% (P = 0.048) faster ethanol production rate (Table 4). Hence, TMB 3467 had a 8.9% (P = 0.10) faster ethanol production rate compared with the control strain in the presence of xylose (Table 4). Furthermore, the specific uptake rate of xylose by TMB3467 was 34% lower compared with TMB3466 (Table 4). This might be due to improved repression of genes encoding unspecific aldose reductases that can convert xylose to xylitol. Indeed, the only difference between the two strains with regard to product yields was a 34% (P = 0.044) lower xylitol yield by TMB3467 (Table 4), matching the difference in xylose uptake rate very well.

To investigate whether the increased resistance toward xylose-induced inactivation affected a batch fermentation process, two new strains were constructed: TMB3492 (Hxk2p-wt) and TMB3493 (Hxk2p-Y) (Table 1). These strains assimilate xylose via the oxido-reductive pathway, consisting of a xylose reductase (XR) and a xylitol dehydrogenase (XDH) from *Scheffersomyces stipitis* (formerly *Pichia stipitis* [Kurtzman and Suzuki, 2010]) and contain modifications known to improve xylose fermentation, such as increased pentose phosphate pathway and xylulokinase levels [Karhumaa *et al.*, 2005]. In addition, the XR is an engineered variant with improved NADH preference [Runquist *et al.*, 2010]. The fermentation of 20 g/L glucose and 50 g/L xylose was evaluated in anaerobic batch cultivations (Fig. 3). TMB3493 had between 10% and 57% higher maximum product yields and consumption yields per gram biomass during growth on glucose compared with the control strain (data not shown), but only those regarding glycerol and acetate were statistically significant. The maximum glycerol and acetate yields per gram biomass were 10% (P = 0.038) and 23% (P = 0.089) higher, respectively, compared with the control strain (data not shown). However, the yield of biomass per glucose consumed obtained with TMB3493 also decreased by 10% (P = 0.16) which explains the lack of significant differences between the two strains in yields per substrate and in specific production rates (Table 5). The most significant difference with regard to specific production rate during growth on glucose was that of acetate which was 17% higher (P = 0.12) with strain TMB3493. When xylose was the only carbon source, the specific consumption rate of substrate by TMB3493 was 64% faster (P = 0.095) than the control strain (Table 5). The increased uptake rate of xylose led to a 5.6% (P = 0.081) faster xylitol production rate. The results also suggest that strain TMB3493 can utilize the higher xylose uptake rate and increase the growth rate for a short period after glucose is depleted. During the period of fastest xylose

consumption strain TMB3493 had a maximum growth rate more than double that of the control strain (0.027 1/h and 0.013 1/h, respectively) (Table 5). Although this difference is statistically significant at $P = 0.037$, there are simply too few data points within the short time period in question to calculate reliable regression curves. Furthermore, due to the limited extension of this growth rate it has no impact on the overall productivity of the fermentation process or yield of products. Hence, there were no statistically significant differences between the two strains with regard to product yields per consumed xylose (Table 5) or per total amount of sugar consumed (data not shown).

DISCUSSION

Several studies have been made on Hxk2p active-site by site-directed mutagenesis, mostly focusing on Ser158 or Asp211, i.e. the key catalytic residues involved in phosphate transfer [Kraakman *et al.*, 1999]. In this study we describe the first condensed, rationally designed combinatorial library [Reetz and Wu, 2008; Sandström *et al.*, 2012] targeting the active-site in Hxk2p and the subsequent screening for mutations in the *HXK2* gene beneficial for resisting xylose-induced inactivation. This resulted in the identification of a protein variant, with the single amino acid substitution Phe159Tyr, which provides an increased glucose-phosphorylating activity in the presence of xylose.

The Phe159Tyr substitution does not impact negatively on the catalytic activity (Fig. 2),which is consistent with a widespread occurrence of tyrosine in position 159 among several hexokinases. For example, the Tyr159 is found in *S. cerevisiae* Hxk1p [Kuser *et al.*, 2008] and also in Hxk1p from the xylose-utilizing *Scheffersomyces stipitis* (NCBI RefSeq: XP_001386689). The occurrence of Tyr159 in the only hexokinase enzyme present in *S. stipitis* strongly indicates that it is beneficial for resisting xylose-induced inactivation. The residue Tyr159 is pointing towards the ATP-binding pocket (Fig. 4). The extension of the residue 159 with hydroxyl functionality generates a more polar environment at the edge of the glucose-binding pocket. It is conceivable that the tyrosyl residue can contribute as an electron rich draw on the phosphate group in the transition state, which could result in a lowered risk of autophosphorylation of the spatially close Ser158. Subsequent studies will however be needed to know whether the novel substitution impacts the i) enzyme kinetics, ii) potential for autophosphorylation, iii) tolerance to autophosphorylation, iv) xylose affinity and v) regulatory mechanism(s).

The screening method used to isolate the Hxk2p-Y variant was designed to be very fast and at the same time allow cells to grow at maximum growth rate under the given conditions. Having a fast screening method was expected to reduce the chance of obtaining unknown mutations through adaptation as populations cultivated continuously for less than 20 generations are unlikely to have undergone significant adaptive modifications [Sauer, 2001]. In the current experiment the population was exposed to xylose for less than 15 generations

which is well below the suggested limit. This low number of generations would give rise to less than 0.05 spontaneous mutations per genome [Drake, 1991] which makes adaptive mutations very unlikely. In this particular case, however, unknown mutations are of little concern since it is the *HXK2* gene which is of interest and not the final strain. Still, the short cultivation time in the adopted method reduced the risk of biofilm formation. Cells attached to surfaces will use the nutrients in the medium flowing past them, leaving less available for the cells in suspension. Hence, the attached cells and suspended cells are competing for the available nutrients leading to an inefficient selection for fast-growing strains [Gostomski *et al.*, 1994]. There is however a significant drawback with the currently adopted method: loss of selection pressure. The decrease in cell concentration during the washout reduces the capacity to consume glucose. Hence the residual glucose will inevitably accumulate over time, preventing xylose from entering the cells and act on the Hxk2p enzymes. In order to avoid this problem, further screening may be performed using e.g. a turbidostat [Bryson, 1952; Gostomski *et al.*, 1994], which could operate very closely to the maximum growth rate of the population while maintaining a low residual glucose concentration and high selection pressure from xylose.

The significant differences observed between strains TMB3466 and TMB3467 in xylose uptake rate and xylitol production at steady state in the presence of xylose (Table 4) suggest that Hxk2p has a role in the regulation of the endogenous xylose pathway in *S. cerevisiae*. There are five genes in *S. cerevisiae* encoding putative xylose reductases: *YDL124W*, *YJR096W*, *GCY1*, *GRE3* and *YPR1* [Träff *et al.*, 2002]. The protein encoded by *YDL124W* does, however, not show any activity with xylose and cannot support xylose utilization when overexpressed [Träff *et al.*, 2002; Wenger *et al.*, 2010]. Only the last two genes have been shown to support xylose utilization when expressed alone in the absence of the other genes encoding aldose reductases [Wenger *et al.*, 2010]. Since the *GRE3* gene is not present in the parental strain TMB3042 (Table 1), none of the strains constructed in this study carry this gene. Hence, the observed conversion of xylose to xylitol is most likely catalysed by the *GCY1* and *YPR1* gene products. The BioGRID database of genetic and physical interactions (http://thebiogrid.org) lists one study in which a negative genetic interaction between *HXK2* and *GCY1* has been identified [Costanzo *et al.*, 2010]. In this particular case the *hxk2-Δ gcy1-Δ* double mutant formed a smaller colony size than expected, but the implications of this phenotype cannot be fully evaluated since no information about the growth medium was provided. Nevertheless, Hxk2p is known to regulate the expression of genes required for utilization of alternative carbon sources such as sucrose and galactose through the physical interactions with Med8p (*SUC2*) [de la Cera *et al.*, 2002] and Rpt5p (*GAL1-10*) [Guerrero *et al.*, 2008]. If xylose is also considered an alternative carbon source by *S. cerevisiae* it is plausible that the genes required for its utilization are also regulated by Hxk2p. Further information is needed to confirm this hypothesis.

One application of the new Hxk2p-Y variant would be in the production of ethanol from lignocellulosic materials. The hydrolysates produced from some of those materials are often rich in xylose. Our hypothesis was that expressing the new variant, with increased activity and possibly improved repressive capability in

the presence of xylose, would increase the ethanol productivity by increasing the sugar consumption rate. This hypothesis is based on the experimental results from several studies, showing that Hxk2p acts as an activator of *HXT1* expression and as a repressor of *HXT2* and *HXT4-7* [Randez-Gil *et al.*, 1998b; Schuurmans *et al.*, 2008]. Hxt1p is a sugar transporter with low affinity and high transport capacity when glucose or xylose are present at high concentrations; Hxt4p-7p, on the other hand, are high affinity, low capacity transporters [Saloheimo *et al.*, 2007]. It has been shown that mainly the low capacity transporters are present when xylose is the sole carbon source, even at high concentrations [Wahlbom *et al.*, 2003; Jin *et al.*, 2004; Salusjärvi *et al.*, 2006; Runquist *et al.*, 2009b]. This makes the transport process inefficient since the available transporters easily become saturated with xylose. If Hxk2p can be expressed and fully functional in the presence of xylose, it might be enough to shift the expression of genes encoding transporters toward high capacity transporters, which would lead to an increased uptake rate at high concentrations. The results presented here from anaerobic batch fermentation of glucose and xylose did indeed show a faster xylose uptake rate by the strain with the Hxk2p-Y variant (Table 5) which is in good agreement with the hypothesis. The increased uptake rate did, however, not lead to an increased production of ethanol but rather seemed to enable a faster initial growth rate on xylose. Unfortunately the extent of this growth period was very short indicating that the improved transport capacity must be combined with other regulatory factors (metabolites and proteins) reminiscent from glucose metabolism. Apparently the xylose metabolism cannot sustain the optimal levels of these factors and therefore the effect disappears as they are converted or degraded. Hence, this positive effect had no influence on the final yields or productivity. It is also possible that the XR/XDH pathway is not optimized for a faster uptake rate which might lead to an accumulation of xylose intracellularly. As the uptake rate slows down the conversion of xylose to xylitol by the XR reduces the intracellular concentration of xylose to a low level and thus prevent inactivation of Hxk2p through a built-in detoxification process. Therefore the effect of the Hxk2p-Y variant is only observed during the early stage of xylose fermentation. The most appropriate application of the Hxk2p variant might therefore be in strains designed for fermentation of only the glucose fraction while the pentose fraction is used in a subsequent process using another organism. The results from the batch experiments suggest that the use of the Hxk2p-Y variant leads to increased product yields per biomass at the expense of growth rate and biomass yield per substrate during fermentation of glucose. Similar results were also observed in the glucose limited chemostat experiments but further replicate experiments are required to statistically confirm this behaviour. Nevertheless, the results presented here show that the Hxk2p-Y variant does not impact the fermentation of glucose negatively. The two strains expressing the Hxk2p-Y variant, TMB3467 and TMB3493, both had higher yields of glycerol and acetate than the corresponding control strain during fermentation of glucose. This might reflect a higher need to re-oxidise NADH to NAD and to reduce NADP to NADPH as glycerol formation involves the former process while acetate formation involves the latter. NADH is formed in the catabolic utilization of the sugar substrate as well as in biosynthetic reactions. Such reactions also require

NADPH to form the macromolecules which are used to form cell biomass. In the continuous cultivations TMB3467 did indeed have a higher yield of biomass from glucose, but TMB3493 produced less biomass per gram glucose in batch cultivation than the control strain. This raises questions whether Hxk2p is involved in the regulation of key redox reactions in anabolic pathways and to what extent the xylose-induced inactivation modulates this regulation to affect biomass formation. Further investigations of the transcriptional changes that occur in these strains as a response to xylose-induced inactivation of the Hxk2p proteins are required to answer these questions.

ACKNOWLEDGEMENTS

We wish to gratefully acknowledge the following students for their significant contributions to this work: Mirna Sallaku for performing the structural analysis, Tarinee Boonyawan for creating the triple-deletion strain and Celina Borgström for creating the quadruple-deletion strain. We also wish to thank Swedish National Energy Agency (Energimyndigheten, Project No. P35350-1) for financial support.

Table 1. Strains and plasmids used in this study

Name	Relevant genotype	Reference
Plasmids		
p424	*TRP1*	[Mumberg *et al.*, 1995]
p426	*URA3*	[Mumberg *et al.*, 1995]
pUG6	LoxP-*KanMX*-LoxP	[Güldener *et al.*, 1996]
pUG6AUR	LoxP-*AUR1*-LoxP	[Johansson, 2001]
pUG62AUR-HXK1USDS	*HXK1*(-294 – -21 bp), *HXK1*(+1780 – +1999 bp), LoxP-*AUR1*-LoxP	This study
YIplac128	*LEU2*	[Gietz and Sugino, 1988]
YIplac211	*URA3*	[Gietz and Sugino, 1988]
YIpDR1	YIplac128:TDH3p-*GXF1*-CYC1t	[Runquist *et al.*, 2009a]
YIpDR7	YIplac211:TDH3p-*XYL1*(N272D)-ADH1t; PGK1p-*XYL2*-PGK1t	[Runquist *et al.*, 2010]
YIpBB5	YIplac128:HXK2p-*HXK2*-HXK2t	This study
YIpBB8	YIplac128:TDH3p-*HXK2*-CYC1t	This study
YIpBB8Y	YIplac128:TDH3p-*HXK2*(F159Y)-CYC1t	This study
Yeast strains		
TMB3042	CEN.PK2-1C; *gre3*-Δ; *his3*::PGK1p-XKS1-PGK1t, *HIS3*; *tal1*::PGK1p-TAL1-PGK1t; *tkl1*::PGK1p-TKL1-PGK1t; *rki1*::PGK1p-RKI1-PGK1t; *rpe1*::PGK1p-RPE1-PGK1t; *trp1*, *ura3*, *leu2*	[Karhumaa *et al.*, 2005]
TMB3460	TMB3042; *hxk2-Δ*::*TRP1*; *ura3, leu2*	This study
TMB3461	TMB3460; *hxk1-Δ1*::*URA3*; *leu2*	This study
TMB3462	TMB3461; *glk1-Δ*::LoxP-*KanMX*-LoxP; *leu2*	This study
TMB3463	TMB3462; *hxk1-Δ2*::LoxP-*AUR1*-LoxP; *leu2*	This study
TMB3466	TMB3463; *leu2*::YIpBB8	This study
TMB3467	TMB3463; *leu2*::YIpBB8Y	This study
TMB3490	TMB3460; *ura3*::YIpDR7; *leu2*	This study
TMB3492	TMB3490; *leu2*::YIpBB8	This study
TMB3493	TMB3490; *leu2*::YIpBB8Y	This study

Table 2. Degenerate primers used to introduce mutations in the *HXK2* gene.

Name	Sequence (with wobble positions in bold letters)
Group_1_f	5'-CATTGGGTTTCACCTTTA**S**CT**W**CCCAGCTTCTCAAAAC-3'
Group_1_r	5'-GTTTTGAGAAGCTGGG**W**AG**S**TAAAGGTGAAACCCAATG-3'
Group_2_f	5'-GAAGGTATCTTGCAAA**R**ATGGACTA**R**AGGTTTTGATATTCC-3'
Group_2_r	5'-GGAATATCAAAACCT**Y**TAGTCCAT**Y**TTTGCAAGATACCTTC-3'
Group_3_f	5'-GTTGCTTTGATAAACGA**K**A**S**CACCGGTACTTTGGTTG-3'
Group_3_r	5'-CAACCAAAGTACCGGTG**S**T**M**TCGTTTATCAAAGCAAC-3'
Group_4_f	5'-GAAACTAAGATGGGTGTT**WW**CTTC**R**GCA**S**CG**S**AGTCAATGGTGCTTAC-3'
Group_4_r	5'-GTAAGCACCATTGACT**S**CG**S**TGC**Y**GAAG**WW**AACACCCATCTTAGTTTC-3'
Group_5_f	5'-CAATGGCCATCAACTGTGA**K**TAC**K**GCTCCTTCGATAATGAAC-3'
Group_5_r	5'-GTTCATTATCGAAGGAGC**M**GTA**M**TCACAGTTGATGGCCATTG-3'
Group_6_f	5'-CAGGCCAACAAACCTTTGA**K**AAAATGTCTTCTGGTTAC-3'
Group_6_r	5'-GTAACCAGAAGACATTTT**M**TCAAAGGTTTGTTGGCCTG-3'

Table 3. Amino acid residues chosen for mutagenesis, the alternative residues in each position and the codon degeneracy used.

#	Region	Selected residue	Alternative residue(s)	Codon degeneracy [a]
1	1	Ser158	Thr	ASC
2		Phe159	Tyr	TWC
3	2	Arg173	Lys	ARA
4		Lys176	Arg	ARA
5	3	Asp211	Glu	GAK
6		Thr212	Ser	ASC
7	4	Ile231	Asp/Phe/Tyr	WWC
8		Gly233	Ser	RGC
9		Thr234	Ser	ASC
10		Gly235	Ala	GSA
11	5	Glu269	Asp	GAK
12		Gly271	Cys	KGC
13	6	Glu302	Asp	GAK

[a] Codon degeneracy: S = C or G; W = A or T; R = A or G; K = G or T

Table 4. Specific consumption and production rates (g/g CDW/h) and yields (g/g sugar) in anaerobic glucose-limited chemostat cultures of TMB3466 (Hxk2p-wt) and TMB3467 (Hxk2p-Y). Values are given as mean ± standard deviation of four measurements from two biological experiments.

	Glucose steady state		Glucose + xylose steady state	
	TMB3466	**TMB3467**	**TMB3466**	**TMB3467**
Specific rates (mmol/g CDW/h)				
Glucose	-12.9±0.08	-13.2±0.5	-10.9±0.4	-12.5±0.3
Xylose	–	–	-2.75±0.59	-1.82±0.27
Glycerol	2.19±0.03	2.76±0.29	2.34±0.41	2.53±0.04
Acetate	0.15±0.02	0.23±0.09	0.21±0.08	0.20±0.02
Ethanol	20.6±2.43	21.7±1.0	21.3±1.9	23.2±0.6
Xylitol	–	–	0.32±0.09	0.22±0.05
CO_2 [a]	21.6±2.44 [b]	22.9±0.9	22.4±1.8	24.3±0.6
Yields (g/g sugar)				
Glycerol	0.087±0.001	0.107±0.015	0.092±0.022	0.092±0.004
Acetate	0.004±0.001	0.006±0.002	0.006±0.002	0.005±0.000
Ethanol	0.391±0.045	0.402±0.003	0.395±0.010	0.404±0.018
Xylitol	–	–	0.020±0.005	0.013±0.002
Biomass	0.092±0.001	0.094±0.001	0.090±0.007	0.089±0.001
CO_2	0.410±0.044	0.422±0.002	0.414±0.007	0.423±0.017
Carbon balance (%)	99.1±8.7 [b]	103.7±1.5	102.2±1.1	103.1±3.5
Redox balance (%)	98.6±8.6 [b]	103.4±1.6	101.9±1.3	102.8±3.5

[a] The production rate of CO_2 was calculated from the production rates of ethanol, acetate and biomass according to the following relationships: 1 mol/mol ethanol, 1 mol/mol acetate and 0.1 mol/C-mol biomass.

[b] The high standard deviation of these values is due to a single deviating measurement of ethanol in one experiment.

Table 5. Maximum specific consumption and production rates and yields in anaerobic batch fermentation of 20 g/L glucose and 50 g/L xylose by TMB3492 (Hxk2p-wt) and TMB3493 (Hxk2p-Y). Values are given as mean ± standard deviation of two independent experiments.

	Glucose phase		Xylose phase	
	TMB3492	**TMB3493**	**TMB3492**	**TMB3493**
μ_{max} (1/h)	0.35±0.02	0.34±0.01	0.013±0.000	0.027±0.004
Specific rates (mmol/g CDW/h)				
$r_{max,glc}$	-20.6±3.2	-21.8±0.4	–	–
$r_{max,xyl}$	–	–	-3.48±0.35	-5.72±0.99
$r_{max,xylt}$	–	–	0.909±0.017	0.960±0.014
$r_{max,glyc}$	6.31±0.49	6.61±0.42	0.085±0.041	0.052±0.037
$r_{max,ac}$	1.04±0.02	1.22±0.09	0.040±0.021	0.028±0.005
$r_{max,etoh}$	39.1±5.6	41.3±2.5	1.60±0.40	1.34±0.98
Yields (g/g sugar)				
$Y_{xylt/s}$	–	–	0.261±0.007	0.270±0.003
$Y_{glyc/s}$	0.129±0.005	0.127±0.007	0.028±0.001	0.027±0.000
$Y_{ac/s}$	0.015±0.002	0.015±0.000	0.009±0.003	0.008±0.002
$Y_{etoh/s}$	0.398±0.012	0.392±0.036	0.251±0.003	0.255±0.009
$Y_{X/s}$	0.078±0.005	0.070±0.002	0.056±0.013	0.055±0.008

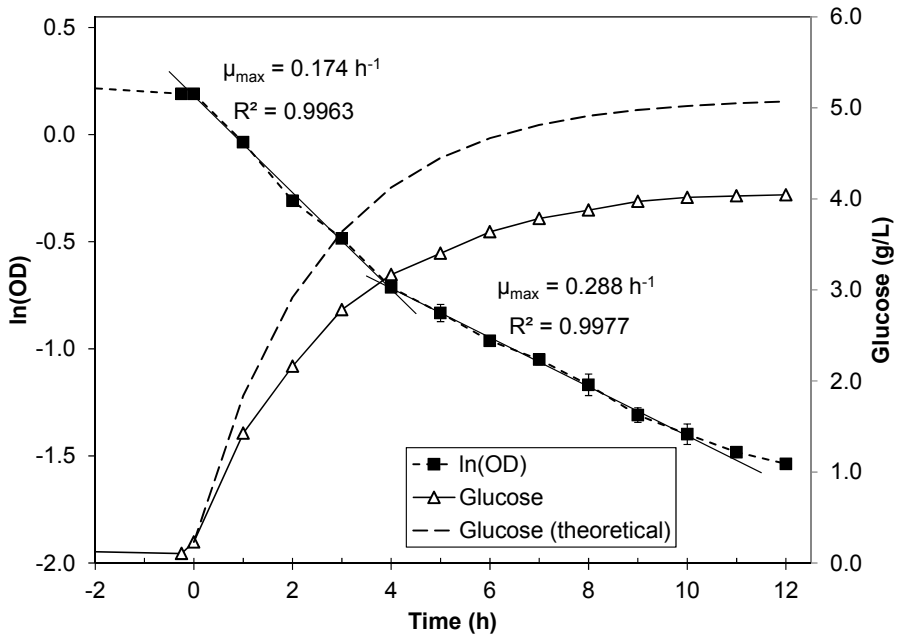

Figure 1. Selection of Hxk2p variants.
The selection of Hxk2p variants was performed in anaerobic glucose limited chemostat cultivation with feed containing 5 g/L glucose and 50 g/L xylose. After 96 h of continuous cultivation of TMB3463 transformed with the *HXK2*-library at D = 0.072 1/h, the dilution rate was increased to D = 0.40 1/h (indicated as t = 0 h). During the washout the specific growth rate was calculated from the equation d ln(OD)/dt = $\mu_{max} - D$. The natural logarithm of OD is shown as filled squares. The washout profile displays two growth phases and the switching point occurs when the residual glucose concentration exceeds 3 g/L (triangles). After 10 h the glucose concentration stabilized at 4 g/L which reduced the selection pressure by inhibiting the uptake of xylose and thus slowed down the washout of cells. The theoretical accumulation of glucose (dashed line) was calculated according to $S = S_{in} + (S_0 - S_{in}) \cdot e^{(-D \cdot t)}$.

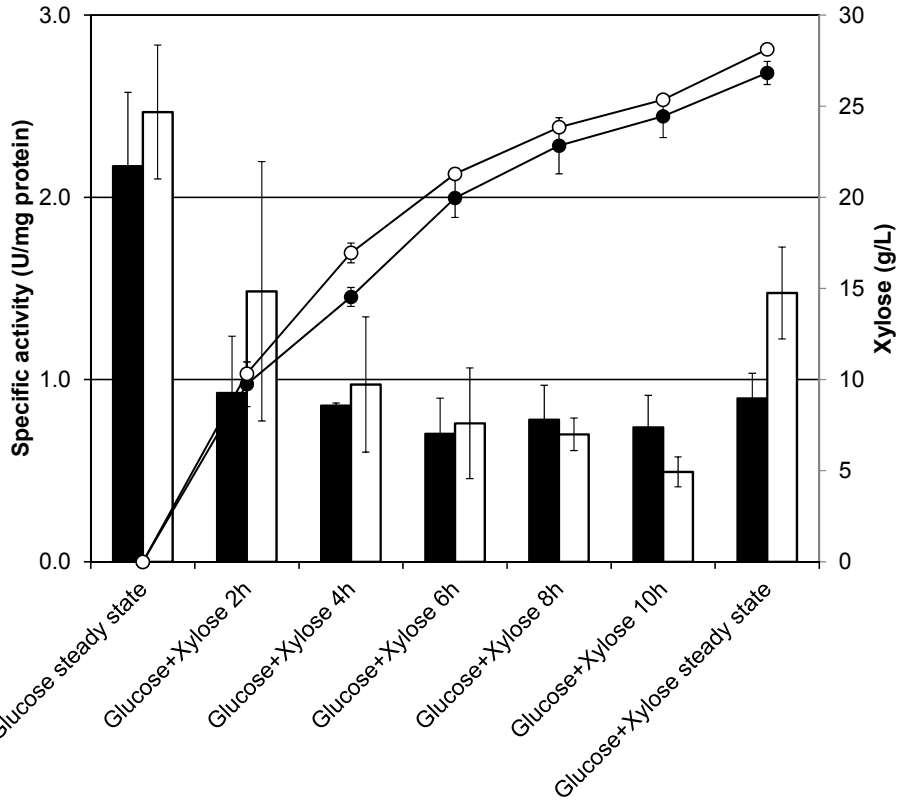

Figure 2. Specific glucose phosphorylating activity during xylose-induced inactivation of Hxk2p-wt and Hxk2p-Y

Specific glucose phosphorylating activity (bars) in strains TMB3466 (Hxk2p-wt) (filled bars/circles) and TMB3467 (Hxk2p-Y) (open bars/circles) in anaerobic glucose-limited chemostat cultivations. At steady state on glucose the two strains exhibited similar activity but during the accumulation of xylose (circles) the wild type enzyme seemed to become inhibited faster than the variant. At steady state in the presence of xylose the variant had 64% higher specific activity compared with the wild-type. Specific activities were determined from duplicate biological experiments. At steady state conditions two different samples were collected with at least 2.5 volume changes in between.

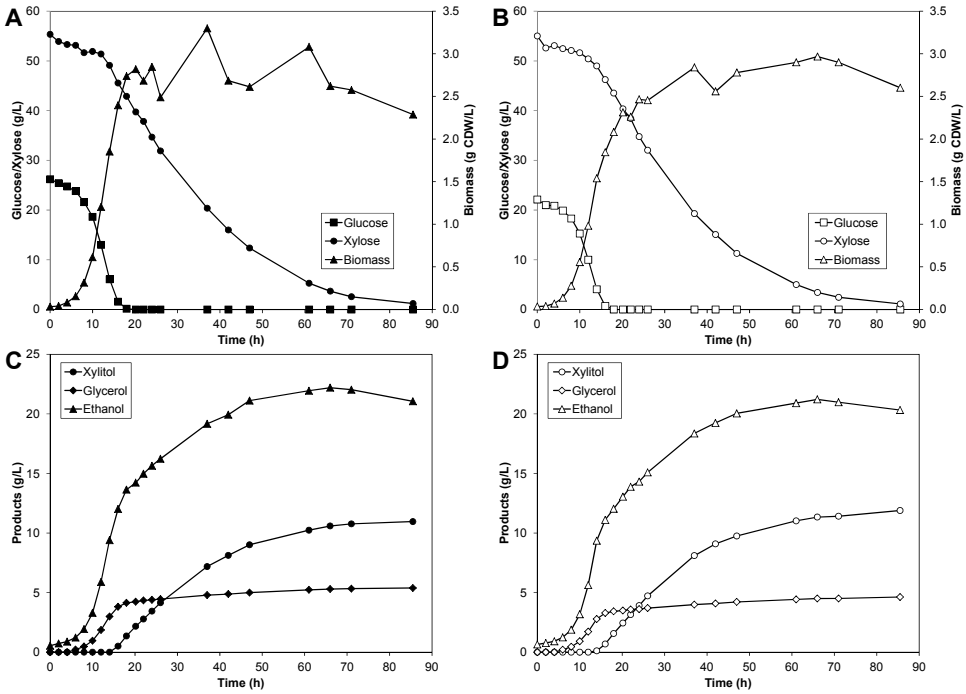

Figure 3. Anaerobic batch fermentation profiles of a glucose/xylose mixture.
Fermentation profiles of substrate consumption, biomass and product formation of TMB3492 (Hxk2p-wt) (**A** and **C**) and TMB3493 (Hxk2p-Y) (**B** and **D**) Fermentation was performed in 2X YNB medium containing 20 g/L glucose and 50 g/L xylose. Figures show representative values from one experiment out of two biological duplicates.

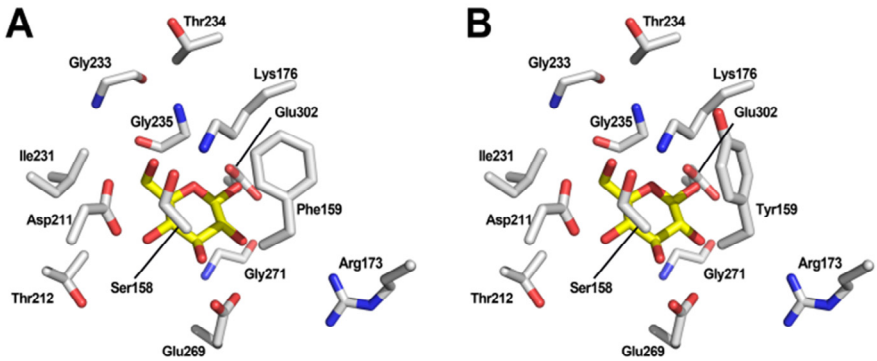

Figure 4. Homology models of the Hxk2p active site.
The key residues in the active site of Hxk2p that were selected for mutagenesis are displayed with corresponding label (see also Table 5). The positions of the Phe159 and Tyr159 residues are shown in A) and B), respectively. Both figures show the orientation of the β-D-glucopyranose structure (yellow colour) in the active site.

REFERENCES

1. **The PyMOL Molecular Graphics System, Version 1.5.0.4 Schrödinger, LLC.** [http://www.pymol.org]
2. Ahuatzi D, Herrero P, de la Cera T, Moreno F: **The glucose-regulated nuclear localization of hexokinase 2 in *Saccharomyces cerevisiae* is Mig1-dependent.** *J Biol Chem* 2004, **279**(14):14440-14446.
3. Ahuatzi D, Riera A, Pelaez R, Herrero P, Moreno F: **Hxk2 regulates the phosphorylation state of Mig1 and therefore its nucleocytoplasmic distribution.** *J Biol Chem* 2007, **282**(7):4485-4493.
4. Arnold K, Bordoli L, Kopp J, Schwede T: **The SWISS-MODEL workspace: a web-based environment for protein structure homology modelling.** *Bioinformatics* 2006, **22**(2):195-201.
5. Barnard EA: **Hexokinases from yeast.** *Methods Enzymol* 1975, **42**:6-20.
6. Bennett WS, Jr., Steitz TA: **Structure of a complex between yeast hexokinase A and glucose. I. Structure determination and refinement at 3.5 A resolution.** *J Mol Biol* 1980, **140**(2):183-209.
7. Bergdahl B, Heer D, Sauer U, Hahn-Hägerdal B, van Niel EW: **Dynamic metabolomics differentiates between carbon and energy starvation in recombinant *Saccharomyces cerevisiae* fermenting xylose.** *Biotechnol Biofuels* 2012, **5**(1):34.
8. Bisson LF, Kunathigan V: **On the trail of an elusive flux sensor.** *Res Microbiol* 2003, **154**(9):603-610.
9. Bryson V: **Microbial Selection Part 2. The turbidostatic selector - A device for automatic isolation of bacterial variants.** *Science* 1952, **116**(3003):48-51.
10. Carlson M: **Glucose repression in yeast.** *Curr Opin Microbiol* 1999, **2**(2):202-207.
11. Costanzo M, Baryshnikova A, Bellay J, Kim Y, Spear ED, Sevier CS, Ding H, Koh JLY, Toufighi K, Mostafavi S, et al: **The genetic landscape of a cell.** *Science* 2010, **327**(5964):425-431.
12. de la Cera T, Herrero P, Moreno-Herrero F, Chaves RS, Moreno F: **Mediator factor Med8p interacts with the hexokinase 2: Implication in the glucose signalling pathway of *Saccharomyces cerevisiae*.** *J Mol Biol* 2002, **319**(3):703-714.
13. DelaFuente G: **Specific inactivation of yeast hexokinase induced by xylose in the presence of a phosphoryl donor substrate.** *Eur J Biochem* 1970, **16**(2):240-243.
14. Drake JW: **A constant rate of spontaneous mutation in DNA-based microbes.** *Proc Natl Acad Sci U S A* 1991, **88**(16):7160-7164.
15. Fernandez-Garcia P, Pelaez R, Herrero P, Moreno F: **Phosphorylation of yeast hexokinase 2 regulates its nucleocytoplasmic shuttling.** *J Biol Chem* 2012, **287**(50):42151-42164.
16. Fernandez R, Herrero P, Fernandez MT, Moreno F: **Mechanism of inactivation of hexokinase PII of *Saccharomyces cerevisiae* by D-xylose.** *J Gen Microbiol* 1986, **132**:3467-3472.
17. Fernandez R, Herrero P, Gascon S, Moreno F: **Xylose-induced decrease in hexokinase PII activity confers resistance to carbon catabolite repression of**

invertase synthesis in *Saccharomyces carlsbergensis*. *Arch Microbiol* 1984, **139**(2-3):139-142.
18. Firth AE, Patrick WM: **Statistics of protein library construction.** *Bioinformatics* 2005, **21**(15):3314-3315.
19. Gancedo C, Flores CL: **Moonlighting proteins in yeasts.** *Microbiol Mol Biol Rev* 2008, **72**(1):197-210.
20. Gancedo JM: **Yeast carbon catabolite repression.** *Microbiol Mol Biol Rev* 1998, **62**(2):334-361.
21. Gancedo JM, Clifton D, Fraenkel DG: **Yeast hexokinase mutants.** *J Biol Chem* 1977, **252**(13):4443-4444.
22. Gietz RD, Schiestl RH: **High-efficiency yeast transformation using the LiAc/SS carrier DNA/PEG method.** *Nat Protoc* 2007a, **2**(1):31-34.
23. Gietz RD, Schiestl RH: **Large-scale high-efficiency yeast transformation using the LiAc/SS carrier DNA/PEG method.** *Nat Protoc* 2007b, **2**(1):38-41.
24. Gietz RD, Sugino A: **New yeast-*Escherichia coli* shuttle vectors constructed with in vitro mutagenized yeast genes lacking six-base pair restriction sites.** *Gene* 1988, **74**(2):527-534.
25. Gostomski P, Muhlemann M, Lin YH, Mormino R, Bungay H: **Auxostats for continuous-culture research.** *J Biotechnol* 1994, **37**(2):167-177.
26. Guerrero C, Milenković T, Pržulj N, Kaiser P, Huang L: **Characterization of the proteasome interaction network using a QTAX-based tag-team strategy and protein interaction network analysis.** *Proc Natl Acad Sci U S A* 2008, **105**(36):13333-13338.
27. Güldener U, Heck S, Fielder T, Beinhauer J, Hegemann JH: **A new efficient gene disruption cassette for repeated use in budding yeast.** *Nucleic Acids Res* 1996, **24**(13):2519-2524.
28. Hahn-Hägerdal B, Karhumaa K, Fonseca C, Spencer-Martins I, Gorwa-Grauslund MF: **Towards industrial pentose-fermenting yeast strains.** *Appl Microbiol Biotechnol* 2007, **74**(5):937-953.
29. Hamacher T, Becker J, Gardonyi M, Hahn-Hägerdal B, Boles E: **Characterization of the xylose-transporting properties of yeast hexose transporters and their influence on xylose utilization.** *Microbiology* 2002, **148**(Pt 9):2783-2788.
30. Heidrich K, Otto A, Behlke J, Rush J, Wenzel KW, Kriegel T: **Autophosphorylation-inactivation site of hexokinase 2 in *Saccharomyces cerevisiae*.** *Biochemistry* 1997, **36**(8):1960-1964.
31. Herrero P, Martinez-Campa C, Moreno F: **The hexokinase 2 protein participates in regulatory DNA-protein complexes necessary for glucose repression of the *SUC2* gene in *Saccharomyces cerevisiae*.** *FEBS Letters* 1998, **434**(1-2):71-76.
32. Hoog C, Widmalm G: **Free energy simulations of D-xylose in water and methyl D-xylopyranoside in methanol.** *J Phys Chem B* 2001, **105**(27):6375-6379.
33. Horton RM, Hunt HD, Ho SN, Pullen JK, Pease LR: **Engineering hybrid genes without the use of restriction enzymes: gene splicing by overlap extension.** *Gene* 1989, **77**(1):61-68.

34. Jin YS, Laplaza JM, Jeffries TW: ***Saccharomyces cerevisiae*** **engineered for xylose metabolism exhibits a respiratory response.** *Appl Environ Microbiol* 2004, **70**(11):6816-6825.
35. Johansson B: **Metabolic Engineering of the Pentose Phosphate Pathway of Xylose Fermenting *Saccharomyces cerevisiae*.** *Doctoral Thesis.* Lund University, Division of Applied Microbiology; 2001.
36. Karhumaa K, Hahn-Hägerdal B, Gorwa-Grauslund MF: **Investigation of limiting metabolic steps in the utilization of xylose by recombinant *Saccharomyces cerevisiae* using metabolic engineering.** *Yeast* 2005, **22**:359-368.
37. Klimacek M, Krahulec S, Sauer U, Nidetzky B: **Limitations in xylose-fermenting *Saccharomyces cerevisiae*, made evident through comprehensive metabolite profiling and thermodynamic analysis.** *Appl Environ Microbiol* 2010, **76**(22):7566-7574.
38. Kraakman LS, Winderickx J, Thevelein JM, De Winde JH: **Structure-function analysis of yeast hexokinase: structural requirements for triggering cAMP signalling and catabolite repression.** *Biochem J* 1999, **343 Pt 1**:159-168.
39. Kurtzman C, Suzuki M: **Phylogenetic analysis of ascomycete yeasts that form coenzyme Q-9 and the proposal of the new genera *Babjeviella*, *Meyerozyma*, *Millerozyma*, *Priceomyces*, and *Scheffersomyces*.** *Mycoscience* 2010, **51**(1):2-14.
40. Kuser P, Cupri F, Bleicher L, Polikarpov I: **Crystal structure of yeast hexokinase PI in complex with glucose: A classical "induced fit" example revised.** *Proteins* 2008, **72**(2):731-740.
41. Lobo Z, Maitra PK: **Physiological role of glucose-phosphorylating enzymes in *Saccharomyces cerevisiae*.** *Arch Biochem Biophys* 1977, **182**(2):639-645.
42. Maitra PK: **A glucokinase from *Saccharomyces cerevisiae*.** *J Biol Chem* 1970, **245**(9):2423-2431.
43. Menezes LC, Pudles J: **Specific phosphorylation of yeast hexokinase induced by xylose and ATPMg. Properties of the phosphorylated form of the enzyme.** *Arch Biochem Biophys* 1977, **178**(1):34-42.
44. Miyazaki K: **Creating random mutagenesis libraries by megaprimer PCR of whole plasmid (MEGAWHOP).** *Methods Mol Biol* 2003, **231**:23-28.
45. Mumberg D, Muller R, Funk M: **Yeast vectors for the controlled expression of heterologous proteins in different genetic backgrounds.** *Gene* 1995, **156**(1):119-122.
46. Pelaez R, Herrero P, Moreno F: **Functional domains of yeast hexokinase 2.** *Biochem J* 2010, **432**(1):181-190.
47. Randez-Gil F, Herrero P, Sanz P, Prieto JA, Moreno F: **Hexokinase PII has a double cytosolic-nuclear localisation in *Saccharomyces cerevisiae*.** *FEBS letters* 1998a, **425**(3):475-478.
48. Randez-Gil F, Sanz P, Entian KD, Prieto JA: **Carbon source-dependent phosphorylation of hexokinase PII and its role in the glucose-signaling response in yeast.** *Mol Cell Biol* 1998b, **18**(5):2940-2948.

49. Reetz MT, Wu S: **Greatly reduced amino acid alphabets in directed evolution: making the right choice for saturation mutagenesis at homologous enzyme positions.** *Chem Commun (Camb)* 2008(43):5499-5501.
50. Runquist D, Fonseca C, Rådstrom P, Spencer-Martins I, Hahn-Hägerdal B: **Expression of the Gxf1 transporter from *Candida intermedia* improves fermentation performance in recombinant xylose-utilizing *Saccharomyces cerevisiae*.** *Appl Microbiol Biotechnol* 2009a, **82**(1):123-130.
51. Runquist D, Hahn-Hägerdal B, Bettiga M: **Increased expression of the oxidative pentose phosphate pathway and gluconeogenesis in anaerobically growing xylose-utilizing *Saccharomyces cerevisiae*.** *Microb Cell Fact* 2009b, **8**.
52. Runquist D, Hahn-Hägerdal B, Bettiga M: **Increased ethanol productivity in xylose-utilizing *Saccharomyces cerevisiae* via a randomly mutagenized xylose reductase.** *Appl Environ Microbiol* 2010, **76**(23):7796-7802.
53. Saloheimo A, Rauta J, Stasyk OV, Sibirny AA, Penttila M, Ruohonen L: **Xylose transport studies with xylose-utilizing *Saccharomyces cerevisiae* strains expressing heterologous and homologous permeases.** *Appl Microbiol Biotechnol* 2007, **74**(5):1041-1052.
54. Salusjärvi L, Pitkanen JP, Aristidou A, Ruohonen L, Penttilä M: **Transcription analysis of recombinant *Saccharomyces cerevisiae* reveals novel responses to xylose.** *Appl Biochem Biotechnol* 2006, **128**(3):237-261.
55. Sambrook J, Fritsch EF, Maniatis T: **Molecular cloning: A laboratory manual**. Cold Spring Harbor: Cold Spring Harbor Laboratory Press; 1989.
56. Sandström AG, Wikmark Y, Engström K, Nyhlen J, Backvall JE: **Combinatorial reshaping of the *Candida antarctica* lipase A substrate pocket for enantioselectivity using an extremely condensed library.** *Proc Natl Acad Sci U S A* 2012, **109**(1):78-83.
57. Sassner P, Galbe M, Zacchi G: **Techno-economic evaluation of bioethanol production from three different lignocellulosic materials.** *Biomass Bioenergy* 2008, **32**(5):422-430.
58. Sauer U: **Evolutionary engineering of industrially important microbial phenotypes.** *Adv Biochem Eng Biotechnol* 2001, **73**:129-169.
59. Schuller HJ: **Transcriptional control of nonfermentative metabolism in the yeast *Saccharomyces cerevisiae*.** *Curr Genet* 2003, **43**(3):139-160.
60. Schuurmans JM, Boorsma A, Lascaris R, Hellingwerf KJ, de Mattos MJT: **Physiological and transcriptional characterization of *Saccharomyces cerevisiae* strains with modified expression of catabolic regulators.** *FEMS Yeast Res* 2008, **8**(1):26-34.
61. Smith FC, Davies SP, Wilson WA, Carling D, Hardie DG: **The SNF1 kinase complex from *Saccharomyces cerevisiae* phosphorylates the transcriptional repressor protein Mig1p in vitro at four sites within or near regulatory domain 1.** *FEBS Letters* 1999, **453**(1-2):219-223.
62. Treitel MA, Kuchin S, Carlson M: **Snf1 protein kinase regulates phosphorylation of the Mig1 repressor in *Saccharomyces cerevisiae*.** *Mol Cell Biol* 1998, **18**(11):6273-6280.

63. Träff KL, Jönsson LJ, Hahn-Hägerdal B: **Putative xylose and arabinose reductases in *Saccharomyces cerevisiae*.** *Yeast* 2002, **19**(14):1233-1241.
64. Wahlbom CF, Otero RRC, van Zyl WH, Hahn-Hägerdal B, Jönsson LJ: **Molecular analysis of a *Saccharomyces cerevisiae* mutant with improved ability to utilize xylose shows enhanced expression of proteins involved in transport, initial xylose metabolism, and the pentose phosphate pathway.** *Appl Environ Microbiol* 2003, **69**(2):740-746.
65. Van Vleet JH, Jeffries TW: **Yeast metabolic engineering for hemicellulosic ethanol production.** *Curr Opin Biotechnol* 2009, **20**(3):300-306.
66. Wenger JW, Schwartz K, Sherlock G: **Bulk segregant analysis by high-throughput sequencing reveals a novel xylose utilization gene from *Saccharomyces cerevisiae*.** *PloS Genetics* 2010, **6**(5).
67. Verduyn C, Postma E, Scheffers WA, Van Dijken JP: **Effect of benzoic acid on metabolic fluxes in yeasts: a continuous-culture study on the regulation of respiration and alcoholic fermentation.** *Yeast* 1992, **8**(7):501-517.

Bergdahl *et al.*:Engineering yeast hexokinase 2 for improved tolerance toward xylose-induced inactivation

ADDITIONAL FILE 1

Contents

Construction of the mutated *HXK2* megaprimer

The strategy used to construct the mutated *HXK2* megaprimer is outlined in Figure S1 and the primers used in addition to those listed in Table 2 in the main text are listed in Table S1.

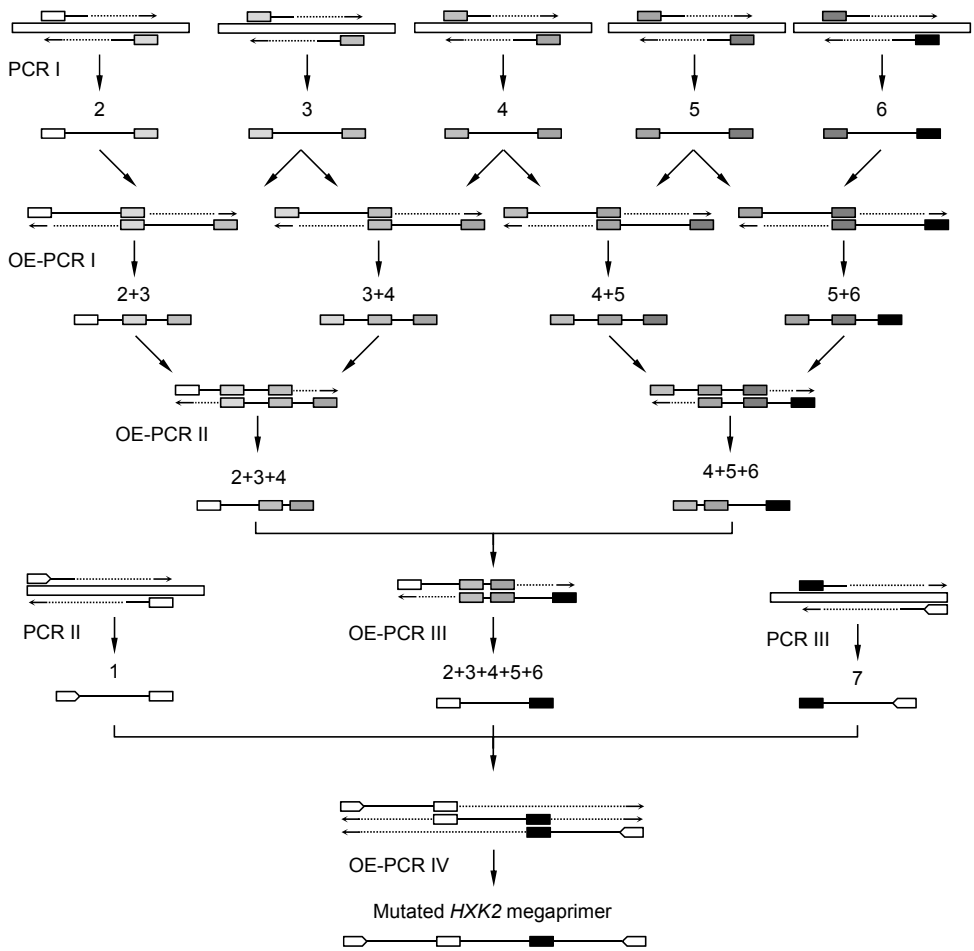

Figure S1. Construction of the mutated *HXK2* megaprimer

Table S1. Primers used in addition to those listed in Table 2 in the main text.

Name	Sequence
Yip128-F1	5'-GGCCTTTTGCTGGCCTTTTG-3'
Yip128-R1	5'-AAGGGGGATGTGCTGCAAGG-3'

Unless stated otherwise the PCR reactions contained 1X HF Buffer, 0.2 mM of each dNTP, 0.01 U/µL Phusion Hotstart DNA Polymerase II and 0.5 µM each of forward and reverse primers. The reaction volume was 50 µL. OE-PCR reactions contained 30 fmol of each fragment. DNA fragments amplified by PCR were purified using GeneJet PCR Purification Kit (Thermo Scientific, USA) unless stated otherwise.

PCR I: Mutated fragments were amplified from YIpBB5 using the following PCR program: 30 s denaturation at 98 °C, 30 cycles of 10 s denaturation at 98 °C, 5 s annealing and extension at 72 °C and 1 cycle of 10 min extension at 72 °C. Primers were used according to the following scheme:

Fragment 2: Group_1_f and Group_2_r
Fragment 3: Group_2_f and Group_3_r
Fragment 4: Group_3_f and Group_4_r
Fragment 5: Group_4_f and Group_5_r
Fragment 6: Group_5_f and Group_6_r

PCR II: The non-mutated fragments were amplified from YIpBB5 using the following PCR program: 30 s denaturation at 98 °C, 20 cycles of 10 s denaturation at 98 °C, 15 s annealing at 72 °C (-0.5 °C/cycle), 30 s extension at 72 °C, 16 cycles of 10 s denaturation at 98 °C, 15 s annealing at 62.4 °C, 30 s extension at 72 °C and 1 cycle of 10 min extension at 72 °C. Primers were used according to the following scheme:

Fragment 1: Yip128-F1 and Group_1_r
Fragment 7: Group_6_f and Yip128-R1

OE-PCR I: The two fragments were joined using 1X GC buffer in the reaction mix and the following PCR program: 30 s denaturation at 98 °C, 16 cycles of 10 s denaturation at 98°C, 30 s annealing at 70 °C (-0.5 °C/cycle) and 30 s extension at 72 °C. At this point the reaction was halted at 4 °C until primers had been added after which the program was repeated. The program was finished with a final 10 min extension at 72 °C. The primers were added to a final concentration of 0.52 µM according to the following scheme:

Fragment 2+3: Group_1_f and Group_3_r
Fragment 3+4: Group_2_f and Group_4_r
Fragment 4+5: Group_3_f and Group_5_r
Fragment 5+6: Group_4_f and Group_6_r

OE-PCR II: The two fragments were joined using the same procedure as in OE-PCR I. The primers were added to a final concentration of 0.52 µM according to the following scheme:

Fragment 2+3+4: Group_1_f and Group_4_r
Fragment 4+5+6: Group_3_f and Group_6_r

OE-PCR III: The two fragments were joined using the same procedure as in OE-PCR I. The primers Group_1_f Group_6_r and were added to a final concentration of 0.52 µM.

OE-PCR IV: The three fragments were joined using the following PCR program: 30 s denaturation at 98 °C, 16 cycles of 10 s denaturation at 98°C, 30 s annealing at 70 °C (-0.5 °C/cycle), 30 s extension at 72 °C and 1 cycle of 5 min extension at 72 °C. At this point the reaction was halted at 4 °C until primers had been added after which the program was repeated. The program was finished with a final 10 min extension at 72 °C. The primers Yip128-F1 and Yip128-R1 were added to a final concentration of 0.52 µM.

The final megaprimer was purified from 0.8% agarose gel using the QIAquick Gel Extraction Kit (Qiagen, Germany).

Generating the plasmid library using the MEGAWHOP procedure

The MEGAWHOP reaction mixture (50 µL) contained the following: 1X HF Buffer, 0.2 mM of each dNTP, 503 ng of HXK2 megaprimer, 50.1 ng of template plasmid YIpBB5 and 0.02 U/µL Phusion Hotstart DNA Polymerase II. The whole plasmid amplification was performed using the following PCR program: 30 s denaturation at 98 °C, 25 cycles of 10 s denaturation at 98 °C, 15 s annealing at 58 °C and 3 min extension at 72°C.

After completing the PCR reaction, 0.8 µL *Dpn*I (20 U/µL) was added to 40 µL of the MEGAWHOP reaction mixture and incubated for 2 h at 37°C. AT the same time a negative control (40 µL) containing 1X HF Buffer and 1 ng/µL YIpBB5 was treated equally. 2 µL and 5 µL of *Dpn*I-treated MEGAWHOP reaction was used to transform commercial heat shock competent *E. coli* NEB5α (High Efficiency, New England Biolabs, USA) according to the suppliers instructions. Transformants were selected on solid LB-medium supplemented with 100 mg/L ampicillin. Both transformations generated ca. 7700 cfu/mL. 5 µL of the negative control did not result in any transformants. Five additional transformation reactions of NEB5α were performed generating a total *E. coli* library of 57,370 ± 3261 cfu. These transformants were inoculated in 100 mL of LB-medium supplemented with 100 mg/mL of ampicillin and grown for 16 h at 37 °C. The resulting culture was aliquoted in 25% glycerol and stored at -80 °C.

Part of the culture was used to purify and sequence the plasmids. This confirmed that all mutations were present in the plasmid mix (Fig. S2).

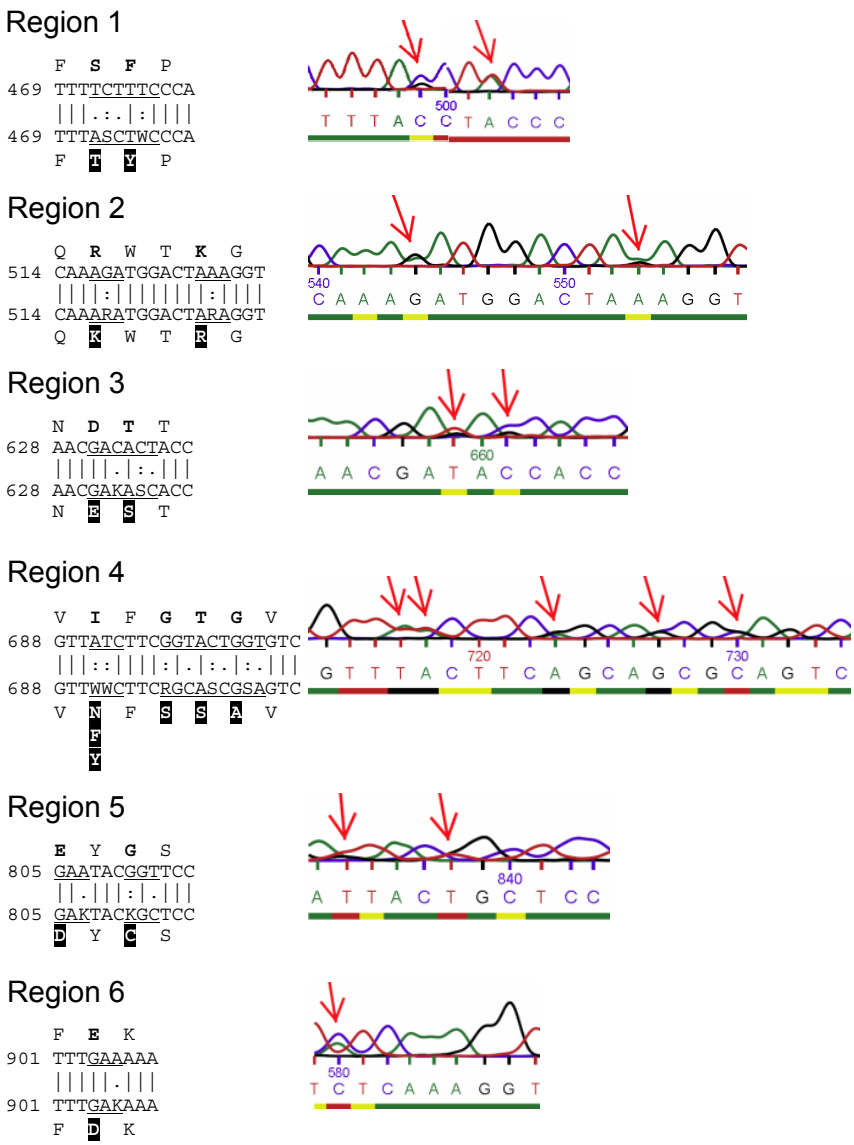

Figure S2. Sequencing of the *HXK2*-library
The nucleotide sequences of the mutated regions are shown to the left. The top sequence is the native sequence and the bottom sequence contains the introduced degeneracy. Codons that were modified are underlined and the native and alternative amino acid residues are indicated with bold and white-on-black letters. The left panel shows the corresponding region from the electropherogram. Arrows indicate the point of the degeneracy and the dual signals show that the mutations are indeed introduced in the megaprimer.

Construction of strains TMB3460, TMB3461 and TMB3462

Unless stated otherwise the PCR reactions contained 1X HF Buffer, 0.2 mM of each dNTP, 0.01 U/µL Phusion Hotstart DNA Polymerase II and 0.5 µM each of forward and reverse primers (Table S2). The reaction volume was 50 µL. OE-PCR reactions contained 200 fmol of each fragment. DNA fragments amplified by PCR were purified from 0.8% agarose gel using the QIAquick Gel Extraction Kit (Qiagen, Germany) unless stated otherwise.

Verification of correct integration and gene deletion was performed using the primers listed in Table S3 and the following reaction mix: 1X DreamTaq Buffer, 0.2 mM of each dNTP, 0.3 µM each of forward and reverse primers and 1 U/µL DreamTaq DNA Polymerase.

Table S2. Primers used to construct deletion cassettes.

Name	Sequence
HXK2_US_f	5'-GGTACCTAGAAATGGCTATCATGC-3'
HXK2_US_r	5'-TATATATAGTAATGTCGTTTATTTAATTAGCGTACTTATTATGTGTGG-3'
HXK2_DS_f	5'-GATAGGGTTGAGTGTTGTTACTTAATTTGTAAATTAAGTTTGAACAACAAG-3'
HXK2_DS_r	5'-AGAAGAATCCACGCGTAAAAATCG-3'
TRP1_f	5'-TAAGTACGCTAATTAAATAAACGACATTACTATATATATAATATAGGAAG-3'
TRP1_r	5'-CTTAATTTACAAATTAAGTAACAACACTCAACCCTATCTAGGTC-3'
HXK1_US_f	5'-TGGCGTGGGGTGGGGTGATT-3'
HXK1_US_r	5'-GTTAAGCCAGCCCCGACACCGGGCACGTGCGGGAGTTT-3'
HXK1_DS_f	5'-GTCTATCAGGGCGATGGCCCGCGACCCAGATTGCAGAAGATCCC-3'
HXK1_DS_r	5'-AGGTGCCCTTGCTAGCAT-3'
URA3_f	5'-AAACTCCCGCACGTGTGCCCGGTGTCGGGGCTGGCTTAAC-3'
URA3_r	5'-GGGATCTTCTGCAATCTGGGTCGCGGGCCATCGCCCTGATAGAC-3'
GLK1_US_f	5'-AGAGGAGGCGAGCAGCAGGG-3'
GLK1_US_r	5'-GTCGACCTGCAGCGTACGAAAGTGCCCACCGTTTGAGCGT-3'
GLK1_DS_f	5'-ATCAGATCCACTAGTGGCCTATGCGACAGCCTCGCCCTCTTCCGT-3'
GLK1_DS_r	5'-CGGGCAGTGCAGTGTGAGGG-3'
loxPKanMX_f	5'-ACGCTCAAACGGTGGGCACTTTCGTACGCTGCAGGTCGAC-3'
loxPKanMX_R	5'-ACGGAAGAGGGCGAGGCTGTCGCATAGGCCACTACCTCTTCCGT-3'

Table S3. Primers used to confirm correct integration and gene deletion.

Name	Sequence	Application
HXK2_823US_f	5'-ACCACACGCATGCCTTCATTCC-3'	Chromosomal integration
TRP1_71_r	5'-GCGGCCTCTGTGCTCTGCAA-3'	
HXK2_773_f	5'-TTCCACCATCTGCTCCAATGGC-3'	Gene deletion
HXK2_1248_r	5'-TGCAGCAATGTGACCGGTCTTG-3'	
HXK1_1510US_f	5'-AGCGGTTCGCTTCCAGCACC-3'	Chromosomal integration
URA3_120_r	5'-GGTGGTACGAACATCCAATGAAGCA-3'	
HXK1_547_f	5'-GTCGAAGGCCACGATGTCGTCC-3'	Gene deletion
HXK1_1282_r	5'-CCCTTAGCGGCGGCTTCCTT-3'	
GLK1_1050US_f	5'-ACGGCGACAGCCGGTTGGCTT-3'	Chromosomal integration
kanMX_32_r	5'-CGCGGCCTCGAAACGTGAGT-3'	
GLK1_433_f	5'-CCGGACGAGTTGGCCAAGGG-3'	Gene deletion
GLK1_1434_r	5'-CCTCTCACCCTCGGCACCCA-3'	

Construction of TMB3460 (*hxk2-Δ*)

The upstream and downstream fragments flanking the *HXK2* gene were amplified from genomic DNA from *S. cerevisiae* CEN.PK2-1C using the following PCR program: 30 s denaturation at 98 °C, 30 cycles of 10 s denaturation at 98 °C, 30 s annealing at 65 °C (-0.5 °C/cycle), 15 s extension at 72 °C and 1 cycle of 10 min extension at 72 °C.

The auxotrophic marker cassette *TRP1* was amplified from plasmid p424 using the following PCR program: 30 s denaturation at 98 °C, 30 cycles of 10 s denaturation at 98 °C, 30 s annealing at 65 °C (-0.5 °C/cycle), 1 min extension at 72 °C and 1 cycle of 10 min extension at 72 °C.

The deletion cassette HXK2_US-TRP1-HXK2_DS was created by OE-PCR using the following PCR program: 30 s denaturation at 98 °C, 16 cycles of 10 s denaturation at 98 °C, 30 s annealing at 68 °C (-0.5 °C/cycle) and 1 min extension at 72 °C. At this point the reaction~~s~~ was halted at 4 °C until primers HXK2_US_f and HXK2_DS_r had been added after which the program continued: 30 s denaturation at 98 °C, 20 cycles of 10 s denaturation at 98°C, 30 s annealing at 63 °C (-0.4 °C/cycle) and 1 min extension at 72 °C. The program was finished with a final 10 min extension at 72 °C.

The amplified deletion cassette was purified and used to transform TMB3042. Transformants were selected on solid YNB medium with 2% glucose, 50 mg/L uracil and 220 mg/L leucine. Correct integration was verified by PCR amplification from chromosomal DNA of randomly selected colonies using

primers HXK2_823US_f and TRP1_71_r. One positive clone was named TMB3460.

Construction of TMB3461 (*hxk2-Δ hxk1-Δ1*)

The upstream and downstream fragments flanking the *HXK1* gene were amplified from genomic DNA from *S. cerevisiae* CEN.PK2-1C. The auxotrophic marker cassette *URA3* was amplified from plasmid p426. All fragments were amplified using the following PCR program: 30 s denaturation at 98 °C, 30 cycles of 10 s denaturation at 98 °C, 30 s annealing at 65 °C (-0.5 °C/cycle), 1 min s extension at 72 °C and 1 cycle of 10 min extension at 72 °C.

The deletion cassette HXK1_US-URA3-HXK1_DS was created by OE-PCR using the following PCR program: 30 s denaturation at 98 °C, 16 cycles of 10 s denaturation at 98 °C, 30 s annealing at 68 °C (-0.5 °C/cycle) and 1 min extension at 72 °C. At this point the reaction was halted at 4 °C until primers HXK1_US_f and HXK1_DS_r had been added after which the program continued: 30 s denaturation at 98 °C, 20 cycles of 10 s denaturation at 98°C, 30 s annealing at 67 °C (-0.4 °C/cycle) and 1 min extension at 72 °C. The program was finished with a final 10 min extension at 72 °C.

The amplified deletion cassette was purified and used to transform TMB3460. Transformants were selected on solid YNB medium with 2% galactose and 220 mg/L leucine. Correct integration was verified by PCR amplification from chromosomal DNA of randomly selected colonies using primers HXK1_1510US_f and URA3_120_r. One positive clone was named TMB3461.

Construction of TMB3462 (*hxk2-Δ hxk1-Δ1 glk1-Δ*)

The upstream and downstream fragments flanking the *GLK1* gene were amplified from genomic DNA from *S. cerevisiae* CEN.PK2-1C. The antibiotic marker cassette LoxP-KanMX-LoxP was amplified from plasmid pUG6. All fragments were amplified using the following PCR program: 30 s denaturation at 98 °C, 30 cycles of 10 s denaturation at 98 °C, 30 s annealing at 67 °C (-0.5 °C/cycle), 1 min extension at 72 °C and 1 cycle of 10 min extension at 72 °C.

The deletion cassette GLK1_US-[LoxP-KanMX-LoxP]-GLK1_DS was created by OE-PCR using the following PCR program: 30 s denaturation at 98 °C, 16 cycles of 10 s denaturation at 98°C, 30 s annealing at 68 °C (-0.5 °C/cycle) and 1 min extension at 72 °C. At this point the reaction was halted at 4 °C until primers GLK1_US_f and GLK11_DS_r had been added after which the program continued: 30 s denaturation at 98 °C, 20 cycles of 10 s denaturation at 98°C, 30 s annealing at 68.5 °C (-0.4 °C/cycle) and 1 min extension at 72 °C. The program was finished with a final 10 min extension at 72 °C.

The amplified deletion cassette was purified and used to transform TMB3461. Transformants were selected on solid YNB medium with 2% galactose, 220 mg/L leucine and 200 mg/L geneticin. Correct integration was verified by PCR amplification from chromosomal DNA of randomly selected colonies using primers GLK1_1050US_f and kanMX_32_r. One positive clone was named TMB3462.

Investigation of the glucose phosphorylating activity in strain TMB3462 revealed a significant level of activity despite confirmation of all deletion cassettes. Amplification of each gene using specific primers (Table S3) revealed that *HXK1* was still present in the genome (Fig. S3).

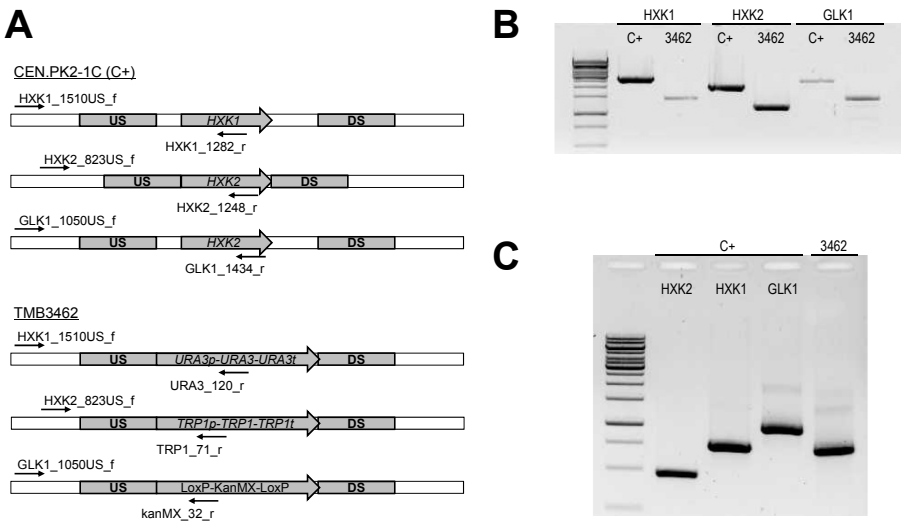

Figure S3. Verification results of integration and gene deletion.
A) Primers used with template from CEN.PK2-1C (positive control) and TMB3462. **B**) Amplification results of the set-up shown in (A). **C**) Amplification of each gene using specific primers listed in Table S3. The reaction with template from TMB3462 contained primers for all genes.

Construction of the screening strain TMB3463

Generation of plasmid pUG62AUR

To facilitate the use of pUG6AUR, a new multiple cloning site was created near the LoxP site upstream of the aureobasidin A resistance gene using linkers. These linkers consisted of two long oligonucleotides, 37 and 35 bases, respectively, and were complimentary except for the sticky ends. These were instead complementary to the restriction sites *Sal*I and *Nde*I present in the pUG6AUR plasmid. All in all, the linkers included six different restriction sites; *Sal*I, *Kpn*I, *Sma*I, *Sph*I, *Avr*II and *Nde*I (Fig. S4).

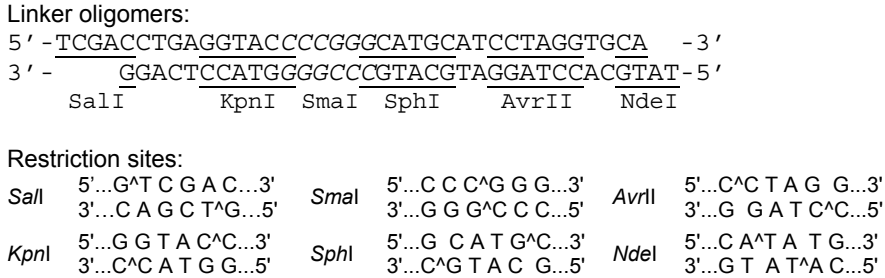

Figure S4. Illustration of the 39 bases long linker used to create a multiple cloning site into the pUG6AUR plasmid.

The linker oligomers were annealed to each other by mixing 500 pmol of each oligonucleotide with 6 µmol NaCl in 1X DreamTaq Buffer (final volume 30 µL) and incubation at 100 °C in a Thermocycler for 5 minutes. The temperature was then lowered slowly at 1 °C/min until a temperature of 4 °C was reached. The salt was removed through alcohol precipitation. 1 mL 99.5 % ethanol was added to the 30 µL mix and incubated at -80 °C for 10 min. The tube was centrifuged for 12 min at 4 °C and the supernatant was discarded. The pellet was washed once with 500 µL of 70% ethanol after which the pellet was dried in room temperature for 10 min. The small pellet was finally dissolved in 25 µL TE buffer giving an estimated concentration of 20 µM (ca. 475 ng/µL).

The annealed linkers were ligated to pUG6AUR, previously digested with *Sal*I and *Nde*I, in a 20 µL reaction containing the following: 1X Fast Digest Green Buffer, 50 ng/µL linker, 12.5 ng/µL linear pUG6AUR, 5% (w/v) PEG 4000, 0.5 mM ATP and 0.125 U/µL T4 DNA Ligase. The ligation mixture was incubated at room temperature for 60 min after which the ligase was inactivated at 70 °C for 5 min. 2 µL of the ligation mix was removed and diluted to a final concentration of 2.5 ng plasmid/µL. 5 µL of the diluted ligation mix was used to transform heat

shock competent *E. coli* NEB5α. Transformants were selected on LB-medium with 100 mg/L ampicillin. Successful ligation was determined by digesting the purified plasmids with *Kpn*I/*Sph*I or *Kpn*I/*Avr*II which are specific for the presence of the linker. The resulting plasmid was named pUG62AUR (Fig. S5).

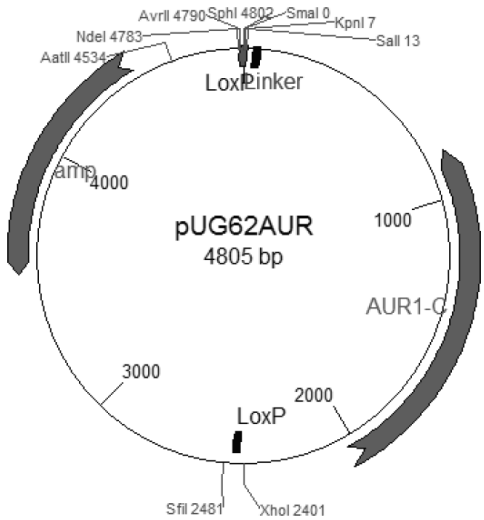

Figure S5. The pUG62AUR plasmid with a multiple cloning site consisting of the *Avr*II, *Sph*I, *Sma*I and *Kpn*I restriction sites.

Construction of TMB3463 (*hxk2-Δ hxk1-Δ1 glk1-Δ hxk1-Δ2*)

Unless stated otherwise the PCR reactions contained 1X GC Buffer, 0.2 mM of each dNTP, 0.01 U/µL Phusion Hotstart DNA Polymerase II and 0.5 µM each of forward and reverse primers (Table S4). The reaction volume was 50 µL. DNA fragments amplified by PCR were purified from 0.8% agarose gel using the QIAquick Gel Extraction Kit (Qiagen, Germany) unless stated otherwise.

Verification of correct integration and gene deletion was performed using the primers listed in Table S5 and the following reaction mix: 1X DreamTaq Buffer, 0.2 mM of each dNTP, 0.3 µM each of forward and reverse primers and 1 U/µL DreamTaq DNA Polymerase.

Table S4. Primers used to amplify additional fragments upstream and downstream the *HXK1* gene. Restriction sites are indicated in bold.

Name	Sequence	Restriction site
HXK1_US2_f	5'-TAG**GCATGC**GCATTGGTACCTTAGGACCGTTGAG-3'	SphI
HXK1_US2_r	5'-CG**CCTAGG**GATTGAGTTGTTTGGGTGAGTTTG-3'	AvrII
HXK1_DS2_f	5'-ACT**GGTACC**TTGGTCTTCTTCATGCATCATTTCA-3'	KpnI
HXK1_DS2_r	5'-TTG**GCATGC**ATCAGCTATAAGAGACGAAATTGCT-3'	SphI

Table S5. Primers used to confirm correct integration and gene deletion.

Name	Sequence	Application
HXK1_1510US_f	5'-AGCGGTTCGCTTCCAGCACC-3'	Chromosomal integration
AmpR-R130	5'-AATGATACCGCGAGACCCAC-3'	
HXK1_547_f	5'-GTCGAAGGCCACGATGTCGTCC-3'	Gene deletion
HXK1_1282_r	5'-CCCTTAGCGGCGGCTTCCTT-3'	

The additional upstream and downstream fragments flanking the *HXK1* gene were amplified from genomic DNA from *S. cerevisiae* CEN.PK2-1C using the following PCR program: 30 s denaturation at 98 °C, 5 cycles of 10 s denaturation at 98 °C, 15 s annealing at 60.9 °C, 8 s extension at 72 °C, 25 cycles of 10 s denaturation at 98 °C, 20 s annealing and extension at 72 °C and 1 cycle of 10 min extension at 72 °C.

The purified upstream and downstream fragments were digested with *Sph*I/*Avr*II and *Kpn*I/*Sph*I, respectively. The digested fragments were ligated to pUG62AUR, previously digested with *Kpn*I/*Avr*II, using a 3:1 molar ratio of insert to vector and an incubation time of 2 h at room temperature. 5 µL of the ligation mix was used for transformation of heat shock competent *E. coli* NEB5α. Transformants were selected on LB-medium with 100 mg/L ampicillin. Successful ligation was determined by colony PCR using primers HXK1_DS2_f and HXK1_US2_r and the resulting plasmid was named pUG62AUR-HXK1USDS (Fig. S6).

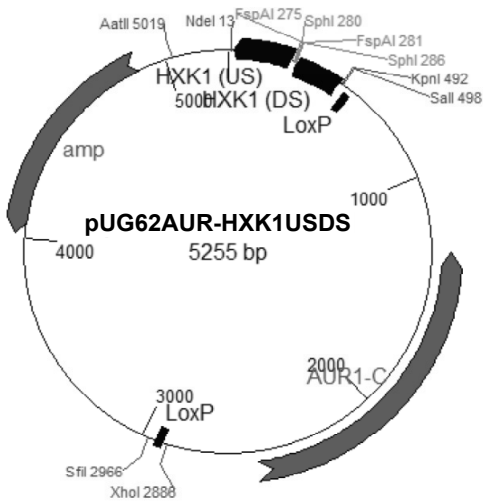

Figure S6. The pUG62AUR-HXK1USDS plasmid containing homologous regions flanking the *HXK1* gene.

TMB3462 was transformed with pUG62AUR-HXK1USDS, linearized with *Fsp*I, according to High efficiency protocol. Before plating the transformants the

cells were resuspended in 1 mL of YP with 2% galactose and incubated at 30 °C for 2.25 h. Transformants were selected on solid YNB medium containing 2% galactose, 220 mg/L leucine and 0.15 mg/L aureobasidin A. Correct integration was verified by colony PCR on randomly selected colonies using primers HXK1_US_f and AmpR-R130. Attempts to amplify the *HXK1* gene using primers HXK1_547_f and HXK1_1282_r did not result in any amplification, indicating the gene had been deleted. This was confirmed by a very low glucose phosphorylating activity in one positive clone which was named TMB3463 (Fig. S7).

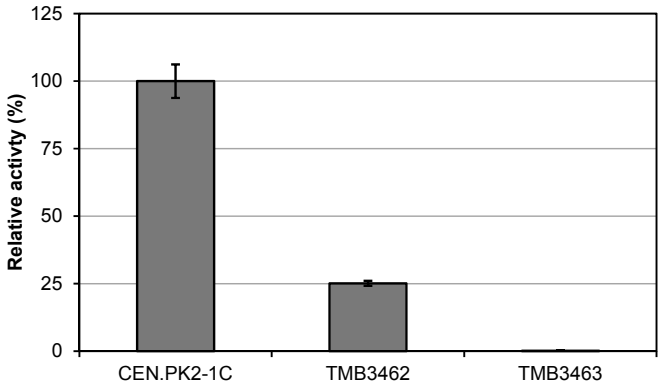

Figure S7. The glucose phosphorylating activity in strains TMB3462 (3Δ) and TMB3463 (4Δ) relative to the wild-type CEN.PK2-1C strain.

***Bergdahl et al.*: Engineering yeast hexokinase 2 for improved tolerance toward xylose-induced inactivation**

ADDITIONAL FILE 2

Selection experiment I

Strain TMB3463 was transformed with 300 µg of the plasmid library from *E. coli* according to the method outlined in the main text. The resulting library size was comparable with that described in the main text. However, instead of inoculating the transformants directly in a bioreactor they were allowed to recover in 100 mL of YNB medium with 2% galactose in a 1 L shake flaks for 6 h at 30 °C. The cells were subsequently harvested and aliquoted in 20% glycerol and stored at -80 °C. Propagation was performed by inoculating one thawed vial in 300 mL YNB medium with 2% glucose at an initial OD of 0.4. After 92 h the OD had reached 10 and the cells were harvested and aliquoted in 20% glycerol and stored at -80 °C.

The selection experiment was started by inoculating a thawed aliquot in 50 mL of YNB medium with 2% glucose in a 500 mL shake flask at an initial OD of 0.1. The pre-culture was grown over night in an orbital shaker at 30 °C and 180 rpm and used to inoculate a bioreactor containing 1000 mL mineral medium with 1% glucose at OD = 0.15. After cultivating the transformants in aerobic batch mode the experiment was carried out as described in the main text.

In this experiment it took 10 h to reduce the OD from 1.2 to 0.16 after the washout had been initiated (Fig. S8). During the first 2 h the cells were unable to increase the growth rate, but as the concentration of glucose increased the transport of xylose into the cells became inhibited and the cells were eventually able to grow at a rate of 0.21 1/h. In comparison, the transformants pre-grown in galactose were able to grow at a rate of 0.17 1/h immediately upon increasing the flow rate and it took 4 h before the concentration of glucose had increased enough to inhibit the transport of xylose into the cells and the growth rate increased to 0.29 1/h. Hence this population showed a higher glucose consumption rate which is also displayed in the large deviation from the theoretical accumulation profile of glucose. Due to the higher growth rate it took 12 h to reduce the OD from 1.2 to 0.2. The large differences in the washout profiles of the two experiments indicate that the population pre-grown in galactose is capable of having a higher metabolic activity in the presence of xylose. This is shown by the higher growth rate, reduced glucose accumulation, higher glycerol concentration and higher CO_2 content in the exhaust gas (Fig. S8).

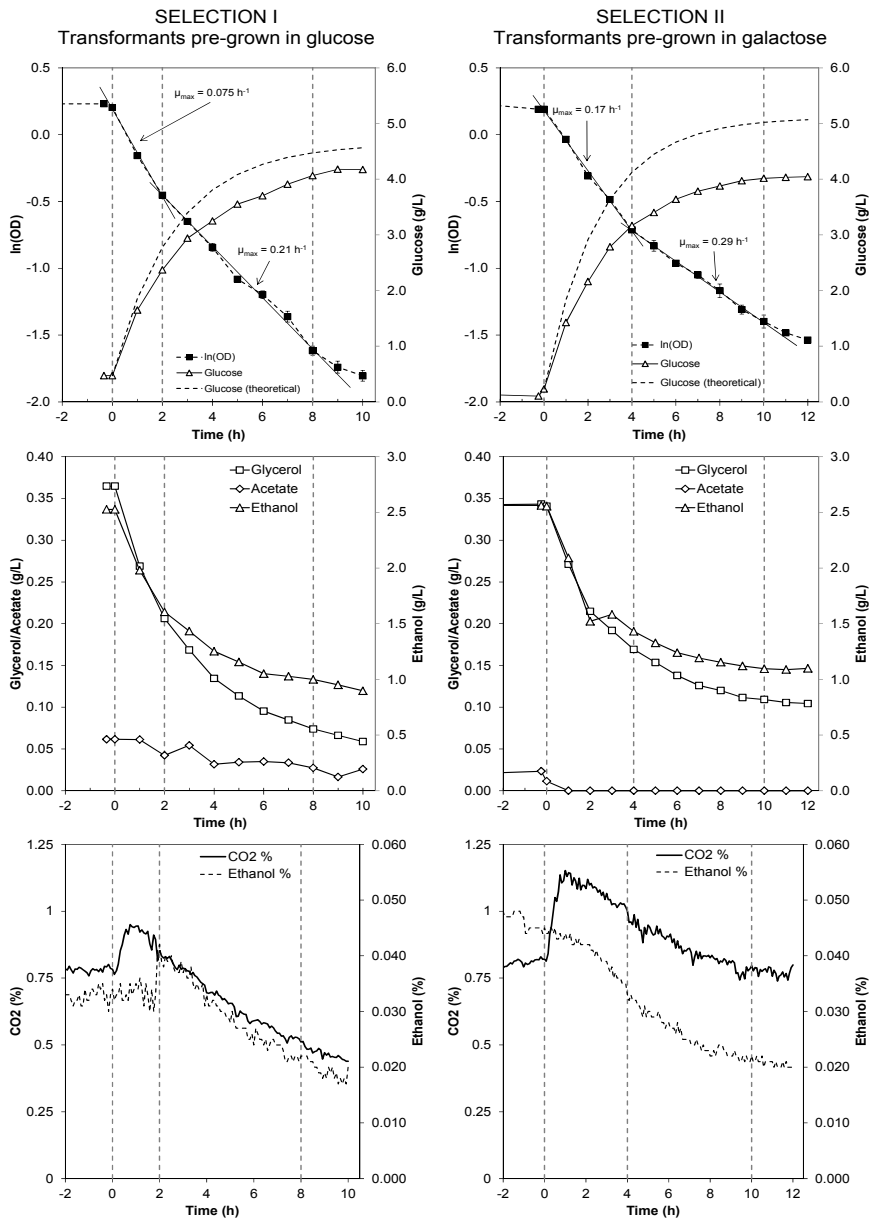

Figure S8. Washout profiles from two selection experiments.
In both cases was strain TMB3463 (*hxk2Δ hxk1Δ*1 *glk1Δ hxk1Δ*2) transformed with the plasmid library. Selection I was started with transformants pre-grown on glucose whereas Selection II was started with transformants pre-grown on galactose. Several features indicate that the population of transformants in Selection II are more metabolically active in the presence of xylose. These features are: higher growth rate, reduced glucose accumulation, higher glycerol concentration and higher CO_2 content in the exhaust gas.